Investigating the Interaction between the Hepatitis C Virus Core Protein and the Cellular DEAD-box Protein DDX3 and its Importance in Virus Replication

Allan G. N. Angus

A thesis presented for the degree of Doctor of Philosophy

Faculty of Biomedical and Life Sciences

University of Glasgow

MRC Virology Unit

Church Street

Glasgow

G11 5JR

April 2010

Abstract

Hepatitis C virus (HCV) is a major cause of chronic hepatitis worldwide. Present estimates predict that approximately 130 million people are infected with HCV with the majority of all infections progressing to chronicity, ultimately leading to fibrosis, cirrhosis and hepatocellular carcinoma. The virus, which belongs to the family *Flaviviridae*, has a single-stranded RNA genome of positive polarity that codes for a unique polyprotein of approximately 3000 amino acids.

Core protein forms the viral nucleocapsid and is the most highly conserved of all the viral proteins. As well as playing a central role in virion assembly, core has been shown to modulate several cellular processes mainly due to its interaction with several host factors. One such cellular interacting partner of core protein is the DEAD-box RNA helicase DDX3. Although, the binding of these two proteins has been shown by yeast-two hybrid screening and co-immunoprecipitation (co-IP) assays, an authentic interaction is yet to be demonstrated in cells replicating the HCV JFH1 infectious clone. Nevertheless, IF analysis of JFH1-infected cells has shown a proportion of DDX3 is redistributed to distinct cytoplasmic sites where it colocalises with core, implying that these two proteins interact during virus replication. Six JFH1 core alanine mutants (F24A, G27A, I30A, G33A, V34A and Y35A) are known to disrupt this core-DDX3 colocalistion without altering viral genome replication following direct electroporation of viral RNA into cells. All mutants release infectious virus particles, except $JFH1_{G33A}$. However, substantial reductions in RNA replication levels were observed at early time points following infection of naïve cells with the infectious mutant virus particles. Furthermore, the G33A mutation appears to allow the viral genome some degree of elasticity as during the serial passaging of G33A-electroporated cells, a progressive increase in infectious virus particles was observed. Based on the diverse phenotypes of these mutants it is difficult to conclude as to which effects (if any) are directly related to the core-DDX3 interaction. In addition, DDX3 has become a topical host factor in HCV research following recent studies demonstrating that its knockdown from target cells causes an overwhelming reduction to HCV replication. However, these studies failed to demonstrate if the core-DDX3 interaction had any functional relevance to this effect.

The aim of this study was to clearly define the role of the core-DDX3 interaction in HCV replication. Using highly specific antibodies, a co-IP assay was developed that was

sensitive enough to detect an interaction between these two proteins from JFH1 RNA-electroporated cell lysates. Co-IP analysis of the 6 JFH1 core mutants revealed that only one of these ($JFH1_{Y35A}$) appeared to completely abolish DDX3 binding. Detailed analysis of this mutant revealed its replication properties resembled those of the WT virus following both electroporation of the viral RNA into cells and infection of naïve cells with the virus particles, demonstrating that the core-DDX3 interaction is dispensable for virus replication in cell culture. In addition, DDX3 knockdown experiments revealed that as for $JFH1_{WT}$, the replication of $JFH1_{Y35A}$ was equally sensitive to the depletion of endogenous DDX3 levels from target cells, indicating that the requirement of DDX3 for HCV replication is unrelated to its interaction with the viral core protein. Interestingly, sucrose gradient studies showed that DDX3 protein sedimented with the extracellular core protein from $JFH1_{WT}$ virus particles. Analysis of the $JFH1_{Y35A}$ virus particles found them to be less dense with a lower content of DDX3, alluding to the exciting possibility of DDX3 being a novel component of the virion. The results of this study indicate that the core-DDX3 interaction is not the mechanism through which HCV utilises this host factor for its replication. However, DDX3 may be incorporated into virus particles through its association with the nucleocapsid. Investigating the latter possibility is the subject of our future work.

In a separate study, the replication properties of $JFH1_{G33A}$ and $JFH1_{F24A}$ were fully characterised. These two mutants were chosen for further analysis as they possessed unique properties relating to the virus proliferation in cell culture. Of the original 6 JFH1 core mutants, only $JFH1_{G33A}$ had a defect in secreting infectious virus particles. Upon passaging of cells electroporated with this mutant infectious particle production increased and eventually achieved peak titers similar to WT. The increase in infectivity consistently coincided with the appearance of a second mutation in close proximity to the originally mutated residue 33. Although, similar results were reported previously for this mutant by Dalrymple, (2007), the present study extended this work by confirming that these second-site changes were compensatory mutations, which rescued the infectivity of $JFH1_{G33A}$. In contrast to the assembly defect of $JFH1_{G33A}$, $JFH1_{F24A}$ was efficient at secreting infectious virus following electroporation, however the infection kinetics of these particles was considerably lower than those derived from $JFH1_{WT}$. Further analysis, suggested the delayed infection of $JFH1_{F24A}$ virus was likely due to an early event in the HCV lifecycle following entry into the cell and prior to the release of the infectious genome. Identifying the importance of glycine 33 in infectious virus assembly and phenylalanine 24 in virus spread provides the basis for further studies into the role that core plays in virus

proliferation in cell culture. In its totality, this study has uncovered important details regarding the role of core, DDX3 and the core-DDX3 interaction in the HCV lifecycle.

Table of Contents

Abstract……I

Figures, Tables and Appendices..……IX

Publications……...XII

Acknowledgements……XIII

Author's Declaration……..XIV

Abbreviations……XV

One and Three letter Amino Acid Abbreviations……....XXI

1. Introduction……..1

1.1. Discovery of Hepatitis C Virus……..1

1.2. Virion Properties and Classification……..1

1.3. Transmission and Epidemiology……2

1.4. Natural History of Infection……...4

1.4.1. Acute Hepatitis C……..…….4

1.4.2. Chronic Hepatitis C……4

1.4.3. Cirrhosis and Hepatocellular Carcinoma…….....5

1.5. Immunological Response to HCV Infection……..5

1.5.1. Innate Immunity……5

1.5.2. Adaptive Immune Response……...6

1.5.2.1. Cellular Immune Response……6

1.5.2.2. Humoral Immune Response….....7

1.6. Pathobiological changes Induced by HCV Infection…….....8

1.6.1. Immune-Mediated Damage in Chronic HCV Infection…….....8

1.6.2. HCV Cytopathogenicity…….....9

1.7. Treatment of HCV Infection……10

1.8. Genome Organisation……...11

1.8.1. Untranslated RNA Segments……...12

1.8.2. HCV-Encoded Proteins……13

1.8.2.1. Core Protein.....13

1.8.2.2. E1 and E2…….13

1.8.2.3. p7.....14

1.8.2.4. NS2.....15

1.8.2.5. NS3 and NS4A.....16
1.8.2.6. NS4B.....17
1.8.2.7. NS5A.....17
1.8.2.8. NS5B.....19
1.9. Systems to Study HCV Replication…….21
1.9.1. Animal Models…….21
1.9.2. *In Vitro* Systems to Study HCV……...22
1.9.2.1. Replicons….....22
1.9.2.2. HCVpp……..….....23
1.9.2.3. HCVcc……..23
1.10. The HCV Lifecycle……..24
1.10.1. Virus Attachment and Entry…….....24
1.10.2. Genome Translation and RNA Replication…….....27
1.10.3. HCV Assembly…….....28
1.11. HCV Core Protein……30
1.11.1. Structural Determinants…….....30
1.11.2. The Core-LD Association and Virus Production……...……..31
1.11.3. Core is the Viral Nucleocapsid…….32
1.11.4. Alternative Reading Frame Protein……...……...32
1.11.5. Conserved RNA Stem Loop Structures……...……34
1.11.6. Pathogenic Effects of Core……...34
1.11.6.1. Apoptosis……...…...34
1.11.6.2. Transformation…….....36
1.11.6.3. Immune Response…….....37
1.11.6.4. Transcription…….....39
1.11.6.5. Lipid Metabolism…….....40
1.11.6.6. Host Cell Proteins Interacting with Core…….....41
1.12. DEAD-Box proteins……42
1.13. DDX3……...42
1.13.1. Cellular Localisation of DDX3……...…….43
1.13.2. Splicing…….....43
1.13.3. Innate Immune Response……...……..44
1.13.4. Apoptosis……..45
1.13.5. Tumourigenesis……45
1.13.6. Protein Translation……...47
1.13.7. Virus Replication……..48

1.13.7.1. HIV-1…….....48
1.13.7.2. HBV…….49
1.13.7.3. HCV……...……..50
1.14. Aims……51
2. Materials and Methods……..52
2.1. Materials……...52
2.1.1. Chemicals…….52
2.1.2. Kits……...53
2.1.3. Cells……..53
2.1.4. Transfection Reagents……..54
2.1.5. Cell Culture Growth Medium……..54
2.1.6. Primary Antibodies……..54
2.1.7. Secondary Antibodies……..55
2.1.8. Clones……...56
2.1.9. Bacterial Strains……...58
2.1.10. Solutions……...59
2.1.10.1. Bacterial Expression…….59
2.1.10.2. DNA Manipulation……...59
2.1.10.3. SDS-PAGE……...59
2.1.10.4. Western Immunoblotting……..60
2.1.10.5. Cell Lysis……..60
2.1.10.6. Tissue Culture……..60
2.1.11. Oligonucleotide Synthesis……61
2.1.12. siRNAs…….61
2.2. Methods……61
2.2.1. Tissue Culture Maintenance……61
2.2.1.1. Cell Passaging……..61
2.2.1.2. Long Term Storage of Cells…….61
2.2.2. Production of Electrocompetent Bacterial Cells……..62
2.2.3. DNA Manipulation……...62
2.2.3.1. Quantitation of DNA……62
2.2.3.2. Restriction Enzyme Digestion of DNA……62
2.2.3.3. Ligation of DNA Fragments……63
2.2.3.4. Transformation of Electrocompetent *E.coli* Cells…63
2.2.3.5. Small Scale Plasmid Preparation from Transformed Bacteria…….……63

2.2.3.6. Large Scale Plasmid Preparation from Transformed Bacteria……63
2.2.3.7. Isolation and Purification of DNA from Agarose Gels……...64
2.2.3.8. Site-Directed Mutagenesis……...64
2.2.3.9. Introducing Core Mutations into pJFH1……..65
2.2.3.10. Preparation of HCV cDNA for Sequencing…….66
2.2.3.11. Polymerase Chain Reaction (PCR) Amplification of DNA.....66
2.2.3.12. Nucleotide Sequencing…….67
2.2.3.13. Restriction Digestion of pJFH1 for *In Vitro* Transcription……68
2.2.4. RNA Manipulation……...68
2.2.4.1. *In Vitro* Transcription…….……..68
2.2.4.2. Preparation of Total RNA……....68
2.2.4.3. Preparation of Extracellular HCV RNA……...69
2.2.5. Introduction of DNA/RNA into Eukaryotic Cells……69
2.2.5.1. Transfection of DNA……....69
2.2.5.2. Electroporation of RNA……...70
2.2.6. Reverse Transcription-Quantitative PCR (RT-qPCR).....70
2.2.6.1. First-Strand cDNA Synthesis……...70
2.2.6.2. REAL-TIME PCR……71
2.2.7. Generation of JFH1 Virus……73
2.2.7.1. Measuring Virus Infectivity…….73
2.2.7.2. Analysis of Virus Replication……..74
2.2.8. Detection of Cellular and Viral Proteins……..75
2.2.8.1. Sample Lysis for SDS-PAGE Analysis……...75
2.2.8.2. Denaturing Polyacrylamide Gel Electrophoresis (SDS-PAGE)…….....…..…76
2.2.8.3. Western Immunoblotting……..…….....76
2.2.9. Immunoprecipitation (IP) of DDX3…….77
2.2.10. Co-immunoprecipitation (Co-IP) of HCV Core Protein……..77
2.2.11. Sedimentation Equilibrium Gradient Analysis……77
2.2.12. RNA Interference…….78
2.2.13. Indirect Immunofluorescence (IF)……79
3. Results……80

3.1. The Importance of the core-DDX3 Interaction in HCV RNA replication and Infectious Particle Production……..80
3.1.1. Introduction……..80
3.1.2. Characterisation of DDX3 Antibodies…….81
3.1.3. Demonstrating an Interaction between Core and DDX3 in Cells Replicating JFH1…….....82
3.1.4. DDX3 Associates with HCV Core on LDs……..83
3.1.5. Core Residues Required for DDX3 Interaction…….....84
3.1.6. Detailed Characterisation of JFH1 Core Mutants……86
3.1.7. Effect of DDX3 Knockdown on HCV Replication…..……..88
3.1.8. DDX3 Sediments with Extracellular Core Protein……...89
3.1.9. Discussion……....91
3.2. Identification of Core Mutations that Determine Infectious Virus Assembly and Productive Infection…….....94
3.2.1. Introduction……..94
3.2.2. The Role of Phenylalanine 24 in Virus Replication and DDX3 Binding…….....95
3.2.3. Effects of Core Mutation G33A on Infectious Virus Assembly…..98
3.2.4. $JFH1_{F24A}$ and $JFH1_{G33A/V34A}$ have Reduced Virus Spread…….101
3.2.5. Discussion……..102
4. Conclusions……...105
4.1. Summary…...…….106
4.2. The Core-DDX3 Interaction and HCV Replication……...106
4.3. Requirement of DDX3 for HCV Replication……...…..107
4.4. Is DDX3 a Component of the Virion?.....109
4.5. The Core-DDX3 Interaction and HCV-Associated Pathogenesis……..111
4.6. The Importance of Core Residue Glycine 33……...…..113
4.7. The Importance of Core Residue Phenylalanine 24……...……114
4.8. Finishing Statement...…….116
References…….117

Figures, Tables and Appendices

Chapter 1 Figures

Figure 1.1. HCV subtype distribution worldwide

Figure 1.2. Signalling pathways in the innate immune response to HCV infection

Figure 1.3. HCV evasion from the innate immune response

Figure 1.4. The interaction of different arms of the HCV-adaptive immune response

Figure 1.5. General features of the HCV genome and polyprotein processing

Figure 1.6. Proposed secondary and tertiary structure of the HCV 5' UTR, together with a small portion of the core-coding sequence, from genotype 1b infectious clone (HCV-N)

Figure 1.7. Predicted secondary structure of the HCV 3' UTR from the genotype 1b Con1 isolate

Figure 1.8. *In vitro* systems for the study of HCV replication, entry, and infectivity

Figure 1.9. Model of the HCV Lifecycle

Figure 1.10. Current model for HCVentry

Figure 1.11. The role of the core-LD association in virion assembly

Figure 1.12. Hypothetical model of assembly and secretion of VLDL and HCV virions in hepatocytes

Figure 1.13. Model for the release of HCV core protein from the ER membrane

Figure 1.14. Schematic representation of the four predicted core RNA secondary structures

Figure 1.15. Diagram illustrating the 9 conserved motifs of DEAD-box proteins flanked by variable N- and C-termini

Chapter 3 Figures

Figure 3.1. Characterisation of two anti-DDX3 antibodies

Figure 3.2. Interaction of HCV core with cellular DDX3

Figure 3.3. Images of JFH1-infected Huh-7 cells probed with different antibodies

Figure. 3.4. Localisation of DDX3 and JFH1 core on LDs

Figure 3.5. Localisation of DDX3 and $JFH1_{DP}$ core on LDs

Figure 3.6. Localisation of DDX3 in cells replicating JFH1 core mutants

Figure 3.7. Identification of core residues critical for its interaction with DDX3

Figure 3.8. Mutations in core do not disrupt its association with LDs

Figure 3.9. Analysis of JFH1 core mutant viruses

Figure 3.10. Further characterization of the JFH1 core mutants

Figure 3.11. Infection kinetics of JFH1 core mutants

Figure 3.12. Requirement of DDX3 for HCV replication

Figure 3.13. Requirement of DDX3 for HCV genome synthesis and protein expression

Figure 3.14. Detection of DDX3 on virus particles

Figure 3.15. Biochemical and biophysical properties of $JFH1_{WT}$ and $JFH1_{Y35A}$ virus particle

Figure 3.16. $JFH1_{WT}$ virus is not neutralised by anti-DDX3 antibodies

Figure 3.17. BLOSUM62 substitution matrix

Figure 3.18. Venn diagram relating a selection of physico-chemical properties from the 20 standard amino acids

Figure 3.19. Structures of the amino acids relevant to this study

Figure 3.20. Replication of JFH1 phenylalanine core mutants following electroporation

Figure 3.21. Infection kinetics of the JFH1 phenylalanine core mutant viruses

Figure 3.22. The localisation of DDX3 in cells replicating the phenylalanine core mutants

Figure 3.23. Analysis of the core-DDX3 interaction from the phenylalanine mutants

Figure 3.24. NS5A expression from $JFH1_{G33A}$-electroporated and -infected cells

Figure 3.25. Requirement of $JFH1_{G33A}$ for virus release

Figure 3.26. Reversion properties of $JFH1_{G33A}$

Figure 3.27. Second-site mutations compensate $JFH1_{G33A}$ virus assembly

Figure 3.28. Infection kinetics of double core mutant viruses

Figure 3.29. The localisation of DDX3 in cells replicating the double core mutants

Figure 3.30. Analysis of JFH1 core double mutant viruses

Figure 3.31. $JFH1_{G33A/V34A}$ and $JFH1_{F24A}$ have reduced virus spread

Figure 3.32. Effect of core mutations on the predicted structures of stem loops SL47 and SL87

Figure 3.33. NMR model of core residues 2-45 proposed by Ladaviere *et al*. (Protein Data Bank I.D.1CWX)

Tables

Table 1. Risk factors for developing chronic HCV infection

Table 2. Risk factors for advanced progression of liver fibrosis

Table 3. Time to development of cirrhosis in representative cohorts of immunocompetent and different groups of immunosuppressed HCV patients

Table 4. Cellular and viral proteins shown to interact with HCV core protein

Table 5. Numbers of host proteins found on enveloped viruses by MS

Appendices

Appendix 1. Primers used for core mutagenesis and sequencing

Appendix 2. Binding of mAbs to JFH1-electroporated Huh-7 cell lysates when used alone or in combination with other mAbs

Appendix 3. Binding of core antibodies to $JFH1_{I30A}$, $JFH1_{G33A}$-electroporated Huh-7 cell lysates

Publications

Publications from this work (accompanying material)

Angus, A.G., Dalrymple, D., Boulant, S., McGivern, D.R., Clayton, R.F., Scott, M.J., Adair, R., Graham, S., Owsianka, A.O., Targett-Adams, P., Li, K., Wakita, T., McLauchlan, J., Lemon, S.M. and Patel, A.H. (2010). Requirement of cellular DDX3 for hepatitis C virus replication is unrelated to its interaction with the viral core protein. *J Gen Virol* **91**, 122-132.

Publications obtained from personal contribution to other studies

Dhillon, S., Witteveldt, J., Gatherer, D., Owsianka, A.M., Zeisel, M.B., Zahid, M.N., Rychłowska, M., Foung, S.K., Baumert, T.F., Angus, A.G. & Patel, A.H. (2010). Mutations within a conserved region of the hepatitis C virus E2 glycoprotein that influence virus-receptor interactions and sensitivity to neutralizing antibodies. *J Virol* **84**, 5494-5507.

Hughes, M., Gretton, S., Shelton, H., Brown, D.D., McCormick, C.J., Angus, A.G., Patel, A.H., Griffin, S. & Harris M. (2009). A conserved proline between domains II and III of hepatitis C virus NS5A influences both RNA replication and virus assembly. *J Virol* **83,** 10788-96.

Iro, M., Witteveldt, J., Angus, A.G., Woerz, I., Kaul, A., Bartenschlager, R. & Patel A.H. (2009). A reporter cell line for rapid and sensitive evaluation of hepatitis C virus infectivity and replication. *Antiviral Res* **83**, 148-55.

Vieyres, G., Angus, A.G., Haberstroh, A., Baumert, T.F., Dubuisson, J. & Patel A.H. (2009). Rapid synchronization of hepatitis C virus infection by magnetic adsorbtion. *J Virol Methods* **157**, 69-79.

Witteveldt, J., Evans, M.J., Bitzegeio, J., Koutsoudakis, G., Owsianka, A.M., Angus, A.G., Keck, Z.Y., Foung, S.K., Pietschmann, T., Rice, C.M. & Patel AH. (2009). CD81 is dispensable for hepatitis C virus cell-to-cell transmission in hepatoma cells. *J Gen Virol* **90**, 48-58.

Acknowledgements

Many Thanks to –

The MRC and Professor Duncan McGeoch for allowing me the opportunity to undertake my PhD at the MRC Virology Unit.

My supervisor, Dr Arvind Patel, for his outstanding support and guidance throughout the practical and writing stages of my PhD.

Dr David Dalrymple for the JFH1 core mutant clones.

All past and present members of lab 106a, but particularly Dr Richard Adair for his experimental expertise, Dr Ania Owsianka and Dr Susan Graham for their technical support and Gaby and Sim for their friendship and experimental assistance.

Dr John McLauchlan and his past lab members Dr Paul Targett-Adams and Dr Steeve Boulant for providing reagents and confocal microscopy assistance.

Professor Mark Harris and Dr Steve Griffin for reagents and experimental advice.

Dr Takaji Wakita for the JFH1 plasmid and Dr Charles Rice for the NS5A antibody.

Dr Francois Penin and Dr Derek Gatherer for their expert advice on protein structural analysis.

Finally, I would like to thank my family, particularly my parents, for their support throughout my academic career.

Author’s Declaration

This work was completed at the University of Glasgow between October 2006-2009 and has not been submitted for another degree. All work presented in this thesis was obtained by the author’s own efforts, unless otherwise stated.

Abbreviations

°C	degrees celcius
%	percentage
µ	micro (10^{-6})
ADRP	adipocyte differentiation-related protein
AIG	anchorage independent growth
ALT	alanine aminotransferase
aa	amino acid
Amp	ampicillin
Apo	apolipoprotein
APS	ammonium persulphate
APC	antigen presenting cell
ARFP	alternative reading frame protein
ATP	adenosine-5'-triphosphate
ATRA	all-trans-retinoic acid
bp	base pair(s)
BPB	bromophenol blue
BSA	bovine serum albumin
BVDV	bovine viral diarrhoea virus
C-	carboxy-terminus
CAP-Rf	core associated protein-RNA helicase full-length
cccDNA	covalently closed circular DNA
cdk	cyclin-dependent kinase
cDNA	complementary DNA
c-FLIP	FLICE-like inhibitory protein
CHO	chinese hamster ovary (cells)
cIAP	cellular inhibitor of apoptosis protein-1
CLDN	claudin
CPE	cytopathic effect
CRM1	chromosome maintainance region 1
CSFV	classical swine fever virus
CTL	cytotoxic T lymphocyte
CypA	cyclophilin A

DAPI	4’,6-diamidino-2-phenylindole
DISC	death-inducing signaling complex
dH_2O	deionised molecular biology grade water
DMEM	Dulbecco’s modified eagles media
DMSO	dimethyl sulphoxide
DNA	deoxyribonucleic acid
DNase	deoxyribonuclease
DNTPs	deoxynucleotides triphosphates
DV	dengue virus
EBPs	eIF4E inhibitory proteins
E.coli	Escherichia coli
ECL	enhanced chemiluminescence
EDTA	ethylenediaminetetra-acetic acid
ELISA	enzyme-linked immunosorbant assay
eIF	eukaryotic translation initiation factor
EM	electron microscopy
EMCV	encephalomyocarditis virus
EP-PCR	error prone PCR
ER	endoplasmic reticulum
FAH	fumaryl acetoacetate hydrolase
FCH	fibrosing cholestatic hepatitis
FCS	foetal calf serum
FFU	focus-forming unit(s)
FLICE	FADD-like interleukin-1-beta-converting enzyme
g	gram
GAG	glycosaminoglycan
GFP	green fluorescent protein
GSK3	glycogen synthase kinase-3
h	hour(s)
HAV	hepatitis A virus
HBV	hepatitis B virus
HCC	hepatocellular carcinoma
HCl	hydrochloric acid
HCV	hepatitis C virus
HCVcc (virus)	HCV cell culture-derived virus
HCVpp	HCV pseudoparticles

HDL	high-density lipoprotein
HeBS	HEPES-Buffered Saline
hnRNP K	heterogenous nuclear ribonucleoprotein K
HGG	hypogammaglobulinaemia
HGV	hepatitis G virus
HIV	human immunodeficiency virus
HL	hydrophobic loop
HRP	horseradish peroxidase
Huh-7	human hepatoma 7 (cells)
HVR	hypervariable region
IF	indirect immunofluorescence
IFN	interferon
IgG	immunoglobulin G
IL	interleukin
IRES	internal ribosome entry site
IRF-3	IFN regulatory factor 3
ISG	IFN-stimulated gene
JFH	Japanese fulminant hepatitis
kb	kilobase pair(s)
kDa	kilodalton(s)
LB	L-Broth
LB2	immunoprecipitation buffer
l	litre(s)
LD	lipid droplet
LDL	low-density lipoprotein
LDLR	low-density lipoprotein receptor
LEL	large extracellular loop
LT	liver transplant
LT-βR	lymphotoxin-β receptor
LVP	lipoviroparticle
m	milli (10^{-3})
m	metre(s)
M	molar
mAb	monoclonal antibody
MAF	membrane-associated foci
Mcl-1	human myeloid cell factor 1

min	minute
m.o.i	multiplicity of infection
MPT	mitochondrial permeability transition
mRNA	messenger RNA
mRNPs	messenger ribonulceoprotein particles
MS	mass spectrometry
MTOC	microtubule organising centre
MTP	microsomal triglyceride transfer protein
nano	(10^{-9})
N-	amino terminus
NANBH	non-A, non-B hepatitis
Neo/G418	neomycin phosphotransferase
NH_4OAc	ammonium acetate
NLS	nuclear localization signals
NS	non-structural
NTBC	2-(2-nitro-4-trifluoro-methylbenzoyl)-1,3-cyclohexanedione
2-5’ OAS	2’5’ oligoadenylate synthetase
OCLN	occludin
OD	optical density
ORF	open reading frame
pAb	polyclonal antibody
PAGE	polyacrylamide gel electrophoresis
PBS(A)	phosphate-buffered saline
PBST	PBS(A)–Tween
PBMC	peripheral blood mononuclear cells
PCR	polymerase chain reaction
pgRNA	pregenomic RNA
pH	potential of hydrogen
PI	protease inhibitor
PKA	protein kinase A
PKC	protein kinase C
PKR	protein kinase R
PTB	polypyrimidine tract binding protein
RC-DNA	relaxed circular
RdRp	RNA-dependent RNA polymerase
RIG-I	retinoic-acid-inducible gene I

RNA	ribonucleic acid
RNAi	RNA interference
RNase	ribonuclease
r.p.m	revolutions per minute
RRE	Rev responsive element
RT-PCR	reverse transcription PCR
RT-qPCR	reverse transcription-quantitative PCR
s	second(s)
SCID	severe combined immunodeficiency
SDS	sodium dodecyl sulphate
sE2	soluble E2
SGR	subgenomic replicon
shRNA	short hairpin RNA
siRNA	small inhibitory RNA
SOCS3	suppressor of cytokine signaling-3
SP	signal peptidase
SPP	signal peptide peptidase
SR-BI	scavenger receptor class B member I
STAT-C	specifically targeted antiviral therapy for hepatitis C
SVR	sustained viral response
TAP	tip-associated protein
TBE	tick-borne encephalitis
$TCID_{50}$	50% tissue culture infective dose
TEMED	N'N'N'N'-tetramethylethylene-diamine
TVR	teleprevir
TMD	transmembrane domain
TNF	tumour necrosis factor
TRIF	Toll/interleukin-1 receptor/resistance domain-containing adaptor inducing IFN
TRIS	2-Amino-2-(hydroxymethyl)-1,3-propanediol
TV	trypsin/versene
U	unit
µ	micro
UTR	untranslated region
UV	ultraviolet
V	volts

VLDL	very-low density lipoprotein
wt	wild-type
w/v	weight/volume ratio
YFV	yellow fever virus
YTB	yeast tryptose broth

One and Three Letter Amino Acid Abbreviations

Amino acid	Three letter code	One letter code
Alanine	Ala	A
Arginine	Arg	R
Asparagine	Asn	N
Aspartic acid	Asp	D
Cysteine	Cys	C
Glutamine	Gln	Q
Glutamic acid	Glu	E
Glycine	Gly	G
Histidine	His	H
Isoleucine	Ile	I
Leucine	Leu	L
Lysine	Lys	K
Methionine	Met	M
Phenylalanine	Phe	F
Proline	Pro	P
Serine	Ser	S
Threonine	Thr	T
Tryptophan	Trp	W
Tyrosine	Tyr	Y
Valine	Val	V

1. Introduction

1.1. Discovery of Hepatitis C Virus

Following the development of serologic tests for hepatitis A virus (HAV) and hepatitis B virus (HBV) during the 1970s, it became apparent that most cases of transfusion-associated hepatitis were caused by another unknown agent, designated “non-A, non-B hepatitis” or NANBH (Feinstone *et al.*, 1975; Prince *et al.*, 1974). Studies in chimpanzees confirmed that the blood-borne NANBH agent was transmissible and caused by a small, lipid-enveloped virus (Alter *et al.*, 1978; Tabor *et al.*, 1978). Then in 1989, Michael Houghton and collegues used chimpanzee plasma with high concentrations of NANBH to identify a virally encoded antigen belonging to an agent with an RNA genome, subsequently termed “hepatitis C virus” (HCV) (Choo *et al.*, 1989). Further characterisation found that HCV contained a positive sense, single-stranded RNA genome approximately 9.6 kb in length (Choo *et al.*, 1991).

1.2. Virion Properties and Classification

HCV has a genetic organisation similar to that of flaviviruses and pestiviruses and has been classified within the *Flaviviridae* family as a unique member in the Hepacivirus genus (Choo *et al.*, 1991; Robertson *et al.*, 1998; Takamizawa *et al.*, 1991). Members of the *Flaviviridae* family include the flaviviruses such as yellow fever virus (YFV) and tick-borne encephalitis virus (TBE), the pestiviruses such as bovine viral diarrhoea virus (BVDV), classical swine fever virus (CSFV) and GBV-A, -B and hepatitis G (HGV) viruses (Linnen *et al.*, 1996). *Flaviviridae* comprise a positive single-stranded RNA genome encoding a polyprotein composed of structural and non-structural proteins (Reed & Rice, 2000). The genomes of *Flaviviridae* are encapsidated by an icosahedral capsid, which is surrounded by an outer envelope (Clarke, 1997), and is assumed to be the case for HCV. Transmission studies in chimpanzees first showed that HCV virions were relatively small in size (between 30 and 60 nm) and contained a lipid envelope by using filtration and chloroform inactivation methods, respectively (Feinstone *et al.*, 1983; He *et al.*, 1987). In

line with this, HCV particles observed from human plasma by electron microscopy were approximately 50 nm in diameter and could be gold-labelled with antibodies to the HCV envelope proteins (Kaito *et al.*, 1994).

In density gradients, HCV RNA containing particles from clinical isolates exhibit a broad distribution and unusually low buoyant densities (Andre *et al.*, 2002; Miyamoto *et al.*, 1992; Nielsen *et al.*, 2006; Thomssen *et al.*, 1992). These properties are likely due to HCV particles associating with very low- and/or low-density lipoproteins (VLDLs and LDLs) (Andre *et al.*, 2002; Nielsen *et al.*, 2006). These complexes, called lipoviroparticles (LVPs) have very low buoyant densities of approximately 1.08 g/ml. In addition, HCV has been reported to associate with immunoglobulins, and these complexes exhibit a buoyant density of 1.17 – 1.21 g/ml (Choo *et al.*, 1995; Hijikata *et al.*, 1993b; Thomssen *et al.*, 1993). However, the density of infectious HCV determined by inoculating chimpanzees was found between 1.09 – 1.11 g/ml (Bradley *et al.*, 1991). In line with this, the HCV RNA derived from highly infectious patient plasma was also found in very low density fractions (~1.09 g/ml) (Hijikata *et al.*, 1993b). The recent development of a robust HCV cell culture infection system (HCVcc) has allowed the biophysical and biochemical nature of the HCV virion to be further characterised. Gradient analysis showed HCVcc RNA containing particles sedimented to a density of approximately 1.15 g/ml (Wakita *et al.*, 2005). The HCV structural proteins core, E1 and E2 were also detected at this density confirming for the first time that these proteins are components of the virion. Electron microscopy (EM) analysis of these HCVcc particles showed the virus HCV has an inner ring of 30-35 nm (thought to be the capsid) and an overall diameter of 50-65 nm (Wakita *et al.*, 2005). Another study measuring the specific infectivity (the ratio of viral RNA divided by the infectious titer) of HCVcc particles by gradient analyses found the most infectious material sedimented at densities between 1.09-1.11 g/ml (Lindenbach *et al.*, 2005), consistent with the peak of infectivity for HCV *in vivo* (see above). In addition, a more recent study has shown HCVcc virions are also associated with VLDLs (Chang *et al.*, 2007). Thus, HCVcc virus particles appear to be biophysically similar to those found *in vivo*.

1.3. Transmission and Epidemiology

HCV is regarded as a major human pathogen and recent estimates predict that 2.2 % (~130 million) of the world's population are infected with the virus (Alter, 2007). HCV infection

is most commonly transmitted by percutaneous exposure to blood or blood products. In economically developing countries, HCV is largely transmitted through unhygienic medical practices and other percutaneous routes such as intravenous drug use. In economically developed countries, the vast majority of new cases are associated with injection drug use. Most descriptions of global HCV epidemiology depend on HCV seroprevalence studies. These studies are typically cross-sectional in design and only performed in select populations, such as blood donors or patients with chronic liver disease, which are not representative of the community or region in which they reside. Despite population-based studies representative of an entire community being far more useful, this kind of study is not possible in most regions of the world. Therefore, in many countries the exact magnitude of the problem has not been defined (Lavanchy, 1999). Nevertheless, for several years the World Health Organisation has reported data on the worldwide prevalence of HCV infection, founded on both submitted data and published studies (Shepard *et al.*, 2005). Although HCV is endemic worldwide, there is a large degree of geographic variability in its distribution. HCV is estimated to infect approximately 0.6 % and 2 % of the UK and US population, respectively (Thomson, 2009). Fewer data are available for developing countries, where it is believed that HCV prevalence is generally higher. For example, Egypt has the highest reported seroprevalence rate with 22 % of the total population being infected (Shepard *et al.*, 2005). This high percentage is the result of the country's anti-schistosomal therapy programme, which until the 1970s involved intravenous administration of drugs using reusable syringes (Frank *et al.*, 2000).

The distribution of the different HCV genotypes also varies between countries. HCV is classified into at least six major genetic groups that on average over the complete genome differ in 30–35 % of nucleotide sites. Each of these six major genetic groups contain a series of more closely related subtypes that typically differ from each other by 20–25 % in nucleotide sequences (Simmonds, 2004). This variation is likely the result of the error prone replication of HCV and the high production rate of 10^{12} particles/day (Neumann *et al.*, 1998). Although the population-based samples are not consistently available, the geographic distribution of HCV genotypes can be mapped using online databases (Fig. 1.1). Genotypes 1-3 have a worldwide distribution and account for almost all infections in the western world with 1a and 1b being the most common.

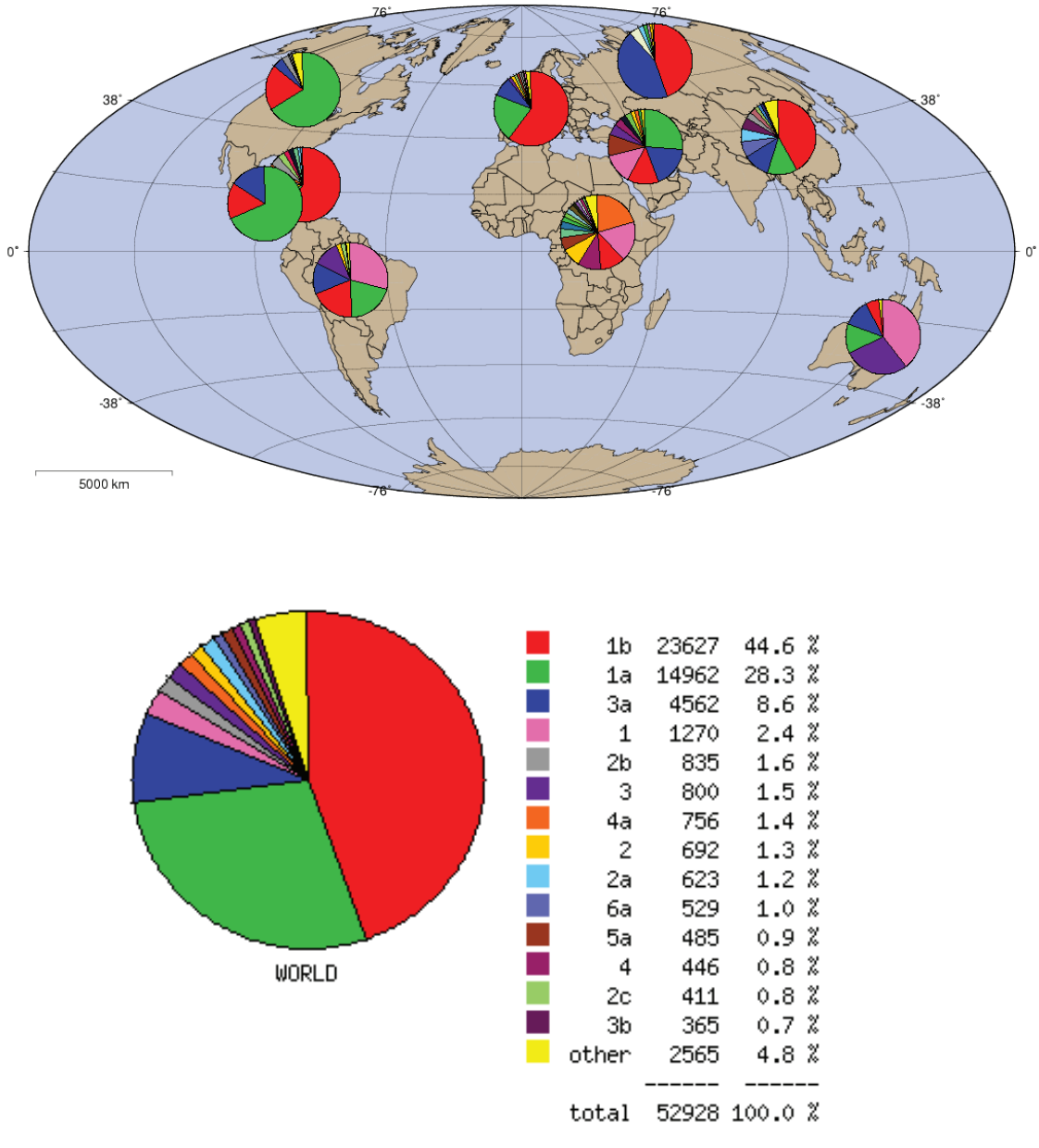

Figure 1.1. HCV subtype distribution worldwide.

The geographic and subtype distribution is shown for the 52, 928 sequences available online at http://hcv.lanl.gov (accessed November 12, 2009).

1.4. Natural History of Infection

HCV is a significant cause of both acute and chronic hepatitis. The clinical course of hepatitis C is variable with no single typical course or natural history of disease, but instead a broad clinical spectrum of disease presentations and outcomes (Hoofnagle, 1997).

1.4.1. Acute Hepatitis C

Acute HCV infection is marked by the detection of HCV RNA in the serum within 1 to 2 weeks post-exposure (Farci *et al.*, 1991; Thimme *et al.*, 2001). However, acute infection is infrequently diagnosed because the majority of acutely infected individuals are asymptomatic. Indeed, in the transfusion setting, where acute onset of HCV infection has been best documented, 70-80 % of cases were found to be asymptomatic (McCaughan *et al.*, 1992). In the few individuals (20-30 %) developing clinical symptoms, these are evident by 3-12 weeks post-exposure and may include malaise, weakness, anorexia, and jaundice (Alter & Seeff, 2000; Thimme *et al.*, 2001). Serum alanine aminotransferase (ALT) levels, signifying hepatocyte necrosis, begin rising 2-8 weeks post-exposure, and frequently reach levels of greater than 10 times the normal upper limits (Farci *et al.*, 1991; Thimme *et al.*, 2001). Resolution of acute infection occurs in 15-40 % of patients, signalled by clearance of HCV RNA from blood, the return of serum ALT to normal levels, and the disappearance of symptoms, usually within 2-12 weeks (Hoofnagle, 1997). Acute infection can be severe but fulminant liver failure is rare (Farci *et al.*, 1996a).

1.4.2. Chronic Hepatitis C

Chronic hepatitis C infection is diagnosed by the detection of HCV RNA in the blood for at least 6 months after infection. In general, prospective studies have shown that 60-85 % of acutely infected patients will develop chronic infection (NIH Consensus, 2002). Once chronic, HCV infection usually persists for decades, causing insidious and progressive liver damage in most patients. Most patients (80 %) remain asymptomatic for 10-30 years despite having moderate to severe chronic liver disease (Hoofnagle, 1997; Sharara, 1997). There are many risk factors involved in the development of chronic HCV infection,

including the age at time of infection, gender, ethnicity, and the development of jaundice during the acute infection (Table 1).

1.4.3. Cirrhosis and Hepatocellular Carcinoma

Structural liver damage, known as fibrosis implies possible progression to extensive tissue scarring called cirrhosis. The time from HCV infection to cirrhosis is dependent on multiple internal host factors, and cannot be predicted in an individual patient (Table 2). In a large cohort study by Poynard *et al*. (1997) the median duration of infection for progression to cirrhosis was estimated to be 30 years, with host factors including ageing, alcohol consumption and male sex having a strong association with fibrosis progression. Also, 10-20 year follow-up studies show that cirrhosis develops in 20-30 % of patients (Di Bisceglie *et al.*, 1991; Haber *et al.*, 1995; Seeff *et al.*, 1992; Takahashi *et al.*, 1993; Vaquer *et al.*, 1994). The progression to cirrhosis is often clinically silent, and some patients are not known to have hepatitis C until they present with the complications of end-stage liver disease or hepatocellular carcinoma (HCC). Virtually all HCV-related HCC occurs among patients with cirrhosis. Once cirrhosis is established, HCC develops at an annual rate of 1-4 % (NIH Consensus, 2002).

1.5. Immunological Response to HCV Infection

1.5.1. Innate Immunity

After HCV infection, the innate immune system is the first response prior to the appearance of the adaptive or specific response and is designed to combat the infection before the virus has a chance to replicate and produce progeny (Pavio & Lai, 2003). This is achieved by a series of intracellular signaling events that lead to the production of an antiviral state directly within the infected hepatocyte and indirectly within the surrounding tissue (Fig. 1.2).

Risk Factors	Reference
Age at time of infection > 25 years	Alter *et al*. (1999), Bellentani & Tiribelli (2001)
Male gender	Kenny-Walsh (1999), Wiese *et al*. (2000)
African American race	Seeff *et al*. (2001), Villano *et al*. (1999)
No Jaundice or symptoms during acute infection	Villano *et al*. (1999), Wiese *et al*. (2000)
HIV infection	Thomas *et al*. (2000)

Table 1. Risk factors for developing chronic HCV infection.

Risk Factors	Reference
Alcohol consumption (>30 g/ day in males, >20 g/ day in females)	(2002)
Age at time of infection > 40 years	Poynard *et al*. (1997)
Male gender	Poynard *et al*. (1997)
Coinfection with HIV	Benhamou *et al*. (1999), Di Martino *et al*. (2001), Ragni & Belle (2001)
Coinfection with HBV	Zarski *et al*. (1998)
Immunosuppression	Benhamou *et al*. (1999), Berenguer *et al*. (2000), Bjoro *et al*. (1994), Bjoro *et al*, (1999)

Table 2. Risk factors for advanced progression of liver fibrosis.

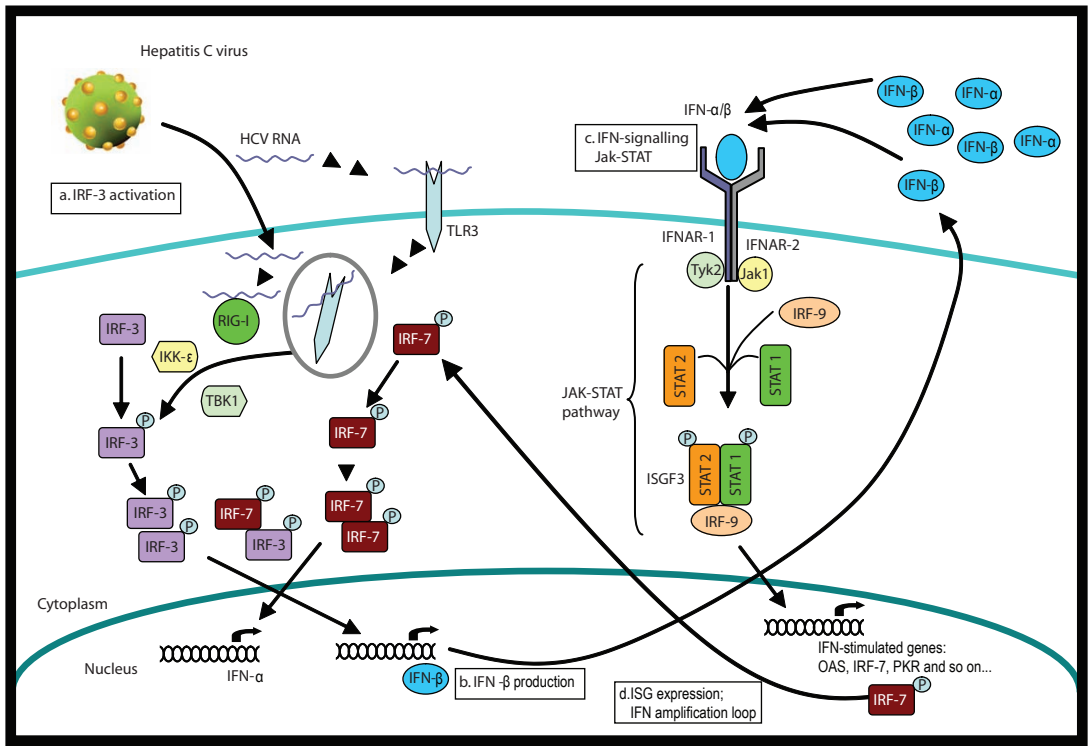

Figure 1.2. Signalling pathways in the innate immune response to HCV infection.

(a) The HCV RNA from the infecting virus is presented to recognition receptors expressed in the host cell. In hepatocytes, retinoic-acid-inducible gene I (RIG-I) and Toll-like receptor 3 (TLR3) signalling comprise the two major host defense pathways triggered by double-stranded RNA. The viral RNA of HCV contains extensive regions of secondary double-stranded RNA structure and is sufficient for this recognition, which leads to the phosphorylation and activation of interferon regulatory factor (IRF)-3 by the Tank-binding kinase 1 (TBK1) or I-kappa-B kinase-ε (IKK-ε) protein kinases. The dimer of phospho-IRF-3 translocates to the cell nucleus and binds the promoter regions of IRF-3 target genes, including IFN-β. (b) IRF-3 activation results in IFN-β production and secretion from the infected cell. (c) IFN-β binding to the IFN-α/β receptor signals the activation of the Tyk2 and Jak1 protein kinases that directs the phosphorylation and assembly of a STAT1–STAT2 heterodimer and trimeric IFN-stimulated gene factor 3 (ISGF3) complex containing IRF-9. The ISGF3 complex localizes to the nucleus, where it binds and directs the expression of IFN-stimulated genes (ISGs). (d) The IRF-7 transcription factor is an ISG expressed in many tissue types in response to IFN. IRF-7 phosphorylation, dimerization and heterodimerization with IRF-3 allow it to bind the promoter region of IFN-α genes resulting in the expression of IFN-α subtypes that further signal ISG expression. This increases the abundance of RIG-I and viral recognition signalling components whose persistent signalling acts to amplify IFN production and anti-viral action within host cells. Adapted from Gale & Foy (2005).

Since acute HCV infection is silent in most cases, very few data on the innate immune response are available from the acute phase in humans. Interestingly, studies using experimentally infected chimpanzees found that during acute infection, HCV-infected hepatocytes induce the transcription of numerous interferon (IFN)-stimulated genes (ISGs). However, this response appears to have no effect on the viral titer or outcome of infection, suggesting HCV can evade these antiviral effects by blocking the subsequent functions of ISGs (Su *et al.*, 2002). Indeed, HCV has been shown to successfully avoid several aspects of the innate immune response, including expression of IFN-β, IFN signalling, and antiviral activities of IFN-induced proteins (Fig. 1.3) hence, the low percentage of patients that are able to resolve infection during the acute stage. Such activities are also likely to result in defects to the adaptive immune response, thereby contributing to HCV persistence in chronic infection.

1.5.2. Adaptive Immune Response

The adaptive immune response is divided into two major types of effector: cellular effectors comprised of cytotoxic T lymphocytes (CTL), and humoral effectors comprised of antibodies secreted by activated B lymphocytes (Pavio & Lai, 2003) (Fig. 1.4).

1.5.2.1. Cellular Immune Response

Initial studies of acutely HCV-infected patients revealed that a strong CD4+ T cell response to several HCV antigens in the initial phase of acute HCV infection is associated with viral clearance (Diepolder *et al.*, 1995; Missale *et al.*, 1996). CD4+ T cell responses are directed mainly against non-structural proteins of HCV and often target the same immunodominant epitopes within the non-structural protein NS3 (Neumann-Haefelin *et al.*, 2005). Studies of the role of virus-specific CD8+ T cells in acute HCV infection showed that patients with a self-limited course of HCV infection mount vigorous and multispecific CD8+ T cell responses, targeting up to eight to twelve epitopes (Gruner *et al.*, 2000; Lechner *et al.*, 2000; Neumann-Haefelin *et al.*, 2005). HCV-infected patients who develop chronic infection typically have only weak, oligo-/mono-specific or no virus-specific CD4+ and CD8+ T cell responses in the acute (Diepolder *et al.*, 1995; Gruner *et al.*, 2000; Lechner *et al.*, 2000; Missale *et al.*, 1996) and chronic phase of infection

(Battegay *et al.*, 1995; Chang *et al.*, 2001; Koziel *et al.*, 1993; Koziel *et al.*, 1995; Lauer *et al.*, 2002; Neumann-Haefelin *et al.*, 2005; Rehermann *et al.*, 1996; Wong *et al.*, 2001). Viral escape mutations have been proposed to contribute to such failure, thereby promoting viral persistence. Indeed, viral amino acid (aa) substitutions that inhibit CD4+ and CD8+ T cell recognition have been reported in chronically infected patients and chimpanzees (Chang *et al.*, 1997; Frasca *et al.*, 1999; Kaneko *et al.*, 1997; Tsai *et al.*, 1998; Weiner *et al.*, 1995).

1.5.2.2. Humoral Immune Response

Studies of the humoral response have revealed the presence of antibodies to virtually all viral antigens during the course of HCV infection in humans and chimpanzees (Bhattacherjee *et al.*, 1995; Mink *et al.*, 1994; Mondelli *et al.*, 1994; Nasoff *et al.*, 1991). However, the most attention has been focused on the envelope glycoproteins (E1E2) as anti-envelope antibodies have been shown to partially protect chimpanzees against infection (Choo *et al.*, 1994). The impact of neutralising antibodies in the resolution of acute infection is poorly understood. The analysis of neutralizing responses has been hampered by the heterogenous nature of patient cohorts as well as HCV strains. These reasons likely explain why many studies assessing antibody-mediated neutralization in acute hepatitis C failed to reveal a clear association between neutralizing antibodies and viral clearance (Ishii *et al.*, 1998; Lavillette *et al.*, 2005; Logvinoff *et al.*, 2004; Steinmann *et al.*, 2004). The above problems were absent in one study using serum samples from a group of homogenous patients in a long-term follow-up of a single-source outbreak of HCV (Pestka *et al.*, 2007). This unique cohort comprised young healthy females, infected with the same HCV genotype 1b strain by intravenous transmission. In these patients, viral clearance was associated with the rapid induction of neutralizing antibodies in the acute phase of infection and loss of neutralizing antibodies after recovery from infection. In contrast, chronic HCV infection was characterized by a complete absence of or reduced capacity to neutralize the transmitted virus in the early phase of infection and a delayed induction of neutralizing antibodies in the late phase of infection. This study highlights two important findings. First, the rapid induction of neutralizing antibodies during the early phase of infection may help control HCV infection. Secondly, HCV can persist despite the induction of antibodies neutralizing the transmitted virus. The later point is likely explained by viral escape from antibody-mediated neutralization by the existence of quasispecies with distinct viral variants in infected individuals changing constantly over

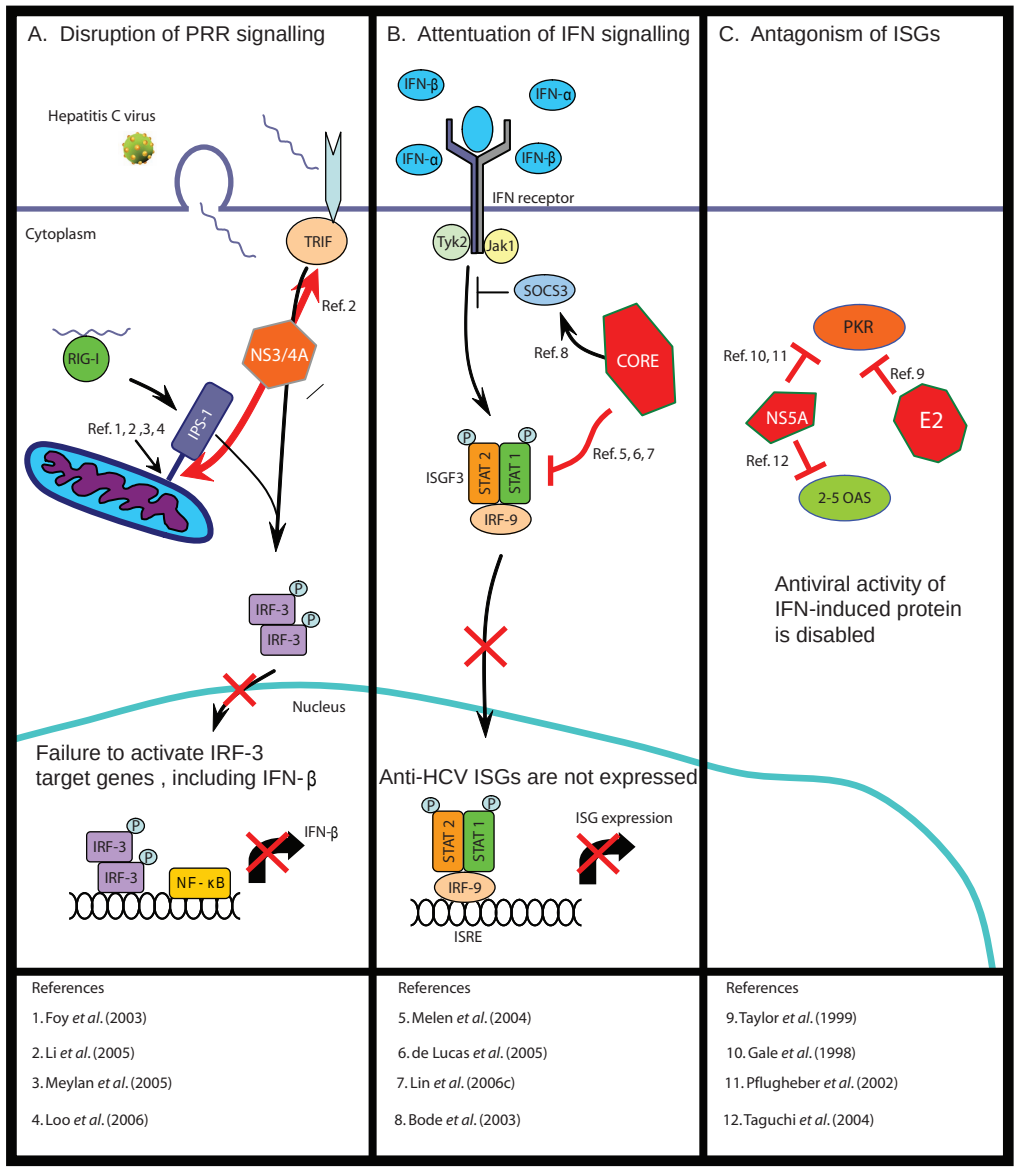

Figure 1.3. HCV evasion from the innate immune response.

(A) NS3/4A blocks RIG-I and TLR3 signalling. RIG-I activation by HCV induces a conformational change that facilitates its interaction with the innate immune adaptor proteins IPS-1. This leads to assembly of a complex on the mitochondria that signals downstream to activate the kinases IKK-ε and TBK1, which phosphorylate the transcription factors IRF-3 and IRF-7. The HCV NS3/4A protease cleaves IPS-1 to release it from the mitochondrial membrane thereby abolishing RIG-I-mediated signal transduction. NS3/4A also cleaves TRIF (Toll/interleukin-1 receptor/resistance domain-containing adaptor inducing IFN), the signaling adaptor molecule for TLR3, to prevent TLR3-mediated antiviral signaling. (B) HCV core protein blocks the Jak/STAT pathway. HCV core protein directly binds to STAT1 to prevent its phosphorylation and subsequent activation of downstream anti-HCV ISGs. HCV core protein also induces expression of the suppressor of cytokine signaling-3 (SOCS3), a negative regulator of the Jak/STAT signaling pathway, causing a decreased STAT1 activation in response to type I IFN. (C) HCV proteins directly interfere with the two ISGs Protein Kinase R (PKR) and 2'5' oligoadenylate synthetase (2-5 OAS). Both the HCV NS5A and E2 protein bind PKR and inhibit its activation. NS5A also blocks the antiviral function of 2–5 OAS through a direct interaction. Adapted from Horner & Gale (2009).

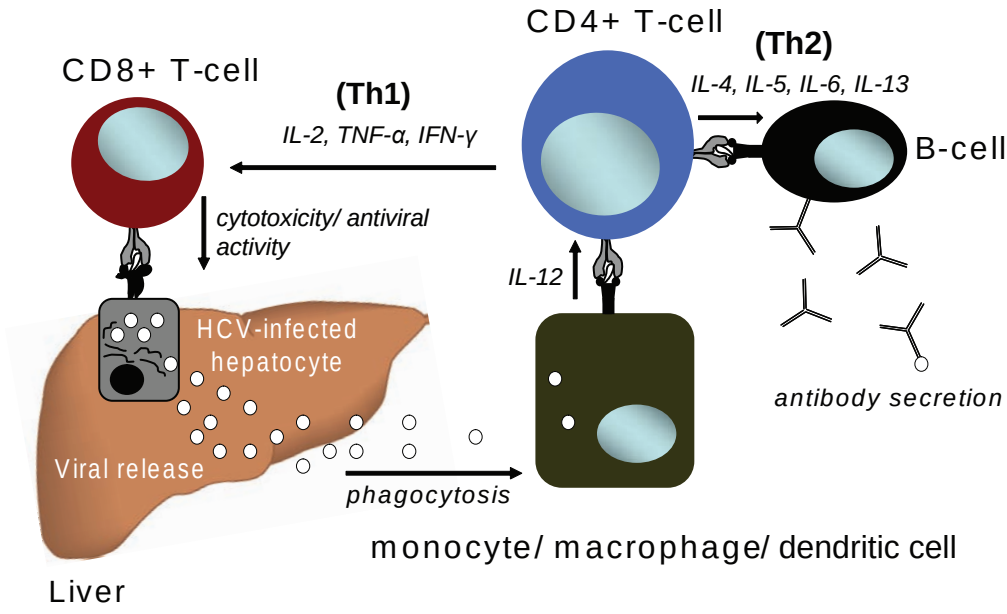

Figure 1.4. The interaction of different arms of the HCV-adaptive immune response.

Specific CD4+ T helper cells recognise viral peptides bound to HLA class II molecules present on the surface of professional antigen presenting cells (APCs) (e.g monocytes, macrophages, B cells, dendritic cells). CD4+ T cell activation results in the development of either Th1 or Th2 helper cells. Th1 cells secrete interleukin (IL)-2, tumour necrosis factor alpha (TNF-α), and IFN-γ, which then stimulate the development of CD8+ Cytotoxic T Lymphocytes (CTLs). Th2 cells, promote the development of virus-specific antibody producing B cells through secretion of IL-4, IL-5, IL-10. Specific CTLs recognise viral peptides bound to HLA class I molecules on the surface of infected hepatocytes leading to the elimination of infected cells. CD8+ T cells perform important non-cytolytic effector functions as well, including the secretion of cytokines such as IFN-γ and TNF-α that can inhibit viral replication without killing the infected cell (Neumann-Haefelin *et al.*, 2005; Pavio & Lai, 2003). Adapted from Diepolder *et al*. (1998).

time. Such rapid evolution is likely to be a result of the high mutation (10^{-3} per nucleotide per generation) and replication rate (~10^{12} virions per day) of HCV in humans (Neumann *et al.*, 1998). Indeed, another study using serum samples collected from a chronically infected patient, demonstrated that the neutralizing antibody response lags behind the rapidly evolving glycoprotein sequences present within the quasispecies population (von Hahn *et al.*, 2007). The highest rate of aa substitutions occurred in the most genetically variable segment of the envelope protein known as hypervariable region 1 (HVR1). This region comprises a ~30 aa stretch at the N-terminus of E2 that is highly tolerant to aa substitutions and is subject to strong selection pressure. HVR1 is a target for anti-HCV neutralising antibodies and assumed to exist as a polypeptide loop on the surface of the virion (Kato *et al.*, 1992a; Kato *et al.*, 1992b; Weiner *et al.*, 1991). In infected patients the appearance of anti-HVR1 antibodies can alter the quasispecies, selecting variants that are less reactive to such antibodies. This indicates that HVR1 harbours a neutralisation epitope that is the site of escape mutations from the humoral immune response (Farci *et al.*, 1996b; Kato *et al.*, 1993; Weiner *et al.*, 1992). In line with this, HCV-infected patients with humoral immunodeficiency display slower evolution of aa sequence changes within HVR1 compared to immunocompetent patients (Booth *et al.*, 1998). This suggests that in the absence of a virus specific antibody response no selection of mutant viruses occurs. It has been suggested that HVR1 may function as an immunologic decoy during infection by masking a deeper, more highly conserved structure within the envelope, such as a cellular receptor recognition site (Ray *et al.*, 1999). Importantly, deletion of HVR1 does not eliminate the ability of HCV to infect chimpanzees, suggesting that it is not critical for viral entry or release (Forns *et al.*, 2000).

1.6. Pathobiological Changes Induced by HCV Infection

1.6.1. Immune-Mediated Damage in Chronic HCV-Infection

Immunophenotyping of intrahepatic infiltrating inflammatory cells in patients with chronic HCV infection revealed a predominance of CD4+ and CD8+ T cells, implying that the host immune system is involved in liver disease pathogenesis (Onji *et al.*, 1992). Also, patients with mild HCV-related liver disease have been shown to have a strong HCV-specific CD4+ T cell proliferative response in peripheral blood in comparison to patients with active liver disease (Botarelli *et al.*, 1993; Hoffmann *et al.*, 1995). In terms of

immmunopathogenesis one explanation for this finding is that HCV-specific CD4+ T cells are compartmentalized in the liver of patients with active liver disease and, hence, there is a low frequency of HCV-specific CD4+ T cells in peripheral blood. Also, in chronically infected patients the frequency of HCV-specific CD8+ T cell precursors was found to be higher in liver than in peripheral blood, suggesting active recruitment of HCV-specific CD8+ T cells in liver. The detection of HCV-specific CD8+ T cell activity in liver was associated with lower levels of viraemia and higher levels of disease activity, providing support for their involvement in the control of viral infection and their contribution to disease (Nelson *et al.*, 1997). Therefore, the majority of the liver damage experienced in patients who fail to clear the virus is most likely due to compartmentalisation of HCV-specific CD4+ and CD8+ T cells.

1.6.2. HCV Cytopathogenicity

The majority of evidence indicates that HCV is not significantly cytopathic in the non-immunosuppressed state. Arguments against a direct viral cytopathic effect (CPE) include, little correlation between intrahepatic HCV load and disease activity (McGuinness *et al.*, 1996), minimal or no hepatocyte damage occurring despite viraemia (Brillanti *et al.*, 1993), and low levels of HCV RNA detected in patient sera with HCV-associated fulminant hepatitis (Farci *et al.*, 1996a). These observations taken together with the evidence of immunopathogenesis imply that hepatocellular damage is immune-mediated rather viral derived.

However, histological examination of HCV-infected livers in early studies showed morphological alterations of cellular architecture such as cell shrinkage, cell rounding and nuclear pycnosis, which are characteristics of CPE (Bamber *et al.*, 1981; Dienes *et al.*, 1982). More recent histological observations supporting a CPE specifically induced by HCV include hepatocellular steatosis, and fibrosing cholestatic hepatitis (FCH). Hepatocellular steatosis is characterized by lipid accumulation in the hepatocyte cytoplasm and is found in 41-73 % of patients with chronic hepatitis C. This virus-induced steatosis is primarily associated with genotype 3 infection, correlates with serum HCV RNA levels, and disappears after successful antiviral therapy (Castera *et al.*, 2005). FCH, initially described in HBV infection, is a severe and progressive form of liver dysfunction seen in a small subset of organ transplant recipients (Doughty *et al.*, 1998; Schluger *et al.*, 1996; Toth *et al.*, 1998). Manifested by rapidly progressive liver failure, FCH is characterized

histologically by hepatocyte ballooning, cholestasis, minimal inflammation, and periportal fibrosis. The pathogenesis of HCV-induced FCH has been attributed to unrestrained viral replication within hepatocytes in the absence of an effective cellular immune response, culminating in a direct CPE (Rosenberg *et al.*, 2002).

In addition, patients with impaired cellular responses suffer a more severe course of liver disease than immunocompetent patients (Einav & Koziel, 2002). This is particularly evident in HCV-infected liver transplant (LT) patients, those co-infected with human immunodeficiency virus (HCV/HIV) or those suffering from hypogammaglobulinaemia (HGG). As shown in Table 3 these groups of patients have extremely rapid cirrhosis progression rates compared to immunocompetent patients. Based on this rationale the lack of an efficient immune response in such patients would allow widespread viral replication and thus, a direct HCV-induced CPE could well be the pathogenic mechanism responsible for the liver damage observed. Unfortunately, the scarcity and divergence of data available on the viral load within these studies make it difficult to comment on the association between viral load and disease severity. Together, these data suggest that the pathobiological changes induced by HCV infection are a result of both the immune response and direct viral CPE.

1.7. Treatment of HCV Infection

The current reference treatment of naïve patients with chronic hepatitis C is the combination therapy with pegylated IFN-α plus ribavirin (Gotto & Dusheiko, 2004). The mechanisms through which IFN and ribavirin exert their anti-HCV effects are currently unknown. The main aim of HCV treatment is to interfere with progression of chronic hepatitis to cirrhosis by the eliminating the virus at an early stage of the disease. Clearance of virus is possible and the aim of therapy is to achieve undetectable HCV RNA 6 months following therapy (sustained viral response, SVR). This is maintained long-term and is significantly associated with reduction in inflammation and fibrosis (Poynard *et al.*, 2002). However, only 40-50 % of individuals infected with HCV genotypes 1 or 4 obtain a SVR, compared with 80 % of patients infected with genotypes 2 or 3 (Soriano *et al.*, 2009). To date, there is no published data on the treatment outcome in patients with genotypes 5 and 6. Unfortunately, as well as the limited response rate in treated patents, therapy is costly, and can cause severe side effects including myalgia, fever, headaches, haemolytic anaemia and severe depression (Fried *et al.*, 2002). Consequently, more effective and better-

Patient group	Time to cirrhosis (years)	References
Immunocompetent	30/ 13-42	Poynard *et al*. (1997)
HIV-HCV	6. 9-28	Soto *et al*. (1997) Benhamou *et al*. (1999) Martinez-Sierra *et al*. (2003) Mohsen *et al*. (2003)
LT	1-5	Gane *et al*. (1996) Prieto *et al*. (1999) Feray *et al*. (1999) Berenguer *et al*. (2000)
HGG	1. 5-15	Bjoro *et al*. (1999) Christie *et al*. (1997)

Table 3. Time to development of cirrhosis in representative cohorts of immunocompetent and different groups of immunosuppressed HCV patients.

tolerated therapies to treat HCV infection are urgently required. Indeed, the recent advances in understanding the HCV lifecycle through the development of HCV replicons (autonomously replicating genomes) and cell culture infectious systems have enabled the production of STAT-C (specifically targeted antiviral therapy for hepatitis C) compounds designed to specifically inhibit HCV replication. The goal of future HCV therapy is to generate antiviral drugs that are less toxic, more potent, and allow shorter duration of therapy than the current standard treatment. Ideally, such compounds should have the capacity to cure the majority of patients between 12-24 weeks of therapy. The NS3/4A protease (required for cleavage of the viral polyprotein) and the NS5B RNA dependent RNA polymerase are currently the two most promising targets for the design of specific HCV inhibitors (Soriano *et al.*, 2009). Teleprevir (TVR) is the most promising drug candidate from the protease inhibitors designed to target NS3/4A. TVR was designed using structure based drug-design techniques and its proof of concept was demonstrated by the elimination of HCV RNA from cell lines harbouring replicons (Lin *et al.*, 2006a; Lin *et al.*, 2006b). Phase 2 clinical trials of TVR used in combination with pegylated IFN-α and ribavirin produced promising results. This novel triple therapy attained a SVR in 62 % of patients with only 12 weeks of therapy, compared to 48 % after 48 weeks using standard therapy. The trial found the main side effects of TVR were skin rashes, nausea and anaemia. The compound is currently being tested in phase 3 clinical trials (Soriano *et al.*, 2009). In terms of HCV polymerase inhibitors, R-1626 was one of the promising candidates that underwent clinical trails. R-1626 is a nucleoside analogue that acts as a chain terminator preventing elongation of the nascent RNA strand, thereby blocking HCV replication. Although, this drug demonstrated potent antiviral activity against all HCV genotypes in early *in vitro* experiments, during phase II clinical trials, the majority of patients treated with R-1626 in combination with pegylated IFN or pegylated IFN and ribavirin suffered severe neutropenia. Moreover, a high rate of HCV infection relapse occurred after completion of therapy (Pockros *et al.*, 2008). As a result, the development of R-1626 was halted at the end of 2008.

1.8. Genome Organisation

The genome of HCV is a positive-sense, single-stranded RNA molecule approximately 9.6 kb in length. The genome comprises a long (~3000 aa) open reading frame (ORF), encoding structural and non-structural (NS) proteins, flanked by two untranslated regions (UTRs) at the 5’ and 3’ ends. The structural proteins, located in the N-terminal region,

include the core protein, the envelope proteins E1 and E2 and probably p7. The non-structural region of the ORF comprises six proteins, NS2, NS3, NS4A, NS4B, NS5A and NS5B (Fig. 1.5).

1.8.1. Untranslated RNA Segments

Depending on the isolate, the HCV 5' UTR is approximately 341 nucleotides long and has a highly conserved sequence with up to 85 % similarity shared between HCV isolates (Bukh *et al.*, 1992). The predicted secondary structure of the 5'UTR shows 4 highly structured domains (domains I to IV) (Fig. 1.6) (Honda *et al.*, 1999). HCV contains an internal ribosomal entry site (IRES) spanning domains II, III and IV of the 5' UTR, and includes the first 24-40 nucleotides of the core-coding sequence (Honda *et al.*, 1996b; Reynolds *et al.*, 1996). The HCV IRES allows cap-independent translation initiation of the viral ORF (Tsukiyama-Kohara *et al.*, 1992; Wang *et al.*, 1993) and is capable of binding directly to the 40S ribosome subunit in the absence of any protein translation initiation factor (Pestova *et al.*, 1998). Domains II and III directly contact and position 40S ribosomal subunit at the AUG codon for core protein and thus these domains are essential for genome translation (Honda *et al.*, 1996a; Honda *et al.*, 1996b). Domain IV is not required for ribosome binding, although the structural stability of this region is inversely proportional to translation efficiency (Honda *et al.*, 1996a). In addition to its importance in translation, the 5' UTR is also essential for genome replication. Domains I and II are sufficient for viral RNA synthesis, although the efficiency of this process is enhanced by the presence of the complete 5' UTR (Friebe *et al.*, 2001; Kim *et al.*, 2002).

A number of host factors are known to associate with the HCV 5' UTR and regulate both replication and translation of the viral genome. These include, polypyrimidine tract binding protein (PTB) (Ali & Siddiqui, 1995), La autoantigen (Ali & Siddiqui, 1997) and poly (rC)-binding protein (Fukushi *et al.*, 2001). Each of these factors influences viral RNA replication, while PTB and La autoantigen are also required for translation (Domitrovich *et al.*, 2005; Fukushi *et al.*, 2001). Another cellular protein known to bind the 5' UTR is heterogenous nuclear protein L (Hahm *et al.*, 1998), although the function of this interaction remains to be determined. A recent study discovered that the liver-specific microRNA-122 (miR-122) base pairs at two locations within the unstructured region between domains I and II of the 5' UTR sequence. This binding is essential for both viral

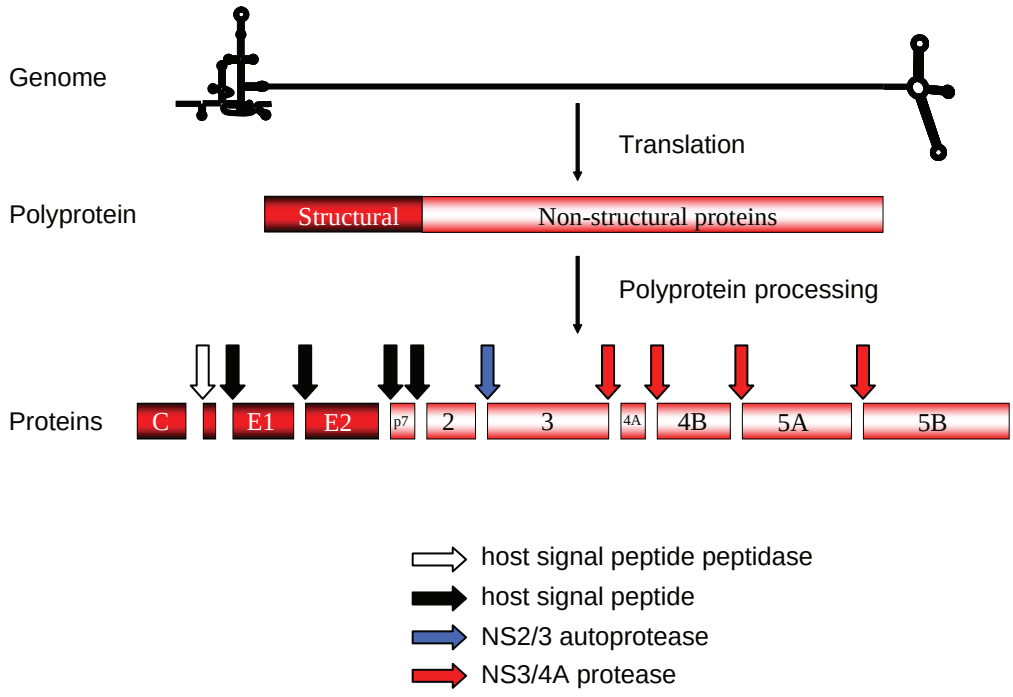

Figure 1.5. General features of the HCV genome and polyprotein processing.

5' and 3' UTRs flank the HCV ORF, which generates a single polyprotein with structural proteins (nucleocapsid protein or core, envelope glycoproteins E1 and E2, and probably p7) grouped at the N-terminus followed by the nonstructural proteins (NS2-5B). The polyprotein is cleaved into the 10 individual HCV proteins by both host and viral proteases through complex co- and posttranslational events. Adapted from Tellinghuisen *et al.* (2007) .

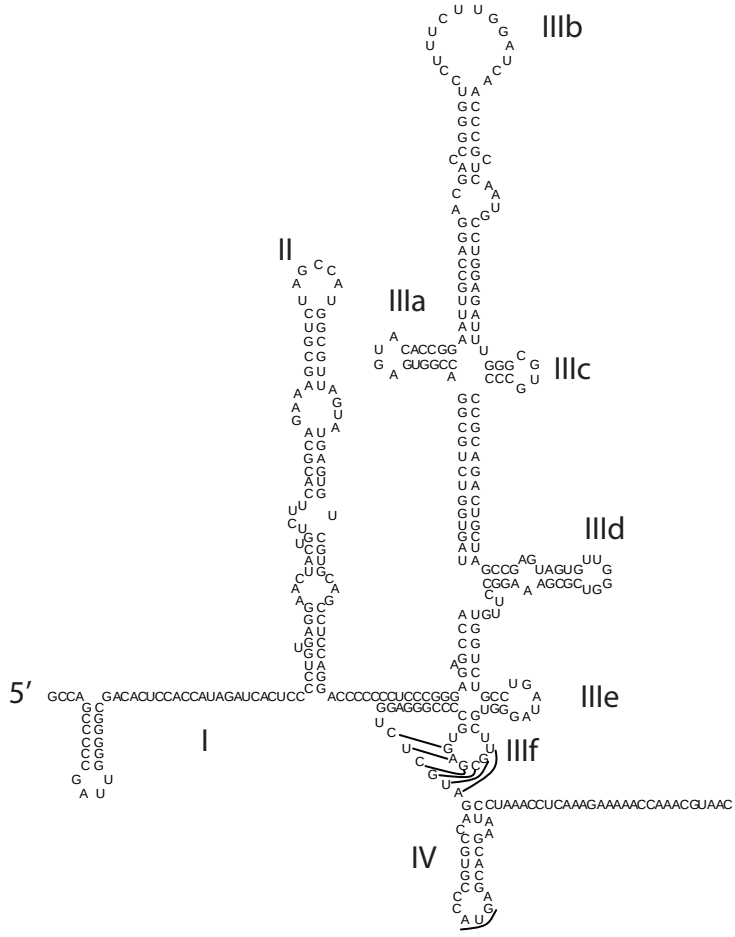

Figure 1.6. Proposed secondary and tertiary structure of the HCV 5' UTR, together with a small portion of the core-coding sequence, from genotype 1b infectious clone (HCV-N).

Major structural domains (I through IV) and subdomains (IIIa through IIIf) are indicated with Roman numerals and the initiator AUG codon within stem-loop IV is underlined. Adapted from Honda *et al*. (1999).

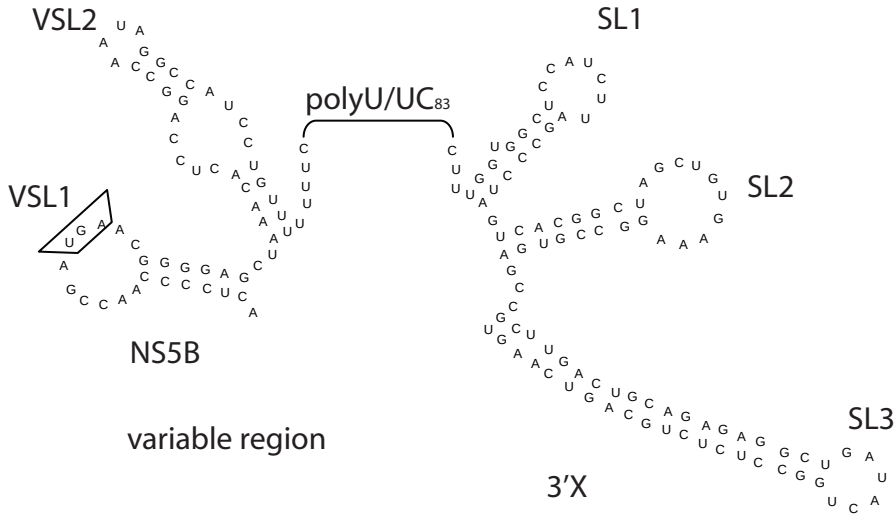

Figure 1.7. Predicted secondary structure of the HCV 3' UTR from the genotype 1b Con1 isolate.

The positions of the two stem-loops (VSL1 and VSL2) in the variable region, the 83 nucleotide poly (U/UC) tract, and the three stem-loops (SL, SL2 and SL3) in the 3'X-tail are indicated. The stop codon of the polyprotein ORF is boxed. Adapted from Friebe & Bartenschlager (2002).

RNA replication (Jopling *et al.*, 2008; Jopling *et al.*, 2005) and translation (Henke *et al.*, 2008).

The HCV 3' UTR has a tripartite structure comprising a variable region which is poorly conserved between genotypes, a poly (U/UC) tract and a highly conserved, 98 nucleotide sequence known as the 3' X tail (Kolykhalov *et al.*, 1996). Biochemical and structural studies have confirmed two stem loops in the variable region (VSL1 and VSL2) and three stem loops in the 3' X-tail (SL1, SL2 and SL3) (Fig. 1.7) (Blight & Rice, 1997; Tanaka *et al.*, 1996). VSL1 and VSL2 are dispensable for RNA replication in cell culture (Friebe & Bartenschlager, 2002) and for HCV infectivity in chimpanzees (Yanagi *et al.*, 1999). The poly (U/UC) region is variable in length and composition, consisting of uridine residues that are interspersed with occasional cytidine residues. This segment must be at least 26 nucleotides in length to permit viral RNA replication (Friebe & Bartenschlager, 2002). Deletion of any one of the 3' X-tail stem-loops prevents replication in cell culture (Friebe & Bartenschlager, 2002; Yi & Lemon, 2003) as well as infectivity in chimpanzees (Yanagi *et al.*, 1999) Aside from roles in replication, the 3' UTR also stimulates IRES-mediated translation of viral RNA. This stimulation was stronger in hepatoma cell lines (Huh-7 and HepG2) compared to non-hepatoma lines (BHK and HeLa) (Song *et al.*, 2006). It has been proposed that the 3' UTR enhances IRES-dependent translation by increasing the efficiency of termination (Bradrick *et al.*, 2006). Several of the cellular proteins shown to interact with the 5' UTR also bind to the 3' UTR including PTB and La autoantigen (Ito *et al.*, 1998; Spangberg *et al.*, 1999; Wood *et al.*, 2001), although the functional significance of these interactions have yet to be determined.

1.8.2. HCV-Encoded Proteins

1.8.2.1. Core Protein

The properties of core protein are discussed in detail in section 1.11.

1.8.2.2. E1 AND E2

The viral envelope glycoproteins E1 and E2 are located on the surface of the virion and mediate particle interaction with cellular receptors. Both proteins are critical for virus entry

into host cells (Bartosch *et al.*, 2003a) as well as the assembly of infectious virus particles (Wakita *et al.*, 2005). Following genome translation, E1 and E2 are liberated from the viral polyprotein following proteolytic cleavage by host cell signal peptidases (Fig. 1.5) (Miyamura & Matsuura, 1993). Both proteins are classed as type I transmembrane proteins having an N-terminal ectodomain translocated into the endoplasmic reticulum (ER) lumen, and a C-terminal hydrophobic anchor inserted into the ER membrane (Op De Beeck *et al.*, 2001). E1 and E2 associate with each other as a noncovalent heterodimeric complex and it is believed that the correct conformational folding of either protein is dependent on the expression of the other (Deleersnyder *et al.*, 1997; Michalak *et al.*, 1997). E1 and E2 undergo asparagine (N) – linked glycosylation with each protein possessing 6 and 11 potential sites, respectively (Lavie *et al.*, 2007). It is believed that these glycans function in protein folding, receptor interactions and sensitivity to neutralising antibodies (Goffard *et al.*, 2005; Helle *et al.*, 2007; Lavie *et al.*, 2007; Lozach *et al.*, 2003).

1.8.2.3. p7

The tenth HCV-encoded cleavage product to be identified was the p7 polypeptide, which is located at the junction between the structural and nonstructural proteins of the HCV polyprotein (Lin *et al.*, 1994a). Whether p7 corresponds to a structural or non-structural protein remains to be determined. Cleavage of p7 from the polyprotein is mediated by a host signal peptidase, which, due to the presence of an E2-p7-NS2 precursor and stable E2-p7 form, is likely to occur post-translationally (Lin *et al.*, 1994a). p7 is a polytopic membrane protein harbouring two transmembrane domains (TMDs) connected by a cytoplasmic loop with both its N- and C termini orientated towards the ER lumen (Carrere-Kremer *et al.*, 2002). In studies using recombinant expression plasmids, p7 has been found localised to ER (Carrere-Kremer *et al.*, 2002; Isherwood & Patel, 2005) and mitochondrial membranes (Griffin *et al.*, 2005), with a small fraction also being detected at the plasma membrane (Carrere-Kremer *et al.*, 2002). However, a more recent report suggests that HA-tagged p7, expressed from the full-length HCVcc infectious RNA, localises solely to the ER (Haqshenas *et al.*, 2007). Interestingly, the p7 polypeptide has been shown to exhibit ion channel activity in artificial membranes (Griffin *et al.*, 2003; Pavlovic *et al.*, 2003). In accordance with these data, p7 has been shown to oligomerize *in vitro* and form hexameric structures indicative of ion channels (Griffin *et al.*, 2003; Luik *et al.*, 2009). Also, this p7 function can be inhibited by amantadine, a compound that inhibits the influenza A-encoded M2 ion channel activity (Griffin et al., 2003). p7 is not required for RNA replication

(Lohmann *et al.*, 1999), but injection of viral RNAs harbouring p7 deletions into chimpanzees has shown that the protein is essential for HCV infectivity *in vivo* (Sakai *et al.*, 2003). Using the HCVcc system, it has been demonstrated that deletion of p7 eliminates infectious virus production and furthermore, that this block occurs prior to the assembly of HCV virions (Jones *et al.*, 2007; Steinmann *et al.*, 2007a). In line with this, compensatory and adaptive mutations in p7 have been shown to enhance virus production (Kaul *et al.*, 2007; Murray *et al.*, 2007; Russell *et al.*, 2008; Yi *et al.*, 2007). Interestingly, two recent studies have shown that several inhibitory compounds known to interfere with the p7 ion channel activity *in vitro* also repress the release of infectious virus particles in the HCVcc system (Griffin *et al.*, 2008; Steinmann *et al.*, 2007b). Strikingly, Griffin *et al.* (2008) found moderate effects of these inhibitors on virus entry, suggesting p7 may be a component of the virion. Together, these data suggest that the ion channel activity of p7 is critical for its role in HCV propagation, highlighting this protein as an attractive target for antiviral therapies.

1.8.2.4. NS2

NS2 functions in the proteolytic cleavage of the NS2/NS3 junction (Fig. 1.5). The catalytic activity of this protease requires the C-terminal half of NS2 and the N-terminal one-third of NS3 (Grakoui *et al.*, 1993b; Hijikata *et al.*, 1993a). This NS2/NS3 enzyme has been described as a cysteine proteinase (Pallaoro *et al.*, 2001). The crystal structure of the NS2 C-terminal region reveals a dimeric cysteine protease with two composite active sites. For each active site, the catalytic histidine and glutamate residues are contributed by one monomer, and the nucleophilic cysteine by the other (Lorenz *et al.*, 2006). NS2 associates with ER membranes and is predicted to be a polytopic membrane protein with possibly 4 TMDs (Santolini *et al.*, 1995; Yamaga & Ou, 2002). It was recently shown that residues 3-23 of NS2 form an interrupted α-helix that is likely to serve as the first TMD (Jirasko *et al.*, 2008). NS2 is the only NS protein that is not required for RNA replication (Jones *et al.*, 2007; Lohmann *et al.*, 1999). Although, full-length NS2 has been shown to be important for the assembly of infectious particles in HCVcc, this effect is independent of the proteins proteolytic function (Jirasko *et al.*, 2008; Jones *et al.*, 2007). Interestingly, the crossover sites for generating infectious inter/intragenotypic chimeric HCVcc genomes containing the NS3-NS5B region from strain JFH1 and the structural genes from other genotypes have been mapped to the NS2 junction (Gottwein *et al.*, 2009; Lindenbach *et al.*, 2005; Pietschmann *et al.*, 2006). Numerous studies have also identified adaptive mutations in

NS2 that enhance HCVcc virus production (Gottwein *et al.*, 2009; Russell *et al.*, 2008; Yi *et al.*, 2007), further supporting the role of this protein in the virus assembly pathway. Interactions between NS3, NS4A and a p7-E1-E2 complex have been reported for NS2 (Flajolet *et al.*, 2000; Kiiver *et al.*, 2006; Selby *et al.*, 1994; Steinmann *et al.*, 2007a). In line with this, a recent HCVcc study identified compensatory mutations in E1, E2, NS3 and NS4A that could suppress the virus assembly defects caused by several engineered mutations within conserved NS2 residues (Phan *et al.*, 2009). Thus, NS2 likely contributes to virus assembly in concert with other structural and non structural proteins.

1.8.2.5. NS3 and NS4A

NS3 is a multifunctional protein, containing a serine protease within its N-terminal third (Bartenschlager *et al.*, 1993; Grakoui *et al.*, 1993a; Hijikata *et al.*, 1993a; Tomei *et al.*, 1993) and an NTPase/helicase within its C-terminal two-thirds (Kim *et al.*, 1995; Suzich *et al.*, 1993). The NS4A polypeptide functions as a co-factor for both these enzymatic activities. The NS3 serine protease domain facilitates 4 cleavage events, acting in cis to liberate itself from the HCV polyprotein (Section 1.8.2.4) and in trans to produce the N-termini of NS4B, NS5A and NS5B (Bartenschlager *et al.*, 1993; Grakoui *et al.*, 1993a; Lin *et al.*, 1994b; Tomei *et al.*, 1993) (Fig. 1.5). The C-terminal domain of NS4A is required for efficient cleavage of the downstream polyprotein, especially at the NS4B/5A cleavage site (Bartenschlager *et al.*, 1994; Failla *et al.*, 1994). The C-terminal two-thirds of NS3 encodes a DExH-box RNA helicase whose RNA unwinding activity requires an NS3 dimer (Serebrov & Pyle, 2004; Tai *et al.*, 1996). For efficient RNA helicase activity, NS3 requires both its protease domain and its NS4A cofactor (Beran *et al.*, 2009; Frick *et al.*, 2004; Pang *et al.*, 2002). The crystal structure of the NS3 helicase shows a Y-shaped molecule composed of 3 subdomains (Kim *et al.*, 1998; Yao *et al.*, 1997). While this structure provides important insights into the mechanisms behind its nucleotide unwinding activities, the exact function(s) of this RNA helicase in the virus lifecycle remains unknown. NS3 has no TMD but is targeted to ER through its non-covalent association with the central domain of NS4A (Wolk *et al.*, 2000). NS3 is essential for viral RNA replication (Lohmann *et al.*, 1999), and depends on both the RNA binding and helicase activity of the protein (Beran *et al.*, 2009). In accordance with these findings, cell culture adaptive mutations have been identified in the protease and helicase regions of NS3, which enhance the RNA replication of subgenomic replicons (SGRs) (Lohmann *et al.*, 2003) (Section 1.9.2). More recently, studies using HCVcc have identified compensatory

mutations in NS3 that rescue the assembly of infectious virus from defective mutant and chimeric genomes (Ma *et al.*, 2008; Phan *et al.*, 2009; Yi *et al.*, 2007). Together, these data indicate NS3 is an important viral protein for RNA replication and infectious particle assembly. In addition to its requirement in NS3 enzymatic activity and membrane targeting, NS4A influences NS5A phosphorylation and HCV RNA replication through its acidic C-terminal region (Lindenbach *et al*., 2007).

1.8.2.6. NS4B

NS4B localises to the ER independent of the other HCV proteins and is believed to have at least 4 TMDs between aa 75-191 that bind the protein tightly to ER membranes (Hugle *et al.*, 2001; Lundin *et al.*, 2003). Upstream of these TMDs, the N-terminal segment is predicted to contain an amphipathic α-helix (Elazar *et al.*, 2004) and a fifth TMD (Lundin *et al.*, 2003). One likely function of NS4B is to induce ER membrane alterations required for the formation of viral RNA replication complexes. These structures induced by NS4B expression are referred to as the membranous web (Egger *et al.*, 2002; Gosert *et al.*, 2003) or membrane-associated foci (MAF) (Gretton *et al.*, 2005). Other NS proteins have been shown to localise to these structures, including NS3, NS4A, NS5A and NS5B (Elazar *et al.*, 2004; Hugle *et al.*, 2001). Importantly, disrupting the ability of NS4B to bind to ER membranes leads to a loss of proteins at these foci in addition to abolishing replication of the viral genome (Elazar *et al.*, 2004). Thus, these NS4B-induced membrane alterations are likely to create an environment suitable for viral RNA replication. Cell culture adaptive mutations within NS4B that significantly enhance the RNA replication levels of SGRs have been reported (Lohmann *et al.*, 2003). Also, recent studies that performed detailed mutagenesis of NS4B revealed specific aa changes with the ability to enhance as well as abolish RNA replication of SGRs (Jones *et al.*, 2009; Lindstrom *et al.*, 2006). In HCVcc, NS4B mutations were identified that could influence the level of infectious virus release (Jones *et al.*, 2009). Together, these data indicate NS4B functions in the formation of replication complexes, RNA replication and infectious particle release.

1.8.2.7. NS5A

NS5A is composed of 3 domains that are separated by low complexity sequences (LCS I and LCS II) (Tellinghuisen *et al.*, 2004). Preceding domain I is an N-terminal amphipathic

α-helix that anchors the protein to ER membranes and disruption of this structure leads to a loss in membrane binding and viral RNA replication in SGRs (Brass *et al.*, 2002; Elazar *et al.*, 2003). Domain I is the most conserved NS5A domain and is capable of binding a single zinc atom per molecule, which is required for SGR RNA replication (Tellinghuisen *et al.*, 2004). The crystal structure of domain I reveals that it may dimerise to form a basic groove that could accommodate a single-strand RNA molecule (Tellinghuisen *et al.*, 2005). In line with this, NS5A has been shown to bind to the 3' ends of both positive- and negative-strand HCV RNA (Huang *et al.*, 2005). Replication enhancing mutations have also been identified in domain I using SGRs, highlighting the important role of this domain in RNA replication (Blight *et al.*, 2000; Lohmann *et al.*, 2003). Domains II and III are poorly characterised compared to domain I. Recent studies have suggested that domain II is flexible and disordered in nature (Liang *et al.*, 2006), while domain III is mostly unstructured (Hanoulle *et al.*, 2009). Deletion analyses have shown that large portions of domain II and the entire domain III are dispensable for SGR and HCVcc RNA replication (Appel *et al.*, 2008; Tellinghuisen *et al.*, 2008b). While, a nearly complete deletion of domain II had little effect on HCVcc virus production, large domain III deletions significantly impaired virus infectivity (Appel *et al.*, 2008; Hughes *et al.*, 2009; Masaki *et al.*, 2008). It has recently been reported that core and NS5A associate with LDs, an event that is crucial for virus assembly in HCVcc (Section 1.10.3). Moreover, mutations within domain I of NS5A prevent its association with LDs, severely impairing virus production as a result (Miyanari *et al*., 2007). Interestingly, Appel *et al*. (2008) found that the deletions in domain III that impaired virus production did not prevent NS5A-LD attachment but instead abolished its association with core protein on LDs.

NS5A is a phosphoprotein that exists in hypophosphorylated and hyperphosphorylated forms (Tanji *et al*., 1995). It is not known which of the numerous potential phosphorylation sites in NS5A are relevant to these forms. However, accumulating evidence suggests that hypophosphorylation primarily targets residues in domains II and III, whereas the hyperphosphorylation sites cluster in and around domain I (Huang *et al.*, 2007b). A recent study showed that mutation of two separate clusters (CLA and CLB) of domain III serine residues impaired the hypophosphorylation of NS5A. While the RNA replication of both mutants was unaltered, CLB had severely impaired virus production of HCVcc while CLA was unaffected (Masaki *et al.*, 2008). The effect of CLB was later found to be caused by these mutations disrupting a direct interaction of NS5A with core protein, resulting in a loss of NS5A-LD association. One study found that reducing NS5A hyperphosphorylation by mutating serine clusters around domain I resulted in enhanced SGR RNA synthesis

(Appel *et al*., 2005). More recently, a single serine residue in domain III was identified that impaired NS5A hyperphosphorylation, had no effect on HCVcc RNA replication but almost completely abolished virus production (Tellinghuisen *et al*., 2008a). Overall, these data suggest NS5A is a key mediator of viral RNA replication and virus production through distinct mechanisms.

1.8.2.8. NS5B

NS5B is the HCV RNA-dependent RNA polymerase (RdRp) that synthesises the positive and negative-strand viral RNAs during RNA replication. NS5B can initiate RNA synthesis *de novo*, a mechanism that is likely to operate *in vivo* (Luo *et al.*, 2000; Oh *et al.*, 1999; Zhong *et al.*, 2000). NS5B is capable of copying HCV genomes in the absence of other viral or cellular factors (Behrens *et al.*, 1996; Lohmann *et al.*, 1997). However, in cell culture an interaction between NS5A and NS5B is critical for the RNA replication of SGRs (Shimakami *et al.*, 2004). NS5B associates to the ER membrane via a C-terminal TMD, which is critical for SGR RNA replication (Ivashkina *et al.*, 2002; Moradpour *et al.*, 2004). NS5B contains motifs common to all RdRps, including the GDD sequence that represents the hallmark signature of most polymerases (Bartenschlager *et al.*, 2004). The crystal structure of NS5B has been determined by several groups (Ago *et al.*, 1999; Biswal *et al.*, 2005; Bressanelli *et al.*, 1999; Lesburg *et al.*, 1999; Simister *et al.*, 2009). As with other nucleic acid synthesising enzymes, it was found to be a typical right-hand polymerase with a central palm domain harbouring the catalytic GDD motif and the fingers and thumb domains on either side creating a channel for binding the RNA template. Extensive interactions between the fingers and thumb domains result in a completely enclosed active site, a feature shared with other RdRps. A recent study reported the RdRp from the JFH1 strain exhibited a far greater capacity to initiate RNA synthesis *de novo* than the closely related J6 strain RdRp. The crystal structure of JFH1 NS5B revealed a more closed conformation than a genotype 2a consensus structure and previously reported HCV polymerase structures. This closed conformation is more suited for single-stranded RNA binding, which may promote more efficient *de novo* initiation (Simister *et al.*, 2009). These observations may in part explain the outstanding replication efficiency of SGRs and full-length genomes harbouring the JFH1 replicase compared to those tested from other isolates.

1.9. Systems to Study HCV Replication

1.9.1. Animal Models

Until very recently, the restrictive host range of HCV limited animal studies to chimpanzees. Indeed, the chimpanzee model was first used to characterise the physicochemical properties of the NANBH agent, prior to the cloning of HCV from plasma collected from a persistently infected chimpanzee in 1989 (Section 1.1). However, it was not until 1997 that the first functional full-length HCV molecular clones were established. Two genomes constructed from a genotype 1a isolate (strain H77) could establish productive infection in chimpanzees after intrahepatic inoculation with *in vitro* transcripts (Kolykhalov *et al.*, 1997; Yanagi *et al.*, 1997). Other infectious clones have since been reported in chimpanzees (Bartenschlager & Sparacio, 2007). The chimpanzee is an ideal model for HCV infection given their genetic similarity to humans (98.5 %) and their disease progression following a clinical course similar to that seen in human patients. Despite the invaluable contributions this model has made to HCV research, due to limited availability, expense and the ethical issues which arise from their use, chimpanzees have not been utilised for anti-HCV drug discovery. This knowledge will best be attained through a widely available and easily accessible animal model for HCV (Grakoui *et al.*, 2001). Rodents are regarded the most suitable for all biological studies given their short gestation period, small size and low cost. Although, rodents are naturally non-receptive to HCV infection, if maintained in an immunosuppressed state, they can undergo successful transplantation with human hepatocytes allowing viremia to develop. The most successful HCV rodent model has been the Alb-uPA transgenic mouse developed in mice with severe combined immunodeficiency (SCID). These mice contain an additional copy of the urokinase-type plasminogen activator (uPA) expressed from an albumin (Alb) promoter. The Alb-uPA transgene overexpression is hepatotoxic and results in homozygous mice with severe liver damage (Heckel *et al.*, 1990). This defect, in combination with severe immunodeficiency allows the mice livers to be repopulated with non-transgenic human hepatocytes that are susceptible to HCV infection (Mercer *et al.*, 2001). Inoculation of mice with virus obtained from HCVcc or the sera from HCV positive patients leads to a rapid increase in viremia that is sustained over several weeks (Lindenbach *et al.*, 2006; Mercer *et al.*, 2001; Meuleman *et al.*, 2008; Vassilaki *et al.*, 2008). This model has

demonstrated *in vivo* infection can be prevented by inhibitory antibodies targeting the viral glycoproteins (Law *et al.*, 2008; Vanwolleghem *et al.*, 2008) and the HCV cellular receptor CD81 (Meuleman *et al.*, 2008). Such chimeric mice have also been used for the study of pharmacokinetics and drug toxicity (Katoh *et al.*, 2008; Vanwolleghem *et al.*, 2007). Thus, these xenotransplanted humanized mice hold great potential as a means of assessing drug efficacy. The uPA mouse model, however, has certain limitations that include excessive mortality, low breeding efficiency, transgene reversion, and overall colony management (Meuleman & Leroux-Roels, 2008). Robust HCV propagation has recently been described in a new triple knockout transgenic mouse model (the $Fah^{-/-}Rag2^{-/-}Il2rg^{-/-}$ mouse) that solves many of the problems described for the uPA-SCID mouse (Bissig *et al*., 2010). Suitable immunodeficiency is created by crossing $Fah^{-/-}$ mice with both the $Rag2^{-/-}$ mice, which are depleted of mature B and T lymphocytes and $Il2rg^{-/-}$ mice, which have impaired B, T and NK cell development (Bissig *et al.*, 2007). The absence of the enzyme fumaryl acetoacetate hydrolase (FAH) from these mice leads to an accumulation of toxic tyrosine catabolites within mouse hepatocytes. The selection pressure for transplanted human hepatocytes can be regulated by the drug, 2-(2-nitro-4-trifluoro-methylbenzoyl)-1,3-cyclohexanedione (NTBC), which prevents the toxicity caused by the lack of FAH, while human hepatocytes stay healthy due to the human homolog. This growth disadvantage for mouse hepatocytes and positive selection for transplanted human hepatocytes allows the human cells to expand and repopulate up to 95 % of the murine liver. The advantage of this regulatable system is that animals with low human chimerism can be put back on the drug NTBC and hence do not undergo liver failure and eventually death. Highly repopulated triple knockout mice could be stably infected with different HCV strains including a genotype 1a clinical isolate, HCVcc genotype 2a and HCVcc genotype 1b/2a and 1a/2a chimeras. Viral infection could be sustained for more than 6 months and be passaged from one chimeric mouse to another. Importantly, the mice were suitable for antiviral drug screening (Bissig *et al*., 2010). Pathogenesis and immunity studies are limited in chimeric mice, as the animals lack a functional immune system to avoid the rejection of the xenograft. Transgenic mice carrying HCV proteins have been used in a vast number of studies to investigate the pathogenic properties of these proteins on the host. Despite some contradictory results, transgenic mice have provided a wealth of information on the effects of HCV and specific viral proteins on lipid metabolism, HCC and the immune response (Kremsdorf & Brezillon, 2007).

1.9.2. In Vitro Systems to Study HCV

In terms of studying HCV in cell culture, three major systems were developed between 1999 and 2005 that have proved invaluable in the study of the HCV life cycle. These are replicons, retrovirus-based HCV pseudoparticles (HCVpp), and HCVcc (Fig. 1.8).

1.9.2.1. Replicons

Despite the development of HCV molecular clones that could infect chimpanzees, efficient and reproducible replication of these clones could not be achieved in cell culture for reasons unknown. The first major breakthrough for analysing HCV RNA replication in cell culture came in 1999 with the development of the SGR (Lohmann *et al.*, 1999). The first SGR was a bicistronic construct, derived from a genotype 1b strain, Con1. The first cistron encoded the neomycin phosphotransferase (*neo*) gene and was translated under the control of the HCV IRES. The second cistron encoded the NS3-5B HCV region and was translated under the control of the EMCV IRES. Following electroporation of these *in vitro* transcribed RNAs into Huh-7 cells, and subsequent G418 selection, a small number of resistant colonies supporting autonomously replicating HCV RNAs could be generated. While this system was a major advancement in the propagation of HCV genomes in cell culture, the replication of these RNA species was relatively inefficient as only small populations of resistant cell clones could be obtained. Subsequent studies identified two main reasons responsible for the amplification of genomes within certain cell populations: cell culture adaptive mutations and host cell permissiveness. Cell culture adaptive mutations were found in each of the HCV NS proteins although they tended to cluster in NS5A. Upon insertion into the parental replicon several of these adaptive mutations were shown to increase RNA replication levels to various extents (Blight *et al.*, 2000; Krieger *et al.*, 2001; Lohmann *et al.*, 2001). In addition to cell culture adaptive mutations, the efficiency of replicon RNA replication is also determined by the selection of particular cells that are highly permissive. This comes from the observation that removal of the replicon from a cell clone by IFN treatment often results in cell clones that sustain greater levels of RNA replication compared to naïve Huh-7 cells. The exact reason for the higher permissiveness is largely unknown, but for one particular cell clone, designated Huh-7.5 (Blight *et al.*, 2002), a defective IFN response caused by a mutation in the RIG-I gene was

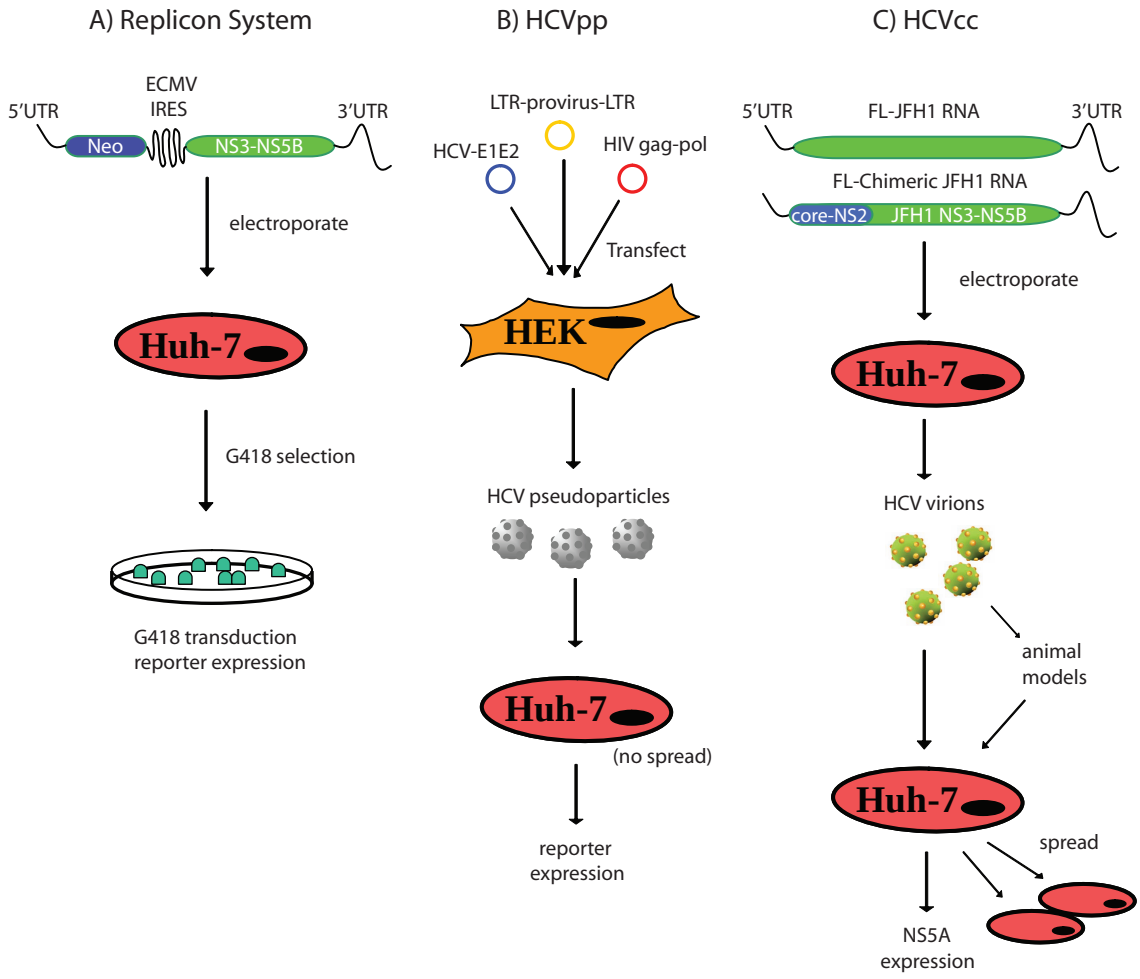

Figure 1.8. *In vitro* systems for the study of HCV replication, entry, and infectivity.

(A) HCV SGRs, allow for the study of viral RNA replication in cell culture. Bicistronic replicon RNAs, encoding a selectable marker, under control of the HCV IRES in the first cistron and the HCV non-structural NS3-NS5B proteins under the control of the encephalomyocarditis virus (EMCV) IRES in the second cistron, are electroporated into Huh-7 cells and derived sub-lines. RNA replication results in the expression of the selectable marker and allows for selection of cell colonies that support viral RNA replication. (B) HCVpp allows for the study of HCV entry. Recombinant retrovirus particles that contain HCV envelope glycoproteins on their surface are produced in HEK-293T cells by co-transfecting plasmids encoding the HCV glycoproteins, retroviral or lentiviral core and polymerase proteins and a proviral genome harbouring a reporter gene. Following infection of permissive cell lines, the retrovirus genomes express a reporter gene, such as luciferase, allowing for a quantitative measure of cell entry. (C) HCVcc allows for the study of the entire HCV lifecycle. This system uses either JFH1 HCV genomic RNA or chimeric versions of this genome. Electroporation of these RNAs into permissive cell lines allows for viral RNA replication and the production of infectious particles that can infect naïve cells. Productive infection can be monitored by several methods allowing the detection of intracellular viral RNA or protein levels. Adapted from Tellinghuisen *et al*. (2007).

shown to be involved (Sumpter *et al.*, 2005). The advancements in the understanding of the SGR system led to the development of autonomously replicating full-length genomic replicons harbouring the entire HCV ORF (Blight *et al.*, 2003; Ikeda *et al.*, 2002; Pietschmann *et al.*, 2002). However, none of these genomes supported the production of infectious virus particles. In 2003, a SGR based on a genotype 2a strain (JFH1) isolated from a patient with fulminant hepatitis was described. In contrast to the other replicon systems, the JFH1 SGR was capable of highly efficient replication (Kato *et al.*, 2003) without the need for cell selection or cell culture adaptive mutations. It was the unique properties of this unusual strain that led to the establishment of the first cell culture infectious system for studying the complete HCV lifecycle.

1.9.2.2. HCVpp

In 2003, several groups reported the production of infectious lentiviral particles bearing HCV E1 and E2 glycoproteins, known as HCVpp (Bartosch *et al.*, 2003a; Drummer *et al.*, 2003; Hsu *et al.*, 2003). These particles were generated by co-transfection of 293T cells with plasmids encoding the HCV glycoproteins, retroviral or lentviral core and polymerase proteins and a packaging competent but replication defective proviral genome harbouring a reporter gene, such as GFP or luciferase. HCVpp have a tropism for human liver cells and are neutralised by anti-HCV glycoprotein antibodies, confirming HCVpp as a valid system for studying HCV entry.

1.9.2.3. HCVcc

Electroporation of *in vitro* transcribed full-length JFH1 RNA into Huh-7 cells resulted in HCV replication and secretion of infectious particles that could spread in culture (Wakita *et al.*, 2005). A slightly later study demonstrated this genome could generate peak virus titers of 10^4 -10^5 infectious units/ml. The productive infection of these virus particles in Huh-7 cells was relatively slow, however, the infection kinetics of JFH1 was found to be improved using the highly permissive Huh-7-derived clonal cell line Huh-7.5.1 cells (Zhong *et al.*, 2005). Huh-7.5.1 cells were developed by curing the Huh-7.5 I/5A-GFP-6 replicon cell line with IFN-γ. The exact reason for these cells improving the virus infection kinetics is currently unknown. At the same time as the full-length JFH1 cell culture infectious clone was described, Charlie Rice and collegues reported an infectious chimeric

clone harbouring the JFH1 NS3-NS5B fused to the core-NS2 region of a different genotype 2a isolate, J6 (Lindenbach *et al.*, 2005). Using Huh-7.5 cells, this chimera could produce similar virus titers to those reported for JFH1 in Huh-7.5.1 cells (Zhong *et al.*, 2005). A later study improved the virus release of this chimera by altering the fusion junction from NS2/NS3 to a breakpoint within NS2 after the first predicted transmembrane segment (Pietschmann *et al.*, 2006). The findings of Lindenbach *et al*. (2005) and Pietschmann *et al.* (2006) were generalized and have since been used to produce viable JFH1 chimeras covering all 6 HCV genotypes (Gottwein *et al.*, 2009). Thus, today there are many derivatives of the HCVcc system with different chimeric viruses and Huh-7-derived cells. The intragenotypic chimera (Jc1) remains the most efficient at virus release, with peak titers 1-2 logs greater than JFH1 after transfection in Huh-7 or Huh-7.5 cells (Griffin *et al.*, 2008; Pietschmann *et al.*, 2006; Shavinskaya *et al.*, 2007).

1.10. The HCV Lifecycle

All evidence to date suggests the HCV lifecycle is entirely cytoplasmic. A hypothetical model of the complete replication lifecycle is schematically represented in Fig. 1.9. The different stages of the replication cycle including HCV entry, genome replication and virus assembly and release are discussed in detail in the following sections.

1.10.1. Virus Attachment and Entry

HCV entry is initiated by the initial binding of virus particles to attachment factors which are believed to be glycosaminoglycans (GAGs) (Barth *et al.*, 2003; Koutsoudakis *et al.*, 2006), low density lipoprotein receptor (LDLR) (Agnello *et al.*, 1999; Chang *et al.*, 2007; Germi *et al.*, 2002; Molina *et al.*, 2007) and C-type lectins such as DC-SIGN and L-SIGN (Cormier *et al.*, 2004a; Lozach *et al.*, 2004; Lozach *et al.*, 2003). Upon attachment at least four receptors are important for particle internalization. These include CD81 (Pileri *et al.*, 1998), scavenger recepotor B-1 (SR-BI) (Scarselli *et al.*, 2002) and the tight junction proteins claudin-1 (CLDN-1) (Evans *et al.*, 2007) and occludin (OCLN) (Benedicto *et al.*, 2009; Liu *et al.*, 2009; Ploss *et al.*, 2009) (Fig. 1.10)

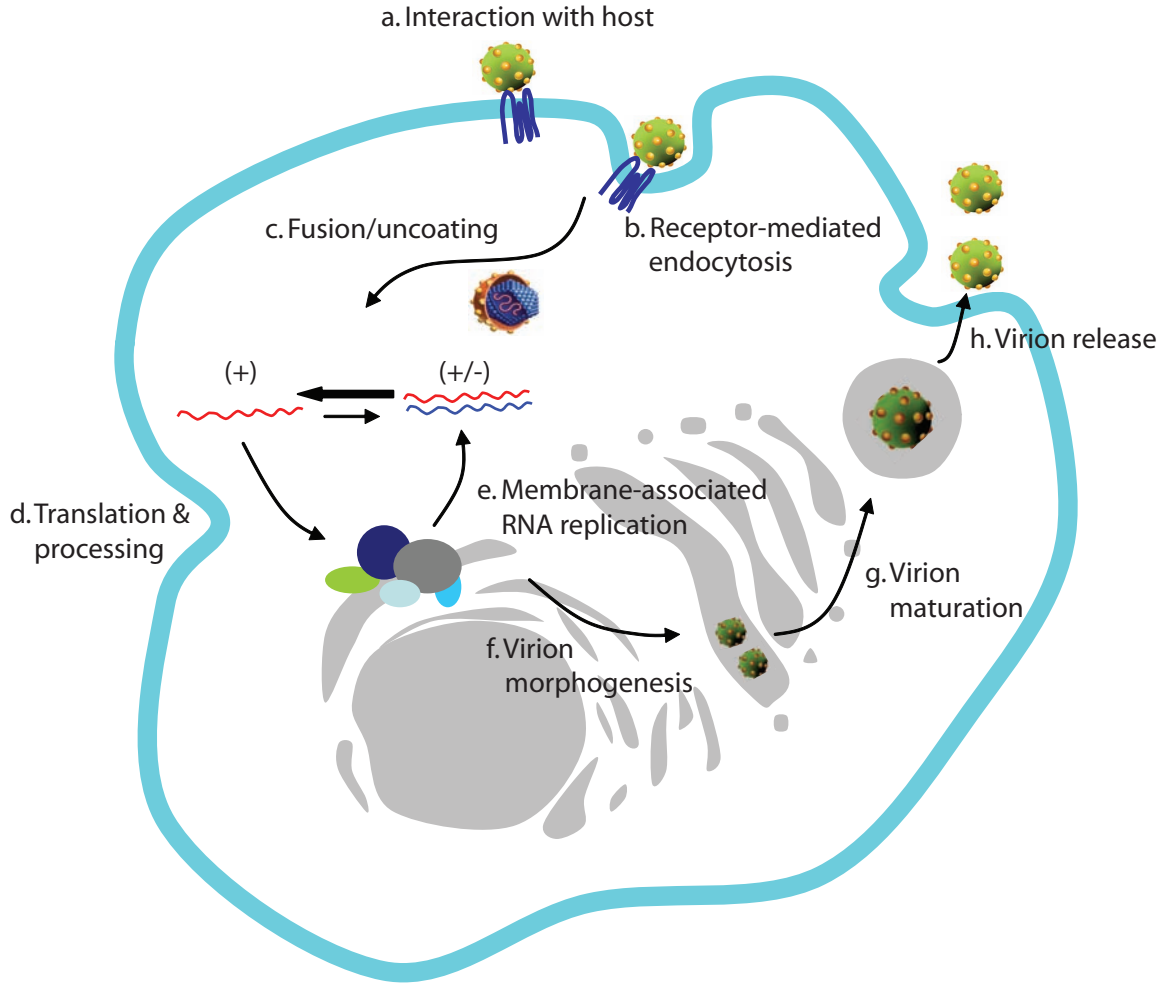

Figure 1.9. Model of the HCV lifecycle.

(a) HCV binding to cell-surface receptor molecules leads to (b) receptor-mediated endocytosis (c) into a low-pH vesicle. Following HCV glycoprotein mediated membrane fusion, the viral genome is liberated into the cytosol. (d) The viral RNA functions as a template for translation of the HCV ORF that is processed into the 10 mature HCV proteins. (e) Viral RNA replication occurs within membrane-associated replication complexes (membranous web). (f) Replication occurs through a positive-strand replicative intermediate to produce progeny RNA, a portion of which is encapsidated. (g) Particles are enveloped by budding into the lumen of the ER where they are thought follow the cellular secretory pathway and, during this transit, maturation of particles occurs. (h) Mature virions are secreted from the cell, completing the life cycle (h). Adapted from Tellinghuisen *et al*. (2007).

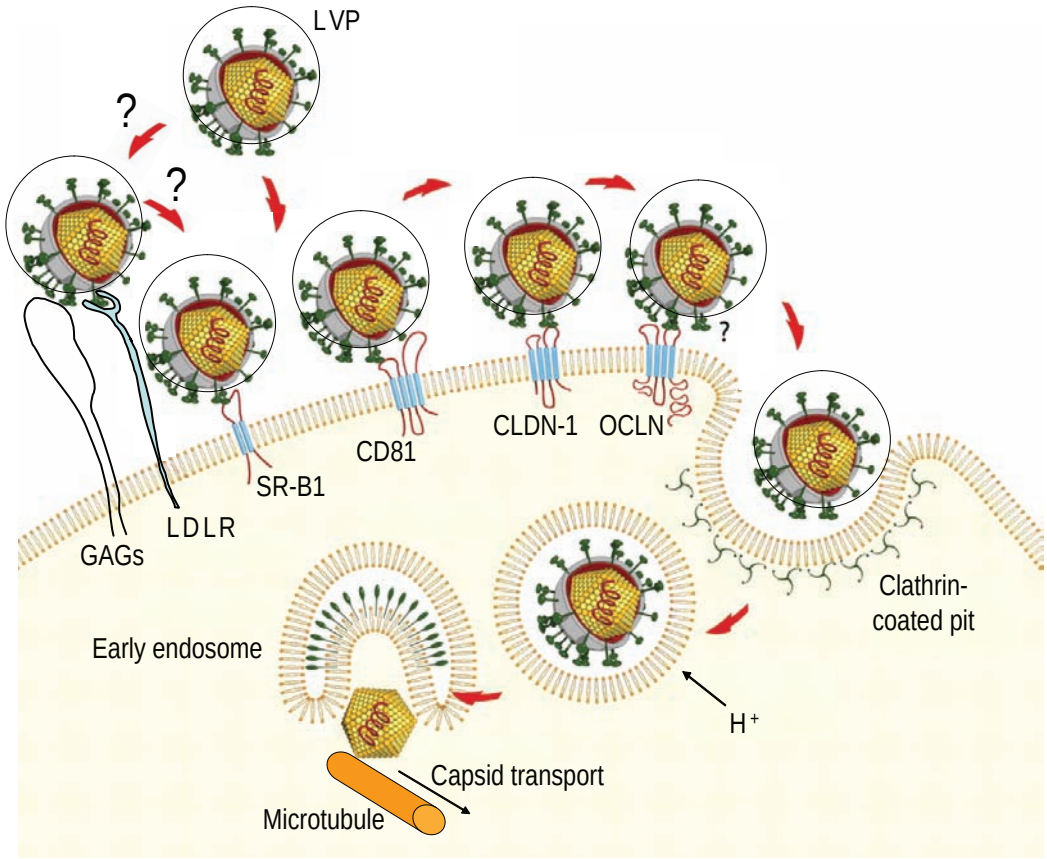

Figure 1.10. Current model for HCV entry.

Initial host-cell attachment may involve GAGs. Through the association of HCV with LDLs and VLDLs, the LDLR may also function at the early entry steps. After cell-surface binding, the virion interacts with four entry factors including SR-B1, CD81 and the two tight junction proteins CLDN-1 and OCLN. Following these interactions, the HCV particle is internalised by clathrin-mediated endocytosis where acidification of the endosome induces HCV glycoprotein-mediated membrane fusion. Once liberated into the cell cytosol, the genome containing nucleocapsid interacts with microtubules, which facilitate its transport to the ER where genome translation and RNA replication take place. Adapted from Burlone & Budkowska (2009).

SR-B1 is expressed in various mammalian tissues with the highest levels found in the liver and adrenal glands. SR-B1 has two TMDs and is a multi-ligand receptor for various classes of lipoproteins including HDL, LDL and VLDL (Acton *et al.*, 1996; Acton *et al.*, 1994). SR-B1 was first identified as a putative receptor based on its ability to bind soluble, truncated E2 (sE2) via HVR1 (Bartosch *et al.*, 2003b; Scarselli *et al.*, 2002). However, sE2 is not representative of E2 structures on the HCV virion (Owsianka *et al.*, 2001) and an interaction between SR-B1 and the E1E2 heterodimers has yet to be confirmed. The lipoproteins associated with the HCV virion have also been proposed to interact with this receptor (Maillard *et al.*, 2006). Despite the uncertainty as to how HCV interacts with SR-B1, the specificity of this receptor to the viral entry process has been confirmed using both the HCVpp (Bartosch *et al.*, 2003b; Voisset *et al.*, 2005) and HCVcc systems (Catanese *et al.*, 2007; Grove *et al.*, 2007; Kapadia *et al.*, 2007). Evidence from recent HCVcc studies has shown SR-B1 to be involved in an early step of the virus/cell recognition prior to the other receptors (Catanese *et al*., 2010; Evans *et al*., 2007).

The first identified and best characterised HCV receptor is CD81, a member of the tetraspanin family of transmembrane proteins. This widely expressed cell surface protein has various functions including tissue differentiation, cell-cell adhesion and immune cell maturation (Levy *et al*., 1998). It consists of a small and a large extracellular loop (LEL) with four TMDs. CD81 was identified as a putative receptor through the binding of its LEL to sE2 (Pileri *et al*., 1998) as well as E1E2 heterodimers (Cocquerel *et al*., 2003). CD81 has been confirmed as an essential HCV entry factor by utilising HCVpp (Bartosch *et al*., 2003a; Cormier *et al*., 2004b; Zhang *et al*., 2004) and HCVcc (Lindenbach *et al*., 2005; Wakita *et al*., 2005; Zhong *et al*., 2005). Inhibition assays with HCVcc using anti-CD81 antibody suggest CD81 acts subsequent to initial virus binding, possible via SR-BI (Catanese *et al*., 2010).

The most recently identified receptors are the tight junction proteins CLDN-1 (Evans *et al*., 2007) and OCLN (Benedicto *et al*., 2009; Liu *et al*., 2009; Ploss *et al*., 2009), which are both required for HCVpp and HCVcc entry. Tight junctions are major components of cell-cell adhesion complexes that maintain cell polarity by forming an intramembrane barrier that regulates the diffusion of certain molecules (Shin *et al*., 2006). Tight junctions possess several important liver functions in hepatocytes, such as bile formation and secretion. CLDN-1 contains two extracellular loops and four TMDs with the first extracellular loop being required for HCVpp entry (Evans *et al*., 2007). Experiments to date have failed to detect an interaction between the viral glycoproteins and CLDN-1 (Evans *et al*., 2007;

Krieger *et al*., 2009). However, several studies have shown an association between CD81 and CLDN-1, implying these two entry factors act in a cooperative manner during HCV entry (Harris *et al*., 2008; Krieger *et al*., 2009). Similar kinetics of inhibition was shown for HCVcc and HCVpp by anti-CLDN-1 and anti-CD81 antibodies. Also, anti-CLDN-1 antibodies that could disrupt this CLDN-1-CD81 association were able to reduce sE2 and HCVcc binding to permissive cells (Krieger *et al*., 2009). Therefore, it is plausible that CLDN-1 may potentiate CD81 association with HCV particles by way of E2 interactions. Two other members of the CLDN family, CLDN-6 and CLDN-9, have also been shown to mediate HCVcc entry (Meertens *et al*., 2008; Zheng *et al*., 2007). OCLN contains four transmembrane regions and two extracellular loops (Furuse *et al*., 1993). A direct interaction has been shown between OCLN and E2 from HCVcc-infected cells, indicating the association of HCV with OCLN during entry is facilitated by this interaction (Liu *et al*., 2009). The expression of SR-BI, CD81, CLDN-1 and OCLN renders murine and hamster cells permissive for HCVpp infection, which strongly suggests these four proteins represent the complete set of cell surface receptors required for HCV entry (Ploss *et al*., 2009).

Following attachment to these specific receptors HCV internalisation likely occurs via clathrin-mediated endocytosis, with delivery of the nucleocapsid via early endosomes. pH sensitivity is a reasonable indicator for viral entry by endocytosis. Indeed HCVpp and HCVcc entry is sensitive to substances that neutralise the acidic pH of early endosomes (Blanchard *et al.*, 2006; Hsu *et al.*, 2003; Koutsoudakis *et al.*, 2006; Meertens *et al.*, 2006). Furthermore, treatment of cells with agents that disrupt clathrin-coated pit formation or the use of siRNA targeting clathrin, reduces HCVpp and HCVcc entry (Blanchard *et al.*, 2006; Meertens *et al.*, 2006). Once internalised, the virus glycoproteins are proposed to fuse with the membranes of early endosomes (Meertens *et al.*, 2006). The acidic pH of endosomes is likely to trigger the fusion process by inducing conformational changes in the envelope proteins (Op De Beeck *et al.*, 2004). A recent study found that HCV entry is also dependent on an intact microtubule (MT) network. Their HCVcc data suggest that following entry and fusion the nucleocapsid integrates itself into the MT lattice, through an interaction between core and tubulin, for transport of the virus capsid in the infected cell (Roohvand *et al.*, 2009). Presumably the capsid is transported to the sites of genome translation at which point the viral RNA would be released.

1.10.2. Genome Translation and RNA Replication

In mammalian cells, the two methods of translation initiation are cap-dependent and cap-independent. The prior represents the standard mode for most cellular mRNAs where translation initiation begins with the recruitment of the 40S ribosomal subunit to the mRNA 5'-terminal m^7GpppN cap structure. The cap-independent method involves the interaction of ribosomes with an IRES, which is utilised by some cellular transcripts as well as some positive-strand RNA viruses including HCV (Shih *et al.*, 2008). Following infection, the HCV genome is liberated into the cytoplasm where it serves as an mRNA for the synthesis of viral proteins. The HCV IRES, located at the 5' end of the genome, binds and directs the ribosome to the initiator codon within the core gene where translation begins (Section 1.8.1). No viral factors are required for the translation of the HCV genome (Pestova *et al.*, 1998). Translation occurs at ER membranes, which produces a single polyprotein that undergoes co- and post-translational cleavage events facilitated by viral and cellular proteases to generate the structural and NS proteins (Figure 1.5). As with all positive-sense RNA viruses, once sufficient translation of HCV RNA has occurred, a molecular switch is believed to direct the initiation of RNA replication within a membrane bound replication complex (Novak & Kirkegaard, 1994).

Indeed, a specific membrane alteration, named the membranous web, was identified as the site of RNA replication in Huh-7 cells containing SGRs. Importantly, these structures have also been recently observed in HCVcc-infected Huh-7 cells (Goueslain *et al.*, 2009). These structures, believed to be derived from ER membranes, contain positive- and negative-strand viral RNA and the HCV NS proteins (Egger *et al.*, 2002; Gosert *et al.*, 2003; Mottola *et al.*, 2002; Quinkert *et al.*, 2005; Waris *et al.*, 2004). These viral RNA and NS proteins are ribonuclease and protease resistant, indicating that these structures may enclose and protect the viral replication components from the intracellular environment (El-Hage & Luo, 2003; Quinkert *et al.*, 2005; Waris *et al.*, 2004). Within these replication compartments, the instigation of HCV RNA synthesis occurs by an unknown mechanism but likely involves the *de novo* initiation of RNA replication by NS5B. Using the positive-strand genome NS5B generates a negative-strand template that is then used to amplify multiple positive-strand RNA molecules (Lohmann *et al.*, 1999; Negro *et al.*, 1992; Takehara *et al.*, 1992). During this process the complementary negative-strand RNA is believed to form a double-stranded RNA molecule with the positive-strand that acts as a

recycling template for the synthesis of nascent positive-stranded RNA (Targett-Adams *et al.*, 2008a). Quantitative analyses of these replication compartments formed by replicons estimate that an active replicase complex consists of one negative-strand RNA, up to ten positive-strand RNAs and several hundred NS proteins (Quinkert *et al.*, 2005). Replicon studies have shown negative-strand RNAs are detectable at 4 hours post-electroporation, implying that these RNA replication compartments form rapidly after virus entry (Binder *et al.*, 2007).

1.10.3. HCV Assembly

Recent HCVcc studies have shown HCV core protein to be a central instigator in the virion assembly process. Core protein is targeted to lipid droplets (LDs) (Section 1.11.2), and disruption of this process in HCVcc prevents infectious virus production (Boulant *et al.*, 2007; Miyanari *et al.*, 2007). Detailed analyses revealed that core protein recruits the HCV NS and envelope proteins as well as the viral replication complexes to these sites. NS5A also aids in the recruitment of the NS proteins and replication complexes to these sites and harbours residues in domain I that target this protein to LDs (Section 1.8.2.7). Indeed, mutating these residues reduced the level of NS5A, NS proteins and viral RNAs to these sites but did not effect the core-LD association. These effects correlated with an impairment in infectious virus release. Thus, the recruitment of the viral replication compartments to these viral assembly sites occurs in a core- and NS5A-dependent manner. EM analyses of infected cells revealed a proportion of LDs were located in close proximity to membrane cisternae (presumably of the ER), an effect not observed in naïve cells. Moreover, virus-like particles were observed (50 nm diameter) in close proximity to these LD-associated membranes that reacted to core- and E2-specific antibodies, arguing that these particles represent true virions and these are indeed the sites of virus assembly (Miyanari *et al.*, 2007).

It is core protein alone that induces the initial redistribution of LDs from their native disperse cytoplasmic localisation to aggregates around the cell nucleus. The trafficking of LDs is dependent on the MT network and in HCV-infected cells LDs aggregate near the microtubule organisation centre (MTOC) near the nucleus. Interestingly, the disruption of MTs resulted in a reduction in LD redistribution and virus titres, implicating these transport networks in virus assembly. Adipocyte Differentiation Related Protein (ADRP), an abundant protein located on the LD surface, is crucial for maintaining the dispersed

distribution of LDs within the cells. Strikingly, the loading of core protein causes ADRP to be displaced from LDs, an effect that results in their redistribution to ER membranes. Thus, it is hypothesised that core on LDs induces their movement on MTs towards the nucleus through the displacement of ADRP (Boulant *et al.*, 2008). This mechanism may coordinate interactions between RNA replication complexes and virus assembly sites resulting in the LD-associated membranes described by Miyanari *et al*. (2007) (Fig. 1.11).

Although, the sites of virus assembly have been well characterised the molecular events of genome encapsidation and envelopement have yet to be determined in the HCVcc system. Nucleocapsid formation most likely involves an interaction of the core protein with the viral genome. Indeed, several studies have reported an interaction between core protein and HCV RNA (Masaki *et al.*, 2008; Santolini *et al.*, 1994). The RNA binding residues in core were mapped to residues 1-75 (Santolini *et al.*, 1994) and a direct interaction of core protein with the 5' UTR of the genome was shown (Tanaka *et al.*, 2000). Given the main function of the viral core protein is to provide a protective shell for the genome, its ability to multimerise would be an indispensable property for nucleocapsid assembly. Different studies have found residues in both domains I (residues 1-118) and II (residues 119-174) (Section 1.11.1) of core to be involved in homotypic interaction (Matsumoto *et al.*, 1996; Nolandt *et al.*, 1997). In agreement with these finding, residues 1-124 was found to assemble into virus-like particles only in the presence of the HCV 5' UTR RNA, whereas the full-length core could undergo *de novo* assembly in the absence of RNA (Kim *et al.*, 2006). These data suggest domain I of core may be involved in multimerisation upon interaction with RNA while domain II initiates spontaneous multimerization of core during the early stages of capsid formation. Subsequent to nucleocapsid formation, the envelopement stage is thought to occur at ER membranes given that the HCV glycoproteins localise predominantly to the ER (Dubuisson *et al.*, 1994). Interestingly, core has been shown to interact with E1, which may function in the envelopment of the nucleocapsid (Lo *et al.*, 1996).

As described in section 1.2, low density HCV particles isolated both *in vivo* and *in vitro* are associated with host VLDLs and are more infectious than high density particles. Hepatocytes play an essential role in maintaining the lipid homeostasis in the body through the assembly and secretion of VLDLs. Interestingly, LDs provide the bulk of the lipid incorporated into VLDLs. Apolipoprotein B (apo B) and E (apo E) are structural components of VLDL and microsomal triglyceride transfer protein (MTP) is required for the transport of triglyceride to the ER for VLDL assembly (Blasiole *et al*., 2007;

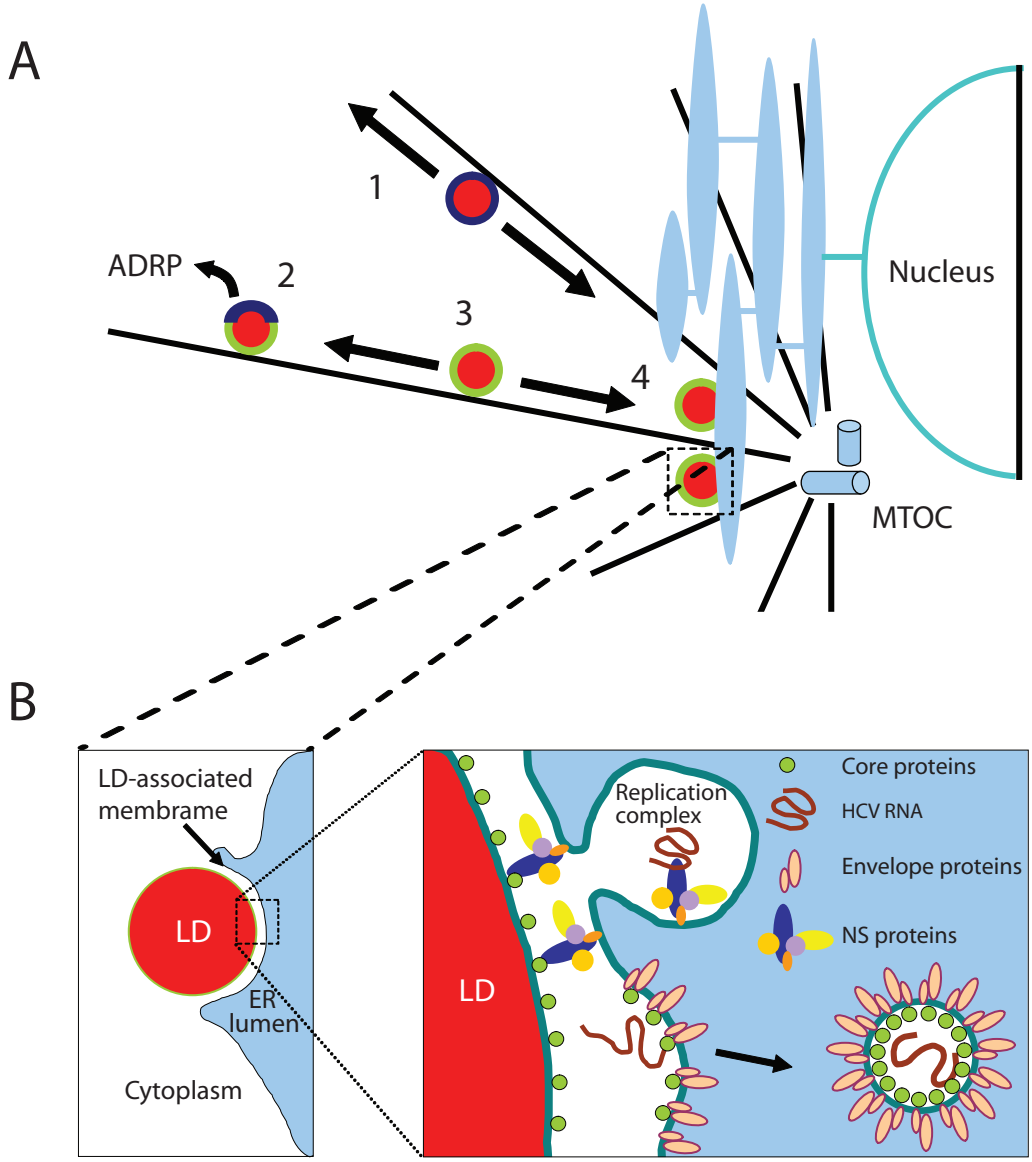

Figure 1.11. The role of the core-LD association in virion assembly.

(A1) ADRP (blue) coated LDs (red) are freely mobile on MT resulting in uniform distribution throughout the cell. (A2) Following infection core protein (green) loads LDs and displaces ADRP (A3) inducing the movement of LDs towards the MTOC and ER membranes. (A4) This redistribution brings LDs in close contact with the HCV RNA replication complexes. (B) LD-associated ER membranes are formed and core recruits the NS proteins, envelope proteins and replication complexes to these sites allowing virus assembly to proceed. Adapted from Boulant *et al*. (2008) and Miyanari *et al*. (2007).

McLauchlan, 2009). Studies using infected patient liver and serum samples suggest that LVPs are comprised of HCV RNA and structural proteins, Apo B, Apo E, Apo C, triglyceride, cholesterol and phospholipids (Andre *et al.*, 2002; Diaz *et al.*, 2006; Meunier *et al.*, 2005; Nielsen *et al.*, 2004; Nielsen *et al.*, 2006; Thimme *et al.*, 2001). As LVPs appear to have characteristics of both lipoproteins and virus particles they are believed to circulate as functional carriers of dietary lipids (Diaz *et al.*, 2006). Recent HCVcc studies have shown the treatment of infected cells with brefeldin, a broad range inhibitor of the secretory pathway, decreased infectious particle secretion and led to an accumulation of intracellular infectious virus. Also, inhibiting the VLDL assembly process using MTP inhibitors or knockdown of apo B and apo E protein expression, prevented both the release of particles and brefeldin induced intracellular accumulation. These treatments caused no alteration to HCV intracellular RNA replication, indicating they inflict a specific block to virion assembly (Chang *et al.*, 2007; Gastaminza *et al.*, 2008; Huang *et al.*, 2007a; Nahmias *et al.*, 2008). Hence, the current model predicts that VLDL and HCV assembly may act in parallel to one another allowing the formation of infectious HCV LVPs that are released from the cell following their trafficking through the secretory pathway (Fig. 1.12).

1.11. HCV Core Protein

1.11.1. Structural Determinants

Sequence analysis of 52 HCV isolates found the core gene to be 573 nucleotides and 191 aas long. With an extremely high level of nucleotide (79.4-99.0 %) and protein (85.3-100 %) sequence similarity, core is the most highly conserved HCV gene (Bukh *et al.*, 1994). Core protein has been divided into 3 domains based on the hydropathicity pattern of its aa sequence (Hope & McLauchlan, 2000). Domain I, spanning residues 1-118, contains a high proportion of basic residues (24 %) along with 2 short hydrophobic domains. Domain II (aa 119-174) is more hydrophobic than domain I with a lower proportion of basic residues. Domain I and domain II are mainly α-helical and the folding of domain I seems to depend on the presence of domain II (Boulant *et al.*, 2005). Domain II contains two amphipathic α-helices at aa 119-136 and 148-164, connected by an unstructured region called the hydrophobic loop (HL). Domain III (residues 175-191) is extremely hydrophobic and acts as the signal sequence that directs the nascent polypeptide chain to the ER membrane and induces translocation of E1 into the ER lumen (Santolini *et al.*, 1994). During the processing of core in the cell, this signal peptide is cleaved by signal

peptidase (SP) releasing the N-terminal end of E1 and leaving core anchored in the ER membrane (Hussy *et al.*, 1996; Liu *et al.*, 1997; Moradpour *et al.*, 1996; Santolini *et al.*, 1994; Yasui *et al.*, 1998). This 191 aa polypeptide is an immature or unprocessed form of core protein, which is named p23 according to its migration size of 23 kDa on a polyacrylamide gel (Ait-Goughoulte *et al.*, 2006; Ogino *et al.*, 2004). Mature or processed core is then generated by a second cleavage event within the core-E1 signal peptide by the signal peptide peptidase (SPP), which releases core from the ER membrane allowing its attachment to LDs (McLauchlan *et al.*, 2002) (Fig. 1.13). The mature core protein has a molecular weight of 21 kDa (p21) (Ait-Goughoulte *et al.*, 2006; Ogino *et al.*, 2004) and is 177 aa long (Ogino *et al.*, 2004; Okamoto *et al.*, 2008). Recent studies using the HCVcc system have shown that the processing of p21 core by SPP is crucial for the production of infectious virus (Okamoto *et al.*, 2008; Targett-Adams *et al.*, 2008b).

1.11.2. The Core-LD Association and Virus Production

The intracellular location of core was first described in studies expressing core in human osteosarcoma (U-2 OS) cells, where the protein localised to the surface of LDs as well as ER membranes surrounding mitochondria (Moradpour *et al.*, 1996). However, the relevance of the core-LD association in the virus lifecycle was realized after observing this localisation in liver biopsies from HCV-infected chimpanzees (Barba *et al.*, 1997). The targeting of core to LDs has been described in a range of cell types including Chinese Hamster Ovary (CHO) (Barba *et al.*, 1997), Baby Hamster Kindney (BHK) (Hope & McLauchlan, 2000), HepG2 (Barba *et al.*, 1997), and Huh-7 cells (McLauchlan *et al.*, 2002; Shi *et al.*, 2002), indicating this association is not cell-type specific. Numerous studies found that this core-LD association was mediated by domain II (Barba *et al.*, 1997; Hope & McLauchlan, 2000; Moradpour *et al.*, 1996) with the two prolines at positions 138 and 143 being critical for this attachment (Hope *et al.*, 2002).

Rouille *et al.* (2006) first showed the core-LD association in HCVcc-infected Huh-7 cells by colocalisation of core protein with ADRP. However, a time course analysis following HCVcc RNA transfection revealed an initial attachment of core to LDs at early time-points (24 h), followed by the progressive loading and eventual covering of the entire organelle at later time-points (48-72h) (Boulant *et al.*, 2007). Interestingly, JFH1 harbouring alanine substitutions at the two proline residues P138 and P143 (PP/AA) produced core protein

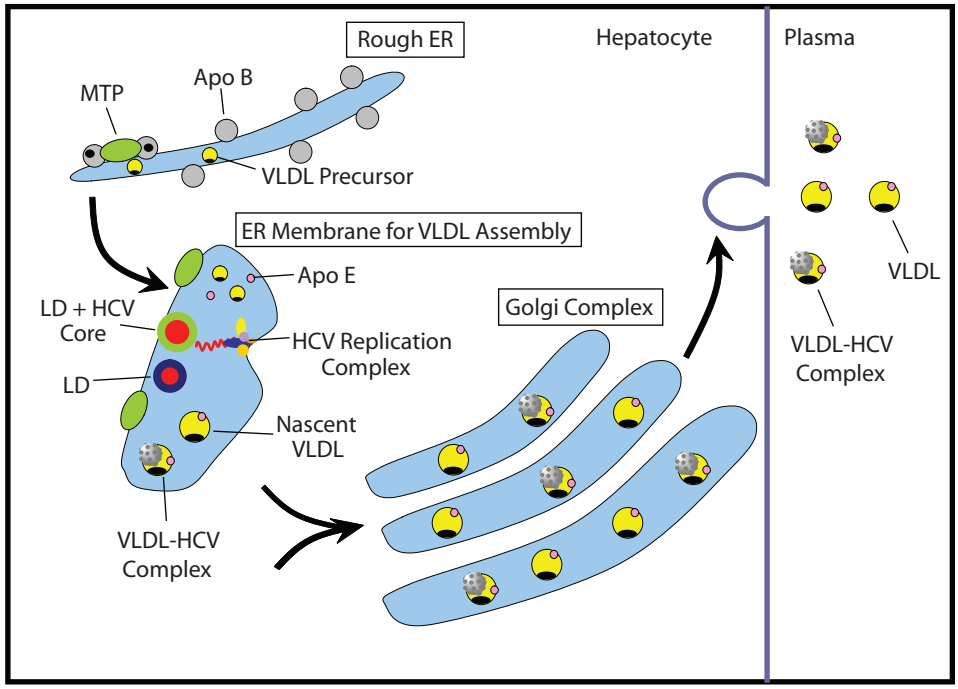

Figure 1.12. Hypothetical model of assembly and secretion of VLDL and HCV virions in hepatocytes.

VLDL assembly begins with the lipidation of newly synthesized apo B in the rough ER by MTP to create a VLDL precursor particle. Following translocation into the lumen of the ER, the MTP-mediated lipidation continues through the fusion of the precursor with LDs, which add the majority of triglycerides and cholesterol to pre-VLDL. Additional lipoprotein components, such as apo E are added to generate mature VLDL that is secreted into the plasma through exocytosis. In infected hepatocytes, virus proteins and replication complexes are concentrated around LD-associated ER membranes, which are believed to allow the co-assembly of virions and lipoprotein particles to produce LVPs. Adapted from Ye (2007).

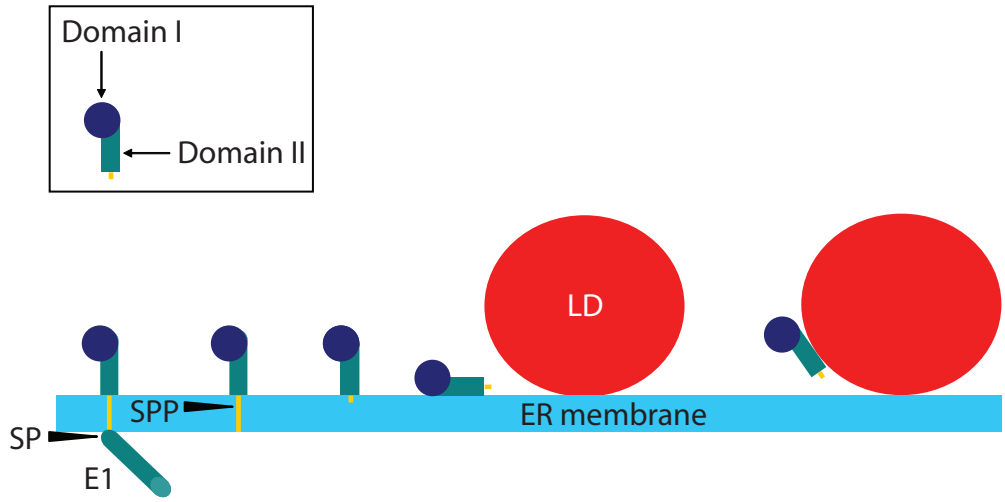

Figure 1.13. Model for the release of HCV core protein from the ER membrane.

During HCV polyprotein processing, the signal peptide between core and E1 is cleaved by SP to produce an immature form of core and the N-terminal end of E1. Subsequent cleavage of the core-E1 signal peptide by SPP liberates mature core protein containing domain I and domain II from the membrane, which then attaches to LDs via domain II. Adapted from McLauchlan *et al*. (2009).

that could attach to LDs but was blocked in its ability to progressively coat LDs following transfection. This defect also correlated with a complete loss in infectious virus production, showing for the first time that the core-LD association functions in the assembly process (Boulant *et al.*, 2007). A slightly later study showed that LD-attached core protein recruits the viral NS proteins, envelope proteins and replication complexes to LD-associated membranes, creating an environment for virion assembly to proceed (Section 1.10.3) (Miyanari *et al.*, 2007).

1.11.3. Core is the Viral Nucleocapsid

The detection of core protein from patient sera (Kashiwakuma *et al.*, 1996; Klein *et al.*, 2004) suggests core is associated with the virus particle. In line with this, *in vitro* studies have shown that core binds RNA and forms multimers; both expected properties of capsid proteins (Section 1.10.3). The availability of HCVcc has allowed the anlaysis of infectious HCV particles and led to a better understanding of core protein and its role as capsid protein for HCV. Indeed, HCVcc has confirmed the presence of core protein within extracellular virus particles (Lindenbach *et al.*, 2005; Wakita *et al.*, 2005). Using HCVcc, a recent study performed extensive mutagenesis across a large part (aa 57-191) of the core-coding region where a total of 34 mutant viruses were constructed each containing alanine changes in blocks of four aas (Murray *et al.*, 2007). This work revealed numerous residues that were critical for infectious virus production but did not alter viral RNA replication. Of the viruses harbouring changes in domain I, all were non-infectious except 4 (69-72, 89-92, 93-96, and 101-104) that displayed minimal infectivity values (~2-3 logs lower than WT). These results demonstrate the importance of these domain I residues in virus assembly, which may be due to impaired RNA binding and/or multimerisation. No mutagenesis within the first 57 residues of domain I was performed to avoid complications caused by the RNA secondary structures (Section 1.11.5) (Tuplin *et al.*, 2004) known to be important for RNA replication (McMullan *et al.*, 2007).

1.11.4. Alternative Reading Frame Protein

Using a newly developed software tool called “Frame splitter” Walewski *et al.* (2001) performed a genome-wide search on HCV with the aim of identifying novel genetic

control elements. By analysing eight highly diverse HCV sequences, this software mapped regions in which synonymous substitutions are suppressed. HCV core was found to contain an unusually high number of such regions and further analysis of viral sequences present in the Genbank database revealed the presence of a +1 alternative reading frame protein (ARFP) in core, also known as the "F" protein. The existence of this putative ARFP in natural HCV infection was confirmed by the presence of anti-ARFP antibodies in sera from HCV-infected patients (Walewski *et al.*, 2001). Cell-free expression studies performed by Xu *et al.* (2001) on a genotype 1a isolate (HCV-1 strain) found F is synthesised as a 17 kDa protein in addition to the 21 kDa mature core. Their data indicate that the F protein translation is initiated at the start codon (AUG) of the main HCV ORF. The ribosome reads in frame until codons 8-11 where it encounters a frame shift-prone region of 10 consecutive alanines, known as the AAA-rich sequence. A +1 frame shift event then occurs facilitating translation of F until termination at the first in-frame stop codon positioned at nucleotides 485-487 (Xu *et al.*, 2001). However, in the absence of the AUG start codon and the AAA-rich sequence, it was found that an F protein could be still generated through internal translation initiation from the AUG codons at positions 85/87 (Vassilaki & Mavromara, 2003). In accordance with these findings, another study reported that F protein synthesis could be initiated at a codon overlapping codon 26 in the main ORF (Baril & Brakier-Gingras, 2005). While the above results were obtained in genotype 1a core, one group found that genotype 1b core could generate F protein via two frame shift events. This double frame shifted protein was produced by a +1 frameshift at codon 42 followed by a rephrasing through a -1 frameshift at position 144 (Boulant *et al.*, 2003). Thus, despite being found in all genotypes (Walewski *et al.*, 2001), the mechanism and size of the F protein generated may be genotype dependent. Although, an F-encoded product has yet to be detected in infected tissue, numerous studies have shown that specific antibodies and cellular immune responses against ARFP antigens are present in HCV-infected patient sera (Bain *et al.*, 2004; Varaklioti *et al.*, 2002; Walewski *et al.*, 2001; Xu *et al.*, 2001). Although, these studies provide strong evidence that the core +1 ORF-derived proteins are produced during natural HCV infection in humans, their biological importance is still unknown. However, it was recently shown that F is not required for virus propagation *in vitro* (HCVcc) or *in vivo* (uPA/SCID mice and chimpanzees) by testing genotype 1a and 2a infectious clones harbouring termination codons that abolish all forms of F protein expression (McMullan *et al.*, 2007; Vassilaki *et al.*, 2008).

1.11.5. Conserved RNA Stem Loop Structures

The HCV RNA encoding the core region contains four highly conserved stem-loop structures (Fig. 1.14), designated SL47, SL87, SL248 and SL443 that were predicted by combining bioinformatic analysis with enzymatic mapping of RNA transcripts (Tuplin *et al.,* 2004). By introducing silent mutations predicted to disrupt these stem-loops two studies have shown that the integrity of SL47 and SL87 are important for the efficient propagation of HCV *in vitro* (HCVcc) and *in vivo* (uPA/SCID mice and chimpanzees) (McMullan *et al.,* 2007; Vassilaki *et al.,* 2008). From experiments with HCVcc, Vassilaki *et al*. (2008) showed that the defects in virus proliferation caused by disrupting these stem-loops was due to a delay in the translation of the viral genome. In addition, this same group found that the remaining stem-loops SL248 and SL443 were not important for HCVcc proliferation.

1.11.6. Pathogenic Effects of Core

1.11.6.1. Apoptosis

Expression of HCV core has been shown to modulate apoptosis through a variety of mechanisms. ER stress leading to apoptosis was shown in HepG2 and Huh-7 cells transiently expressing core, Huh-7 cells harbouring full-length replicons and liver tissue from transgenic mice expressing core (Benali-Furet *et al.,* 2005). Apoptosis can be caused by various stimuli such as oxidative stress, heat shock, ionizing radiation, cytokines and virus infection. The two main apoptotic pathways include the intrinsic or mitochondrial pathway and the extrinsic or death receptor pathway (Elmore, 2007). The intrinsic apoptotic signaling pathways involve various non-receptor-mediated stimuli that trigger an increase in the permeability of the outer mitochondrial membrane. Mitochondria play an important role in the regulation of cell death. They contain many pro-apoptotic proteins such as cytochrome c that are released following Mitochondrial Permeability Transition (MPT) pore formation in the outer membranes. Cytochrome c and other key molecules then activate initiator caspase-9 followed by the effector caspases, primarily caspase-3, -6 and -7, which execute the cell death program. The MPT pores are likely induced by the pro-apoptotic members of the bcl-2 family of proteins, which in turn are activated by

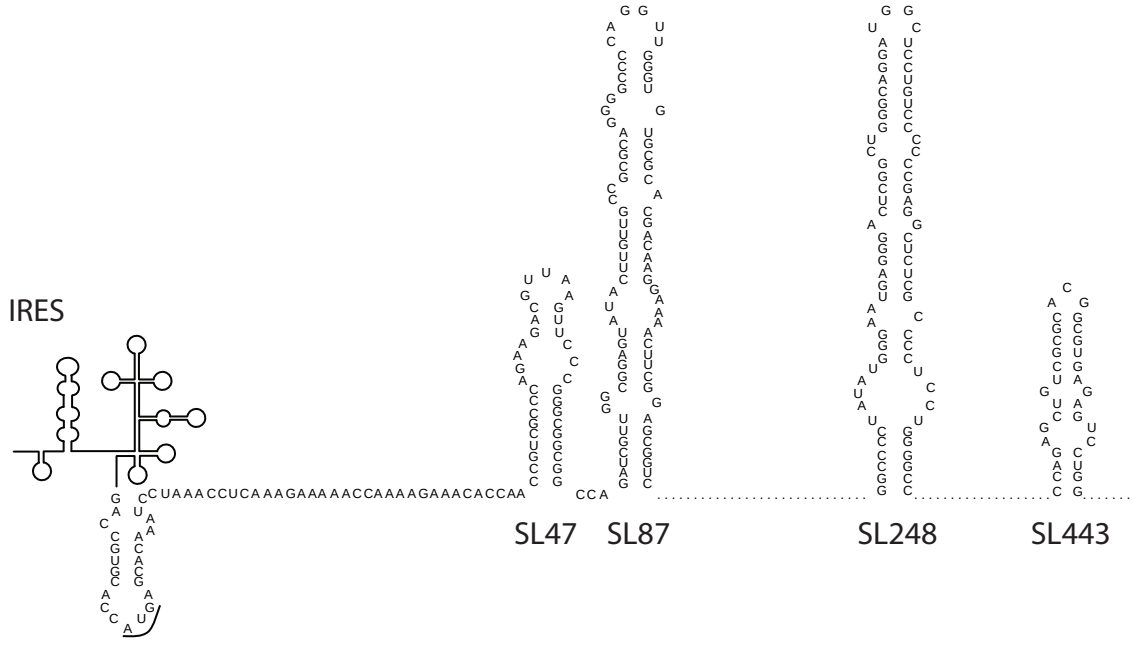

Figure 1.14. Schematic representation of the four predicted core RNA secondary structures.

The structures shown, SL47 (nucleotides 388-423), SL87 (nucleotides 427-507), SL248 (nucleotides 588-665) and SL443 (nucleotides 783-815) are derived from the JFH1 sequence. The polyprotein initiator codon (AUG) is underlined. Adapted from Vassilaki *et al*. (2008).

apoptotic signals such as cell stress, free radical damage or growth factor deprivation (Elmore, 2007). The extrinsic apoptotic signaling cascade is initiated by the activation of death receptors such as Fas, TNF-R1, TRAIL-R1 and TRAIL-R2. To date, the best-characterized ligands and corresponding death receptors include FasL/FasR, TNF-α/TNFR1. The association of Fas ligand to the Fas receptor results in binding to the adaptor protein FADD. The association of TNF ligand with the TNF receptor results in TRADD (adaptor protein) binding followed by the recruitment of FADD and RIP. FADD then associates with initiator caspase-8 via dimerization of the death effector domain. At this point the death-inducing signaling complex (DISC) is formed that promotes autoactivation of initiator caspase-8 and the subsequent activation of the effector caspases, (Elmore, 2007; Igney & Krammer, 2002). Death receptor mediated apoptosis can be inhibited by a protein called FLICE (FADD-like interleukin-1-beta-converting enzyme)-like inhibitory protein (c-FLIP) which binds to FADD and caspase-8, rendering them ineffective (Scaffidi *et al*., 1998). There is also evidence that cross talk exists between the intrinsic and extrinsic pathways whereby molecules in one pathway can influence the other. In certain cell types the amount of active caspase-8 formed at the DISC is insufficient and the mitochondria are used to enhance the apoptotic signal. In this scenario, death receptor recruited caspase-8 cleaves the pro-apoptotic bcl-2 protein, bid, which subsequently induces MPT pore formation (Scaffidi *et al.*, 1998).

Reports describing the influence of core protein on Fas- and TNF-α-mediated apoptosis are somewhat conflicting. In HepG2 cells, core expression has been shown to inhibit (Marusawa *et al.*, 1999) as well as induce (Ruggieri *et al.*, 1997) Fas-mediated apoptosis. Core protein was reported to sensitize HepG2, HeLa and murine BC10ME cells to TNF-α-induced apoptosis, and these effects may be related to the interaction found between core and the cytoplasmic tail region of TNFR1 (Zhu *et al.*, 1998). A follow-up study found that core protein also interacted with the TNF signal transduction molecule FADD in core expressing HEK-293T cells, suggesting that core enhances TNF-α-mediated apoptosis by recruiting FADD to TNFR1 (Zhu *et al.*, 2001). In contrast, two studies found an inhibition of TNF-α-induced apoptosis in MCF7 cells and HepG2 cells expressing core protein (Marusawa *et al.*, 1999; Ray *et al.*, 1998a). More recently, this core-mediated inhibition of TNF-α-induced apoptosis in HepG2 cells was shown to be due to an up regulation of c-FLIP by core, which in turn inhibits the cleavage and activation of caspase-8, thereby inhibiting apoptosis (Saito *et al.*, 2006). The contradictory nature of these reports is likely due to the different cells lines or mode of core expression used.

Core also sensitises all-trans-retinoic acid (ATRA)-induced cell death in MCF-7 cells. The effect is likely due to an interaction between core and Sp110b, a nucleur transcriptional corepressor of the retinoic acid response element that prevents the enhancement of downstream proapoptotic gene expression. Core was shown to sequester Sp110b from the nucleus, thereby releasing the suppressive function of Sp110b and leading to ATRA-induced cell death (Watashi *et al.*, 2003). Core protein interacts with the intracellular domain of the Lymphotoxin-β Receptor (LT-βR), a member of the tumour necrosis factor receptor family involved in cytolytic activation in certain cell types (Chen *et al.*, 1997; Matsumoto *et al.*, 1997). Although, expression of core protein in HeLa cells enhanced LT-βR-mediated apoptosis, this effect was absent in core expressing HepG2 or Huh-7 cells (Chen *et al.*, 1997). A recent study demonstrated that core protein has a functional bcl-2 homology 3 domain near the C-terminal region. This domain was essential for its proapoptotic property and ability to interact with human myeloid cell factor 1 (Mcl-1), a prosurvival member of the Bcl-2 family. This domain is highly conserved among the major HCV genotypes, with the exception of genotypes 2a and 6k, which have V and M residues at position 119, respectively. Interestingly, mutation V119L in the genotype 2a HCVcc significantly increased apoptosis in infected cells and also established an interaction between HCVcc core and Mcl-1 that was absent in the parental form from infected cells. Similarly, replacing L119 to V in genotype 1b core reduced the proapoptotic property of core overexpressed in Huh-7 cells (Mohd-Ismail *et al.*, 2009).

1.11.6.2. Transformation

The suggestion that core functions as an oncogenic protein is a controversial issue. The first indication of the potential oncogenic properties of core came from its ability to alter the transcriptional regulation of cellular proto-oncogenes. These included the transactivation of the human *c-myc* promoter and the suppression of *c-fos* promoter activity by core expression in HepG2 cells (Ray *et al.*, 1995). Another study found p53 activation was enhanced by core protein expressed in Hep3B and HepG2 cells. This resulted in the enhanced expression of the cyclin/cyclin-dependent kinase (cdk) inhibitor $p21^{Waf}$, an effect previously linked to cell cycle suppression (Ko & Prives, 1996). In line with this, Hep3B cell growth was suppressed by core protein expression (Lu *et al.*, 1999). Also, this group found an interaction occurred between core and p53, suggesting core might activate p53 through a direct physical interaction. Another study found core protein interacted with $p21^{Waf}$ (Wang *et al.*, 2000a) and core expression in HeLa or Huh-7 cells lowered $p21^{Waf}$

expression at the post-transcriptional level. Moreover, core negated $p21^{Waf}$–mediated suppression of cyclin/cdk by an undetermined mechanism. This negation may be caused by core-mediated $p21^{Waf}$ degradation or the binding of core to the same C-terminal region of $p21^{Waf}$ known to be involved in its cdk inhibitory activity (Yoshida *et al.*, 2001). A later study by the same group found that core inhibited the synthesis and accumulation of $p21^{Waf}$ and p53 in HeLa cells with the inhibition of $p21^{Waf}$ occurring at the translational level (Oka *et al.*, 2003). However, core protein repressed transcriptional activity of the p53 tumour suppressor when expressed in COS7 and HeLa cells (Ray *et al.*, 1997). In line with this, a later study by the same group found that core expression suppressed $p21^{Waf}$ transcriptional activity when tested in NIH3T3, HepG2 and HeLa cells (Ray *et al.*, 1998b). Core expression was also shown to transform NIH3T3 cells that resulted in core-expressing tumours when inoculated into SCID mice. This transformation and tumourigenicity of core expressing cells coincided with a reduction in p53 transactivation (Smirnova *et al.*, 2006). Core protein can transform primary rat embryo fibroblasts in co-operation with the H-ras, implicating it as a co-factor in the development of HCC (Ray *et al.*, 1996). In line with this, it was demonstrated that the stable expression of core in Rat-1 fibroblasts could induce tumourigenic transformation (Chang *et al.*, 1998).

The most compelling evidence regarding the potential oncogenic properties of core protein came from studies in transgenic mice. Approximately 30 % of transgenic mice expressing core protein developed HCC between 16-19 months from birth, compared to a 0 % incidence in the control mice. Immunologic analysis found that the expression of core protein was higher in the tumours cells than in surrounding normal hepatocytes (Moriya *et al.*, 1997). Several other studies using transgenic mice have failed to observe HCV-induced HCC (Kawamura *et al.*, 1997; Matsuda *et al.*, 1998; Pasquinelli *et al.*, 1997). However, it should be noted that these studies found core expression was barely detectable, and may therefore account for the absence of HCC in these mice.

1.11.6.3. Immune Response

Several lines of evidence implicate core protein in suppression of the immune response to HCV infection. Positive- and negative-strand RNA was found in peripheral blood mononuclear cells (PBMCs) from chronically infected patients, suggesting HCV infection (Lerat *et al.*, 1998). In line with this, a study found that the expression of core and E1 protein using recombinant adenovirus in dendritic cells disrupted their antigen presenting

function, leading to impaired T-cell stimulation (Sarobe *et al.*, 2002). The ability of HCV to enter and replicate in cells from the immune system and the possible dysregulation of normal cell functions associated with core protein expression could be one factor responsible for the establishment of HCV persistence in the host.

The expression of HCV core in mice using recombinant vaccinia virus impaired their protective immune response, including both the antiviral CTL response and IL-2/IFN-γ production (Large *et al.*, 1999). One of the molecular mechanisms of HCV core-mediated immunomodulation was later determined by identification of an interaction between core and the complement receptor gC1qR (Kittlesen *et al.*, 2000). Clq is the natural ligand for gCLqR and is the first molecule to be activated in the classical complement cascade and plays a vital role in modulating both innate and adaptive immunity (Ghebrehiwet *et al.*, 2001). The binding of complement protein C1q to the gCLqR receptor specifically blocks the proliferation of CTLs. HCV core protein mimicked this effect by specifically inhibiting T-cell proliferation, an effect that could be blocked using antibodies against gC1qR1 or HCV core (Kittlesen *et al.*, 2000). Subsequent anlaysis found the core-gClqR interaction impaired activation of the ERK/MEK MAP kinase, which inhibits the transcription of the early genes such as IL-2, thereby suppressing the T cell response (Yao *et al.*, 2001). A significant issue relating to the core/gCLqR-mediated immune suppression in chronic HCV infection is the detection of circulating core protein in the blood of HCV-infected patients that could possibly interact with peripheral T-lymphocytes. Core protein has also been shown to be secreted from transfected cell lines expressing the core gene (Sabile *et al.*, 1999). This idea of circulating core protein suppressing the host immune responses to HCV is supported by high levels of core protein being detected during an early stage of infection before the production of anti-core antibodies (Aoyagi *et al.*, 1999; Urushihara *et al.*, 1994). These results suggest that core-induced immune suppression may play a critical role in establishing and maintaining HCV persistence during early viral infection. Interestingly, the core-gClqR binding causes differential regulation of B-cell and T cell activation. HCV core treatment led to upregulation of IgM and IgG production, cellular proliferation as well as surface receptor expression in B-cells, but to decreased IFN-γ production in T-cells (Yao *et al.*, 2008). Such effects may drive B-cell clonal expansion, a process that is thought to contribute to B-cell lymphoproliferative disorders, such as mixed cryoglobulinaemia and B-cell non-Hodgkin Lymphoma, associated with chronic infection (Racanelli *et al*., 2001; Sansonno & Dammacco, 2005).

1.11.6.4. Transcription

Three putative nuclear localization signals (NLS) are present within domain I of core at residues 38-43, 58-64 and 66-71 (Shih *et al.*, 1993). Interestingly, truncated core protein lacking the hydrophobic domain II region is localized to the nucleus in mammalian cells and deletion studies revealed the first predicted NLS (aa 38-43) plays an important role in this nuclear translocation (Suzuki *et al.*, 1995). The HCV-1 strain encodes a unique 16 kDa species of core (p16) that lacks the C-terminal residues present in the p21 form. This species is mainly localised to the nucleus (Lo *et al.*, 1995) and has been proposed to have regulatory functions on host gene expression (Ray *et al.*, 1995). Also, the p21 species from a genotype 1b core protein was shown to localize to the nucleus as well as the cytoplasm. Experiments using a panel of monoclonal antibodies indicated that these nuclear forms are conformationally distinct to those found in the cytoplasm (Yasui *et al.*, 1998). The existence of such forms of core in the nucleus in addition to a putative DNA binding motif (aa 99-102) (Bukh *et al.*, 1994) within the core protein sequence, suggests it may have a functional role in host gene regulation. Indeed, several studies have shown that core protein can modulate both viral and cellular gene expression. It was demonstrated that core protein could suppress the gene replication and expression of HBV in Huh-7 cells (Shih *et al.*, 1993). Strikingly, these inhibitory effects coincided with the cellular relocalisation of core from the cytoplasm to the nucleus. A follow-up study to this work then demonstrated that core is phosphorylated by protein kinase A (PKA) and C (PKC) and that phosphorylation of Ser-99 and Ser-116 regulated the suppressive acitivity of core on HBV gene expression and replication (Chen *et al.*, 2003). Other studies using reporter plasmids have shown core protein to elevate expression levels in constructs containing the cellular c-myc, SV-40 early promoter and Rous sarcoma virus long terminal repeat (Ray *et al.*, 1995). In addition, core has suppressive effects on the expression from c-fos (Ray *et al.*, 1995), $p21^{Waf}$ (Ray *et al.*, 1998a), p53 (Ray *et al.*, 1997) and HIV-LTR promoters (Ray *et al.*, 1995).

It is unclear if core protein exerts its effects through a direct interaction with each of these promoters. However, the range of promoters affected by core argues for an indirect effect of this viral protein through a common transcription factor. This hypothesis is strengthened by the protein-protein interaction described between core and the cellular transcriptional regulator heterogenous nuclear ribonucleoprotein K (hnRNP K). Furthermore, core protein

could partially reverse the suppressive effect of hnRNP K on the human thymidine kinase promoter. Core protein binds to the proline-rich regions of hnRNP K, which are known to be critical for the interaction of hnRNP K with other cellular factors. Thus, core binding to hnRNP K may disrupt the association of this transcriptional regulator with other cellular protein partners, which in turn affects its proper function within the cell (Hsieh *et al.*, 1998).

1.11.6.5. Lipid Metabolism

A common condition observed in chronically infected HCV patients is steatosis, which is the accumulation of lipids in the liver (Lefkowitch *et al.*, 1993; Scheuer *et al.*, 1992). HCV-induced steatosis appears to be a direct cytopathic lesion mostly seen in patients infected with genotype 3, in whom it correlates directly with the level of viral replication (Section 1.6.2). For reasons unknown, other genotypes are rarely associated with steatosis (Castera *et al.*, 2005; Hezode *et al.*, 2004). Transgenic mice expressing either the full-length HCV genome (Lemon *et al.*, 2000; Lerat *et al.*, 2002; Lerat *et al.*, 2009) or core protein (Moriya *et al.*, 1997) alone can develop steatosis, suggesting a direct involvement of core protein in the development of this condition. In addition, an increase in the proportion of carbon 18 monounsaturated (C18:1) fatty acids, such as oleic and vaccenic acids, was found in the livers of both transgenic mice expressing core and patients with chronic hepatitis C (Moriya *et al*., 2001). Core was found to interact with apolipoprotein AII, a major component of high density lipoproteins, and may be a mechanism by which core alters liver lipid metabolism (Sabile *et al.*, 1999). The numerous studies describing the association of core with LDs and the importance of this association in the viral lifecycle supports this possibility (Section 1.11.2). One mechanism for the induction of steatosis by core protein may be the suppression of lipid secretion as reduced serum levels of cholesterol and apo B have been reported in core-expressing transgenic mice (Perlemuter *et al*., 2002). In line with this, HCVcc infection causes the overproduction of LDs (Miyanari *et al*., 2007) and the RNA replication of SGRs is enhanced by increases in saturated and monounsaturated fatty acids (Kapadia & Chisari, 2005). Together, these data suggest that the regulation of lipid metabolism by the core protein plays crucial roles in the HCV lifecycle, which may in turn result in pathogenic affects.

1.11.6.6. Host Cell Proteins Interacting with Core

A number of host cell proteins have been identified to interact with HCV core protein (Summarised in Table 4). In 1999, three independent studies revealed an interaction between HCV core and a putative cellular RNA helicase belonging to the DEAD-box family. This cellular protein was referred to as DBX (Mamiya & Worman, 1999), CAP-Rf (Core-associated protein-RNA helicase full-length) (You *et al.*, 1999) and DDX3 (Owsianka & Patel, 1999), the latter of which is the term approved by the HUGO/GDB Nomenclature Committee. The interacting domains of the two proteins were mapped to aa 1-59 (Owsianka & Patel, 1999) or 1-40 (You *et al.*, 1999) of core protein, and aa 553-622 (Owsianka & Patel, 1999) or 473-611 (You *et al.*, 1999) of the full-length 662 aa DDX3. Colocalisation between core and DDX3 was observed following the expression of core in Hela or COS-7 cells expressing c-myc-tagged DDX3 (Mamiya & Worman, 1999), Huh-7 cells expressing FLAG-tagged DDX3 (You *et al.*, 1999) and Hela cells expressing endogenous DDX3 (Owsianka & Patel, 1999). The lack of information on the cellular role(s) of DDX3 and the absence of a robust system to study the HCV lifecycle made it difficult to interpret the possible function(s) of this interaction. Nevertheless, there was evidence that this interaction may modulate host gene expression (Mamiya & Worman, 1999; You *et al.*, 1999). The yeast homologue to DDX3, known as Ded1p, functions in translation initiation (Chuang *et al.*, 1997) and a Ded1p-deletion renders yeast non-functional. Interestingly, DDX3 supplied *in trans* rescues these Ded1p-deletion mutants, and this effect is severely inhibited by the co-expression of full-length core protein. These data demonstrate that DDX3 may have an important function in translation initiation, which is disrupted by its interaction with HCV core (Mamiya & Worman, 1999). In accordance with a function of DDX3 in translation, You *et al.* (1999) found DDX3 to upregulate translation from a reporter plasmid in Huh-7 cells. Co-expression of truncated core protein (aa 1-122) significantly enhanced these levels, suggesting this interaction may modulate gene expression regulation in the host. However, given that this truncated form of core is targeted to the nucleus, the *in vivo* relevance of this finding is questionable.

Interacting protein name	Core residues required	Protein residues required	Reference
DDX3	1-59	473-622	Owsianka & Patel (1999), Mamiya & Worman (1999), You *et al*. (1999)
TNFR1	1-115	345-407	Zhu *et al*. (1998)
FADD	1-153	80-205	Zhu *et al*. (2001)
Sp110b	21-80	389-453	Watashi *et al*. (2003)
$LT_{\beta}R$	31-90	338-395	Matsumoto *et al*. (1997)
p53	1-151	366-380	Lu *et al*. (1999)
$p21^{Waf}$	24-52	139-164	Wang *et al*. (2000)
LZIP	-	-	Jin *et al*. (2000)
p73	-	321-353	Alisi *et al*. (2003)
HCV NS5A	-	-	Goh *et al*. (2001), Masaki *et al*. (2008)
gC1qR	26-124	199-259	Kittlesen *et al*. (2000)
Mcl-1	119	-	Mohd-Ismail *et al*. (2009)
14-3-3ε	49-97	165-234	Aoki *et al*. (2000)
hnRNP K	25-91	250-392	Hsieh *et al*. (1998)
ApoAII	160-173	-	Sabile *et al*. (1999)
PA28-γ	44-71	-	Moriishi *et al*. (2003)
Fibrinogen-β	-	-	Ait-Goughoulte *et al*. (2009)
Heat shock 60 kDa protein 1	-	-	Kang *et al*. (2005)
DDX5	-	-	Kang *et al*. (2005)
Cytokeratin 8, 18 and 19	-	-	Kang *et al*. (2005)
Vimentin	-	-	Kang *et al*. (2005)
Solute carrier family 22 member 7 isoform b	-	-	Kang *et al*. (2005)
Hepatocarcinoma high expression protein	-	-	Kang *et al*. (2005)
FK506-binding protein	-	-	Kang *et al*. (2005)
TXNL2	-	-	Kang *et al*. (2005)
MHC class I antigen	-	-	Kang *et al*. (2005)
Low M_w phosphotyrosine protein phosphatase	-	-	Kang *et al*. (2005)
Cofilin	-	-	Kang *et al*. (2005)

Table 4. Cellular and viral proteins shown to interact with HCV core protein.

Interacting protein name	Core residues required	Protein residues required	Assay(s) used	Reference
hnRNP K	25-91	250-392	Yeast-two hybrid, Co-IP, GST-Pulldown, Far western blotting	(Hsieh *et al.*, 1998)
ApoAII	160-173	-	Yeast-two hybrid	(Sabile *et al.*, 1999)
PA28-gamma	44-71	-	Yeast-two hybrid, co-IP	(Moriishi *et al.*, 2003)
Fibrinogen-β	-	-	Yeast-two hybrid, co-IP	(Ait-Goughoulte *et al.*, 2009)
Heat shock 60kDa protein 1	-	-	MALDI-TOF MS	(Kang *et al.*, 2005)
DDX5	-	-	MALDI-TOF MS	(Kang *et al.*, 2005)
Cytokeratin 8, 18 and 19	-	-	MALDI-TOF MS	(Kang *et al.*, 2005)
Vimentin	-	-	MALDI-TOF MS	(Kang *et al.*, 2005)
Solute carrier family 22 member 7 isoform b	-	-	MALDI-TOF MS	(Kang *et al.*, 2005)
Hepatocarcinoma high expression protein	-	-	MALDI-TOF MS	(Kang *et al.*, 2005)
FK506-binding protein	-	-	MALDI-TOF MS	(Kang *et al.*, 2005)
TXNL2	-	-	MALDI-TOF MS	(Kang *et al.*, 2005)
MHC class I antigen	-	-	MALDI-TOF MS	(Kang *et al.*, 2005)
Low M_w phosphotyrosine protein phosphatise	-	-	MALDI-TOF MS	(Kang *et al.*, 2005)
Cofilin	-	-	MALDI-TOF MS	(Kang *et al.*, 2005)

Table 4. Continued…

1.12. DEAD-Box Proteins

The DEAD box protein family, first described in 1989 (Linder *et al.,* 1989), belongs to RNA helicase superfamily 2 (Caruthers & McKay, 2002). DEAD-box proteins act in the unwinding of double-stranded RNA structures and the remodelling of RNA-protein interactions in an ATP-dependent manner. They are found in most organisms and play pivotal roles in nearly all aspects of RNA metabolism including transcription, pre-mRNA splicing, ribosome biogenesis, RNA export, translation and RNA decay. DEAD-box RNA helicases are defined by a cluster of 9 conserved motifs situated in the protein molecules centre and spans a region of approximately 400 aas (Fig. 1.15). In contrast, the N- and C-termini are highly variable in both sequence and length and are thought to be involved in substrate interaction, subcellular localisation and interaction with cellular factors (Cordin *et al.*, 2006). The Q motif is involved in control of ATP binding and hydrolysis as well as RNA substrate affinity (Cordin *et al.,* 2004; Tanner *et al.,* 2003). Motif I, also known as the Walker A motif (Walker *et al.,* 1982), is essential for ATPase and helicase activities. Motif II, also known as the Walker B motif (Walker *et al.*, 1982), gives rise to the name DEAD-box and is involved in ATP-binding and/or ATP hydrolysis (Pause & Sonenberg, 1992; Walker *et al.,* 1982). Motif III is proposed to participate in the linking of ATPase and helicase activities (Pause & Sonenberg, 1992). Motif IV is the least-well studied DEAD-box protein motif, with no definite function assigned as yet (Cordin *et al.,* 2006). Motif V is proposed to be an RNA binding motif (Caruthers *et al.,* 2000) and motif VI is required for RNA binding and ATP hydrolysis (Pause *et al.,* 1993).

1.13. DDX3

DDX3 is a ubiquitous cellular protein belonging to the DEAD-box RNA helicase family. The human genome contains two functional genes of the DDX3 family (Kim *et al.*, 2001). These include DDX3 located on the X chromosome, also termed DDX3X (Park *et al.*, 1998) and the highly homologous (91 %) DDX3Y located on the Y chromosome (Lahn & Page, 1997). While DDX3Y is expressed only in the male germ line, the DDX3X gene is ubiquitously expressed across a wide range of human tissues (Rosner & Rinkevich, 2007). Known homologues of DDX3 include mouse PL10 (Leroy *et al.*, 1989), mDEAD3 (Gee & Conboy, 1994), *Xenopus* An3 (Gururajan *et al.*, 1991) and yeast Ded1 (Jamieson & Beggs,

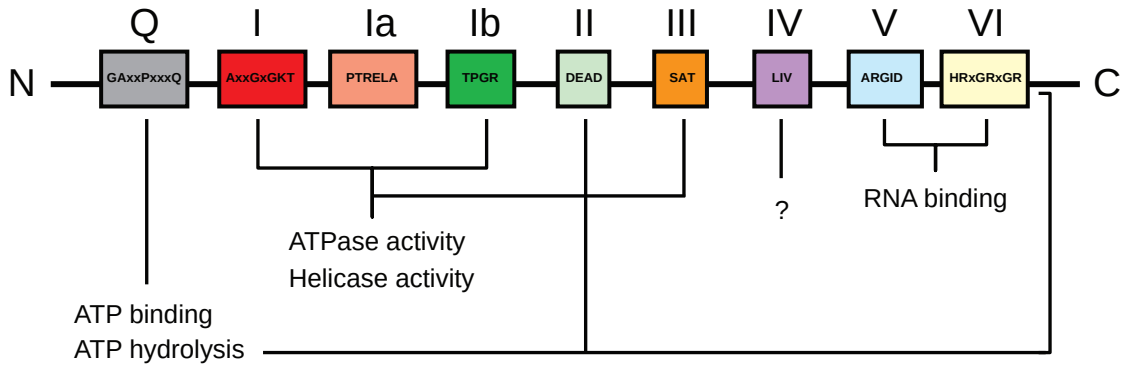

Figure 1.15. Diagram illustrating the 9 conserved motifs of DEAD-box proteins flanked by variable N- and C-termini.

The aa sequence of each motif is detailed in coloured boxes with the motif name listed above. Symbol x represents any residue. The proposed function(s) of each motif are indicated. Adapted from Rocak & Linder (2004).

1991). Since its labelling as a putatitve RNA helicase based on its sequence homology, it has been demonstrated experimentally that DDX3 has ATPase and helicase activities (Franca *et al.*, 2007; Yedavalli *et al.*, 2004). Although, to date the exact cellular functions of DDX3 remain unknown, it has been implicated in numerous cellular processes including splicing, translation, tumourigenesis, nucleo-cytoplasmic RNA shuttling, RNA transport, IFN induction and apoptosis. As the list of cellular processes increases for DDX3 so to does the number of viruses whose replication is dependent on this multifunctional protein. The following sections will summarise the literature available on DDX3 to date.

1.13.1. Cellular Localisation of DDX3

The majority of studies analysing the intracellular distribution of DDX3 have reported this protein to be predominantly cytoplasmic (Franca *et al.*, 2007; Lai *et al.*, 2008; Lee *et al.*, 2008; Mamiya & Worman, 1999; Schroder *et al.*, 2008; Yedavalli *et al.*, 2004). However, DDX3 has been shown to shuttle consistently between the cytoplasm and nucleus in HeLa cells by virtue of the export shuttling protein CRM1 (Chromosome maintainance region 1) which DDX3 binds. Treatment of cells with the CRM1 inhibitor Leptomycin B (LMB) results in DDX3 accumulation in the nucleus (Yedavalli *et al.*, 2004). These results were also reproduced in HEK-293T cells (Schroder *et al.*, 2008). Thus, the high rate of nuclear export may explain why most studies report DDX3 in the cytoplasm. However, two studies have also reported a nuclear localisation of DDX3 in HeLa cells (Owsianka & Patel, 1999; You *et al.*, 1999). This discrepancy may be caused by the antibodies used in each study recognising DDX3 within nuclear complexes more strongly than its cytoplasmic form.

1.13.2. Splicing

Sequence analysis found DDX3 to possess a C-terminal (aa 582-632) arginine/serine rich RS-domain consisting of 7 serine-arginine or arginine-serine dipeptides, similar to that of other splicing factors (Owsianka & Patel, 1999). In HeLa cell nuclei, DDX3 is reported to be present in spliceosomal complexes (Deckert *et al.*, 2006), and also is detected with spliced mRNA as part of mRNPs (messenger ribonulceoprotein particles) (Merz *et al.*, 2007). This suggests DDX3 may not have an active role in splicing, but rather associates with RNPs after splicing for roles such as RNA transport. In line with this, DDX3 is

reported to form part of the Kinesin RNA-transport granules that transport specific populations of mRNAs to the neuronal dendrites for translation. However, knockdown of DDX3 by RNA interference (RNAi) had very little effect on RNA transport, indicating DDX3 may function in other process besides transport (Kanai *et al.*, 2004).

1.13.3. Innate Immune Response

So far, three groups have revealed a function for DDX3 in innate immune signalling through enhancing the induction of anti-viral gene expression in HEK-293T cells. Soulat *et al*. (2008) found DDX3 to be an interacting partner of TBK1. The two related kinases IKK-ε and TBK1 function under the TLR-induced signalling pathway where they phosphorylate and activate IRF-3 and-7 that subsequently activate the IFN-β gene (Figure 1.2). Knockdown of endogenous DDX3 using small inhibitory RNA (siRNA) technology showed DDX3 to be required for TBK1/IRF-3-mediated IFN-β production. Moreover, the phosphorylation of DDX3 by TBK1 was required to stimulate IFN-β production following stimulation of the innate immune response. Also, DDX3 influenced IFN-β gene expression by binding to the IFN-β promoter enhancing region, independent of IRF-3. Given their results and the known functions of DDX3 in transcription initiation (Chao *et al.*, 2006), nuclear export of HIV RNAs (Yedavalli *et al.*, 2004) and cap-dependent mRNA translation (Shih *et al.*, 2008) the authors propose different possible mechanisms for DDX3 in IFN-β activation. The activated TBK1 phosphorylates DDX3 in the nucleus, which is recruited to the IFN promoter for either stimulating transcription of the IFN-β gene and/or nuclear export and translation of the mRNA. Schroder *et al*. (2008) also found DDX3 to be a positive regulator of IFN-β induction. They found DDX3 interacts with IKK-ε after sendai virus infection, thereby contributing to IRF-3 activation. Interestingly, they found the vaccinia virus protein K7 interacted with DDX3 and inhibited its function in the IFN induction pathway. Interestingly, K7 binds to the same N-terminal region of DDX3 (aa 1-139) that is required for its effects on the IFN-β promoter. Therefore, the inhibitory effect of K7 on IFN induction may be caused by the binding of K7 to this region of DDX3 preventing downstream signalling. Also, the most recent report found that DDX3 bound to the RIG-I adaptor protein IPS-I after overexpressing tagged forms of each protein in HEK-293T cells (Oshiumi *et al.*, 2010). IPS-I is an adaptor protein which binds RIG-I following the recognition of viral RNA in the cytoplasm. Using yeast-two hybrid screening residues 622-662 in the C-terminal region of DDX3 were shown to facilitate its interaction with IPS-I. Forced expression of DDX3 and IPS-I in HEK-293T cells also upregulated the IFN-

β promoter activity. These data suggest that DDX3 is required for IPS-I signalling following viral infection, although its exact mechanism in this signaling process remains to be determined. These results together with those from Soulat *et al*. (2008) and Schroder *et al*. (2008) suggest that DDX3 has multiple roles in the innate immune response pathway.

1.13.4. Apoptosis

To date, only two studies have reported DDX3 to function in apoptosis, although the results are somewhat conflicting. Using the non-transformed swiss mouse embryo fibroblast NIH3T3 cell line, Chang *et al*. (2006) found DDX3 knockdown enhanced cellular proliferation and reduced apoptosis. The authors also mentioned preliminary findings that caspase-6 and -9 could not be activated in DDX3 knockdown cells, suggesting that DDX3 functions in the intrinsic apoptotic pathway. In contrast, Sun *et al*. (2008) reported an anti-apoptotic role for DDX3 within the extrinsic signalling pathway. They identified an anti-apoptotic death receptor complex comprising glycogen synthase kinase-3 (GSK3), DDX3 and cellular inhibitor of apoptosis protein-1 (cIAP), which caps the TRAIL-R2 death receptor and inhibits signalling. GSK3 inhibition or DDX3 knockdown released this inhibitory cap to allow stronger apoptotic signalling upon death receptor stimulation. Stimulation of death receptors including TRAIL-R2 disables these proteins causing inactivation of GSK3 and cleavage of DDX3 and cIAP-1 to permit apoptotic signalling. These effects were shown in the transformed HeLa cell line and MDA-MB-231 human breast cancer cells as well as Jurkat cells. It is not possible that DDX3 has a pro-apoptotic effect on the intrinsic pathway (Chang *et al.*, 2006) and an anti-apoptotic effect on the extrinsic pathway (Sun *et al.*, 2008). The differences in the findings from these two studies may be explained by the different cell lines used.

1.13.5. Tumourigenesis

DDX3 has also been reported to function in cell cycle regulation and tumourigenesis. DDX3 was found to be overexpressed in ten liver cancer cell lines (PLC5, Huh-7, Hep3B, SK-Hep1, HepG2, Mahlavu, Huh-6, HCC36, HA22T and Tong) showing anchorage independent growth (AIG) (Huang *et al.*, 2004). Overexpression of DDX3 in AIG-negative Tong cells led to a 60-80-fold increase in transformed colonies in AIG assays. In addition,

this group found that the DDX3 mRNA expression levels were elevated in 64 % of all HCC tissue samples (n=45) tested relative to their adjacent normal tissues. Thus, these data indicate that DDX3 promotes cellular transformation. In contrast, two reports found DDX3 may be down-regulated in liver tumour cells and may affect cell cycle progression via regulation of $p21^{waf}$ gene expression. Firstly, immunohistochemical staining of 41 paraffin embedded HCC specimens revealed that DDX3 expression was decreased in 59 % compared to non-tumour tissue (Chang *et al.*, 2006). Western blot analysis from another 60 HCC specimens found DDX3 expression was lower in 50 % of paired (tumour versus non-tumour) samples. DDX3 knockdown in non-transformed murine fibroblast NIH3T3 cells resulted in the premature entry into S phase and an accelerated proliferation rate. This effect correlated with higher expression levels of cyclin D_1, a key regulator in early-mid G_1 phase, and lower expression levels of $p21^{waf}$ (Chang *et al.*, 2006). Similarly, overexpression of DDX3 protein exerted an inhibitory effect on cell growth in Huh-7 and NIH3T3 cells. Overexpression also led to the upregulation of endogenous $p21^{waf}$ protein expression, which required the ATPase activity of DDX3 but not the helicase activity (Chao *et al.*, 2006). Similar to the report by Chang *et al.* (2006) DDX3 mRNA and protein expression was found to be generally lower in HCC tissue specimens compared to non-tumour specimens (Chao *et al.*, 2006). Furthermore, the vast majority (77 %) of tissue specimens with decreased DDX3 mRNA levels also showed simultaneous $p21^{waf}$ mRNA down-regulation. These two reports provide strong evidence for a role of DDX3 in cell cycle progression and tumourigenicity via regulation of $p21^{waf}$ gene expression. Using the non-tumourogenic human breast epithelial cell line (MCF 10A cells), Botlagunta *et al.* (2008) showed that the carcinogenic compound benzo[a]pyrene diol epoxide increased DDX3 expression levels. Stable overexpression of DDX3 in MCF 10A cells increased AIG, motility and invasion, which are all markers of cellular transformation. However, no correlation between the expression levels of DDX3 and the regulation of $p21^{waf}$ were observed, contrary to previous studies (Chang *et al.*, 2006; Chao *et al.*, 2006). Thus, the data regarding the role of DDX3 in tumourigenesis is some what contradictory with studies describing both tumour suppressor (Chang *et al.*, 2006; Chao *et al.*, 2006) and tumour promoting (Botlagunta *et al.*, 2008; Huang *et al.*, 2004) functions. The reasons for these discrepancies are currently unclear but may be the result of the different cells lines and cancer specimens analysed in each study.

1.13.6. Protein Translation

As described in section 1.11.6.6, Ded1p is a yeast homologue of DDX3, which is required for translation initiation (Chuang *et al*., 1997) and is therefore essential for cell growth. DDX3 supplied *in trans* was able to rescue a functionally crippled yeast containing a lethal Ded1p-deletion mutant (Mamiya & Worman, 1999), suggesting a role for DDX3 in protein translation. In mammalian cells cap-dependent translation initiation is the standard mode of translation for most cellular mRNAs. This process is facilitated by a cap binding complex known as eukaryotic translation initiation factor 4F (eIF4F). This eIF4F complex contains the cap-binding protein eIF4E and adaptor protein eIF4G. The eIF4G protein bridges the mRNA and ribosome by binding to eIF4E and to ribosome associated factor eIF3. The interaction of eIF4G and eIF4E occurs via two conserved motifs and is required for translation initiation and therefore its disruption or reinforcement is an important target for translational control. The eIF4E inhibitory proteins (EBPs) utilize this conserved region to modulate cap-dependent translation by prevention of eIF4F complex formation through the sequestrating of available eIF4E. These EBPs play fundamental roles in cell cycle progression, metabolism, development, tumor formation and responses to various stimuli (Shih *et al.*, 2008).

Shih *et al*. (2008) showed that DDX3 specifically represses cap-dependent translation, but not HCV IRES-mediated translation, in a helicase independent manner. Overexpressing DDX3 in HEK-293T cells showed a dose-dependent decrease in cap-dependent and increase in cap-independent translation. Also, knocking down DDX3 in HeLa cells resulted in an increase in cap-dependent translation but had no effect on cap-independent translation. Moreover, they also showed that DDX3 interacts with eIF4E via the conserved eIF4E binding motif on DDX3 between residues 38-44. Two separate mutations within this binding motif (Y38A and L43A) could disrupt this interaction. Using these mutants they showed that DDX3-eIF4E binding inhibited cap-dependent translation by blocking eIF4E-eIF4G complex formation in HEK-293T cells. Together, the data suggest DDX3 is a novel eIF4E inhibitory protein involved in translation initiation regulation. Previously, this group reported DDX3 to function as a tumour suppressor and ectopic expression in Huh-7 cells inhibited cell proliferation (Chao *et al.*, 2006). Their recent study found a substantial increase in colony formation (20-46 % of control) after overexpressing Huh-7 cells with the DDX3-eIF4E binding mutants Y38A and L43A compared to the WT control (4-6 % of control) (Shih *et al.*, 2008). Together, these data indicate that the DDX3-eIF4E interaction

contributes to the tumour suppressor function of DDX3 in addition to its transactivation of $p21^{waf}$.

Lai *et al*. (2008) reported in HEK-293T cells that DDX3 could interact with Tip-associated protein (TAP), which required aas 536-661 of DDX3. TAP is the major mRNA nuclear export factor. DDX3 bound TAP primarily in the nucleus, and siRNA knockdown of TAP increased the levels of DDX3 in the nucleus and decreased accordingly its levels in the cytoplasm in HEK-293T cells. Therefore, it seems DDX3 can be exported from the nucleus via the TAP-mediated pathway. In addition, DDX3 and TAP associated with stress granules in the cytoplasm of HeLa cells, which are formed after exposure to environmental stress and contain several translation initiation factors that represent stalled translation pre-initiation complexes. DDX3 was shown to interact with the translation initiation factors eIF4A, eIF2-α and PABP1 in HEK-293T cells. DDX3 silencing did not prevent arsenite-induced stress granule formation in HeLa cells, suggesting DDX3 is not required for stress granule assembly. However, overexpression of DDX3 induced stress granule formation in line with the role of DDX3 in general translation repression (Shih *et al.*, 2008). DDX3 knockdown had no effect on the global translation profile of HeLa cells, suggesting DDX3 is not required for general translation in mammalian cells (Lai *et al.*, 2008).

1.13.7. Virus Replication

1.13.7.1. HIV-1

Following HIV-1 entry, the viral RNA genome is reverse transcribed into DNA by the virion associated reverse transcriptase. Following the integration of the provirus into cellular chromosomes, the genome is transcribed. More than 30 different species of HIV-1 mRNAs have been identified to date. Thus, the virus utilizes complex splicing schemes to generate diversity and to maximize its coding capacity. The three general categories of viral mRNAs include genomic, singly spliced, and multiply spliced RNAs. During the early phases in viral infection the multiply spliced mRNAs encoding the Tat, Rev, and Nef proteins predominate in the cytoplasm. Later on in infection, the unspliced and singly spliced RNAs become the major species in the cytoplasm. The Rev protein is a key regulator in this transition (Wang *et al.*, 2000b). The exit of HIV RNAs from the nucleus is a significant issue because unspliced/partially spliced cellular mRNAs are routinely retained in and not permitted for export from the nucleus. The Rev protein binds a highly

secondary structured element called the Rev responsive element (RRE) that is present in all unspliced and partially spliced HIV transcripts. This binding specifically distinguishes, for purposes of nuclear export, viral transcripts from cellular RNAs. In its role of RNA transportation from the nucleus Rev directly interacts with the nuclear export receptor CRM1. CRM1 is required for Rev-mediated export of HIV RNAs (Jeang & Yedavalli, 2006). It was recently shown that DDX3 is a member of the Rev-CRM1-RRE complex through its binding to CRM1 (Yedavalli *et al.*, 2004). This interaction was demonstrated in HeLa cells as well as the Jurkat and MT4 T cell lines. This study also showed for the first time that purified DDX3 could unwind double-stranded RNA in a helicase and ATPase dependent manner. Knockdown of DDX3 expression in HeLa cells using either an anti-sense vector or dominant negative mutants inhibited the export of unspliced/partially spliced HIV-1 RNAs from the nucleus and consequently impaired HIV-1 replication. It was also found that the function of DDX3 within this complex was dependent on its helicase activity and that DDX3 interacted with nucleoporins and localised with the cytoplasmic side of nuclear pores. From their findings, the authors speculated that following the initial delivery of the HIV RNAs by Rev/CRM1 into the nuclear pore the enzymatic unwinding action of DDX3 may facilitate the final release of the HIV-1 RNAs from the cytoplasmic side of the nuclear pore.

1.13.7.2. HBV

HBV is a member of the hepadnavirus family. Infectious virions contain a partially double-stranded, circular but not covalently closed DNA genome referred to as relaxed circular or RC-DNA. During infection, RC-DNA is converted into covalently closed circular DNA (cccDNA) within the host cell nucleus, which serves as a template for the transcription of several genomic and subgenomic RNAs by cellular RNA polymerase II. Of these, the pregenomic RNA (pgRNA) is packaged into progeny capsids and reverse transcribed by the co-packaged viral polymerase (reverse transcriptase) into new RC-DNA genomes (Beck & Nassal, 2007). In the search for host factors that bound the HBV polymerase, Wang *et al*. (2009) identified DDX3 from HEK-293T cells stably expressing FLAG-tagged HBV polymerase. Surprisingly, overexpression of DDX3 in HBV replicating HepG2 cells decreased HBV DNA synthesis in a dose-dependent manner. Also, knockdown of DDX3 from these cells resulted in a dose-dependent increase in HBV DNA synthesis. The impact of DDX3 overexpression or knockdown on HBV genome replication in HEK-293T cells was essentially identical to the results obtained with HepG2 cells, indicating that DDX3

inhibits HBV DNA synthesis in both hepatoma cells and non-hepatoma cells. This was not caused by inhibition of pgRNA encapsidation but instead by DDX3 being incorporated into the viral nucleocapsids to inhibit reverse transcription. Although, these results suggest DDX3 is a cellular host factor restricting HBV genome replication, the exact mechanism and physiological relevance behind these findings remain to be determined. The authors speculate their findings may connect to the previous report by Chang *et al*. (2006) showing a decrease in DDX3 expression levels in HCC tissue samples (Section 1.13.5). HBV might downregulate DDX3 expression during infection to relieve the inhibitory effect of DDX3 on its replication and thereby contribute to the development of HBV-induced HCC.

1.13.7.3. HCV

The importance of DDX3 in HCV replication was first demonstrated in a study that performed a systematic RNAi screen targeting 62 host genes encoding proteins known to interact with HCV RNA, HCV proteins or belonging to cellular pathways thought to modulate HCV infection. These genes were silenced in Huh-7.5 cells that were subsequently infected with HCVcc (Randall *et al.*, 2007). Strikingly, out of all the host genes targeted, DDX3 silencing resulted in the greatest drop in infectious virus release (42-fold) and RNA replication (1800-fold), without affecting cell viability. A slightly later study then carried out a more detailed analysis into the role of DDX3 in HCV replication (Ariumi *et al.*, 2007). DDX3 expression levels were reduced in Huh-7-derived cells through transduction with a lentivirus vector encoding a short hairpin RNA (shRNA) targeting DDX3. Efficient DDX3 knockdown severely impaired intracellular RNA replication (>95 %), core protein expression and colony formation in cells harbouring a replicative full-length genotype 1b HCV replicon (HCV-O). In addition, infection of DDX3 knockdown cells with JFH1 virus caused approximately 90 % reductions in both intracellular HCV RNA levels and core protein release into the supernatant. However, shRNA knockdown of DDX3 only reduced SGR RNA replication by approximately 50 %, suggesting that the requirement of DDX3 for HCV replication applies more to the full-length genomes. To confirm the core protein from HCV-O and JFH1 interacted with DDX3, HEK-293T cells were co-transfected with vectors that expressed core from each genotype and HA-tagged DDX3. Immunoprecipitation of these transfected cell lysates using anti-HA antibody, followed by immunoblotting for core showed strong binding of HCV-O core but very weak binding of JFH1 core to DDX3. In addition, either core protein lacking the N-terminal first 40 aas failed to interact with DDX3 indicating this region

contains the DDX3 binding motif. They next tested the core-DDX3 interaction in Huh-7 derived cells lines harbouring HCV-O or infected with JFH1 by mixing each set of lysates with those from HEK-293T cells overexpressing HA-DDX3 and immunoprecipitating each mixture as before. While the HCV-O core was effectively co-immunoprecipitated, no JFH1 core was detectable. Thus, the core protein from the JFH1 strain appears to have a weaker interaction with DDX3 than the HCV-O core. The authors speculated that the RNA replication of full-length genomes is more impaired by DDX3 knockdown than the SGRs as they possess core. It is possible that core sequesters DDX3 to function in the efficient synthesis of full-length genomes. However, their results clearly made no link between DDX3 knockdown affecting virus replication and the core-DDX3 interaction (Ariumi *et al.*, 2007).

1.14. Aims

The aim of this project was divided into two lines of investigation. The first aim was to use the HCVcc model to characterise the interaction between core and DDX3 during authentic viral replication. To ascertain whether this interaction functions in the viral lifecycle, detailed characterisation studies were performed on a panel of HCVcc core mutants with altered binding affinity to DDX3. Secondly, the importance of two highly conserved core residues in HCVcc replication was investigated, specifically with respect to their roles in infectious particle assembly and productive viral infection.

2. Materials and Methods

2.1. Materials

2.1.1. Chemicals

Chemical / Reagent	Supplier
Absolute ethanol	Bamford Laboratories, UK
30 % Acrylamide/bis solution 37.5:1	Bio-Rad laboratories
Agarose	Melford
2-Amino-2-(hydroxymethyl)-1,3-propanediol (TRIS)	BDH
Ammonium persulphate (APS)	Bio-Rad Laboratories
Ampicillin (Amp)	Melford
Bromophenol blue (BPB)	BDH
Butanol	Fisher Scientific
Chloroform	Sigma
4',6-diamidino-2-phenylindole (DAPI)	Promega
Electroporation cuvettes (1 and 4 mm)	Apollo
Ethanol	Fisher Scientific
Ethidium bromide	Sigma
Glucose	BDH
Glycine	BDH
Isopropanol	Fisher Scientific
β-Mercaptoethanol	Sigma
Methanol	Fisher Scientific
Mung Bean nuclease	NEB
Pipette tips (RNase free)	Starlabs
Phenol	Sigma
Proteinase K	Invitrogen

Restriction enzymes	NEB
Sodium chloride (NaCl)	BDH
Sodium dodecyl sulphate (SDS)	BDH
Sucrose	BDH
N,N,N',N'-Tetramethylethylene-diamine (TEMED)	Sigma
Triton X-100	Sigma
TRIzol	Invitrogen
Tween-20	Bio-Rad Laboratories

2.1.2. Kits

Kit	Source
Advantage® cDNA polymerase Kit	Clonetech
QIAprep Spin Miniprep Kit	Qiagen
QIAquick Gel Extraction Kit	Qiagen
Qiagen Plasmid Maxi Kit	Qiagen
QuickChange Site-Directed Mutagenesis Kit	Stratagene
RNeasy Plus Mini Kit	Qiagen
TaqMan Reverse Transcription Kit	Applied Biosystems
MEGAscript High Yield Transcription Kit	Ambion
MEGAclear Purification Kit	Ambion

2.1.3. Cells

Cells	Description	Source
Huh-7	Human Hepatoma cell line	Jean Dubuisson (CNRS, Institut de Biologie de Lille, Lille, France)
HEK-293T	Human Embryonic Kidney	American Type Culture

	cell line	Collection

2.1.4. Transfection Reagents

Reagent	Source
Lipofectamine RNAiMAX	Invitrogen
Calcium phosphate Transfection Kit	Sigma

2.1.5. Cell Culture Growth Medium

All cell culture media components were supplied by Invitrogen. Huh-7 and HEK-293T cells were grown in complete Dulbecco's modified Eagle's medium (DMEM) supplemented with 10 % fetal calf serum (FCS), 100 U/ml penicillin, 100 μg/ml streptomycin, 0.1 mM non-essential aas and 2 mM glutamine.

2.1.6. Primary Antibodies

The monoclonal antibodies and polyclonal antisera used in this study are listed below:

Antibody	Name	Type	Raised in	Source
Anti-core	C7-50	mAb	Mouse	Bioreagents
Anti-core	R308	pAb	Rabbit	Hope & McLauchlan (2000)
Anti-core	R526	pAb	Mouse	Clayton *et al*. (2002)
Anti-NS5A	9E10	mAb	Mouse	Lindenbach *et al*. (2005)
Anti-NS5A	Anti-NS5A	pAb	Sheep	Macdonald *et al*. (2003)
Anti-E2	AP33	mAb	Mouse	Clayton *et al*.

				(2002)
Anti-E2	ALP98	mAb	Mouse	Clayton *et al.* (2002)
Anti-ADRP	ADRP 4	pAb	Sheep	Targett-Adams *et al.* (2003)
Anti-DDX3	AO196	mAb	Mouse	Angus *et al.* (2010)
Anti-DDX3	R648	pAb	Rabbit	Angus *et al.* (2010)
Anti-GFP	Anti-GFP	mAb	Mouse	Sigma
Anti-α-Tubulin	Anti-Tubulin	mAb	Mouse	Sigma
Anti-CD81	Anti-CD81	mAb	Mouse	BD Biosciences
Anti-core biotinylated	BR526	Biotin labelled pAb R526	Rabbit	A. Owsianka, unpublished
Anti-DDX3 biotinylated	BR648	Biotin labelled pAb R648	Rabbit	Angus *et al.* (2010)

2.1.7. Secondary Antibodies

Antibody	Source
FITC-conjugated donkey anti-sheep IgG	Invitrogen
FITC-conjugated donkey anti-mouse IgG	Invitrogen
FITC-conjugated goat anti-rabbit IgG	Invitrogen
TRITC-conjugated goat anti-mouse IgG	Invitrogen
TRITC-conjugated donkey anti-sheep IgG	Invitrogen
Cy5-conjugated donkey anti-rabbit IgG	Invitrogen
Anti-streptavidin-HRP conjugate	Sigma
Anti-mouse-HRP conjugate	Sigma
Anti-rabbit-HRP conjugate	Sigma

2.1.8. Clones

Name	Vector	Details	Source
pJFH1	pUC	Full-length JFH1 cDNA downstream of the T7 RNA polymerase promoter.	Wakita *et al.* (2005)
pJFH1$_{\Delta E1E2}$	pUC	As pJFH1, except carries a deletion in the envelope glycoprotein sequences situated downstream of the T7 RNA polymerase promoter.	Wakita *et al.* (2005)
pJFH1$_{GND}$	pUC	As pJFH1, except carries a mutation in the NS5B GDD motif, downstream of the T7 RNA polymerase promoter.	Wakita *et al.* (2005)
pJFH1$_{DP}$	pUC	As pJFH1, except carries two mutations in core (P138A and P143A), downstream of the T7 RNA polymerase promoter.	Boulant *et al.* (2007)
pJFH1$_{F130E}$	pUC	As pJFH1, except carries a mutation in core (F130E), downstream of the T7 RNA polymerase promoter.	Boulant *et al.* (2007)
pJFH1$_{VLVL}$	pUC	As pJFH1, except carries four mutations in core (A180V, S183L, C184V and T186L), downstream of the T7 RNA polymerase promoter.	Targett-Adams *et al.* (2008b)
pGEM T-JFH1$_{1-2614}$	pGEM T Easy	Cloning vector containing JFH1 strain nucleotides 1-2614	Dalrymple, (2007)
pJFH1$_{F24A}$	pUC	As pJFH1, except carries a mutation in core (F24A), downstream of the T7 RNA	Dalrymple, (2007)

		polymerase promoter.	
pJFH1$_{G27A}$	pUC	As pJFH1, except carries a mutation in core (G27A), downstream of the T7 RNA polymerase promoter.	Dalrymple, (2007)
pJFH1$_{I30A}$	pUC	As pJFH1, except carries a mutation in core (I30A), downstream of the T7 RNA polymerase promoter.	Dalrymple, (2007)
pJFH1$_{G33A}$	pUC	As pJFH1, except carries a mutation in core (G33A), downstream of the T7 RNA polymerase promoter.	Dalrymple, (2007)
pJFH1$_{V34A}$	pUC	As pJFH1, except carries a mutation in core (V34A), downstream of the T7 RNA polymerase promoter.	Dalrymple, (2007)
pJFH1$_{Y35A}$	pUC	As pJFH1, except carries a mutation in core (Y35A), downstream of the T7 RNA polymerase promoter.	Dalrymple, (2007)
pJFH1$_{\Delta E1E2(Y35A)}$	pUC	As pJFH1, except carries a mutation in core (Y35A) and a large deletion in the envelope glycoprotein sequences, downstream of the T7 RNA polymerase promoter.	A. Patel, unpublished
pJFH1$_{G32D/G33A}$	pUC	As pJFH1, except carries two mutations in core (G32D/G33A), downstream of the T7 RNA polymerase promoter.	A. Angus, this work
pJFH1$_{G33A/V34A}$	pUC	As pJFH1, except carries two mutations in core (G33A/V34A), downstream of the T7 RNA	A. Angus, this work

		polymerase promoter.	
pJFH1$_{G33A/L36S}$	pUC	As pJFH1, except carries two mutations in core (G33A/L36S), downstream of the T7 RNA polymerase promoter.	A. Angus, this work
pJFH1$_{G33A/L37S}$	pUC	As pJFH1, except carries two mutations in core (G33A/L37S), downstream of the T7 RNA polymerase promoter.	A. Angus, this work
pJFH1$_{F24L}$	pUC	As pJFH1, except carries a mutation in core (F24L), downstream of the T7 RNA polymerase promoter.	A. Angus, this work
pJFH1$_{F24I}$	pUC	As pJFH1, except carries a mutation in core (F24I), downstream of the T7 RNA polymerase promoter.	A. Angus, this work
pJFH1$_{F24V}$	pUC	As pJFH1, except carries a mutation in core (F24V), downstream of the T7 RNA polymerase promoter.	A. Angus, this work
pJFH1$_{F24Y}$	pUC	As pJFH1, except carries a mutation in core (F24Y), downstream of the T7 RNA polymerase promoter.	A. Angus, this work
EGFP-DDX3	pEGFP-C1	Full-length DDX3 gene cloned into the *Bam*HI site, in frame to sequences encoding EGFP.	Angus *et al,* (2010)

2.1.9. Bacterial Strains

Plasmids were manipulated and grown in the *Escherichia coli* strain DH5-α.

2.1.10. Solutions

2.1.10.1. Bacterial Expression

Solution	Components
L-Broth (LB)*	170 mM NaCl, 10 g/l Bactopeptone, 5 g/l yeast extract
LB-agar*	LB plus 1.5 % (w/v) agar
Yeast tryptose broth (YTB)*	85 mM NaCl, 16 g/l Bactopeptone, 10 g/l yeast extract

* Prepared in-house by the media department

2.1.10.2. DNA Manipulation

Solution	Components
DNA loading dye	30 % glycerol; 0.25 % BPB
TBE (10x)	8.9 M Tris-borate, 8.9 M boric acid, 0.02 M EDTA (pH 8.0)

2.1.10.3. SDS-PAGE

Solution	Components
Running gel buffer	40 mM Tris, 185 mM Glycine, 0.1 % SDS
Resolving gel buffer	0.5 M Tris-HCl pH 8.9, 0.4 % SDS
Stacking gel buffer	0.5 M Tris-HCl pH 6.9, 0.4 % SDS
Sample loading buffer (reducing)	100 mM Tris-HCl pH 6.9, 2 % SDS, 10 % glycerol, 5 % β-mercaptoethanol, 1 µg/ml bromophenol blue
Sample loading buffer (non-reducing)	100 mM Tris-HCl pH 6.9, 2 % SDS, 10 % glycerol, 1 µg/ml BPB

2.1.10.4. Western Immunoblotting

Solution	Components
Towbin buffer	25 mM Tris-HCl (pH 8.0), 192 mM glycine, 20 % (v/v) methanol
PBS (A)*	170 mM NaCl, 3.4 mM KCl, 10 mM Na_2HPO_4, 1.8 mM KH_2PO_4, 25 mM Tris-HCl (pH 7.2)
PBS (A) –Tween (PBST)	PBS (A), plus 0.05 % (v/v) Tween-20
Blocking buffer	PBST plus 5 % (w/v) dried milk (Marvel)

*Prepared in-house by the media department

2.1.10.5. Cell Lysis

Solution	Components
Immunoprecipitation buffer (LB2)	20 mM Tris-HCl pH 7.4, 20 mM iodoacetamide, 150 mM NaCl, 1 mM EDTA, 0.5 % Triton X-100
Cell Lysis/Co-immunoprecipitation buffer (Masaki Buffer)	20 mM Tris-HCl, pH 7.4, 135 mM NaCl, 0.1 % Triton X-100, 50 mM NAF, 5 mM NA_3VO_4, 1 mM Phenylmethylsulfonyl fluoride (PMSF)

2.1.10.6. Tissue Culture

Solution	Components
Trypsin solution	0.25 % (w/v) Difco trypsin dissolved in PBS(A), 0.002 % (w/v) phenol red
Versene	0.6 mM EDTA in PBS(A), 0.002 % (w/v) phenol red

2.1.11. Oligonucleotide Synthesis

Oligonucleotides were ordered from Sigma.

2.1.12. siRNAs

Two pre-validated siRNA duplexes targeting different regions of the human DDX3 gene (s4004 and s4005) and a negative control siRNA composed of a scrambled sequence were supplied by Appied Biosystems in 1 nM quantities. These were resuspended in RNase free water to yield a stock concentration of 10 µM.

2.2. Methods

2.2.1. Tissue Culture Maintenance

2.2.1.1. Cell Passaging

Huh-7 cells were propagated at 37 °C in complete DMEM in an atmosphere of 5 % CO_2. Cell lines were typically grown in 80 cm^2 or 175 cm^2 tissue culture flasks (Nunc). Passage of cells was carried out when cells reached 90 % confluency by first gently washing cells in ice-cold PBS(A) followed by their removal with trypsin (Sigma) diluted 1:100 in versene (TV). Cells were then resuspended in 10 ml of complete DMEM before re-seeding or use in experiments.

2.2.1.2. Long Term Storage of Cells

Aliquoted cells were stored in DMEM containing 25 % FCS and 10 % DMSO. Aliquots were left overnight at -70 °C before being transferred to -180 °C for long-term storage.

2.2.2. Production of Electrocompetent Bacterial Cells

LB (1 L) was inoculated with 10 ml of fresh overnight *E. coli* DH5-α culture and grown at 37 °C to an OD_{600} of ~0.8. The flask was chilled on ice for 30 min and centrifuged at 4000 r.p.m. for 10 min at 4 °C using a Sorval RC-5B Refrigerated Superspeed Centrifuge. Supernatant was removed and the pellet resuspended in 1 L ice-cold deionised molecular biology grade water (dH_2O). Cells were re-centrifuged as before and resuspended in 500 ml ice-cold dH_2O with 10 % glycerol. Again cells were centrifuged as before and resuspended in 2-3 ml ice-cold dH_2O with 10 % glycerol before being aliquoted into 70 μl aliquots and stored for up to 6 months at -70 °C.

2.2.3. DNA Manipulation

2.2.3.1. Quantitation of DNA

DNA aliquots were diluted 1:50 in dH_2O and the OD measured using a BioPhotometer (Eppendorf).

2.2.3.2. Restriction Enzyme Digestion of DNA

All restriction enzyme digests of plasmid DNA were carried out at 37 °C for at least 1 h unless otherwise specified by the manufacturer. Typically, 10 U of each enzyme per μg DNA were used in a total volume of 50 μl. All reactions were performed using the appropriate enzyme buffers and BSA if necessary.

2.2.3.3. Ligation of DNA Fragments

Gel purified DNA fragments (Section 2.2.3.7) were ligated for 16 h at 16 °C in 10 µl reactions containing 1x ligase buffer and 2 U of T4 DNA ligase. Following ligation, 2 µl DNA was used for electroporation into competent *E. coli* bacteria (Section 2.2.3.4).

2.2.3.4. Transformation of Electrocompetent *E.coli* Cells

Plasmid or ligated DNA (2 µl) was added to 70 µl electrocompetent *E. coli* in a pre-chilled 1 mm gap cuvette and electroporated (1.8 kV, 25 µF, 200 Ω) using a BioRad GenePulser Xcell. The bacteria were then resuspended in 0.5 ml YTB and incubated at 37 °C for 1 h before being plated on LB-agar plates with ampicillin, final concentration 100 µg/ml (LB-agar + Amp). Plates were then incubated overnight at 37 °C.

2.2.3.5. Small Scale Plasmid Preparation from Transformed Bacteria

A single colony from a freshly streaked selective agar plate was picked (Section 2.2.3.4) and used to inoculate a 5 ml culture of LB with ampicillin (LB-Amp). Following culture for 16 h at 37 ºC with vigorous shaking (180 r.p.m.), the bacteria were centrifuged in a Sanyo MSE MicroCentaur at 13,000 r.p.m. and the DNA extracted from the bacterial pellet using the QIAprep miniprep kit according to the manufacturer's instructions.

2.2.3.6. Large Scale Plasmid Preparation from Transformed Bacteria

A single colony from a freshly streaked selective agar plate was picked (Section 2.2.3.4) and used to inoculate a 5 ml starter culture of LB-Amp. Following 8 h incubation, the starter culture was diluted 1:500 into 200 ml of LB-Amp and cultured for 16 h at 37 ºC with vigorous shaking (180 r.p.m.). The bacteria were then harvested by centrifugation at 3000 r.p.m. for 10 min at 4 ºC using a Sorval RC-5B Refrigerated Superspeed Centrifuge.

A large scale DNA preparation was then made from the bacteria using the Qiagen HiSpeed plasmid Maxi kit according to the manufacturer's instructions.

2.2.3.7. Isolation and Purification of DNA from Agarose Gels

This method was employed to resolve DNA fragments produced by PCR (Section 2.2.3.11) or restriction enzyme digestion (Section 2.2.3.2). To separate fragments slab gels containing 0.8 % agarose were prepared in 1 x TBE containing ethidium bromide (1 µg/ml). DNA fragments were run alongside 1 Kbp or 100 bp ladders (NEB). DNA samples were mixed with 0.1 volumes of 10 x DNA loading dye before being loaded into the wells of the gel. Gels were typically run at 100 V in 0.5 x TBE buffer. To purify DNA, fragments were visualised with the aid of long wave UV light and then excised using a clean scalpel. Excised fragments were then purified using the QIAQuick gel extraction kit (Qiagen) according to the manufacturer's instructions.

2.2.3.8. Site-Directed Mutagenesis

Mutagenesis reactions were performed using the QuickChange Site-Directed Mutagenesis kit (Stratagene). Forward and reverse primers for mutagenesis (Appendix 1) were designed to incorporate the desired mutation(s) in the middle of the primer sequence and were between 25 and 45 bases in length, according to the manufacturer's instructions. PCR reactions were performed in a GeneAmp PCR machine (Applied Biosystems) as follows:

Reaction components:

Component	Amount
DNA template	50.0 ng
Forward primer (10 µM)	1.25 µl
Reverse primer (10 µM)	1.25 µl
dNTP mix	1.0 µl
10x reaction buffer	5.0 µl
dH_2O	Up to 50.0 µl

Reaction cycle:

Stage 1

- Hold at 95 °C for 30 s

Stage 2 (6 cycles)

- Hold at 95 ° C for 30 s
- Hold at 55 ° C for 1 min
- Hold at 68 ° C for 6 min

Following PCR, each reaction was chilled on ice for 2 min followed by the addition of DpnI (10 U) to digest the non-mutated dam-methylated parental DNA. Reactions were mixed by pipetting, then centrifuged in a Sanyo MSE MicroCentaur at 13,000 r.p.m. for 1 min, followed by incubation at 37 ºC for 1 h. DpnI-treated DNA was transformed into 50 µl XL1-Blue Supercompetent bacteria. Bacteria were thawed on ice after which 2 µl mutant DNA was added to the competent cells, which were incubated on ice for a further 30 min. DNA-bacteria mixtures were then heat-pulsed at 42 ºC for 45 s and then incubated on ice for a further 2 min. 0.5 ml of YTB pre-heated to 42 ºC was added to each mixture, followed by incubation at 37 ºC for 1 h with shaking at 180 r.p.m. Total cultures were pelleted at 4000 r.p.m using a Sanyo MSE MicroCentaur. for 3 min, resuspended in 50 µl YTB and plated onto LB-agar + Amp and incubated at 37 ºC overnight.

2.2.3.9. Introducing Core Mutations into pJFH1

All core mutations were individually introduced into pGEM T-JFH1$_{1\text{-}2614}$ by site-directed mutagenesis (Section 2.2.3.8). Three colonies from each agar plate were picked and used to prepare plasmid mini-preps (Section 2.2.3.5). Plasmids were sequenced (Section 2.2.3.12) between nucleotides 1-1369 using primers NA7, NA11, NA12, NA13, NA15 and NA18 (Appendix 1). Positive clones were then restriction digested with *Eco*RI and *Bsi*WI (Section 2.2.3.9.1) to remove nucleotides 1-1369 of JFH1, which were subsequently ligated (Section 2.2.3.3) back into the parental pJFH1 vector backbone. The ligation mixture was then transformed into bacteria and used to prepare a plasmid maxi-prep (Section 2.2.3.6). To confirm the fragment had ligated correctly and contained the desired sequence, a diagnostic digest was performed on an aliquot of plasmid preparation using *Eco*RI and *Bsi*WI (Section 2.2.3.9.1) in addition to nucleotide sequencing the insert region

using the same primers as before. Following these checks the plasmids were linearised (Section 2.2.3.13) and used to prepare *in vitro* transcribed viral RNA (Sections 2.2.4.1)

2.2.3.9.1. *Eco*RI/*Bsi*WI Digest Reaction Mix

Component	Volume (µl)
Plasmid DNA	5.0
Buffer 3	2.0
*Bsi*WI	1.0
dH_2O	12.0

The above digest was incubated at 55 ºC/ 1 h. The reaction was then incubated on ice for 2 min to reduce the temperature before adding 1 µl *Eco*RI and incubating at 37 ºC/ 1 h.

2.2.3.10. Preparation of HCV cDNA for Sequencing

Total RNA was extracted from infected Huh-7 cells using the RNeasy kit (Section 2.2.4.2). Total RNA (100 ng) was then subjected to a reverse transcription reaction (Section 2.2.6.1) using 2 pmol of the HCV specific primer NegRT (Appendix 1) to synthesise cDNA from negative-strand viral RNA. After digestion with 1 U RNase H for 20 min at 37 ºC, one quarter of the cDNA reaction was amplified by PCR using core specific primers (Section 2.2.3.11). PCR products were gel purified (Section 2.2.3.7) and sequenced (Section 2.2.3.12).

2.2.3.11. Polymerase Chain Reaction (PCR) Amplification of DNA

PCR was performed to amplify viral cDNA generated from infected cell total RNA. The product of this reaction was to be used for direct sequence analysis (Section 2.2.3.12) and thus it was crucial to obtain high yields of accurately amplified DNA. This was done using the Advantage cDNA polyermase kit (Clonetech), which uses two DNA polymerases simultaneously (KlenTaq-1 and proof-reading enzyme) along with the TaqStart® antibody to provide automatic “hot start” PCR. These components increase the range, accuracy and yield of the PCR reaction. The reaction was performed in a GeneAmp PCR machine (Applied Biosystems) as follows:

Reaction components:

Component	Volume (µl)
dH_2O	36.0
10x cDNA PCR reaction buffer	5.0
cDNA template	5.0
Forward primer (NA11) (10 µM)	1.0
Reverse primer (NA14) (10 µM)	1.0
10 mM dNTP	1.0
DNA polymerase	1.0
Total volume	50.0

Reaction Cycle:

Stage 1

-Hold at 95 °C for 1 min – Denaturation of taq antibody

Stage 2 (35 cycles)

-Hold at 94 °C for 30 s – Denaturation of template

-Hold at 68 °C for 3 min – Primer annealing

Stage 3

-Hold at 68 °C for 3 min – Primer extension

Stage 4

-Hold at 15 °C

The entire PCR reaction was then subjected to agarose gel electrophoresis and the band of interest purified by gel extraction (Section 2.2.3.7).

2.2.3.12. Nucleotide Sequencing

Nucleotide sequencing of plasmid and amplified cDNA was performed using the core specific primers NA11, NA12, NA13 and NA14 (Appendix 1) by GATC biotech, Germany. A minimum of 30 µl of DNA (100 ng/µl) and primers (10 µM) were required for each reaction. Completed sequences were analyzed using Chromas (Applied Biosystems) and NCBI alignment software.

2.2.3.13. Restriction Digestion of pJFH1 for *In Vitro* Transcription

Plasmids were linearised by *Xba*I digestion in a 100 µl reaction in an 1.5 ml RNase-free tube (Ambion) followed by treatment with Mung Bean nuclease to digest the sticky ends (30 °C for 30 min). To clean the template of proteins Proteinase K (final concentration 100 µg/ml) and SDS (final concentration 0.5 %) were added and incubated at 50 °C for 30 min. The template was then treated with 100 µl of neutral phenol-chloroform (25 parts saturated neutral phenol: 24 parts chloroform: 1 part isoamylalcohol), vortexed for 1 min and centrifuged at 13,000 r.p.m. for 2 min using a Sanyo MSE MicroCentaur. The aqueous layer was placed in a fresh RNase-free centrifuge tube and 0.1 volumes 5 M NH_4OAc added along with 3 volumes 100 % ethanol. The sample was stored at -20 °C for 30 min before being centrifuged in a Sanyo MSE MicroCentaur at 13,000 r.p.m. for 15 min to pellet the precipitated DNA. The ethanol was carefully removed from the tube and the pellet dried at room temperature before being resuspended in 30 µl nuclease-free dH_2O. The concentration of linear DNA template was then determined (Section 2.2.3.1).

2.2.4. RNA Manipulation

2.2.4.1. *In Vitro* Transcription

In vitro transcription was carried out using a T7 Megascript kit (Ambion) following the manufacturer's instructions using 1 µg of linear DNA template. The RNA was then purified using the MEGAclear kit to remove nucleotides, short oligonucleotides, proteins, and salts from the RNA. The amount of RNA was obtained by diluting an aliquot of the RNA 1:50 in dH_2O and reading the OD using a BioPhotometer (Eppendorf). Typically, this kit yielded RNA concentrations of 70-100 µg.

2.2.4.2. Preparation of Total RNA

RNA was extracted from cells grown on a 25 cm^2 flask, a 6-well or a 24-well dish using the RNeasy Mini kit (Qiagen) according to the manufacturer's instructions. This kit is

designed to purify up to 100 µg of total RNA from mammalian cells that is ready for use in downstream applications including RT-PCR (Section 2.2.3.11) and RT-qPCR (Section 2.2.6). This technology relies on the selective binding properties of silica-based membranes within microspin columns that bind RNA longer than 200 bases under the high salt buffer conditions. DNase digestion is not required with RNeasy Kits since RNeasy silicamembrane technology efficiently removes DNA without DNase treatment.

2.2.4.3. Preparation of Extracellular HCV RNA

All RNA extractions were performed in RNase-free 1.5 ml tubes (Ambion). Aliquots of viral pellets resupsended in PBS(A) or sucrose gradient fractions were lysed in TRIzol LS reagent to a total volume of 400 µl. Chloroform (110 µl) was added and the sample shaken vigorously for 15 s before being incubated at room temperature for 15 min. Samples were then centrifuged in a Sanyo MSE MicroCentaur at 13,000 r.p.m. for 15 min and the aqueous (upper) phase added to 500 µl isopropanol. This was incubated at room temperature for 10 min before being centrifuged as before. After decanting, the pellet was washed in 75 % ethanol, mixed by vortexing, and centrifuged in a Sanyo MSE MicroCentaur at 13,000 r.p.m. for 10 min. The pellet was then dried at room temperature and resuspended in 20 µl of nuclease-free H_2O (Ambion). RNA was stored at -70 °C or used for quantification by RT-qPCR (Section 2.2.6).

2.2.5. Introduction of DNA/RNA into Eukaryotic Cells

2.2.5.1. Transfection of DNA

The calcium phosphate transfection method was used to introduce plasmid DNA into HEK-293T cells. This method is based upon the formation of a precipitate containing calcium phosphate and DNA. Two million cells were seeded into 90 mm tissue culture dishes in 20 ml complete DMEM 24 h before transfection. In a sterile 1.5 ml eppendorf 8 µg DNA and molecular biology-grade water were added to a total volume of 400 µl followed by 100 µl of 2.5 M $CaCl_2$. In a second 1.5 ml tube, 500 µl of 2x HEPES-Buffered Saline (HeBS), pH 7.05 was added. To prepare the precipitate, the HeBS solution containing sodium phosphate was slowly mixed with the $CaCl_2$ solution containing the

DNA. To do this the HeBS was gently bubbled using an automatic pipette pump attached to a 1 ml sterile serological pipette during which time the $CaCl_2$/DNA solution was added drop wise with a sterile pipette tip. The precipitate was then incubated for 20 min at room temperature. The precipitate was then distributed over the cells in the culture dish in a drop wise fashion using sterile pipette tip followed by gentle agitation for mixing. This DNA-calcium phosphate co-precipitate adheres to the cell surface and is taken up by the cell, presumably by endocytosis. At 24 h post-incubation, the cells were washed once in PBS(A) and lysed for Western immunoblotting (Section 2.2.8.3).

2.2.5.2. Electroporation of RNA

Following trypsin treatment and counting, aliquots of 4 x 10^6 cells were centrifuged in 15 ml centrifuge tubes at 1000 r.p.m. for 5 min at room temperature using a Thermoscientific Heraeus Megafuge 16R. Media was decanted and pelleted cells were washed by resuspension in 10 ml PBS(A), and centrifuged as before. PBS(A) was decanted and cell pellets were resuspended in a total volume of 400 µl PBS(A) and added to a 4 mm gap cuvette along with 10 µg of *in vitro*-transcribed viral RNA. Electroporation was performed using a BioRad GenePulser Xcell (250 V, 950 µF), following the manufacturer's instructions. Cells were then diluted and resuspended in the indicated amount of complete DMEM and seeded into the appropriate tissue culture flask or plate.

2.2.6. Reverse Transcription-Quantitative PCR (RT-qPCR)

RT-qPCR was a two-step protocol involving the reverse transcription of RNA followed by a real-time PCR reaction using either relative or absolute quantification conditions.

2.2.6.1. First-Strand cDNA Synthesis

Reverse transcription of viral and cellular RNAs was performed using the TaqMan Reverse Transcription Reagents Kit. For each reaction 1 µl of RNA was reverse transcribed using the following reaction mix and temperature cycles:

cDNA Synthesis Reaction Mix (1x):

Component	Volume (µl)
10x RT Buffer	2.0
$MgCL_2$	4.4
dNTPs	4.0
Random Hexamers	1.0
RNase Inhibitor	0.4
Multiscribe Reverse Transcriptase	0.5
dH_2O	6.7
RNA	1.0

Reaction Cycle:

Stage 1

- Hold at 25 °C for 10 min

Stage 2

- Hold at 37 °C for 60 min

Stage 3

- Hold at 95 °C for 5 min

Stage 4

-Hold at 4 °C

2.2.6.2. REAL-TIME PCR

2.2.6.2.1. Relative Quantification (RQ)

The relative quantity of viral RNA from electroporated or infected cells was determined by an RQ reaction. The cDNA obtained from the reverse transcription of total intracellular RNA (Section 2.2.6.1) was amplified using both HCV-specific and GAPDH-specific primers (Applied Biosystems) in the presence of FAM™ (HCV-specific) and VIC® (GAPDH-specific) labelled probes. The JFH1 probe and primer sequences are located in the 5' UTR of the viral genome (Appendix 1). Each sample was run in triplicate as a singleplex reaction. The reaction mixes are listed below along with the reaction cycle conditions performed on an Applied Biosystems 7500 Fast Real-Time PCR System using Fast Universal PCR conditions:

Real-Time PCR Reaction Mix for JFH1 RNA:

Component	Volume (µl)
18 µm Forward Primer (Final 900 nm)	1.0
18 µm Reverse Primer (Final 900 nm)	1.0
5 µm FAM JFH1 Probe (250 nm)	1.0
TaqMan Fast Universal Mix (2x)	10.0
dH_2O	5.0
cDNA	2.0

Real-Time PCR Reaction Mix for GAPDH RNA:

Component	Volume (µl)
GAPDH Probe	1.0
TaqMan Fast Universal Mix (2x)	10.0
dH_2O	7.0
cDNA	2.0

Thermal Cycler Protocol:

Stage 1

- Hold at 95 °C for 20 s

Stage 2 (40 cycles)

- Hold at 95 °C for 3 s
- Hold at 60 °C for 30 s

The HCV signals were normalised to the endogenous GAPDH control and data analysed using Applied Biosystems software (SDS version 1.3.1), according to the manufacturer's instructions.

2.2.6.2.2. Absolute Quantification (AQ)

The absolute quantity of viral RNA obtained from purified virus was determined by an AQ reaction. The cDNA obtained from the reverse transcription (Section 2.2.6.1) of extracellular RNA was amplified using the HCV-specific primer/FAM probe combination

described for RQ (Section 2.2.6.2.1). *In vitro*-transcribed JFH1 genomic RNA of known concentration was used as a standard. Serially diluted standard cDNAs and undiluted sample cDNAs were analysed in triplicate and real-time reactions were amplified and analysed under the same Fast Universal PCR conditions as for RQ (Section 2.2.6.2.1).

2.2.7. Generation of JFH1 Virus

In vitro synthesized RNA (10 µg) was electroporated into Huh-7 cells (Section 2.2.5.2). The transfected cells were allowed to rest for 10 min before mixing with fresh medium and seeding into the indicated tissue culture dishes. Following incubation at 37 ^{o}C for the indicated time period, the medium containing the infectious virus progeny was filtered through a 0.45 µm pore-sized membrane before infectivity was determined (Section 2.2.7.1).

2.2.7.1 Measuring Virus Infectivity

Limiting dilution assays were used to quantify the amount of virus infectivity using either the focus forming unit (FFU) assay, as described by Zhong *et al*. (2005) or the 50 % Tissue Culture Infectious Dose ($TCID_{50}$) assay as described by Lindenbach *et al*. (2005). The $TCID_{50}$ assay measures the dilution of virus that will infect 50 % of replicate cell cultures. To determine the virus titer by $TCID_{50}$ assay Huh-7 target cells were seeded at a concentration of 1000 cells per well of a 96-well plate in a total volume of 100 µl complete DMEM. Twenty-four hours later, serial 5 or 10-fold dilutions of cell medium were added, with six wells per dilution. Forty-eight hours later, the medium was removed and the cells were fixed with ice-cold methanol and incubated at -20 °C for 24 h. The cells were then washed three times with PBS(A) and probed with anti-NS5A mAb 9E10 or sheep anti-NS5A pAb at dilutions of 1:20,000 and 1:10,000 in PBST, respectively for 1 h at room temperature. Cells were washed again three times with PBS(A) and bound primary antibody detected by incubation with the appropriate FITC-conjugated secondary antibody at 1:500 dilutions in PBST for 1 h at room temperature. After three washes in PBS(A) the cells were overlaid with 100 µl of dH_2O before visualization under a fluorescent microscope (Nikon Eclipse TS100) to determine the number of positive wells at each dilution. Wells with at least one NS5A-expressing cell were counted as positive, and the $TCID_{50}$ was calculated according to the method of Reed and Muench. An excel

spreadsheet was used to calculate the $TCID_{50}$, which is accessible at the following web link: http://www.med.yale.edu/micropath/pdf/Infectivity%20calculator.xls.

Cell-associated virus was obtained using previously established methods (Gastaminza *et al*., 2006; Shavinskya *et al*., 2008). Cells were electroporated with viral RNA as before and reseeded into a 90 mm tissue culture dish. Forty-eight hours post-incubation, cells were washed once in PBS(A) before being removed from the culture dish using a cell scraper in the presence of 10 ml PBS(A). The cells were then transferred to a 15 ml centrifuge tube and resuspended by rigorous pipetting before being centrifuged at 1000 r.p.m. for 5 min using a Thermoscientific Heraeus Megafuge 16R. After the PBS(A) was decanted, the cell pellet was resuspended in 0.8 ml complete DMEM, and freeze-thawed rapidly three times using dry ice/ethanol and a water bath set to 37 ºC. The samples were centrifuged at 4000 r.p.m. for 5 min using a Thermoscientific Heraeus Megafuge 16R to remove cell debris, and the supernatant assayed by $TCID_{50}$ to determine virus infectivity. Titration of HCVcc by FFU is based on the previously described method for measuring HCV infectivity (Zhong *et al*., 2005). This assay uses an identical infection setup as for $TCID_{50}$, except using only 3 wells per dilution. The immunostaining protocol for HCV positive cells is also the same as $TCID_{50}$. The viral titer is calculated as FFU/ml by the average number of NS5A-positive foci detected at the highest dilution.

2.2.7.2. Analysis of Virus Replication

To measure virus replication at 120 h post-electroporation cells were transfected with the viral RNA, seeded into 10 cm culture dishes and split 1:2 at 48 h post-incubation. After further 72 h incubation, the cells were lysed in RLT buffer (RNeasy kit) to measure the intracellular HCV RNA levels by RT-qPCR assay (Section 2.2.6) and the cell culture medium was harvested for titration by $TCID_{50}$ assay (Section 2.2.7.1). To determine virus replication kinetics over a 72 h period electroporated cells were seeded into 10 cm culture dishes in 15 ml DMEM and incubated at 37 ºC/5 % CO_2 for 4 h. The cells were then washed in 20 ml PBS(A), trypsinized in 2 ml of TV and resuspended in 15 ml DMEM. Next, 14 ml of the cell suspension was pelletted in a Thermoscientific Heraeus Megafuge 16R at 1000 r.p.m./5 min, while the remaining ~1 ml of cells were transferred to a 2 ml cyrotube, pelletted as before and lysed in RLT buffer for RT-qPCR assay. The pelletted cells were then resuspended in 10 ml of DMEM and split 1:3 into 3 T25 flasks in a total volume of 5 ml of medium per flask. Cell lysates and cell culture supernatants were

harvested at 24, 48 and 72 hours for RT-qPCR (Section 2.2.6) and $TCID_{50}$ assay (Section 2.2.7.1), respectively. To measure virus replication after infection, 53,000 naïve Huh-7 cells were seeded into three 6-well culture dishes. For each virus cells were infected at the indicated multiplicity of infection (m.o.i.) in a total volume of 900 µl for 6 h before supplementing with 2 ml of fresh DMEM. At 24, 48, 72 and 96 h cell lysates and culture supernatants were harvested as before. Reseeding cells from 96 h post-infection into a T25 flask with 5 ml of fresh DMEM achieved the 144 h time-point. To monitor virus infectivity during serial passaging, 2 x 10^6 naïve Huh-7 cells were electroporated with the *in vitro*-transcribed viral RNA and seeded into a T80 flask in a total of 25 ml of DMEM. Cells were passaged at the time of subconfluency into a new flask containing 24 ml fresh DMEM. At each passage the cell culture supernatants were harvested and the released virus infectivity determined by $TCID_{50}$ assay (Section 2.2.7.1)

2.2.8. Detection of Cellular and Viral Proteins

2.2.8.1. Sample Lysis for SDS-PAGE Analysis

To detect intracellular antigens, cultured cells were washed once in PBS(A) and either lysed directly in SDS-PAGE sample loading buffer (reducing) or lysed in 500 µl of Masaki buffer. For lysis in sample loading buffer, the lysates were homogenized by passing through a 22-gaugle needle five times before use. Following lysis in Masaki buffer, the lysate was spun briefly (13,000 r.p.m. for 1 min using a Sanyo MSE MicroCentaur) to remove nuclei. After pre-clearing, the clarified lysates (10 or 20 µl aliquots each) were mixed 1:1 with 2x sample loading buffer. To detect extracellular core, 10 ml of each conditioned media were overlaid onto 1 ml of a 20 % (w/v) sucrose cushion made with PBS(A), centrifuged at 25,000 r.p.m. for 4 hours using a Sorvall Discovery 90SE ultracentrifuge, and the pellets were resuspended in 20 µl of Masaki buffer. Lysates were clarified and mixed with sample loading buffer as described. All samples were denatured by boiling at 100 ºC for 5 min before use.

2.2.8.2. Denaturing Polyacrylamide Gel Electrophoresis (SDS-PAGE)

Resolving gels were prepared using acrylamide solution at a final concentration of 10-14 % in 1x resolving gel buffer. Addition of APS (to 0.1 %) and TEMED (to 0.08 %) initiated polymerisation and the solution was immediately poured into the gel assembly apparatus, leaving a gap of ~2 cm from the top. The solution was then overlaid with 1 ml of 100 % butanol. When polymerisation was complete, the butanol was discarded and the gel surface was washed thoroughly with dH_2O. Stacking gels were prepared using acrylamide at a final concentration of 5 % in 1x stacking gel buffer. Again, polymerisation was initiated upon the addition of APS (to 0.1 %) and TEMED (to 0.08 %), before the solution was overlaid onto the resolving gel. A 10-tooth Teflon comb was typically used to form wells in the stacking gel. The gel was allowed to polymerise before removal of the comb. Gels were then loaded into a tank and submerged in running gel buffer. Denatured protein samples were then loaded into each well. Protein markers (Amersham) were also included for protein size determination and empty wells were filled with an equal volume of SDS-PAGE sample loading buffer. Electrophoresis was performed at 100 V until the required separation of protein markers and samples was achieved. Gels were then removed from the apparatus for Western immunoblotting (Section 2.2.8.3).

2.2.8.3. Western Immunoblotting

Proteins separated on polyacrylamide gels were transferred to HybondTM-ECL^{TM} nitrocellulose membranes using a BioRad transblot Semi-Dry blotting device. Transfer was carried out at 25 V for 15 min and membranes were incubated in PBST containing 5 % milk powder to block non-specific binding of antibody. Membranes were washed three times in PBST at room tempertaure and probed with the appropriate antibody (diluted in PBST) for 1 h at room temperature. The membrane was again washed three times with PBST and incubated with the appropriate secondary antibody (diluted in PBST) conjugated to HRP for 1 h at room temperature. Finally the membrane was washed three times in PBST and bound antibody was detected using Enhanced Chemiluminescence Reagents I and II (ECL I & II) (Amersham) in equal ratio. Bands were visualized by autoradiography using Kodak X-OMAT film and a Konica SRX-101-A film processor.

2.2.9. Immunoprecipitation (IP) of DDX3

Approximately 5 x 10^6 Huh-7 cells were washed once with PBS(A) and lysed in 1 ml LB2 and the lysate spun briefly to remove nuclei. Aliquots of 100 µl of the clarified cell lysates were incubated with rotation for 2 h with the anti-DDX3 antibodies described in the text followed by further 2 h incubation with 30 µl Protein G-sepharose beads (Sigma). The immune complexes were then precipitated by centrifugation at 2000 r.p.m. for 2 min using a Sanyo MSE MicroCentaur. Following three washes of the sepharose beads with 1 ml LB2, the immune complexes were analyzed by non-reducing SDS-10 % PAGE (Section 2.2.8.2) followed by Western immunoblotting (Section 2.2.8.3) using biotinylated R648 and anti-streptavidin-HRP conjugate.

2.2.10. Co-immunoprecipitation (co-IP) of HCV Core Protein

Huh-7 cells were electroporated with viral RNA (Section 2.2.5.2) and seeded into 100 mm tissue culture dishes. At 72 h post-incubation, the cells were washed once in PBS(A) and lysed in 0.5 ml of Masaki buffer. The lysates were spun briefly to remove nuclei. After pre-clearing, the clarified lysate was immunoprecipitated overnight with 30 µl of Protein G-sepharose beads that had been pre-incubated overnight with 6 µl of the anti-DDX3 antiserum R648. The immune complex was precipitated with the beads by centrifugation using a Sanyo MSE MicroCentaur at 2000 r.p.m. for 2 min, washed 3 times with 1 ml Masaki buffer, and subjected to non-reducing SDS-14 % PAGE (Section 2.2.8.2) followed by Western immunoblotting (Section 2.2.8.3) using the anti-core mAb C7-50 (1:20,000 dilution) and anti-mouse IgG-HRP conjugate.

2.2.11. Sedimentation Equilibrium Gradient Analysis

Gradients were formed in a 12 ml ultracentrifuge tube (Beckmann) by overlaying 1.3 ml of 20 %, 25 %, 30 %, 35 %, 40 %, 45 %, 50 %, 55 % and 60 % (w/v) sucrose solutions in PBS(A) and incubating at 4 °C overnight. Virus particles obtained at 72 h post-electroporation were purified through 20 % (w/v) sucrose cushions in PBS(A) at 25,000 r.p.m. for 4 h using a Sorvall Discovery 90SE ultracentrifuge. Virus pellets were resuspended overnight in a total of 600 µl of PBS(A) before being added to the 20-60 % continuous gradient. Equilibrium was reached by ultracentrifugation for 24 h at 36,000

r.p.m. at 4 °C using a Sorvall Discovery 90SE ultracentrifuge. Either six 2 ml or twelve 1 ml fractions were collected from the top after which their density was determined. Aliquots of 200 µl were used to determine the infectivity (Section 2.2.7.1) and RNA content (2.2.4.3) of each fraction. The remaining volume was then diluted in PBS(A) to a total volume of 11 ml and pelleted at 25,000 for 4 h using a Sorvall Discovery 90SE ultracentrifuge. The pellets were then lysed in 20 µl of Masaki buffer and subjected to reducing SDS-14 % PAGE (Section 2.2.8.2) following by Western immunoblotting (Section 2.2.8.3) using mAbs AO196 and C7-50.

2.2.12. RNA Interference

To assay virus replication from full-length JFH1 following infection of DDX3 knockdown cells, siRNAs were transfected into naïve Huh-7 cells using the lipofectamine RNAiMax reagent. Transfections were performed in 24-well plates. For each well, 100 µl Optimem-I was mixed with 1 µl lipofectamine and followed by the addition of the siRNAs. For the control transfections 1 µl of scrambled siRNA mix (50 µM) was added to the wells. For the test transfections 0.5 µl of each DDX3 siRNA mix (50 µM) was used. The transfection cocktail was gently mixed by pipetting and incubated for 20 min at room temperature. Wells were then seeded with 1 x 10^4 Huh-7 cells in 900 µl of DMEM, giving a total volume of 1 ml in each well with a final concentration of 50 nM of siRNAs. At 48 h post-incubation, the control and knockdown cells were infected with $JFH1_{WT}$ and $JFH1_{Y35A}$ virus for 4 h and supplemented with 1 ml of fresh DMEM. At 48 h post-infection, the culture medium was harvested and titrated by $TCID_{50}$ assay (Section 2.2.7.1) and the cells lysed in RLT buffer (Section 2.2.4.3) for RT-qPCR assay (Section 2.2.6). The efficiency of DDX3 knockdown at the time of virus infection was determined by lysing control and DDX3 knockdown cells in reducing SDS-PAGE sample loading buffer (Section 2.2.8.1) at 48 h post-transfection and subjecting them to SDS-10% PAGE (Section 2.2.8.2) following by Western immunoblotting (Section 2.2.8.3) with mAb AO196. To measure virus replication of $JFH1_{\Delta E1E2}$ following DDX3 knockdown, 2 x 10^6 naïve Huh-7 cells were electroporated with 10 µg of viral RNA along with siRNAs in a total volume of 0.4 ml PBS(A). In the control cells 10 µl of scrambled siRNA was added and for the test cells 5 µl of each DDX3 siRNA was used. After electroporation, cells were resuspended in 10 ml DMEM and seeded on to 100 mm dishes in a total volume of 15 ml DMEM and incubated at 37 ºC/ 5 % CO_2 for 4 h. The cells were then washed in 20 ml PBS(A), trypsinized using 2 ml of TV and resuspended in 10 ml DMEM. The cells were pelleted at 1000 r.p.m. /5

min using a Thermoscientific Heraeus Megafuge 16R, after which the pellet was resuspensed in 10 ml DMEM. Two 4 ml aliquots were then seeded onto 25 cm^2 culture flasks with the remaining ~2 ml of cells being seeded onto coverslips on a 24-well dish. After 72 h post-incubation, the cells from one culture flasks were lysed in reducing SDS-PAGE sample loading buffer (Section 2.2.8.1) and the remaining flask in RLT buffer (Section 2.2.4.3). The efficiency of DDX3 knockdown was determined by subjecting protein lysates to SDS-10% PAGE (Section 2.2.8.2) followed by Western immunoblotting (Section 2.2.9.3) with mAb AO196. The intracellular HCV RNA levels were determined by RT-qPCR (Section 2.2.6). The coverslips were fixed in methanol for Immunofluorescence analysis (Section 2.2.13).

2.2.13. Indirect Immunofluorescence (IF)

To examine the intracellular expression of HCV proteins, cells on coverslips were fixed in methanol, washed with PBS(A), blocked for 10 min with PBS(A) containing 2 % FCS and incubated at room temperature for 1 h with primary antibody in the blocking buffer. Cells were washed with PBS(A), stained with secondary antibody conjugated with either FITC, TRITC, or Cy5 in blocking buffer for 1 h, washed with PBS(A), and the coverslips mounted on a glass slide and examined with a Zeiss Laser Scanning LSM510 META inverted confocal microscope (Carl Zeiss Ltd., UK). The images were analyzed using LSM510 software. Three-dimensional (3D) reconstructions were performed from Z-stack images collected using optimum intervals. The 3D reconstructions were generated by deconvolving the image stacks by 3D-blind deconvolution using Autodeblur software (MediaCybernetics).

3. Results

3.1. The Importance of the core-DDX3 Interaction in HCV RNA replication and Infectious Particle Production

3.1.1. Introduction

HCV core protein associates with LDs in many different cell lines (Section 1.11.2). Most importantly, recent studies using the HCVcc system have found this association to be crucial for the assembly of infectious virus particles in Huh-7 cells (Boulant *et al.*, 2007; Miyanari *et al.*, 2007). An interaction between core and the cellular DEAD-box RNA helicase DDX3 was first reported by 3 independent studies using yeast-two hybrid screening (Mamiya & Worman, 1999; Owsianka & Patel, 1999; You *et al.*, 1999), and has been confirmed by co-IP assays (Ariumi *et al.*, 2007; You *et al.*, 1999). In line with this, proteomic analysis revealed DDX3 was present in the LD droplet fraction from core expressing Hep39 cells (Sato *et al.*, 2006). Also, the colocalisation between core and DDX3 was confirmed in Huh-7 cells electroporated with JFH1 RNA or infected with the virus (Dalrymple, 2007). RNA silencing of DDX3 drastically reduces JFH1 replication, although it is uncertain if this effect is caused by a reduction in the core-DDX3 interaction or by another direct or indirect mechanism. Six residues (F24, G27, I30, G33, V34 and Y35) in core protein have been identified to disrupt the core-DDX3 interaction when changed to alanine (Dalrymple, 2007). Furthermore, the introduction of these mutations into the full-length JFH1 genome created mutants that replicated in Huh-7 cells but had reduced levels of core-DDX3 colocalisation by IF analysis. Importantly, all viruses released infectious particles except $JFH1_{G33A}$. Upon serial passaging all mutants could be maintained in culture, including $JFH1_{G33A}$ which had acquired infectivity as well as a second mutation adjacent to the original alanine substitution (G32D). Together, these data suggest the interaction between core and DDX3 is not essential for the maintenance of replicating virus in cell culture. However, infection of naïve cells with each mutant virus (F24A, G27A, I30A, G32D/G33A V34A and Y35A) revealed substantially lower levels of intracellular RNA replication and viral protein expression compared to $JFH1_{WT}$

(Dalrymple, 2007). These data would suggest the core-DDX3 interaction is dispensable for persistent infection of JFH1 but nevertheless may be required for enhancing some part of the virus life cycle involving early replication and translation events.

In order to establish the true nature of this virus-host interaction in infected cells and its role in the HCV lifecycle, a co-IP assay was first developed to demonstrate the association of these two proteins in Huh-7 cells harbouring JFH1. Using a highly specific in-house generated anti-DDX3 antiserum and a commercial core mAb, the correct buffer conditions were established to allow efficient pull-down of core protein from cell lysates immunoprecipitated with anti-DDX3. A detailed time course analysis using high resolution confocal microscopy was conducted to understand the association of these two proteins with LDs during virus replication. This analysis was then extended to the six core mutants described above. The newly established core-DDX3 co-IP identified mutants with reduced levels of DDX3 binding. To study the effects of this interaction on virus replication, the levels of intracellular HCV RNA and infectious particle release was examined for particular mutants. One of these mutants was then used to determine the relationship between the core-DDX3 interaction and the inhibitory effects of DDX3 knockdown on HCV replication. This section also investigated if DDX3 is incorporated into extracellular virions through its interaction with core protein.

3.1.2. Characterisation of DDX3 Antibodies

To demonstrate a genuine interaction between two different proteins, it is critical to have highly specific antibodies to either protein, preferably in both mAb and pAb form. Numerous in-house generated mAb and pAb DDX3 antibodies were available for use in this project. Based on recommendations, the mouse mAb anti-DDX3 antibody AO196 and rabbit pAb anti-DDX3 antisera R648 were chosen. The epitope recognised by AO196 has been broadly mapped to the N-terminal end of the protein from residues 1-142 (Scott, 2002). Both mAb AO196 and pAb R648 were previously shown to interact with DDX3 by ELISA, Western blotting and IF (Scott, 2002; Dalyrmple, 2007). By IF analysis, both antibodies recognised only the cytoplasmic form of DDX3 in Huh-7 cells, whereas both nuclear and cytoplasmic forms were identified by immunoblotting (Scott, 2002; Dalyrmple, 2007). To further confirm the specificities of AO196 and R648 for DDX3, their reactivity's were determined by IP using the cytoplasmic extracts obtained from naïve Huh-7 cells. R648 but not the pre-immune control serum specifically immunoprecipitated

DDX3 from a cytoplasmic extract of Huh-7 cells, as did mAb AO196 (Fig. 3.1A). The specificity of both these antibodies was further demonstrated by immunoblotting the total cell extracts from HEK-293T cells transfected with and without green fluorescent protein (EGFP)-DDX3 fusion protein (Fig. 3.1B).

3.1.3. Demonstrating an Interaction between Core and DDX3 in Cells Replicating JFH1

The core-DDX3 interaction was previously demonstrated in cells ectopically expressing HCV genotype 1a core, and in the absence of virus RNA replication and productive infection (Owsianka & Patel, 1999). Despite a recent publication describing an interaction between JFH1 core and DDX3, this was only shown by co-immunoprecipitating the lystates from HEK-293T cells over expressing core and HA-tagged DDX3. Moreover, this study failed to show an interaction between core and DDX3 in JFH1-infected cells (Ariumi *et al.*, 2007). To confirm the core-DDX3 interaction in cells replicating JFH1, the ability of R648 to co-immunoprecipitate core protein was tested from the lysates of Huh-7 cells obtained 72 h post-electroporation with JFH1 *in vitro*-transcribed RNA. The IP buffer (Masaki buffer) recipe was obtained from a recent publication describing an interaction between core and NS5A from JFH1-electroporated cells (Masaki *et al.*, 2008). It was reasoned that this buffer would be suitable for detecting the core-DDX3 binding by co-IP given this buffer was able to preserve an interaction between core and NS5A during co-IP. However, in the initial co-IP assay only very low quantities of core protein were detected using R648 (Fig. 3.2A). In an effort to increase the amount of precipitated core protein, the procedure was repeated in cells lysed with Masaki buffers containing lower concentrations of detergent (Triton-X-100). Reductions in detergent appeared to increase the amount of precipitated core protein, with buffer containing 0.1 % Triton-X-100 achieving the best pull-down (Fig. 3.2B). Using this concentration of Triton in the buffer, the specificity of this co-IP method was confirmed by showing only the immune R648 serum and not the R648 pre-immune serum could precipitate core protein from the cell lysates (Fig. 3.2C). The co-IP results presented in Figs 3.2A-C were obtained through precipitating lysates with 3 µl of R648. To test how the quantity of anti-DDX3 anti-serum affects the levels of core protein precipitated, three separate co-IP experiments were performed, each using different amounts of R648. The levels of core protein detected directly correlated with the amount of R648 added with 6 µl of antibody achieving the greatest pull-down (Fig. 3.2D).

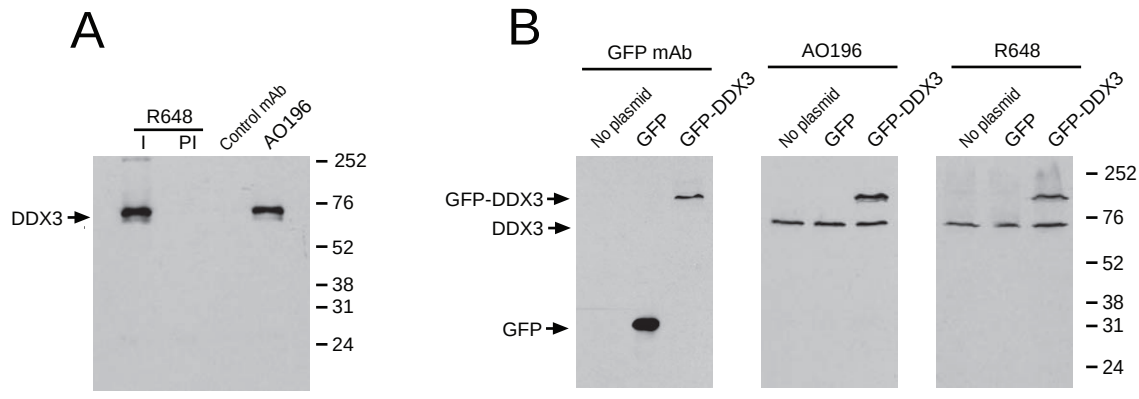

Figure 3.1. Characterisation of two anti-DDX3 antibodies.

(A) Huh-7 cell lysates were immunoprecipitated with the immune (I) and pre-immune (PI) antiserum R648, or mAb AO196 or an isotype control mAb. The immune complexes were then immunoblotted with biotinylated R648. (B) Lysates from HEK-293T cells transfected with a plasmid expressing EGFP alone or an EGFP-DDX3 fusion protein were harvested 24 h after transfection. Cell extracts were immunoblotted using anti-GFP mAb, AO196 and R648.

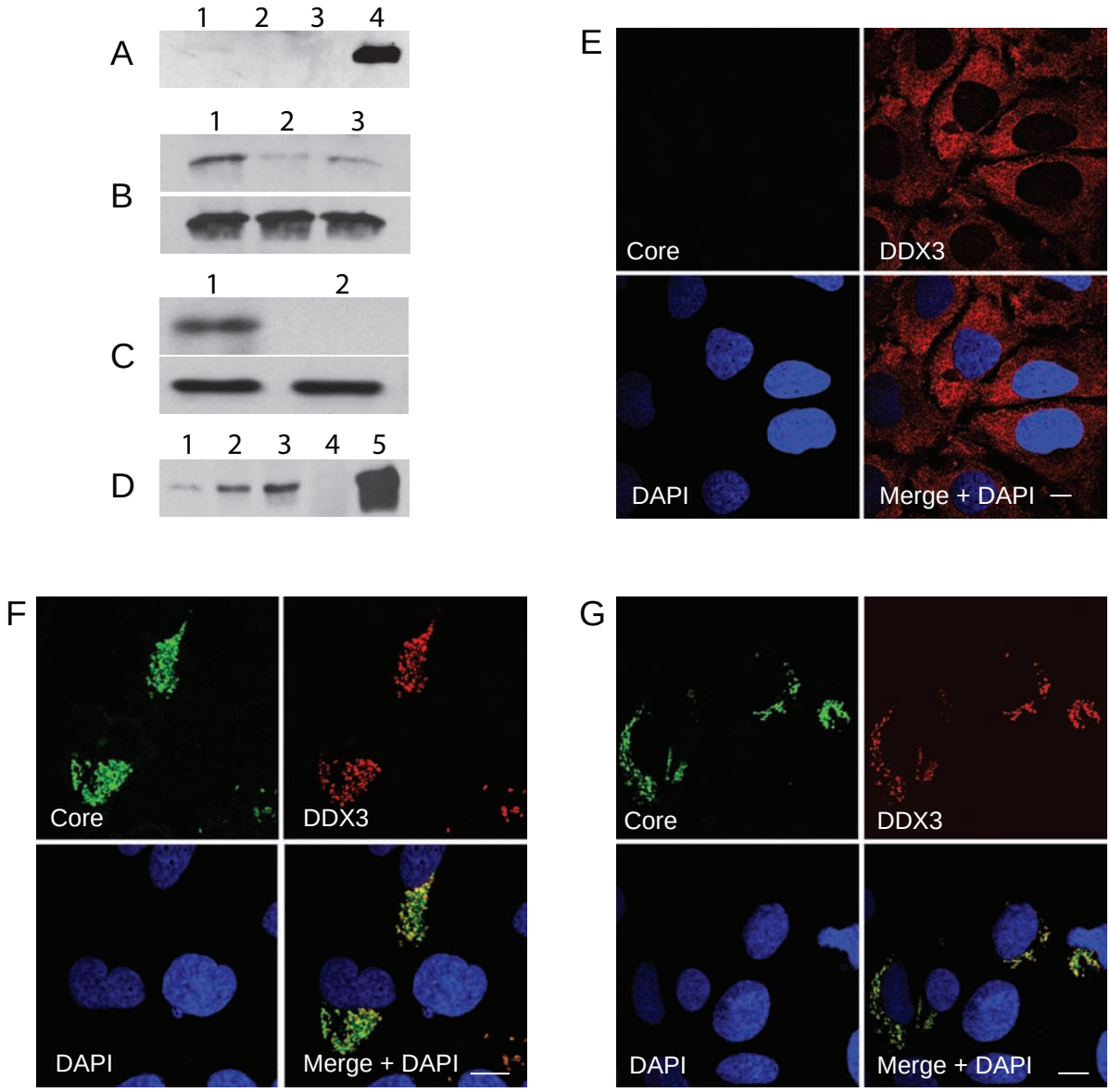

Figure 3.2. Interaction of HCV core with cellular DDX3.

(A) Co-immunoprecipitation of core by R648. Huh-7 cells electroporated with and without 10 µg of JFH1 RNA were lysed at 72 h post-incubation with IP buffer containing 1 % Triton-X-100. The test and control cell lysates were immunoprecipitated with 3 µl R648 and followed by immunoblotting using using anti-core mAb C7-50 (lanes 1 and 2, respectively). One twentieth of the control and test cell lysate used in the co-IP assay was immunoblotted for core as the input control (lanes 3 and 4, respectively). (B) Effect of detergent concentrations on co-IP of core protein. Co-IP was performed on JFH1-electroporated cell lysates as before but containing 0.1 % (lane 1), 0.2 % (lane 2) and 0.5 % (lane 3) of Triton-X-100. Upper and lower panels represent immunoblotting of core protein from precipitated lysates and input control ($1/20^{th}$), respectively. (C) Specificity of the core-DDX3 co-IP assay. (Upper Panel) Co-IP with lysates from JFH1-electroporated cells using 3 µl R648 (lane 1) as before and 3 µl of pre-immune serum (Lane 2). One twentieth of the lysate was loaded as the input control (lower panel). (D) Optimising the co-IP conditions. Lysates from 3 JFH1 electroporations were pooled together and divided into three separate co-IP assays using 1 µl (lane 1), 3 µl (lane 2), and 6 µl (lane 3) of R648. One sixtieth of the pooled lysate was loaded as the input control (lane 5) alongside mock electroporated cell lysates (lane 4). (E-G) Core protein redistributes cytoplasmic DDX3 in JFH1 replicating cells. Naïve (E), JFH1-electroporated (F) and JFH1-infected (G) cells were fixed at 72 h post-incubation and double stained for core (R308) and DDX3 (AO196). Scale bar, 10 µm.

Together, these experiments show a direct interaction occurs between core and DDX3 in cells replicating JFH1. Next, IF analysis was performed by probing naïve, JFH1-RNA electroporated and JFH1-infected Huh-7 cells with anti-DDX3 mAb AO196 and the anti-core pAb R308. As expected, DDX3 had a diffuse cytoplasmic localisation in naïve cells but was redistributed and colocalised with core protein in both JFH1-transfected and -infected cells (Fig. 3.2E-G). These IF results are in agreement with previous data obtained using these antibody combinations in Huh-7 cells harbouring JFH1 (Dalrymple, 2007). It should be noted that the core-bound DDX3 emitted a stronger fluorescent signal compared to the free DDX3 occupying the cell cytoplasm. Thus, adjustment of the core-bound DDX3 signal to prevent overexposure resulted in the apparent loss of free DDX3 from the image. A representative image of core and DDX3 in virus-infected and surrounding non-infected cells taken at two different intensities is depicted in Fig 3.3. Interestingly, the staining of infected cells with R648 allowed the free DDX3 to be visualised without overexposure of the core-bound protein. This observation highlights the diverse staining patterns that can be obtained using different antibodies against the same protein.

3.1.4. DDX3 Associates with HCV Core on LDs

The association of HCV core with LDs is essential for infectious virus production (Boulant *et al.*, 2007; Miyanari *et al.*, 2007). Substitution of core residues P138 and P143 to alanine severely affects coating of LDs by core. Interestingly, both the $JFH1_{WT}$ core and the P138A/P143A (DP) mutant localize at a single site in close juxtaposition to LDs at an early time-point (24 h). However, at later time-points (48 to 72 h), unlike the WT core, the DP mutant fails to fully coat LDs which is coupled to the loss of infectious virus production (Boulant *et al.*, 2007). To gain further insight into the distribution of the core-DDX3 complex in the context of the HCVcc system the localisation of core, DDX3 and LDs was analysed in Huh-7 cells electroporated with $JFH1_{WT}$ RNA at 24, 48 and 72 h. At each time-point post-electroporation core associated with ADRP and the localisation of DDX3 was precisely coincident with both proteins, indicating its redistribution to LDs (Fig. 3.4A-C). Together, these data show that there is a direct correlation between core and DDX3, since DDX3 follows core in coating LDs and it does not associate with LDs without core. To examine the subcellular position of DDX3 and core in relation to ADRP in greater detail, a series of Z-stacks was obtained and used after blind deconvolution to create a 3D model of LDs coated by core, ADRP and DDX3 (Fig. 3.4A-C, i-ii). As reported before, the coating of LDs by core protein occurred in a time-dependent manner. Also, DDX3 by virtue of its

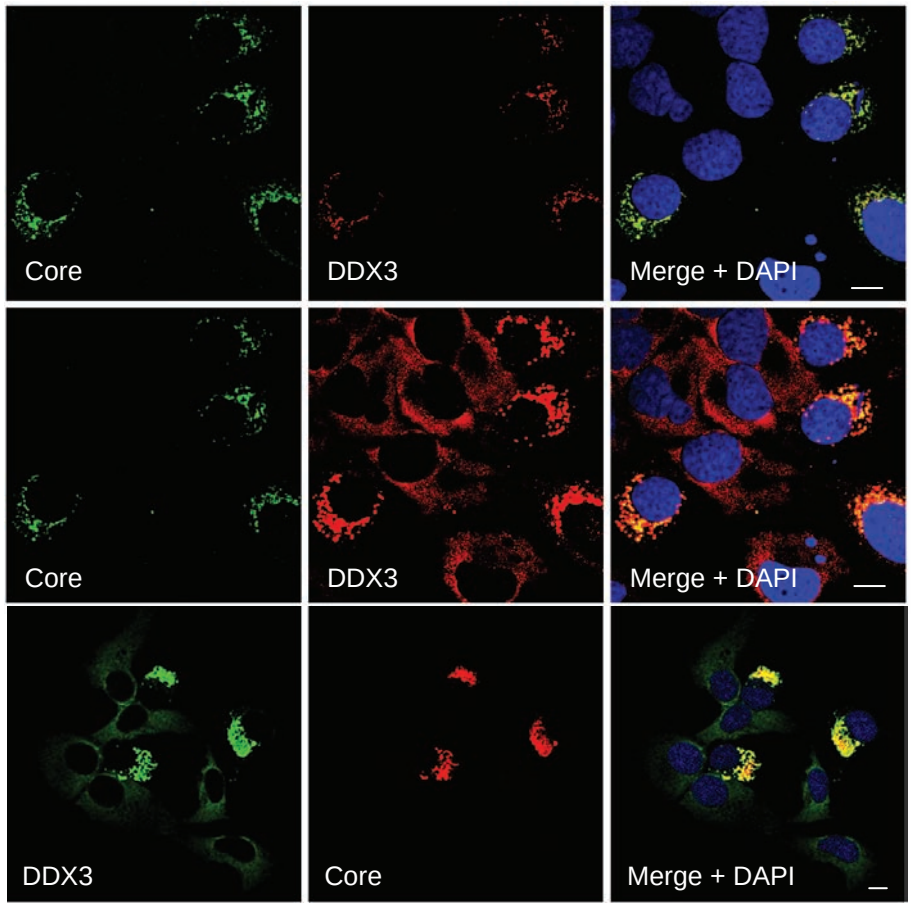

Figure 3.3. Images of JFH1-infected Huh-7 cells probed with different antibodies.

In the upper and middle panels, cells were probed with anti-DDX3 mAb AO196 and anti-core pAb R308. The core-bound DDX3 signal in the top panel was obtained under normal detector gain settings. Enhancement of this signal in the middle panel overexposed core-bound DDX3, but allowed visualization of non-sequestered DDX3. Lower panel, image of JFH1-infected cells probed with anti-DDX3 pAb R648 and anti-core mAb C7-50 taken under normal detector gain settings. Scale bar, 10 µm.

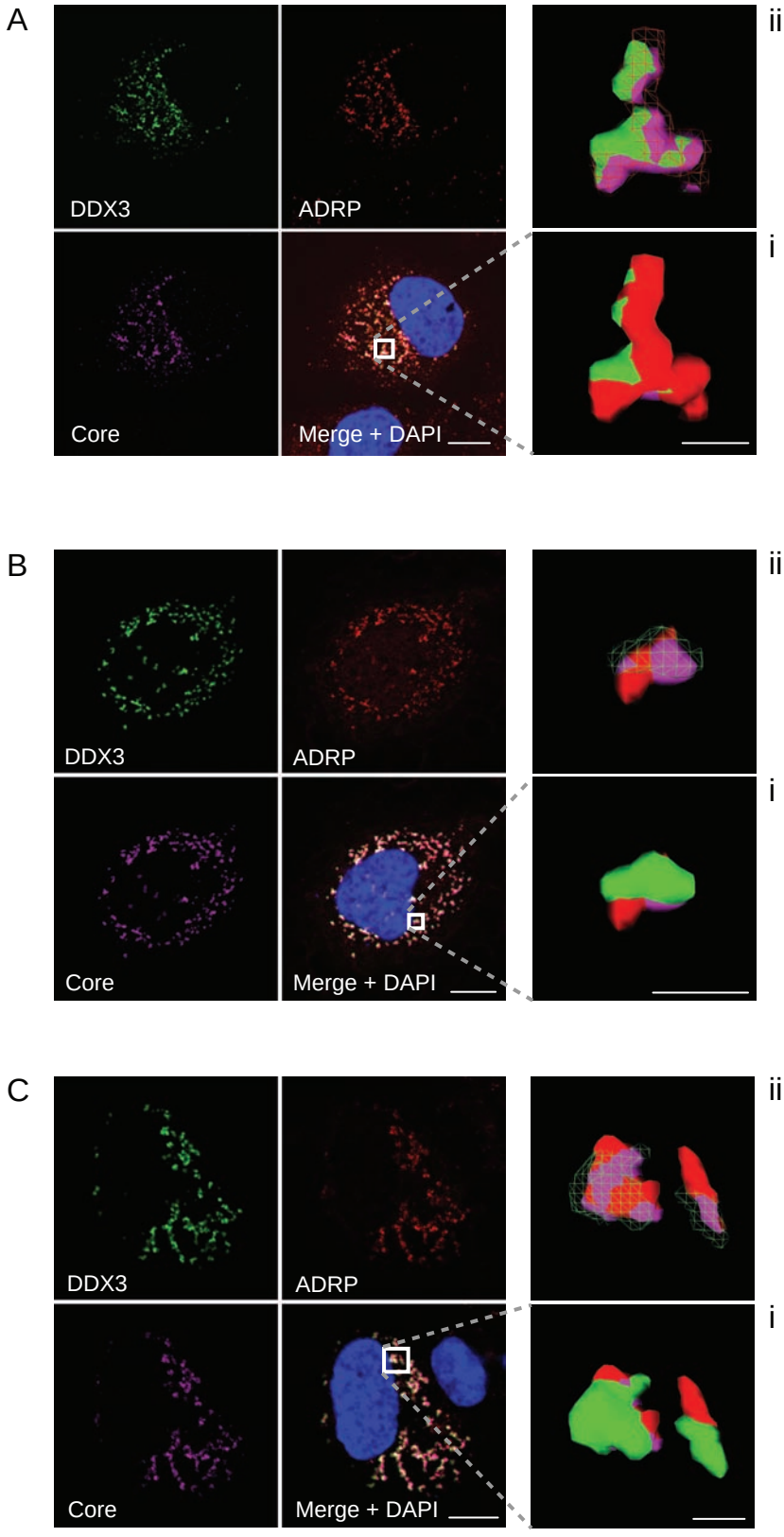

Figure. 3.4. Localisation of DDX3 and JFH1 core on LDs.

Huh-7 cells electroporated with the JFH1 RNA were fixed at 24 (A), 48 (B) and 72 h (C) post-electroporation and probed using antibodies to core (R308), DDX3 (AO196) and ADRP (ADRP 4). Z-stack analysis of all three proteins was performed in each image with the 3D reconstructions of the boxed areas shown (i). A selected area of the 3D image is shown in greater detail (ii) where ADRP is depicted in wire frame at 24 h and DDX3 is in wire frame at 48 and 72 h. Scale bar, 10 µm for confocal images and 1 µm for 3D images.

interaction with core was associated with LDs at all time-points. In cells replicating $JFH1_{DP}$ mutant RNA, the intracellular distribution of DDX3 matched that of core at each time-point analyzed, indicating that the sequestration of DDX3 on LDs by core is independent of the full core-LDs association (Fig. 3.5A-C). Z-stack analyses of each image revealed the DP mutant core failed to fully coat LDs over 72 h, and neither did DDX3 although it still co-localized with core (Fig. 3.5A-C, i-ii). In addition, the localisation of DDX3 was analyzed in cells replicating a JFH1 mutant ($JFH1_{VLVL}$) harbouring four aa substitutions (A180V, S183L, C184V and T186L) at the C-terminal region of core that delays SPP cleavage. A time course analysis revealed the delayed maturation of core affects its ability to coat LD at early times following electroporation (Targett-Adams *et al.*, 2008b). In accordance with these data, at 48 h post-electroporation with $JFH1_{VLVL}$ RNA, there was a mixed population of core protein signals colocalising with ADRP (Fig. 3.6A). Z-stack analyses revealed that both core attached and unattached to LDs were bound by DDX3 (Fig. 3.6A, i-ii). To test if HCV alters the subcellular localisation of DDX3 in the absence of stable core protein expression, cells were electroporated with another JFH1 core mutant ($JFH1_{F130E}$) containing the substitution F130E. This mutation results in the immediate degradation of core protein by the proteasome following its translation but does not effect the stability of the remaining viral proteins (Boulant *et al.*, 2007). At 72 h post-electroporation with $JFH1_{F130E}$ the cytoplasmic distribution of DDX3 was unaltered despite the presence of virus replication as indicated by NS5A expression (Fig. 3.6B).

3.1.5. Core Residues Required for DDX3 Interaction.

It was previously reported that aas 1-59 of core protein are involved in its interaction with DDX3 (Owsianka & Patel, 1999). More recently, Dalrymple (2007) identified six critical residues within this region that were required for the colocalisation of JFH1 core protein with DDX3. As these mutants form the basis of the results presented in the following section it is appropriate to begin by describing briefly how this region was identified. Firstly, a library of mutants was constructed by error prone PCR (EP-PCR). The N-terminal 59 aas of core protein (containing single or multiple aa substitutions generated by EP-PCR) was cloned downstream of GFP in a bacterial expression vector (pKK223-3). ELISA was used to screen the core mutants. Briefly, a soluble GST-DDX3 fusion protein, previously used to delineate the domain of DDX3 interacting with core (Owsianka & Patel, 1999) was immobilized on the ELISA plate and bound mutants were detected using a rabbit polyclonal anti-GFP antiserum. Of 130 clones tested by ELISA, only nine (mutants

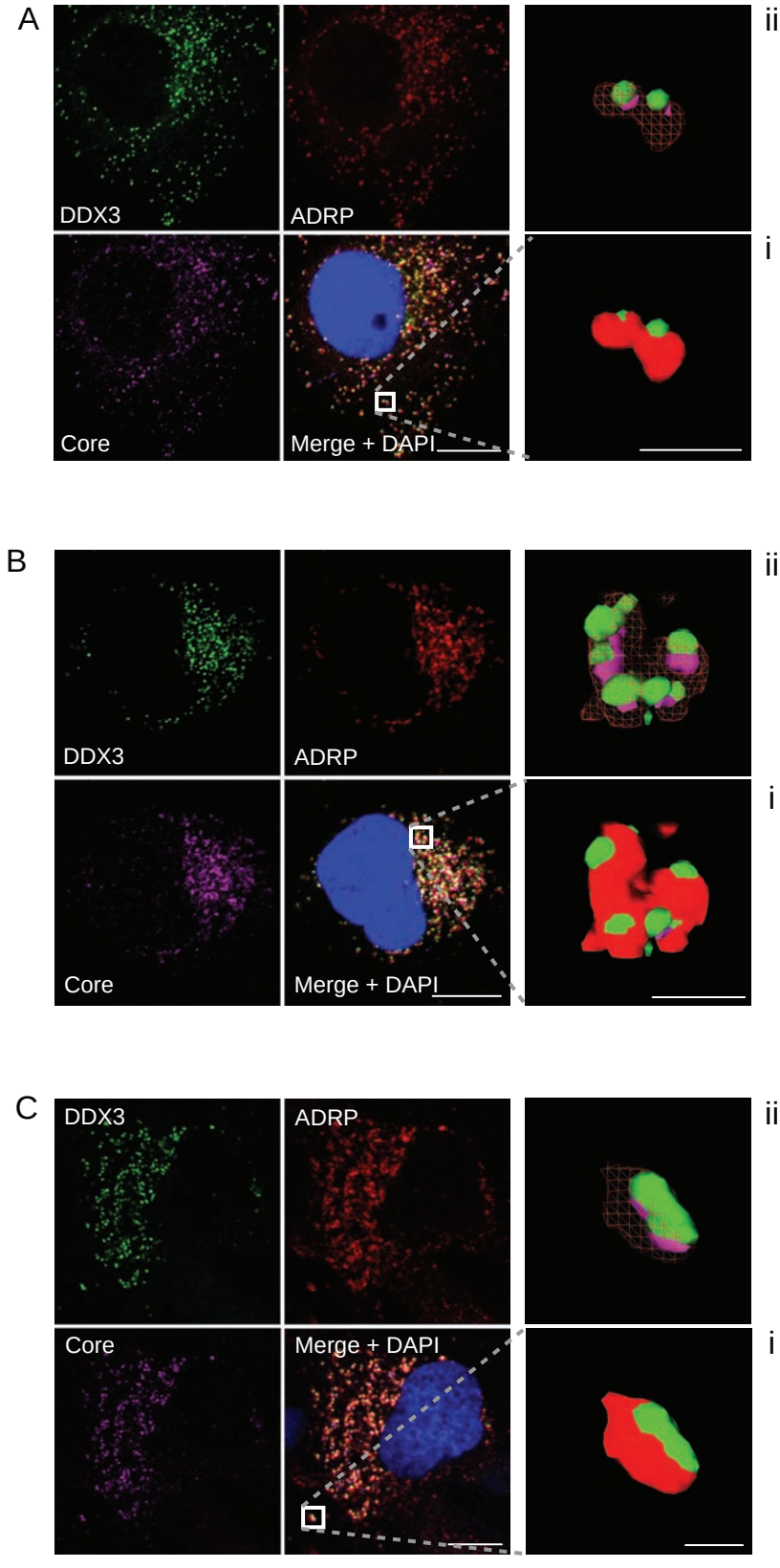

Figure 3.5. Localisation of DDX3 and JFH1$_{DP}$ core on LDs.

Huh-7 cells electroporated with the JFH1$_{DP}$ RNA were fixed at 24 (A), 48 (B) and 72 h (C) post-incubation and probed using antibodies to core (R308), DDX3 (AO196) and ADRP (ADRP 4). Z-stack analysis of all three proteins was performed in each image with the 3D reconstructions of the boxed areas shown (i). A selected area of the 3D image is shown in greater detail (ii) where ADRP is depicted in wire frame at each time point. Scale bar, 10 µm for confocal images and 1 µm for 3D images.

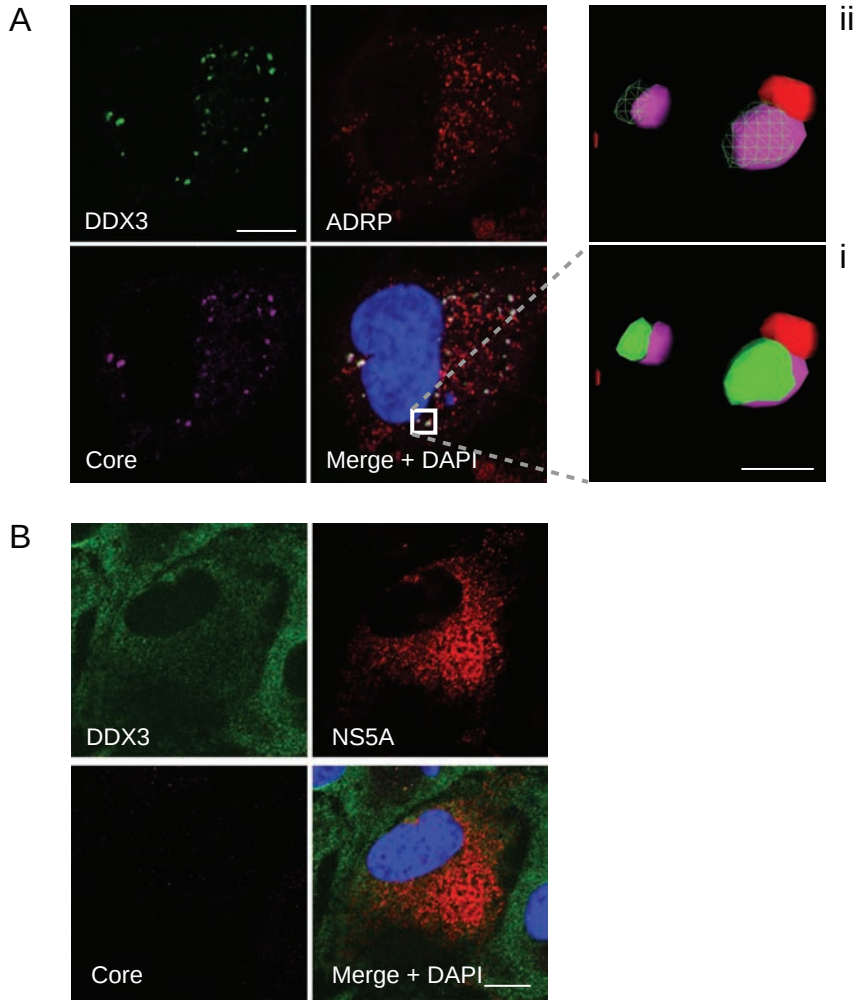

Figure 3.6. Localisation of DDX3 in cells replicating JFH1 core mutants.

(A) Huh-7 cells electroporated with the $JFH1_{VLVL}$ RNA were fixed at 48 h post-incubation and probed using antibodies to core (R308), DDX3 (AO196) and ADRP (ADRP 4). 3D reconstructions of the boxed areas shown (i) and in greater detail (ii) where ADRP is depicted in wire frame. (B) Huh-7 cells electroporated with $JFH1_{F130E}$ RNA were fixed at 72 h post-incubation and probed using antibodies to DDX3 (AO196), NS5A (sheep) and core (R308). Scale bar, 10 µm for confocal images and 1 µm for 3D images.

25, 36, 90, 99, 110, 111, 115, 125 and 126) were found to be defective in binding to GST-DDX3 (Dalrymple, 2007). In order to confirm these results, all 9 mutants were individually sub-cloned into a sequence encoding the HCV genotype 1a strain H77c core, E1 and E2 (pCE1E2) in a mammalian expression vector pcDNA3.1/Zeo+ (Invitrogen), and their expression was analyzed by IF. The results were in accordance with the data from the initial ELISA screen in that all 9 mutated core proteins failed to redistribute DDX3 (Dalrymple, 2007). Instead, DDX3 maintained its typical diffuse cytoplasmic localization in cells ectopically expressing each of these mutated core proteins, similar to that observed in non-transfected cells. Nucleotide sequence analysis showed that each of the mutants carried between one and four aa substitutions (Fig. 3.7). Of interest, mutant 90 had only one aa substitution (I30N), indicating that this residue must be required for the interaction of core with DDX3. All nine mutant proteins had at least one aa substitution in the region spanning residues 24-36, indicating that this region may harbour residues that are critical for the core-DDX3 interaction. To test this hypothesis, site-directed mutagenesis was carried out to revert any mutations outside of this 13 aa region back to the WT residue. These new mutant core 1-59 fragments were then sub-cloned into pCE1E2, and their expression analyzed following transient transfection into Huh-7 cells as above. Again, none of these new core mutants redistributed DDX3 (Dalrymple, 2007), indicating that the 13 aa region between residues 24 and 36 of core is indeed involved in the interaction between core and DDX3. To determine which residues in this 13 aa region were essential, alanine-scanning mutagenesis across aas 24-36, individually substituting each aa in this region with alanine was carried out. As before, these alanine mutant sequences were subcloned into pCE1E2 and transiently transfected into Huh-7 cells. IF analysis revealed seven mutants (P25A, G26A, G28A, Q29A, V31A, G32A and L36A) that showed distinct colocalization between core and DDX3 (similar to that seen with WT HCV core), whilst the other mutants (F24A, G27A, I30A, G33A, V34A and Y35A) displayed no colocalization with DDX3 at all. Thus, these results indicate that core residues F24, G27, I30, G33, V34 and Y35 are critical for its interaction with DDX3. Sequence comparison of core protein from strains H77c (genotype 1a) and JFH1 (genotype 2a) revealed 96.6 % homology within the first 59 residues of core, with the key residues (F24, G27, I30, G33, V34 and Y35) for interaction with DDX3 being fully conserved (Dalrymple, 2007). Thus, recombinant JFH1 genomes each containing one of the six mutations were constructed. Initial analysis of these mutants revealed that they disrupted the colocalisation of core and DDX3 but could spread in cell culture following electroporation (Dalrymple, 2007).

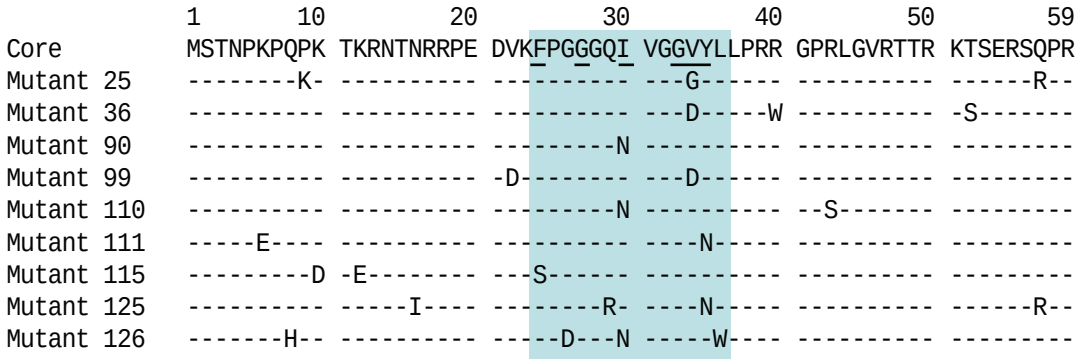

Figure 3.7. Identification of core residues critical for its interaction with DDX3.

Amino acid substitutions in residues 1-59 of core in nine mutants unable to interact with DDX3. Residues in the region 24-36 (shaded box) were targeted for alanine-scanning mutagenesis, which identified residues at positions 24, 27, 30, 33, 34 and 35 (underlined in the sequence at the top) that were critical for DDX3 interaction (Adapted from Dalyrmple, 2002).

3.1.6. Detailed Characterisation of JFH1 Core Mutants

The knockdown of the core-DDX3 interaction in cells replicating the core mutant viruses was shown by IF analysis (Dalrymple, 2007). To verify that these core mutations disrupt the core-DDX3 interaction but not the core-LD association, Huh-7 cells electroporated with each viral RNA were stained for core, DDX3 and ADRP at 72 h post-incubation. As shown from the images in Fig. 3.8, each mutant core, like its WT counterpart, fully associated with LDs. Colocalisation between core and ADRP was found in all cells analysed. However, no core-DDX3 colocalisation was observed for mutants $JFH1_{F24A}$, $JFH1_{G27A}$, $JFH1_{I30A}$ and $JFH1_{Y35A}$, whereas $JFH1_{G33A}$ and $JFH1_{V34A}$ showed colocalisation in 37 and 52 % of cells counted, respectively. Thus, it appears that the latter two core mutations are unable to completely abolish DDX3 binding. Nevertheless, it was unusual to observe differing levels of core-DDX3 colocalisation in cells replicating $JFH1_{G33A}$ and $JFH1_{V34A}$. It is possible that the level of interaction in these cells is governed by the amount of core protein expression, as those cells displaying core-DDX3 colocalisation appear to have higher quantities of core than those lacking colocalisation (Fig. 3.8). These irregularities may also be cell cycle related, with the core-DDX3 interaction for these particular mutants being tightly coupled to a particular phase in cell growth. Importantly, the core-DDX3 colocalisation observations described for each mutant in Fig. 3.8 are consistent with those reported previously (Dalrymple, 2007). Next, the protein expression and virus release of each mutant was tested. To do this Huh-7 cells were electroporated with viral RNA and after 72 h the cell medium was titrated and the cells were lysed for immunoblotting. All mutants were replication active as seen by the expression of NS5A protein at 72 h post-electroporation (Fig. 3.9A). However, differing levels of core expression was observed when immunoblotting these lysates with mAb C7-50. This antibody bound minimally or not at all to $JFH1_{I30A}$ and $JFH1_{G33A}$ core, but had increased affinity for the $JFH1_{V34A}$ protein. To determine whether these differences were due to altered affinity of this mAb to these mutants, the reactivities of the lysates to the pAb R308 were tested. This pAb recognized all core forms equally except $JFH1_{G33A}$, suggesting the altered detection levels observed with mAb C7-50 is due to the mutations $JFH1_{I30A}$, $JFH1_{G33A}$ and $JFH1_{V34A}$ affecting antibody binding (Fig. 3.9A). The smaller quantities of $JFH1_{G33A}$ core detected using R308 suggests this mutation reduces the binding efficiency of both core antibodies. Importantly, there was no detectable change in DDX3 protein levels in any of the electroporated cell cultures tested (Fig. 3.9A). All core mutants released similar quantities of infectious virus into the cell medium at 72 h post-

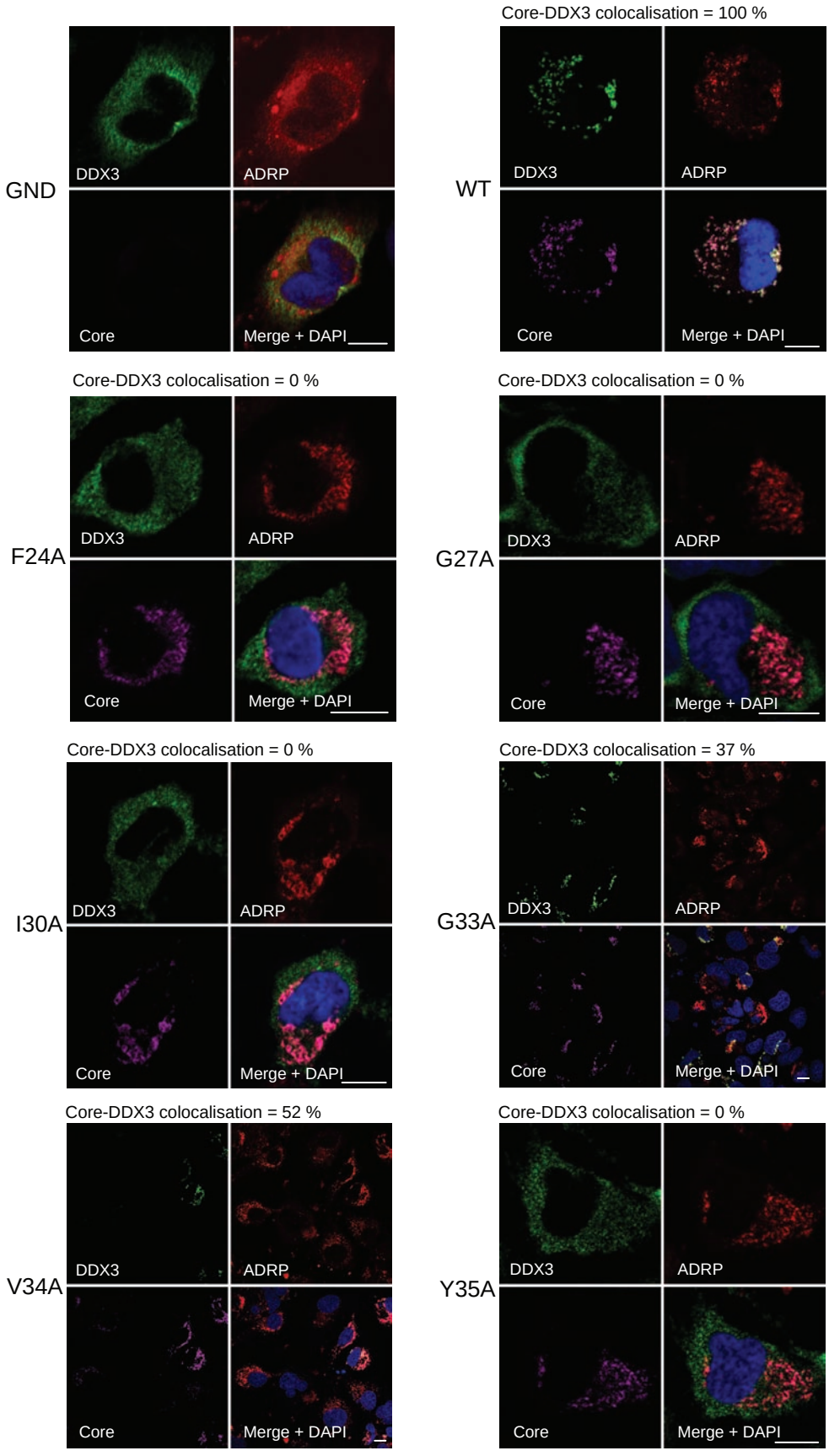

Figure 3.8. Mutations in core do not disrupt its association with LDs.

Huh-7 cells electroporated with the indicated viral RNAs were fixed at 72 h post-incubation and analysed by confocal microscopy for the intracellular distribution of core, DDX3 and ADRP using antibodies R308, AO196 and ADRP 4, respectively. The percentage of cells (n=200) displaying core-DDX3 colocalisation is stated above each image. Bar, 10 µm.

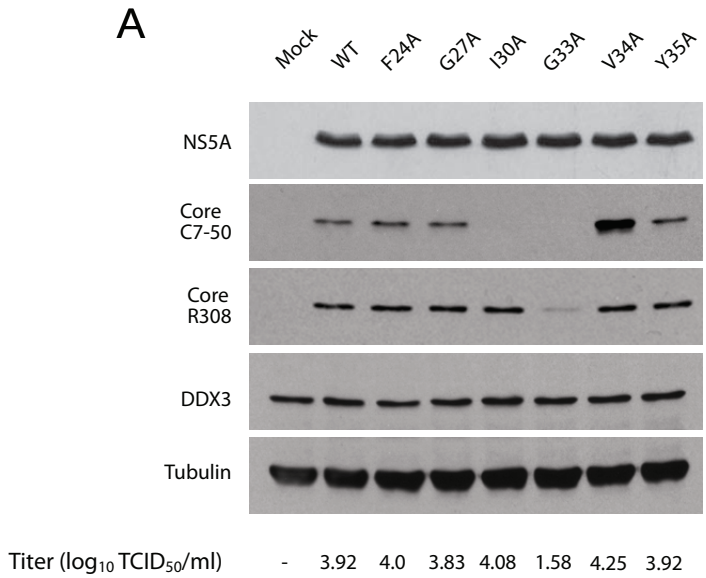

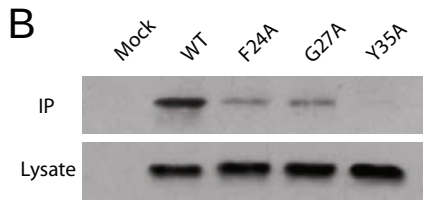

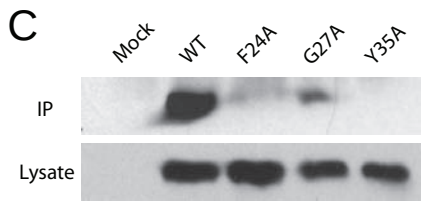

D

Virus	WT	F24A	G27A	Y35A
Titer ($log_{10}TCID_{50}$/ml)	4.17	3.83	3.75	4.0
% Core-DDX3 (n=200)	100	0	0	0
Core Sequence	No change	No change	No change	No change

Figure 3.9. Analysis of JFH1 core mutant viruses.

(A) Huh-7 cells electroporated with viral RNAs as shown were subjected to immunoblotting at 72 h post-incubation using anti-NS5A mAb 9E10, anti-core antibodies mAb C7-50 and pAb R308, anti-DDX3 mAb AO196 and anti-tubulin mAb. The released virus titers from these samples were assayed by $TCID_{50}$ assay. (B and C) The interaction of DDX3 with JFH1 core mutants. Huh-7 cells were electroporated with the indicated viral RNAs and HCV core co-immunoprecipitated at 72 h post-incubation using pAb R648 followed by immunoblotting with mAb C7-50. (D) Persistent infection of Huh-7 cells with the JFH1 core mutant viruses. Cells were infected at an m.o.i. of 0.005 and passaged 1:10 at the time of subconfluency for 5 passages. At passage 5 the infectivity of the culture medium was assayed by $TCID_{50}$ assay, the percentage of cells (n=200) displaying core-DDX3 colocalisation was determined by IF and the viral core gene was sequenced from total cell RNA following RT-PCR.

electroporation, except JFH1$_{G33A}$. However, this difference is unlikely to be caused by disruption of the core-DDX3 interaction, as the remaining mutants do not share this defect.

The co-IP experiment described in section 3.1.3 is a more valid assay than IF to test for alterations to core-DDX3 binding. As core mAb C7-50 was used to establish the co-IP assay, mutants JFH1$_{I30A}$, JFH1$_{G33A}$ and JFH1$_{V34A}$ were excluded from the experiment due to their altered affinity to this antibody. The remaining mutant cores were co-immunoprecipitated by the anti-DDX3 pAb R648 in much lower amounts (JFH1$_{F24A}$ & JFH1$_{G27A}$) than the WT protein or not at all (JFH1$_{Y35A}$), confirming that these changes affect the core-DDX3 interaction (Fig. 3.9, B and C). Together, the results obtained for these mutants in Fig. 3.9A-C, especially JFH1$_{Y35A}$ suggest the core-DDX3 interaction is not required for viral protein expression and infectious virus release at 72 h post-electroporation. Next, the importance of the core-DDX3 interaction in the establishment of persistent infection was tested. Infectious viruses from JFH1$_{F24A}$, JFH1$_{G27A}$ and JFH1$_{Y35A}$ were used to inoculate naïve Huh-7 cells alongside JFH1$_{WT}$ at an equal m.o.i. At the time of subconfluency, these cells were split 1:10 for a total of 5 passages. At passage 5 the cell medium was assayed for infectious virus, the cells were tested for core-DDX3 colocalisation, and the core gene from intracellular viral RNA was sequenced. As summarised in Fig. 3.9D each mutant had similar levels of virus release to the WT indicating that they can persistently infect cells during serial passages. Moreover, their ability to persist was not due a reversion phenotype as IF analysis found no core-DDX3 colocalisation in passage 5 cells and no sequence alterations to the core gene.

Next, the intracellular RNA replication levels of JFH1$_{F24A}$, JFH1$_{G27A}$ and JFH1$_{Y35A}$ were quantified. Huh-7 cells electroporated with RNAs derived from constructs representing the JFH1$_{WT}$, a replication-deficient JFH1$_{GND}$, or the JFH1 core mutants described above were harvested 120 h after electroporation for RNA analysis, while the progeny virus released into the medium was titrated. As expected, JFH1$_{GND}$ did not replicate, whereas all core mutants, like the parental virus, were competent at replicating RNA and releasing virus (Fig. 3.10A and B). Although no effects in virus replication were observed at 120 h post-electroporation, it was possible that differences occured during earlier time-points. To test this theory, the intracellular RNA replication and virus infectivity was measured from electroporated cells at 24, 48 and 72 h post-incubation. In addition, the HCV RNA levels were quantified at 4 h as a measure of transfection efficiency. As seen in Fig. 3.10C, only JFH1$_{G27A}$ displayed considerably lower levels of RNA replication than JFH1$_{WT}$ at 24 and 48 h. However, at 72 h the levels were more comparable to WT. Decreased infectious virus

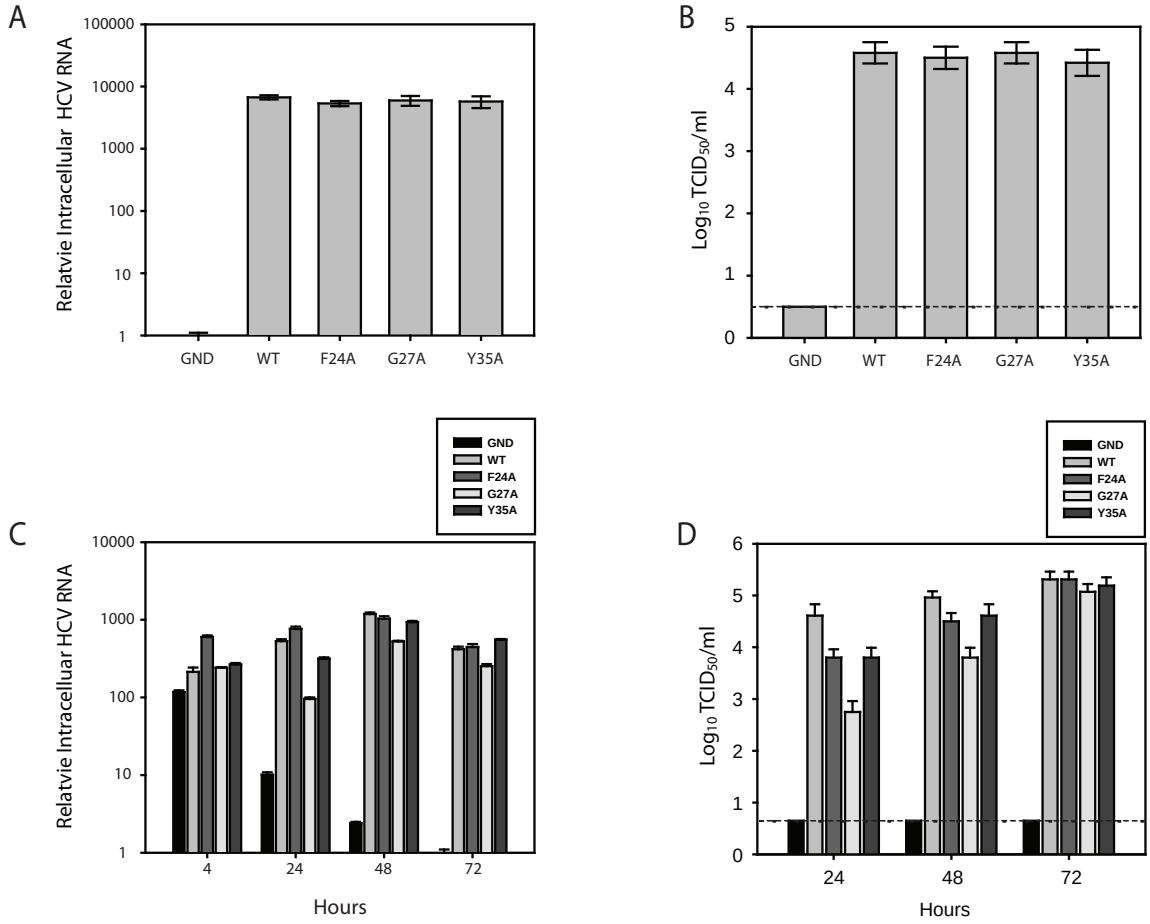

Figure 3.10. Further characterization of the JFH1 core mutants.

(A and B) Huh-7 cells electroporated with $JFH1_{WT}$ and mutant virus RNAs were split at 48 h post-incubation, re-seeded, and incubated for a further 72 h. (A) The relative quantity of intracellular viral RNAs and (B) released infectious virus were quantitated by RT-qPCR and $TCID_{50}$, respectively. The RNA levels were normalized to the GND value. (C and D) At the indicated time points following electroporation the intracellular HCV RNA levels (C) and released virus titers (D) were quantified by RT-qPCR and $TCID_{50}$, respectively. The RNA levels were normalized to the GND value at 72 h. Error bars indicate variability of the assays and dotted line indicates cut-off of the $TCID_{50}$ assay.

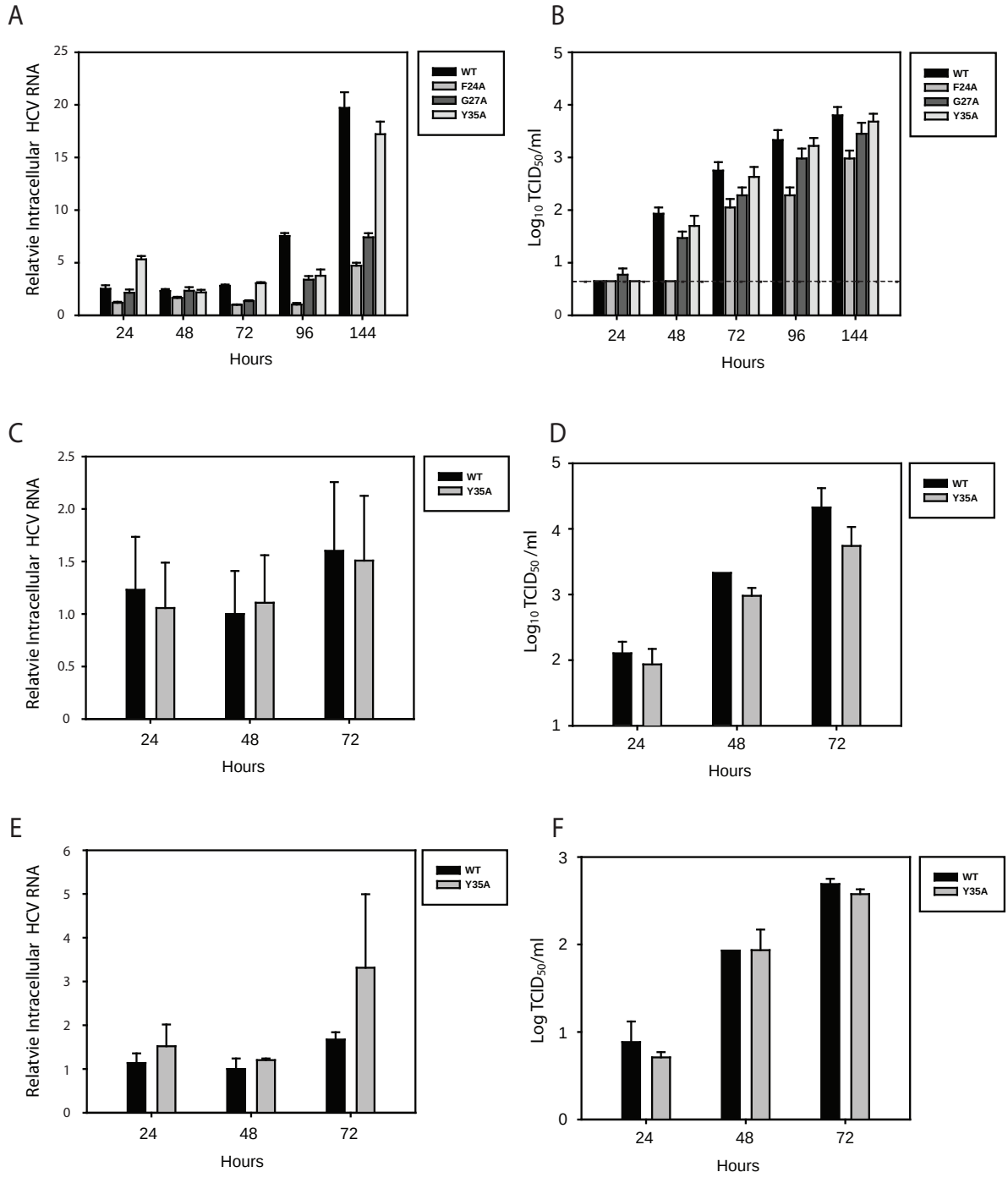

Figure 3.11. Infection kinetics of JFH1 core mutants.

(A and B) Determination of virus yield and intracellular RNA levels following infection. Naïve Huh-7 cells were infected with $JFH1_{WT}$ or the core mutant viruses (obtained from electroporated cells) at an m.o.i. of 0.02. The intracellular viral RNA levels (A) and infectious virus released into the medium (B) were measured over 144 h by RT-qPCR and $TCID_{50}$, respectively. The RNA levels were normalised to $JFH1_{F24A}$ values at 72 h. Error bars indicate variability of the assays and dotted line indicates cut-off of the $TCID_{50}$ assay. (C-F) The intracellular viral RNA levels and released viral titers were measured over 72 h as before following inoculation of naïve Huh-7 cells at an m.o.i. of 0.2 (C and D) and 0.02 (E and F). The RNA levels were normalised to $JFH1_{Y35A}$ values obtained at 24 h (C) and $JFH1_{WT}$ values at 48 h (E). Means and error ranges from two independent infections experiments are shown.

release was observed in each mutant at 24 and 48 h, although these levels achieved parity with $JFH1_{WT}$ by 72 h (Fig. 3.10D). Next, the infectivity and replication efficiency of the core mutant viruses released from electroporated cells was examined. To do this, naïve cells were inoculated at an equal m.o.i. and the released infectious virus progeny and the intracellular viral RNA were measured at various times post-infection. Both the virus yields and RNA replication levels of $JFH1_{Y35A}$ were very similar to $JFH1_{WT}$. In contrast, the replication kinetics of G27A were slightly reduced. However, $JFH1_{F24A}$ displayed the greatest decrease in viral replication and dynamics during the 144 h culture period (Fig. 3.11A and B). The results obtained for $JFH1_{Y35A}$ were the most important for this study as this mutant has the greatest reduction in DDX3 binding yet shows comparable replication levels to $JFH1_{WT}$. To unequivocally show that this mutant possesses no significant alterations to virus replication, two independent infection experiments were performed at an m.o.i. of 0.2 and 0.02. The intracellular HCV RNA and virus release levels were measured over three days. Again, no major alterations to virus replication were observed at either m.o.i. during the infection period, confirming that the fitness of this mutant is unaltered (Fig. 3.11 C-F).

3.1.7. Effect of DDX3 Knockdown on HCV Replication

Recent reports have shown that the silencing of DDX3 from target cells by RNAi impairs HCVcc replication (Ariumi *et al.*, 2007; Randall *et al.*, 2007). To assess the influence of DDX3 abundance on virus infection in the absence of the core-DDX3 interaction, the replication of $JFH1_{WT}$ and $JFH1_{Y35A}$ following infection of cells that had undergone efficient siRNA knockdown of DDX3 was measured. Knockdown of DDX3 protein from Huh-7 cells was demonstrated by immunoblotting using mAbs AO196 and anti-tubulin in combination (Fig. 3.12A). These mAbs are suitable to use in combination as they were known not to cross react with other proteins (Appendix 2). As previously described, DDX3 knockdown cells were substantially less permissive for virus replication than normal cells following infection with $JFH1_{WT}$. Similar reductions in $JFH1_{Y35A}$ replication levels were also observed, indicating that this mutant also relies on endogenous DDX3 levels for replication following infection (Fig. 3.12B-F).

To determine the effects of DDX3 silencing during productive viral RNA replication in the absence of virus assembly, Huh-7 cells were electroporated with $JFH1_{WT}$ and $JFH1_{Y35A}$ genomes lacking the envelope coding genes ($JFH1_{\Delta E1E2}$) along with the DDX3 siRNAs.

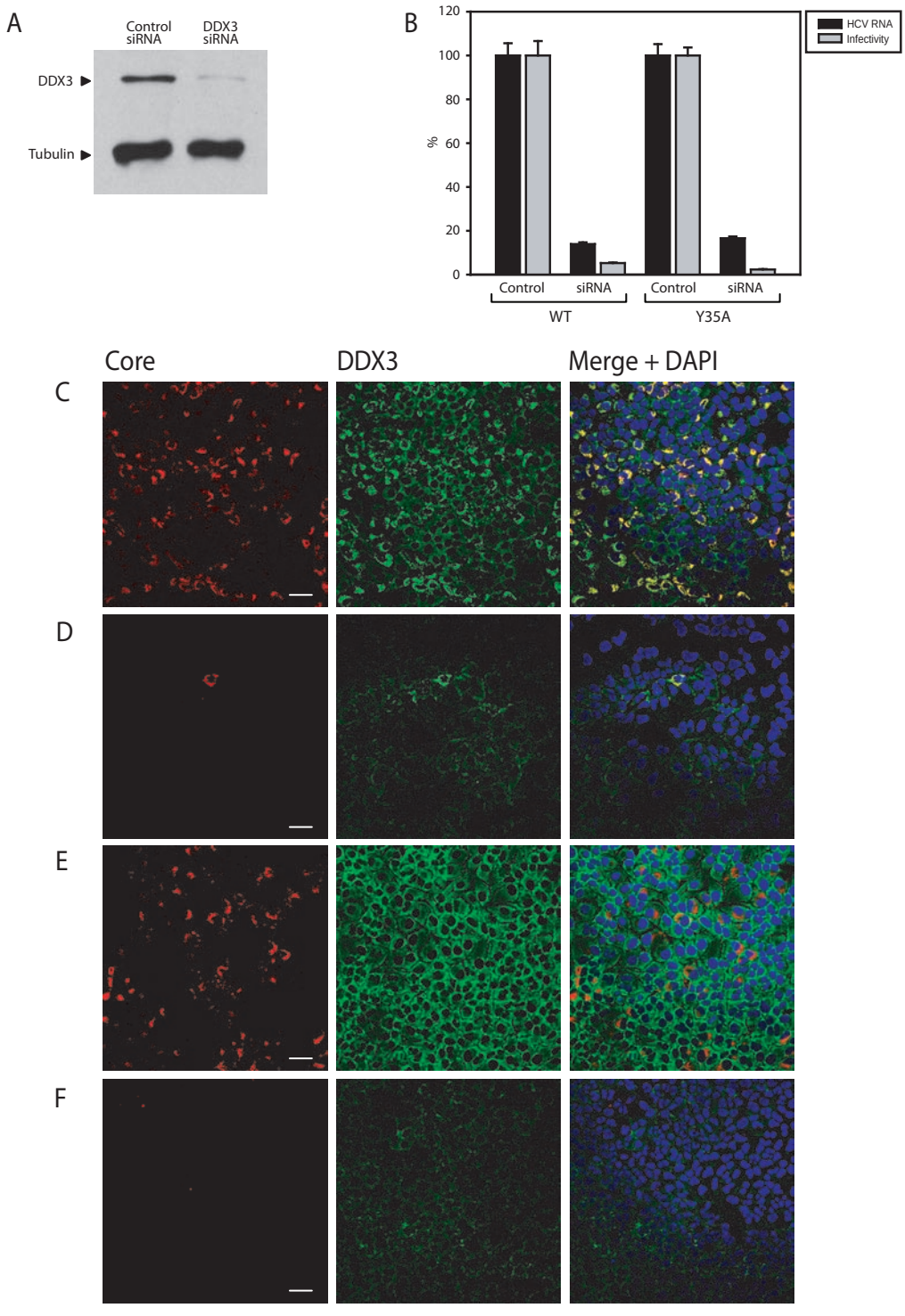

Figure 3.12. Requirement of DDX3 for HCV replication.

(A) Huh-7 cells were lipofected with siRNA duplexes as indicated. Cells were harvested after 48 h and examined by immunoblotting using the anti-DDX3 mAb AO196. (B) Naïve and DDX3-deficient Huh-7 cells were infected with $JFH1_{WT}$ or $JFH1_{Y35A}$ virus. At 48 h post-infection the levels of released virus and intracellular HCV RNA were measured by $TCID_{50}$ assay and RT-qPCR, respectively. Error bars indicate variability of the assays. The HCV RNA levels were normalised to the values obtained from cells harbouring the control siRNAs. (C-F) Cells were transfected with control (C and E) and DDX3 (D and F) siRNAs and infected with $JFH1_{WT}$ (C and D) and $JFH1_{Y35A}$ (E and F) as before. At 48 h post-infection cells were fixed and probed with antibodies to core (C7-50) and DDX3 (R648) for IF analysis. The confocal laser intensities settings were identical for each image. Scale bar, 50 µm.

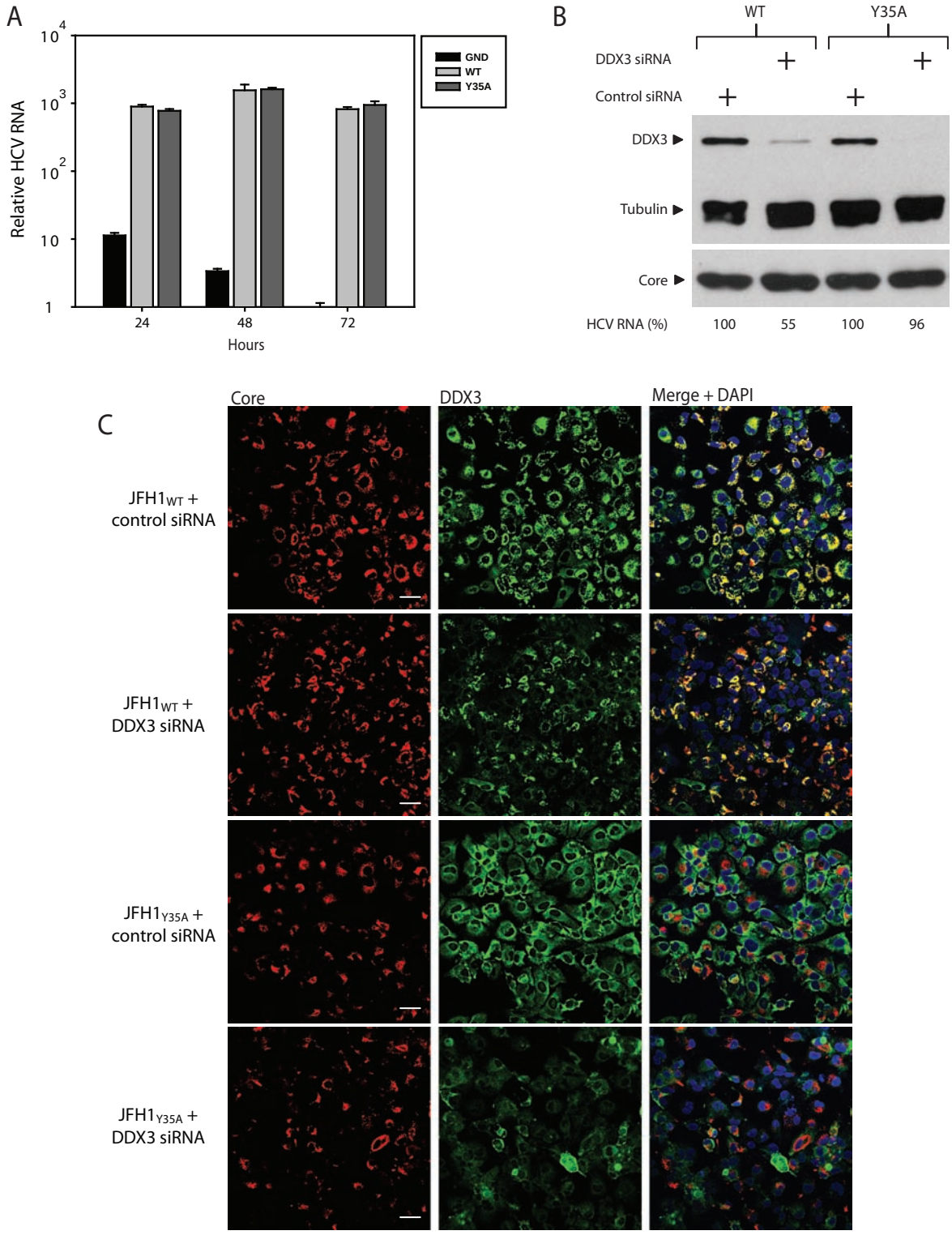

Figure 3.13. Requirement of DDX3 for HCV genome synthesis and protein expression.

(A) RNA replication of $JFH1_{\Delta E1E2(WT)}$ and $JFH1_{\Delta E1E2(Y35A)}$. Huh-7 cells were electroporated with the indicated viral RNAs. At 24, 48 and 72 h post-incubation, Intracellular HCV RNA was quantified by RT-qPCR. HCV RNA levels were normalised to the GND value at 72 h. (B and C) RNA replication of $JFH1_{\Delta E1E2(WT)}$ and $JFH1_{\Delta E1E2(Y35A)}$ in DDX3 silenced cells. (B) Lysates from cells treated with control and DDX3 siRNAs were immunoblotted with antibodies to DDX3 (AO196), tubulin and core (C7-50). The percentage of intracellular HCV RNA levels were quantified as before with the values expressed relative to the control cell readings. (C) At 72 h post-electroporation, cells were fixed and probed with antibodies to core (C7-50) and DDX3 (R648). Scale bar, 50 μm.

The JFH1$_{\Delta E1E2}$ genome is replication-competent but non-infectious (Wakita *et al.*, 2005). The JFH1$_{\Delta E1E2}$ genomes were used in order to exclude possible defects in virus assembly and spread that could result from the removal of DDX3 from the cells and thereby influence the intracellular HCV RNA levels. A JFH1$_{\Delta E1E2}$ genome harbouring the Y35A mutation JFH1 $_{\Delta E1E2(Y35A)}$ was included in this experiment to assess the relationship of core-DDX3 binding on RNA replication during DDX3 silencing. As expected, the RNA replication of JFH1$_{\Delta E1E2}$ was proficient with and without the Y35A mutation in normal Huh-7 cells (Fig. 3.13A). At 72 h following the electroporation of the viral RNAs and DDX3 siRNAs, cells were harvested for immunoblotting, RT-qPCR and IF analysis. As shown in Fig. 3.13B efficient knockdown of DDX3 expression was achieved in cells harbouring the DDX3 siRNAs compared to the control siRNAs. Interestingly, quantification of intracellular HCV RNA found a 45 % reduction for JFH1$_{\Delta E1E2(WT)}$ compared to only a 4 % drop for JFH1$_{\Delta E1E2(Y35A)}$ in DDX3 silenced cells. Strikingly, immunoblotting and IF analysis found no alterations to the core protein expression levels in these samples (Fig. 3.13B and C).

3.1.8. DDX3 Sediments with Extracellular Core Protein

As discussed in section 1.11, core protein is the viral nucleocapsid and is critical for the assembly of infectious particles through its association with LDs. Given the redistribution of DDX3 to LDs in infected cells through its interaction with core protein, it is possible this cellular protein may be incorporated into assembled virions. To test this hypothesis, an initial experiment was performed to determine if core protein could be detected from pelleted cell medium containing infectious virus. Huh-7 cells were electroporated with JFH1$_{GND}$, JFH1$_{\Delta E1E2}$, and JFH1$_{WT}$ RNA and incubated for 72 h before harvesting cell lysates and titrating the cell medium. The TCID$_{50}$ assay indicated the cell medium from the JFH1$_{WT}$ electroporations contained infectious virus titers of 4.1 x 10^4 TCID$_{50}$/ml, whereas no infectivity was released from cells with JFH1$_{GND}$ and JFH1$_{\Delta E1E2}$, as expected. The cell medium from each electroporation was centrifuged through a sucrose cushion and the pellet was lysed in Masaki buffer. Along with aliquots of cell lysates, these extracellular extracts were immunoblotted with core mAb C7-50. As expected, core protein was detected in the cell lysates from the JFH1$_{\Delta E1E2}$ and JFH1$_{WT}$ but not the replication deficient JFH1$_{GND}$ lysates. Importantly, extracellular core protein was detectable in the JFH1$_{WT}$ samples only under short exposure conditions (Fig. 3.14A, upper panel). A longer exposure

revealed a very low level detection of extracellular core protein from the $JFH1_{\Delta E1E2}$ sample (Fig. 3.14A, lower panel). These results are in accordance with a previous report showing $JFH1_{\Delta E1E2}$ electroporated cells can secrete a low level of core protein molecules, although the exact composition of these is unknown (Wakita *et al.*, 2005). Importantly, these results showed that extracellular core protein was detectable from cell medium containing moderate titers of JFH1 virus. Next, to determine if DDX3 associates with the virus, the cell medium from $JFH1_{WT}$ electroporated cells was concentrated, overlayed onto a 20-60 % sucrose gradient and centrifuged to equilibrium. The quantity of infectious virus, HCV RNA and protein levels for core and DDX3 was then determined from the six fractions collected from the top of the gradient by $TCID_{50}$, RT-qPCR and immunoblotting, respectively. As reported previously (Gastaminza *et al.*, 2006), the infectivity of JFH1 sedimented to a lower density than the HCV RNA levels that are mainly comprised of non-infectious virus particles (Fig. 3.14B). The presence of core and DDX3 protein by immunoblotting was examined using mAbs AO196 and C7-50 in combination. These mAbs are suitable to use simultaneously as they were known not to cross react with other proteins (Appendix 2). Strikingly, core and DDX3 protein co-sedimented together and were most prevalent in fractions 3 and 4, which corresponded to the peak HCV RNA content between densities 1.09 and 1.12 g/ml (Fig. 3.14C). These data indicate DDX3 may be incorporated onto HCV RNA containing virus particles and possibly infectious virus particles.

To elaborate on these findings, gradient analyses were performed on $JFH1_{Y35A}$ and $JFH1_{WT}$ extracellular particles. For a more accurate representation of particle sedimentation equilibrium, twelve fractions were collected from these gradients. The buoyant density of the infectious $JFH1_{WT}$ particles were distributed over fractions 3 to 6 (between 1.06 and 1.10 g/ml) (Fig. 3.15A and C), whereas the RNA containing particles were more abundant in fractions 6 and 8 (between 1.10 and 1.12 g/ml) (Fig. 3.15B and D). In contrast, the infectivity of $JFH1_{Y35A}$ was largely present within fraction 4, resulting in a leftward shift in the mean density of the virus (Fig. 3.15A and C). A similar change in density profile was also observed in the $JFH1_{Y35A}$ RNA containing particles (Fig. 3.15B and D), suggesting a significant alteration to the biochemical composition of the mutant particles. To determine if the core-DDX3 interaction was responsible for the observed phenotypic changes in the $JFH1_{Y35A}$ virus, immunoblotting was carried out on each gradient fraction using mAbs AO196 and C7-50. For both $JFH1_{WT}$ and $JFH1_{Y35A,}$ the detected core protein sedimented at similar densities as the peak RNA levels (Fig. 3.15E). Longer exposure found that DDX3 was present in the $JFH1_{WT}$ core containing fractions, whereas its levels were barely

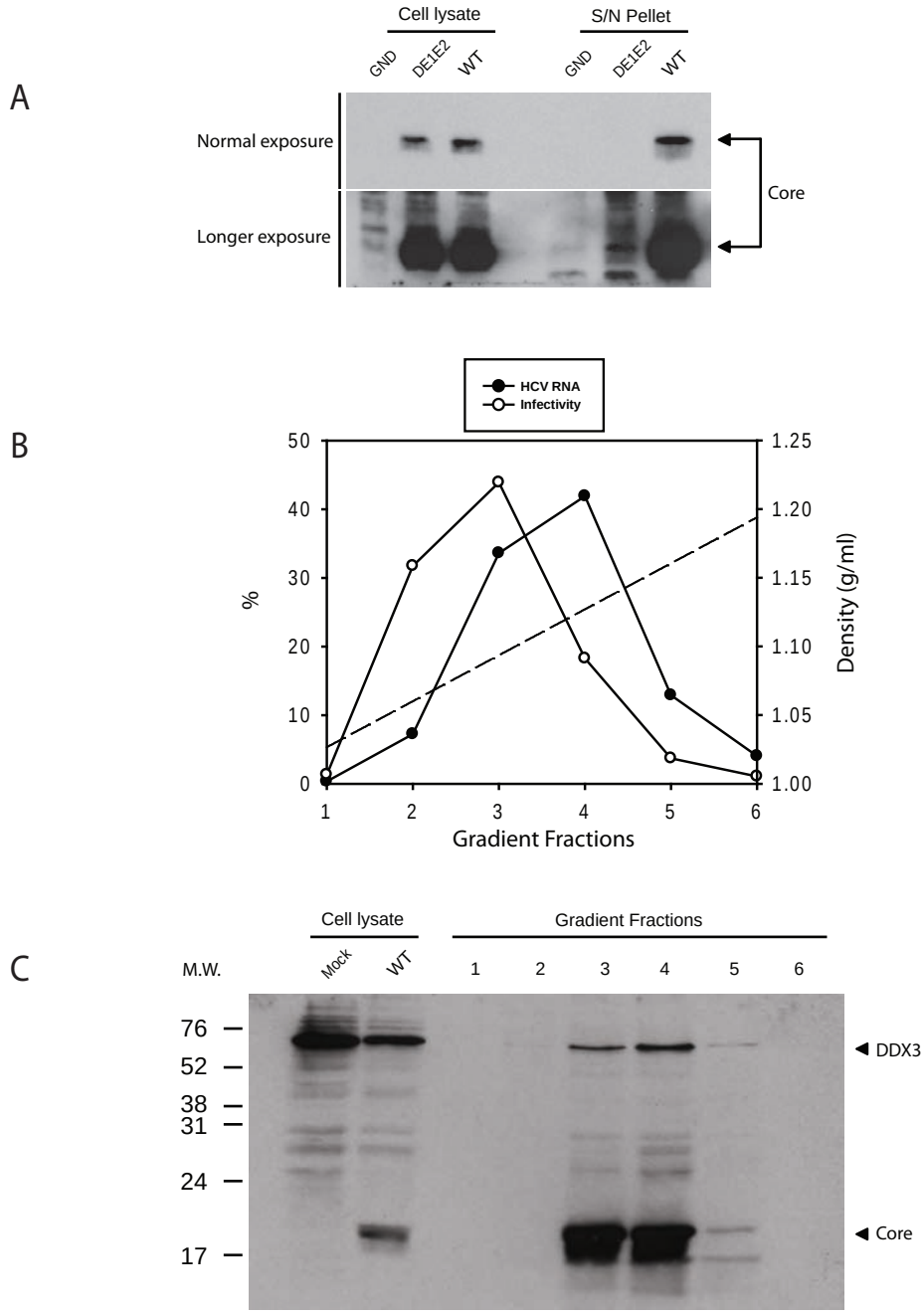

Figure 3.14. Detection of DDX3 on virus particles.

(A) The culture medium from Huh-7 cells electroporated with $JFH1_{GND}$, $JFH1_{\Delta E1E2}$ and $JFH1_{WT}$ was collected and the cells lysed in Masaki buffer. The medium was then pelleted through a 20 % sucrose cushion and the pellet lysed in Masaki buffer. Extracellular lysates were immunblotted with cell lysates ($1/20^{th}$ of total) using core mAb C7-50. Short and long exposures are shown. (B) The infectivity and HCV RNA levels of gradient fractions were determined by FFU assay and RT-qPCR, respectively. (C) Immunoblotting of gradient fractions using mAbs AO196 and C7-50, alongside mock- and JFH1-electroporated cells lysates.

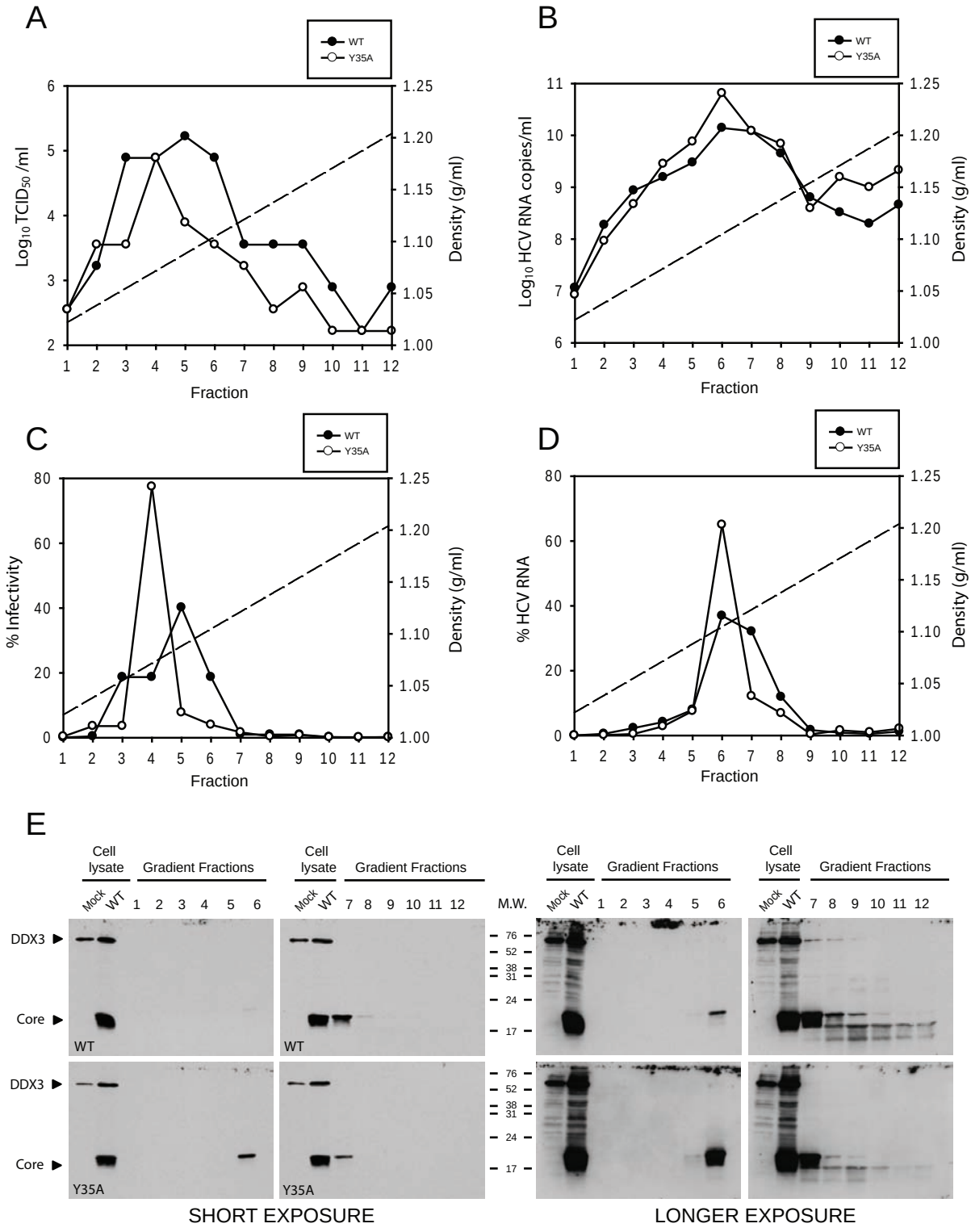

Figure 3.15. Biochemical and biophysical properties of $JFH1_{WT}$ and $JFH1_{Y35A}$ virus particles.

(A-D) Culture medium from Huh-7 cells electroporated with $JFH1_{WT}$ and $JFH1_{Y35A}$ were purified through a 20 % sucrose cushion. The pelleted virus was then subjected to 20-60 % sucrose gradient ultracentrifugation. The infectivity (A and C) and HCV RNA levels (B and D) of gradient fractions were determined by $TCID_{50}$ assay and RT-qPCR, respectively. (E) Immunoblotting of gradient fractions using the anti-DDX3 and anti-core mAbs AO196 and C7-50, respectively. Short and long exposure times are shown.

detectable in the $JFH1_{Y35A}$ core fractions under the same exposure conditions (Fig 3.15E). Thus, these results provide evidence that disruption of the core-DDX3 interaction reduces the incorporation of DDX3 into virus particles. As a consequence the infectious and RNA containing particles assembled are less dense.

As DDX3 is potentially a component of the virion, it was important to test whether anti-DDX3 antibodies could neutralize infection. For this, inhibition assays were performed on $JFH1_{WT}$ virus obtained from electroporated cells using mAb AO196 and pAb R648. Virus was incubated with high concentrations of each antibody, alongside the control antibodies prior to infection of target cells. As expected, the broadly neutralizing anti-E2 mAb AP33 (Owsianka *et al.*, 2005) was capable of almost complete inhibition of infection at concentrations of 100 µg/ml. However, like the non-neutralising anti-E2 mAb ALP98, AO196 was unable to significantly inhibit JFH1 infection. Although, R648 could inhibit infection by ~50 %, a similar effect was observed with the control pre-immune serum. (Fig. 3.16A). Thus, these inhibitory effects are non-specific and likely caused by inhibitory IgGs present in the polyclonal serum. Also, pre-incubation of naïve cells with the DDX3 antibodies prior to infection showed no inhibition in contrast to the >90 % reduction obtained using a well characterized neutralizing mAb to CD81 (Fig. 3.16B), a receptor essential for virus entry into target cells (Section 1.10.1).

3.1.9. Discussion

The data in this section provide novel insights into the redistribution of cellular DDX3 by core protein during productive viral replication. By designing a co-IP assay, the interaction between these two proteins was demonstrated in the HCVcc system. While the colocalisation of DDX3 and core protein in JFH1-infected cells has been previously documented (Dalrymple, 2007), here the exact nature of its redistribution to LDs was dissected. IF analysis found that the redistribution of DDX3 by core protein occurred at early times post-electroporation, suggesting that this interaction takes place immediately following the translation of core protein. Analysis of cells replicating a range of JFH1 domain II and III core mutants demonstrated that the colocalisation of DDX3 with core is independent of the core-LD association. Also, in the absence of core protein the remaining viral proteins had no effect on the cytoplasmic localisation of DDX3. To gain a more detailed insight into the distribution pattern of core and DDX3 in relation to LDs, confocal laser-scanned images of JFH1-electroporated cells were analysed with software designed

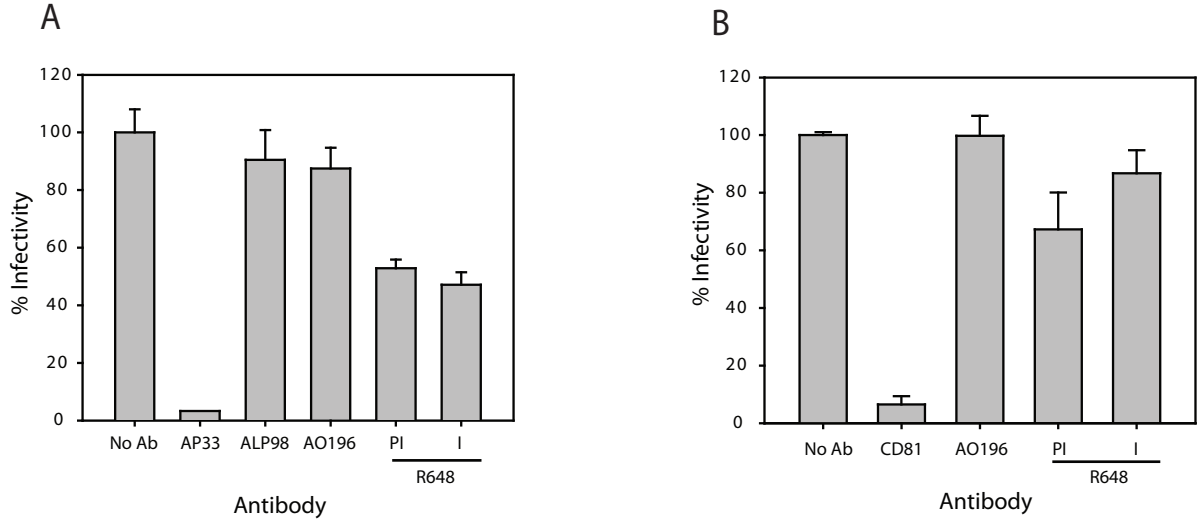

Figure 3.16. JFH1$_{WT}$ virus is not neutralised by anti-DDX3 antibodies.

(A) Approximately 100 FFU of JFH1$_{WT}$ was incubated with 100 µg/ml of mAb AP33, ALP98, AO196 or 1/25 dilution of pAb R648 pre-immune (PI) and immune (I) serum for 1 h prior to infecting Huh-7 cells. At 48 h post-infection, virus infectivity was determined by FFU assay. Percent infectivity was calculated by quantifying viral infectivity in the presence antibodies relative to standard infection. (B) Naïve Huh-7 cells were pre-incubated for 1 h with 40 µg/ml of anti-CD81, 100 µg/ml AO196 and 1/25 dilution of R648 PI and I serum before infection. Cells were then infected with ~100 FFU for 48 h and the infectivity levels determined by FFU assay. Percent infectivity was calculated by quantifying viral infectivity in the presence of inhibitory antibodies relative to a standard infection. Means and error ranges from triplicate infections are shown.

to generate high-resolution 3D reconstructions. The raw z-stack confocal images of the appropriately labelled cells were subjected to deconvolution, a computational 3D-image restoration technique, which serves to remove the unavoidable blurring effect of the point spread function in stacks of optical confocal sections. Regions of interest from the deconvolved z-stacks revealed a tight antigen complex comprising similar ratios of DDX3 and core surrounding ADRP. Thus, this approach provided a more in-depth analysis of the relationships between the DDX3, core and ADRP antigens than that offered by 2D confocal microscopy. However, caution is warranted when interpreting these results as this technique depends crucially on the settings of signal-to-noise and background. Therefore, over- and underestimation of these two parameters during image sampling can lead to artifactual alterations (Landmann & Marbet, 2004). Although, each of the z-stacked images from section 3.1.4 were captured using the appropriate confocal settings with the aim to reduce background and signal-to-noise, one cannot exclude the possibility of artefacts occurring from sub-standard image acquisition.

Given the putative function of DDX3 in RNA metabolism, initial identification of the core-DDX3 interaction led to proposals about its possible role in virus replication and assembly (Mamiya & Worman, 1999; Owsianka & Patel, 1999; You *et al.*, 1999). Recent data using the JFH1 system suggest that HCV RNA replication and virus assembly occur in LD-associated membranes (Boulant *et al.*, 2007; Miyanari *et al.*, 2007). Core protein, which associates with LDs, recruits the viral non-structural proteins, replication complexes and envelope glycoproteins to these sites, allowing virus assembly to proceed in this local environment (Miyanari *et al.*, 2007). Therefore, given that core recruits DDX3 to LDs, it was envisaged that this event may have a function in HCV replication. In keeping with this were the two reports showing reductions in HCVcc replication when DDX3 was removed from the cell by RNAi (Ariumi *et al.*, 2007; Randall *et al.*, 2007). To determine whether this effect on virus replication was pertinent to a reduction in the core-DDX3 interaction, a panel of JFH1 domain I core mutants were characterised. By implementing the co-IP assay, the Y35A mutation was identified as causing the greatest abolition in DDX3 binding. However, this mutant virus still maintained core-LD association and $JFH1_{WT}$ replication levels, suggesting that the core-DDX3 interaction plays no role in virus replication in cell culture.

The data showing RNA silencing impairs $JFH1_{WT}$ infection is in accordance with the previous reports (Ariumi *et al.*, 2007; Randall *et al.*, 2007). In addition to reproducing the deleterious effects of DDX3 knockdown on the $JFH1_{WT}$ replication, a similar phenotype

was also observed for $JFH1_{Y35A}$. These findings provide strong evidence that the requirement of DDX3 for HCV replication is unrelated to its interaction with the viral core protein. Therefore, these data make a clear and important distinction between the effects of siRNA knockdown of DDX3 from the cells and disruption of the core-DDX3 interaction on HCV replication. Intriguing results were also obtained from the simultaneous electroporation of DDX3 siRNAs with $JFH1_{\Delta E1E2(WT)}$ and $JFH1_{\Delta E1E2(Y35A)}$ viral RNAs into cells. While the immunoblotting and IF data provided convincing evidence that efficient DDX3 knockdown caused no deleterious effects to the viral core protein expression from either genome, the $JFH1_{\Delta E1E2(WT)}$ HCV RNA levels were reduced by 45 %. Although, these results are consistent with the data showing ~2 fold reductions in the RNA replication levels of SGRs upon DDX3 knockdown (Ariumi *et al.*, 2007), the RNA levels are contradicted by the unaltered core protein expression levels. Furthermore, the HCV RNA levels of $JFH1_{\Delta E1E2(Y35A)}$ were unaltered by DDX3 silencing, suggesting the Y35A mutation can prevent these reductions in HCV RNA. Another important observation from this experiment is the differential effect of DDX3 silencing prior to virus infection and during viral RNA synthesis. Indeed, the massive reductions in core protein expression demonstrated by IF following infection of DDX3 knockdown cells compared to the unaltered protein expression levels seen in the experiments with $JFH1_{\Delta E1E2}$ genomes, suggest DDX3 functions at an early step in the HCV lifecyle prior to the release of the infectious genome.

Another compelling finding in this section was the co-sedimentation of DDX3 protein with extracellular core protein from $JFH1_{WT}$ electroporated cells. However, this result is puzzling for several reasons. If DDX3 is indeed incorporated into the virion by virtue of the core-DDX3 interaction, it is curious that the disjuncture of these two proteins causes no significant alterations to virus infectivity, as indicated from the phenotype of $JFH1_{Y35A}$. This alludes to DDX3 having no function on the virion during infection and its presence simply being a consequence of its interaction with core protein during viral replication in the cell. On the other hand, it is possible that $JFH1_{Y35A}$ virions possess sufficient levels of DDX3 or a related protein on the particle to fulfil any potential role in virus entry. It is also worth noting that no inhibition of virus infection was found following the incubation of WT virus or target cells with the anti-DDX3 mAb AO196 or pAb R648. However, caution is warranted when interpreting this result as it may be explained by these antibodies being non-neutralising or DDX3 being inaccessible to antibodies rather than DDX3 having no role in infection. Further studies will be necessary to distinguish between these possibilities.

3.2. Identification of Core Mutations that Determine Infectious Virus Assembly and Productive Infection

3.2.1. Introduction

The previous chapter (Section 3.1.6) described 6 alanine mutations in JFH1 core protein that affected the core-DDX3 colocalisation in Huh-7 cells electroporated with each mutant viral RNA. Despite all mutants having reductions in core-DDX3 colocalisation, these viruses were proficient in RNA replication. However, further analysis revealed that the infectious phenotype of two mutants ($JFH1_{F24A}$ and $JFH1_{G33A}$) displayed marked differences to $JFH1_{WT}$. Although the F24A mutation did not affect infectious virus release following electoporation of the viral RNA into cells, it was shown to cause substantial defects to the infection kinetics of the virus particles. To learn more about the function of the F24 residue in virus infection, various aa substitutions were introduced into the JFH1 genome at this position. The effects of these changes were then analysed by measuring the HCV RNA replication levels and infectious virus production of each mutant.

Of all the mutants characterised in section 3.1.6, only $JFH1_{G33A}$ had a reduced capacity to produce infectious virus, as manifested by a 200-fold drop in titer. The virus release defect of $JFH1_{G33A}$ has been reported previously (Dalrymple, 2007). However, in that study infectious virus titers were not detected immediately following electroporation of the viral RNA but instead after five cell passages. The reasons for this discrepancy is possibly due to differences in electroporation efficiency as the titers obtained for $JFH1_{WT}$ from this previous study were substantially lower than those obtained in the present study. Nevertheless, this study revealed that a hallmark of $JFH1_{G33A}$ was its ability to escalate infectious virus release during cell passaging. Furthermore, sequencing of the core gene revealed the presence of a second core aa mutation near the G33A change at the time when infectivity increased (typically passage 5). This phenotype was shown to occur in four independent electroporations, with a different second core mutation being detected in each experiment. The four second-site core mutations reported were G32D, V34A, L36S and L37S (Dalrymple, 2007). However, that study failed to provide conclusive evidence that these were the compensatory mutations responsible for the reversion phenotype of $JFH1_{G33A}$. To further delineate the properties of this mutant, similar passaging experiments

were performed on $JFH1_{G33A}$ electroporated Huh-7 cells. In accordance with the previous report, the infectivity of $JFH1_{G33A}$-progressively increased during cell passaging. Interestingly, sequencing of these fully infectious $JFH1_{G33A}$ genomes revealed the same second-site changes in the core gene reported previously. To confirm that these second-site changes were responsible for the increased $JFH1_{G33A}$ infectivity, each mutation was introduced separately into the original G33A genome. These four double mutants were then characterised alongside $JFH1_{G33A}$ to determine their effects on HCV RNA replication and infectious particle production.

3.2.2. The Role of Phenylalanine 24 in Virus Replication and DDX3 Binding

Although the F24A mutation did not affect the peak infectious virus release following electoporation of the viral RNA into cells, it was shown to cause substantial defects to the infection kinetics of the virus particles (Section 3.1.6). To further assess the dependence of F24 for efficient virus infection, a detailed substitution analysis was performed on this residue. All 6 mutants described in section 3.1.6 were generated by Dalrymple (2007) using alanine-scanning mutagenesis. Alanine was chosen as the replacement residue due to its relatively neutral properties. Alanine is non-polar and not particularly hydrophobic. It is the second smallest aa (behind glycine) containing only a single methyl group for its side chain that is very non-reactive. As a result of its simplicity alanine is present in just about all non-critical protein contexts (Betts & Russell, 2003). It is for these reasons that alanine is frequently chosen in mutagenesis studies aiming to understand the functional properties of particular residues within a protein sequence. While the F24A change potentially highlighted an important function for F24, to more precisely dissect its role in virus infection, substitutions to leucine, isoleucine, valine and tyrosine were introduced into the JFH1 genome. These changes were carefully selected according to the BLOSUM62 mutation matrix as well as the structural and functional properties of each aa. Mutation matrices are sets of numbers that show the propensities of exchanging one aa for another and can be useful as rough guides for how favourable a particular change will be. One of the most common matrices used is BLOSUM (blocks substitution matrix), which is generated from local multiple sequence alignments of protein sequences from a related family (Henikoff & Henikoff, 1992). These matrices are based on the minimum percentage identity of the aligned protein sequences used in deriving them. For example, the standard

BLOSUM62 matrix (Fig. 3.17) corresponds to alignments displaying at least 62 % identity. The scores in a BLOSUM matrix are presented as log-odds scores that measure the logarithm of the probability of two aas occurring in an alignment intentionally and the probability of two aas appearing by chance. A positive score is given to the more favourable substitutions while a negative score is given to the less preferred substitutions. As mutation matrices are based purely on sequence alignments, they do not provide any qualitative information regarding the chemistry involved in particular substitutions. However, such information can be obtained using Taylor classification that explains mutation data through correlation with the physical, chemical and structural properties of aas (Taylor, 1986). The Taylor classification is normally represented in a Venn diagram (Fig. 3.18) where each residue is positioned by multidimensional scaling of Dayhoff's mutation matrix, followed by their grouping to common physico-chemical properties. Thus, the Venn diagram represents a compromise between mutation data and chemistry. Further expert guidance was kindly provided by Dr Francois Penin (Institute de Biologie et Chimie des Protèins, Lyon, France).

BLOSUM62 considers F24A a disfavoured substitution (log-odds score = -2) (Fig. 3.17), which is likely due to the major differences in size and hydrophobicity of phenylalanine and alanine (Fig. 3.18). The differing properties of leucine, isoleucine, valine and tyrosine were selected to allow the effects of aas that are considered disfavourable, neutral and favourable phenylalanine substitutions to be compared in terms of their effects on virus infection. Leucine is a larger and more hydrophobic residue than alanine due to its aliphatic side chains (Figs 3.18 and 3.19). As for alanine, its side chain is very non-reactive and rarely involved in protein function (Betts & Russell, 2003). Leucine is considered to be a neutral substitution for phenylalanine (log-odds score = 0) (Fig. 3.17). Isoleucine has very similar properties to leucine and is also regarded as a neutral substitution (Figs 3.17 and 3.18). However, isoleucine was selected as, unlike leucine, it contains two hydrogen substituents attached to the β-carbon (Cβ-branched) (Fig. 3.19). This feature causes a lot more bulkiness near the protein backbone meaning that this residue is more restrictive to the conformation the main chain can adopt. Valine was selected as its size and hydrophobicity properties fall between those of isoleucine, leucine and alanine (Figs 3.18 and 3.19). Furthermore, valine is Cβ-branched (Betts & Russell, 2003) and considered a less disfavoured substitution than alanine (log-odds score = -1) (Fig. 3.17). Tyrosine was selected as, like phenylalanine, it is an aromatic residue (Fig. 3.19) that is a particularly favoured change for phenylalanine (log-odds score = 3) (Fig. 3.17). Tyrosine is classed as a polar residue as a result of the reactive hydroxyl group on the aromatic ring that makes it

Ala	4																			
Arg	-1	5																		
Asn	-2	0	6																	
Asp	-2	-2	1	6																
Cys	0	-3	-3	-3	9															
Gln	-1	1	0	0	-3	5														
Glu	-1	0	0	2	-4	2	5													
Gly	0	-2	0	-1	-3	-2	-2	6												
His	-2	0	1	-1	-3	0	0	-2	8											
Ile	-1	-3	-3	-3	-1	-3	-3	-4	-3	4										
Leu	-1	-2	-3	-4	-1	-2	-3	-4	-3	2	4									
Lys	-1	2	0	-1	-3	1	1	-2	-1	-3	-2	5								
Met	-1	-1	-2	-3	-1	0	-2	-3	-2	1	2	-1	5							
Phe	-2	-3	-3	-3	-2	-3	-3	-3	-1	0	0	-3	0	6						
Pro	-1	-2	-2	-1	-3	-1	-1	-2	-2	-3	-3	-1	-2	-4	7					
Ser	1	-1	1	0	-1	0	0	0	-1	-2	-2	0	-1	-2	-1	4				
Thr	0	-1	0	-1	-1	-1	-1	-2	-2	-1	-1	-1	-1	-2	-1	1	5			
Trp	-3	-3	-4	-4	-2	-2	-3	-2	-2	-3	-2	-3	-1	1	-4	-3	-2	11		
Tyr	-2	-2	-2	-3	-2	-1	-2	-3	2	-1	-1	-2	-1	3	-3	-2	-2	2	7	
Val	0	-3	-3	-3	-1	-2	-2	-3	-3	3	1	-2	1	-1	-2	-2	0	-3	-1	4
	Ala	Arg	Asn	Asp	Cys	Gln	Glu	Gly	His	Ile	Leu	Lys	Met	Phe	Pro	Ser	Thr	Trp	Tyr	Val

Figure 3.17. BLOSUM62 substitution matrix.

The log-odds score for each of the 210 possible substitutions of the 20 standard aas indicate those changes that are favoured (>0), neutral (0) and disfavoured (<0). Adapted from Henikoff & Henikoff (1992).

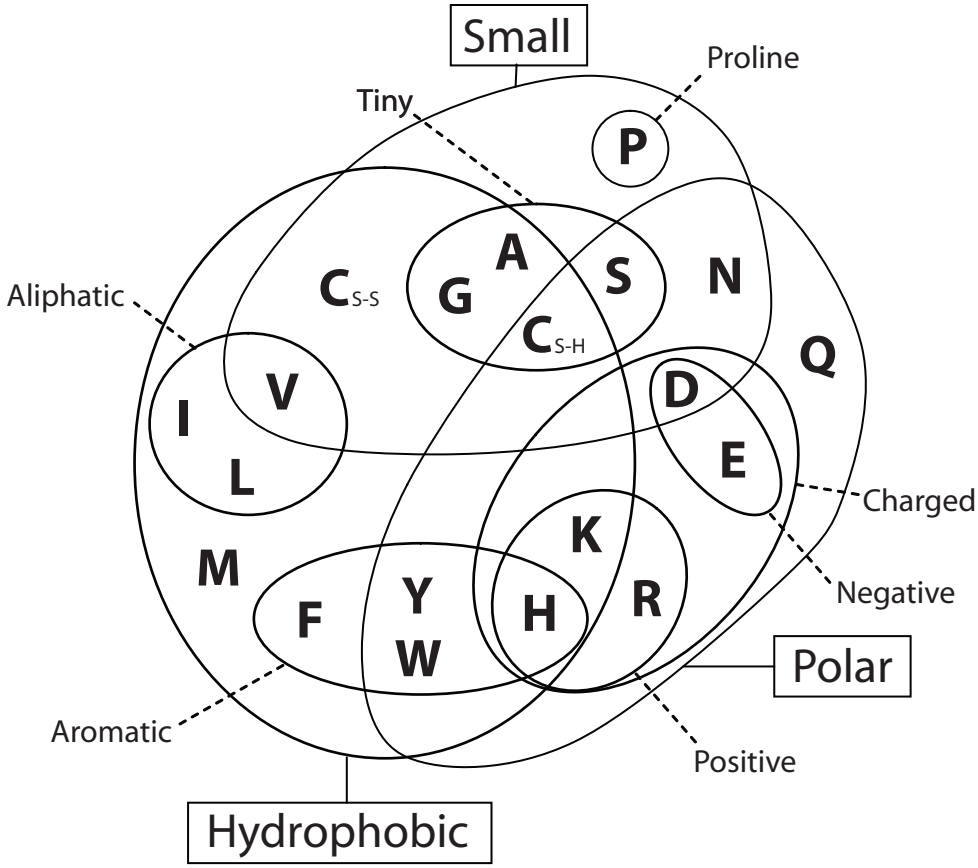

Figure 3.18. Venn diagram relating a selection of physico-chemical properties from the 20 standard aas.

The aas are divided into sets. Two major sets include all aas containing a polar group (polar) and those which exhibit a hydrophobic effect (hydrophobic). A third major set is defined by size (small) and contains the 9 smallest amino acids (with large defined by implication). Within this is an inner set of smaller residues (tiny), which have at most two side chains atoms. Cysteine has an uncertain location as the reduced form (C_{S-H}) has similar properties to serine, whereas the oxidised form (C_{S-S}) may be more comparable to Valine. Other sets include full-charge (charged), which contains the subset positive (negative is defined by implication) and aromatic and aliphatic. Proline was excluded from the main body of the diagram due to its unique backbone properties. Adapted from Taylor (1986).

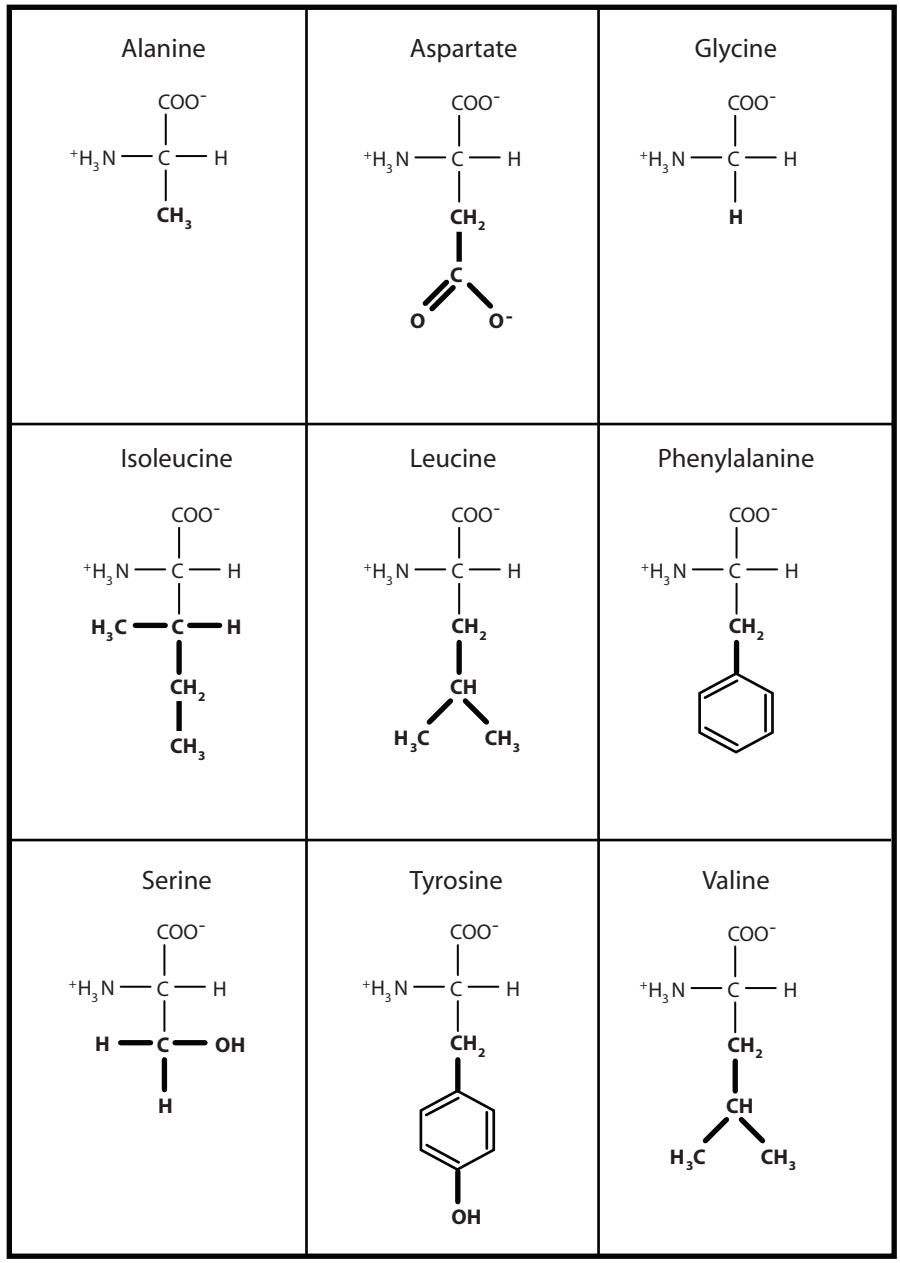

Figure 3.19. Structures of the aas relevant to this study.

Each residue is illustrated in dipolar form consisting of an amino group ($–NH_3^+$), a carboxyl group ($– COOH^-$), a hydrogen atom (–H) and a distinctive side chain (shown in bold) bonded to the α-carbon atom. Adapted from Stryer (1988).

less hydrophobic (Betts & Russell, 2003). Together, this set of mutations will allow the study of two disfavoured changes (alanine and valine), two neutral changes (leucine and isoleucine) and one favourable change (tyrosine) to F24 on JFH1 virus infection. These mutations were introduced into the JFH1 genome using site-directed mutagenesis as described in section 2.2.3.9.

Consistent with the results in section 3.1.6, the RNA replication of $JFH1_{F24A}$ was unaltered post-electroporation, whereas the levels of released virus yield were delayed as seen by the lower titers at 24 and 48 h (Fig. 3.20A and B). No differences in RNA replication were observed for the other F24 mutants; however their virus release levels were slightly altered. The virus release kinetics and peak titers of $JFH1_{F24L}$ and $JFH1_{F24Y}$ were similar to WT, whereas $JFH1_{F24I}$ and $JFH1_{F24V}$ had slightly lower infectivity at each time-point (Fig. 3.20B). Next, the replication kinetics of these phenylalanine mutants was examined following infection. Using virus obtained 72 h post-electroporation, naïve cells were inoculated at an m.o.i. of 0.2 and 0.02 $TCID_{50}$ per cell. The infectious progeny virus release and intracellular viral RNA replication levels were then monitored from these cells over 72 h. The virus release pattern of $JFH1_{F24L}$, $JFH1_{F24V}$ and $JFH1_{F24Y}$ closely mimicked that of $JFH1_{WT}$ (Fig. 3.21A and C). The lower infectivity of $JFH1_{F24I}$ indicates subtle decreases in virus spread. However, the greatest reduction was observed for $JFH1_{F24A}$, which had the lowest infectivity and intracellular RNA replication values at each time-point for each m.o.i. (Fig. 3.21A-D).

Given that the F24A mutation was shown to abrograte core-DDX3 binding (Section 3.1.6), it was important to demonstrate how the other residue changes at this position affected the level of core-DDX3 interaction. As shown in the representative images in Fig. 3.22, IF analysis found varying levels of core-DDX3 colocalisation for each mutant at 72 h post-electroporation. No core-DDX3 colocalisation was observed for $JFH1_{F24A}$, $JFH1_{F24I}$ and $JFH1_{F24V}$; whereas all cells replicating $JFH1_{F24Y}$ displayed complete colocalisation between the two proteins as for $JFH1_{WT}$. Mixed populations of cells were found for $JFH1_{F24L}$ with colocalisation being observed in 9 % of cells counted. Next, the co-IP assay (Section 3.1.3) was performed on Huh-7 cell lysates electroporated with each mutant to test for alterations to the core-DDX3 interaction. Fortunately, all the phenylalanine mutants were recognised by the core mAb C7-50 as shown in Fig. 3.23A by the similar detection levels of core and NS5A in the lysates. The mutant cores were co-immunoprecipitated by the anti-DDX3 antiserum R648 in various amounts compared to $JFH1_{WT}$ (Fig. 3.23B and C). Consistent with our previous findings the F24A mutation reduced the level of core

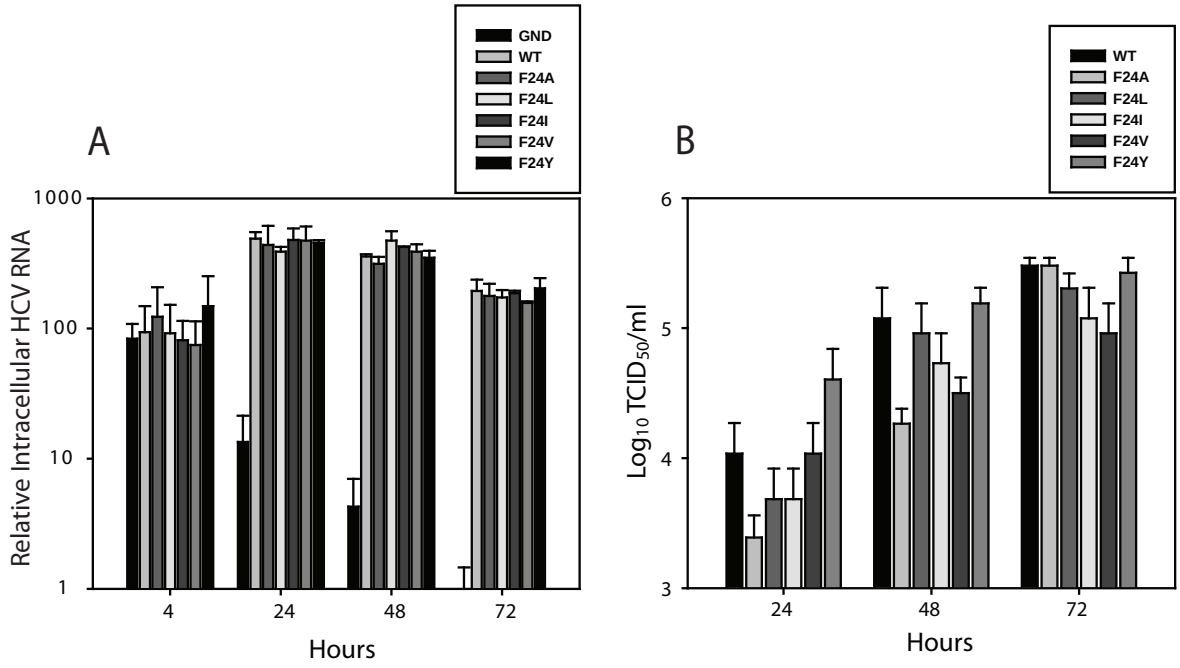

Figure 3.20. Replication of JFH1 phenylalanine core mutants following electroporation.

(A) Intracellular HCV RNA replication and (B) infectious virus production at 24, 48 and 72 h post-electroporation of JFH1 RNA with and without the indicated mutations, as determined by RT-qPCR and $TCID_{50}$, respectively. RNA levels were normalised to GND values at 72 h. Means and error ranges from two independent experiments are given.

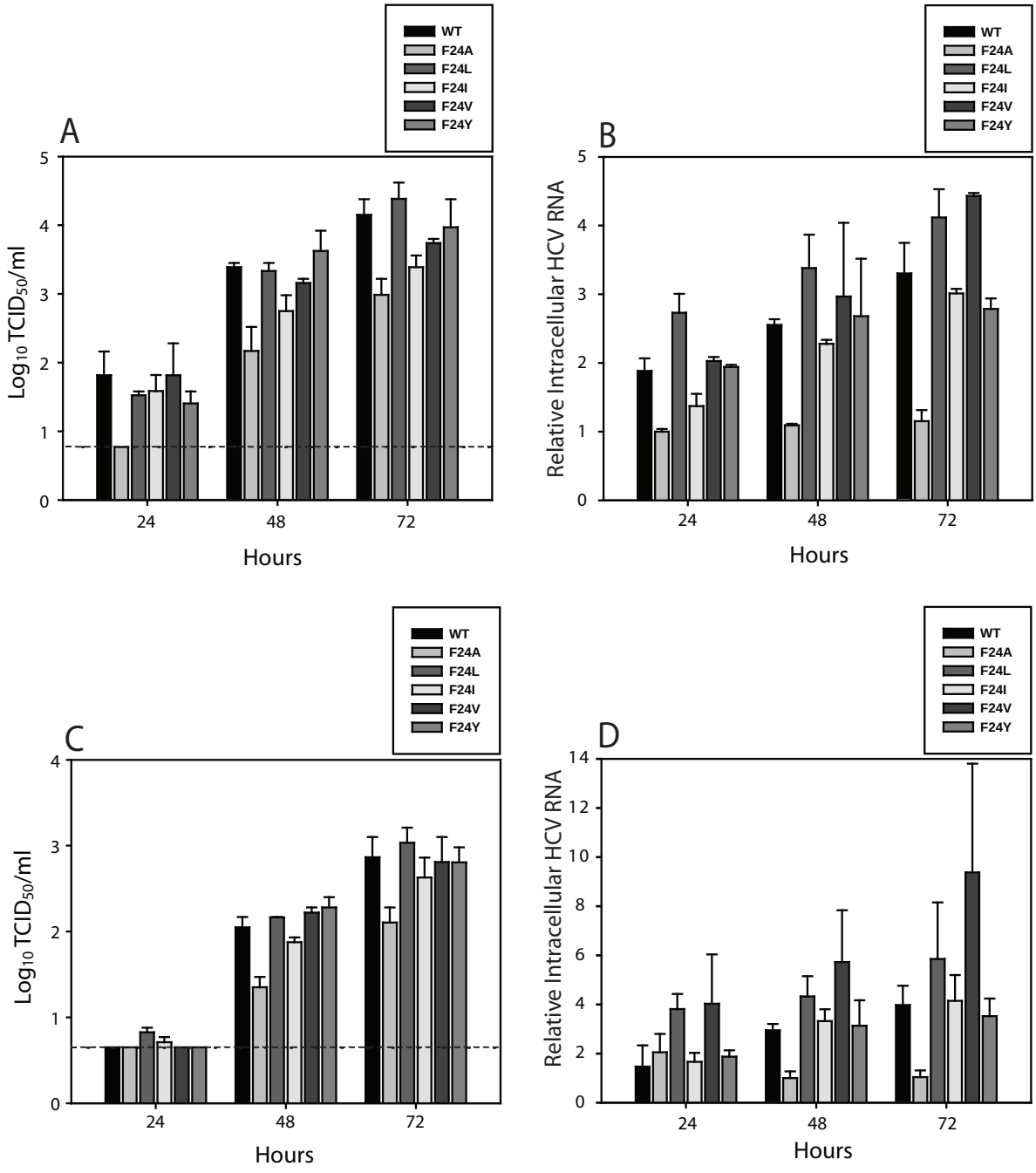

Figure 3.21. Infection kinetics of the JFH1 phenylalanine core mutant viruses.

Naïve Huh-7 cells were infected with $JFH1_{WT}$ or mutant viruses at an m.o.i. of 0.2 (A and B) and 0.02 (C and D) as indicated. At 24, 48, and 72 h post-infection, the released virus yield (A and C) and the intracellular HCV RNA levels (B and D) were determined by $TCID_{50}$ and RT-qPCR, respectively. The RNA levels were normalised to the values from (B) $JFH1_{F24A}$ at 24 h and (D) $JFH1_{F24A}$ at 48 h. Means and error ranges from two independent experiments are given. Dotted line indicates cut-off of the $TCID_{50}$ assay.

being precipitated by anti-DDX3 (Section 3.1.6). Substitution of F24 with L, I and V also caused similar decreases to the core-DDX3 interaction. Remarkably, more F24Y core protein was co-precipitated than WT suggesting the engagement of core with DDX3 is enhanced by this particular mutation (Fig. 3.23B-D). The specificity of the co-IP was confirmed on the cell lysates from $JFH1_{F24Y}$-electroporated cells by showing only the immune R648 serum and not the R648 pre-immune serum could precipitate core (Fig. 3.23E). Importantly, no alteration to the DDX3 expression levels was found in the lysates derived from cells electroporated with each mutant (Fig. 3.23F). Next, the stability of these mutations during persistent infection was measured. Infectious virus from each mutant was used to inoculate naïve Huh-7 cells alongside $JFH1_{WT}$ at an equal m.o.i. At the time of subconfluency, these cells were split 1:10 for a total of 5 passages. At passage 5 the cell medium was assayed for infectious virus, the cells were tested for core-DDX3 colocalisation, and the core gene from intracellular viral RNA was sequenced. As summarised in Fig. 3.23G, each mutant had similar levels of virus release to $JFH1_{WT}$ indicating that they can persistently infect cells during serial passages. Moreover, each mutation appears stable as no changes to the core gene sequence or core-DDX3 colocalisation was observed in passage 5 cells.

3.2.3. Effects of Core Mutation G33A on Infectious Virus Assembly

The images in Fig. 3.24 clearly exhibit the defect of $JFH1_{G33A}$. At 72 h post-electroporation, an equal number of NS5A expressing cells were present for $JFH1_{WT}$ and $JFH1_{G33A}$. However, when naïve cells were inoculated with the culture medium from these electroporated cells, there was a marked reduction in the number of NS5A positive foci for $JFH1_{G33A}$ infected cells compared to $JFH1_{WT}$ (Fig. 3.24B). These data are in agreement with those presented in Fig. 3.9A where no changes in NS5A expression were observed in $JFH1_{G33A}$-electroporated cells, yet the cell culture medium contained a 200-fold reduction in infectious particle numbers compared to $JFH1_{WT}$. Together, these data indicate this mutation does not affect virus RNA replication but grossly impairs infectious virus assembly. To determine more precisely the impact of the G33A mutation on virus assembly, the intracellular and extracellular virus titers were assayed at 48 h post-electroporation. As shown in Fig. 3.25A, the cell-free and cell-associated infectivity of $JFH1_{G33A}$ RNA-electroporated cells was severely compromised, suggesting that this core

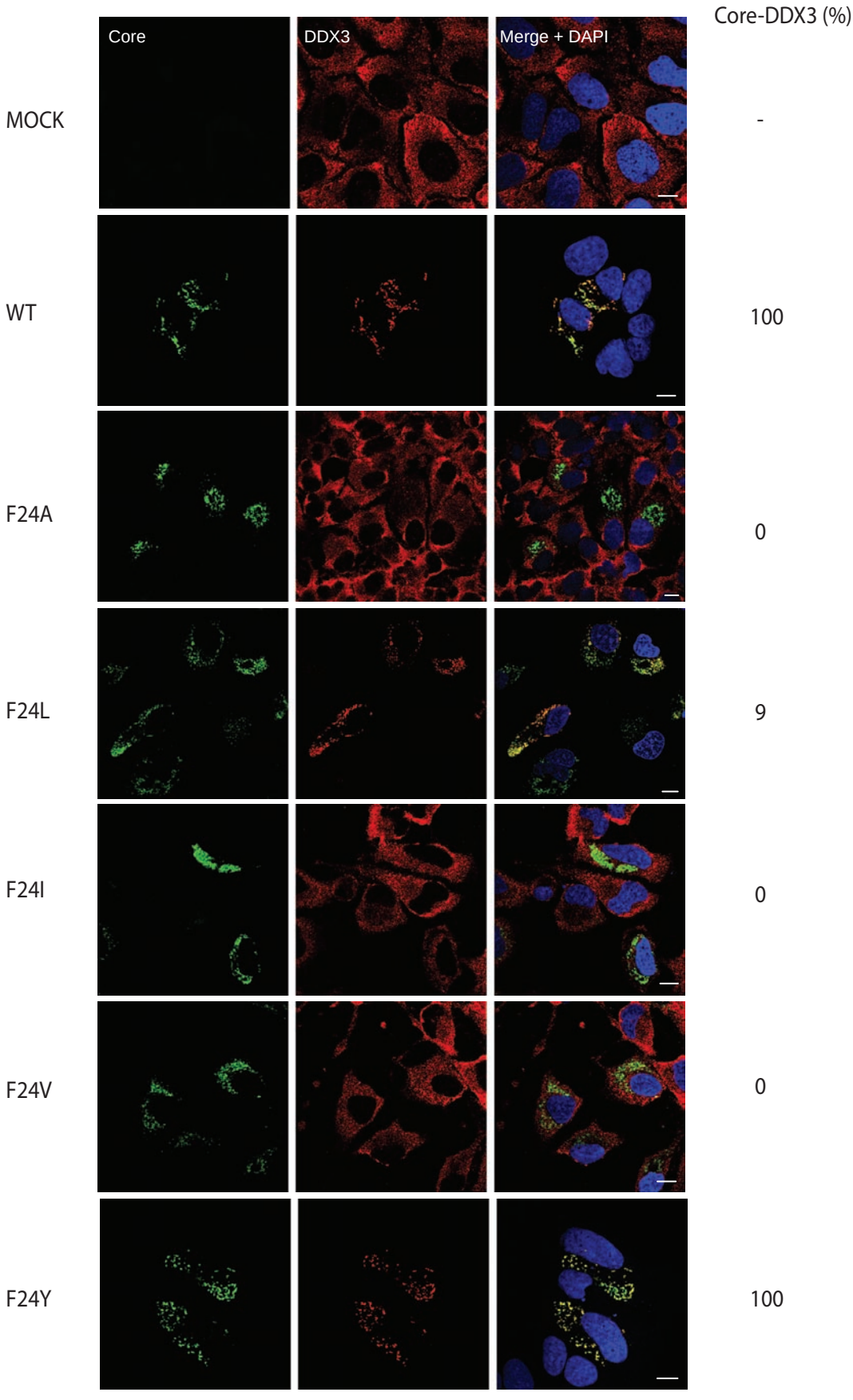

Figure 3.22. Localisation of DDX3 in cells replicating the phenylalanine core mutants.

Huh-7 cells electroporated with the indicated viral RNAs were fixed at 72 h post-incubation and analysed by confocal microscopy for the intracellular distribution of core and DDX3 using R308 and AO196 antibodies, respectively. The percentage of cells (n=200) displaying core-DDX3 colocalisation is stated next to each image. Bar, 10 µm.

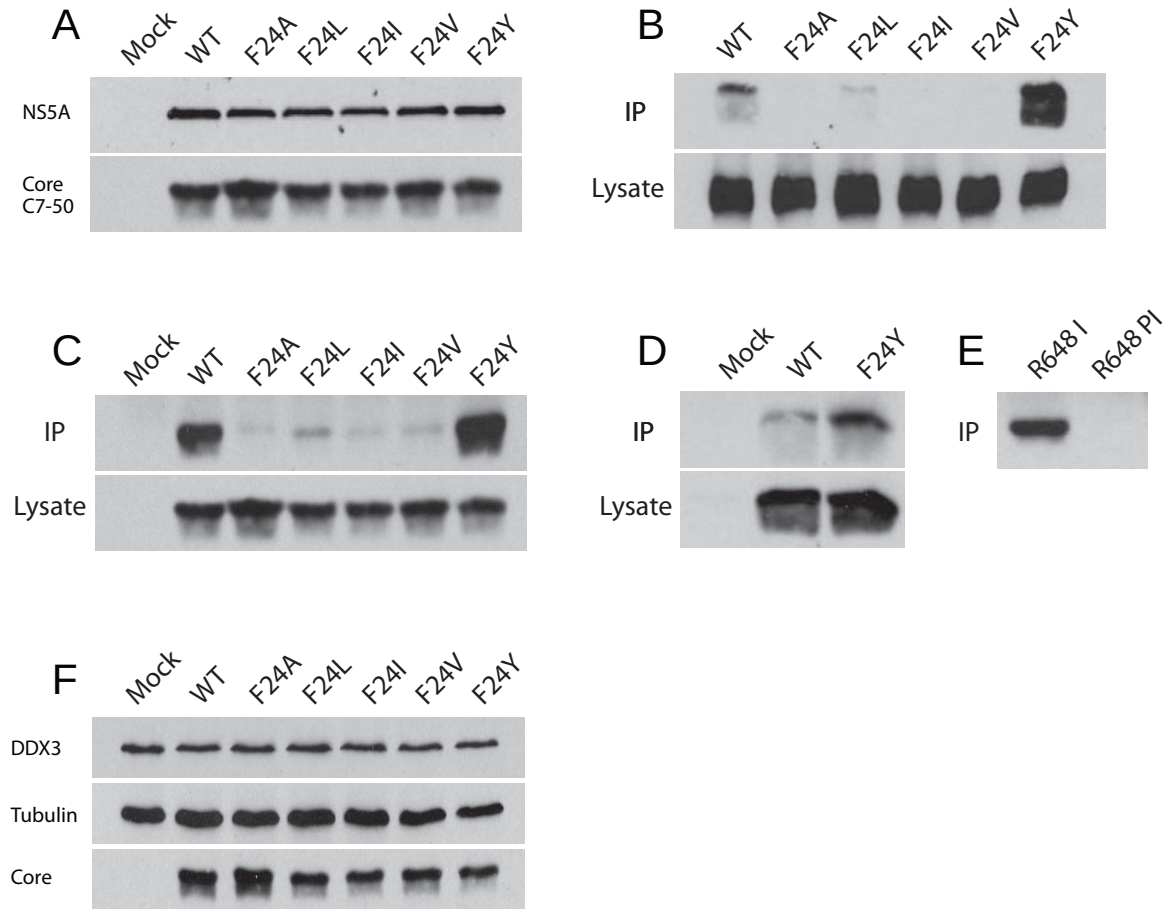

G

Virus	WT	F24A	F24L	F24I	F24V	F24Y
$log_{10}TCID_{50}$/ml	3.5	3.33	4.17	3.5	3.33	4.17
% Core-DDX3	100	0	14	0	0	100
Core Sequence	No change	No change	No change	No change	No change	No change

Figure 3.23. Analysis of the core-DDX3 interaction from the phenylalanine mutants.

(A) Reactivity of mutant core proteins to mAb C7-50. Huh-7 cells were electroporated with the indicated viral RNAs and immunoblotted for core (mAb C7-50) and NS5A (mAb 9E10) at 72 h post-incubation. (B-D) Interaction between DDX3 and the core phenylalanine mutants. HCV core was co-immunoprecipitated from the lysates obtained at 72 h post-electroporation using pAb R648 followed by immunoblotting with mAb C7-50. Upper and lower panels represent immunoblotting of core protein from precipitated lysates and input control ($1/20^{th}$), respectively (E) Specificity of the core-DDX3 co-IP. Lysates from two $JFH1_{F24Y}$ electroporations were pooled together and divided into two co-IP assays. (F) DDX3 expression levels in cells electroporated with the core phenylalanine mutants. Huh-7 cells were electroporated with the indicated viral RNAs and immunoblotted for core (C7-50), DDX3 (AO196) and tubulin at 72 h post-incubation. (G) Persistent infection of Huh-7 cells with the core phenylalanine mutant viruses. Cells were infected at an m.o.i. of 0.005 and passaged 1:10 at the time of subconfluency for 5 passages. At passage 5 the infectivity of the culture medium was assayed by $TCID_{50}$ assay, the percentage of cells (n=200) displaying core-DDX3 colocalisation was determined by IF and the viral core gene was sequenced from total cell RNA following RT-PCR.

mutant has a defect acting prior to infectious particle assembly. To determine what effect this mutation had on the secretion of non-infectious particles, sucrose cushion purification was performed on the cell medium obtained from Huh-7 cells electroporated with the viral RNA from $JFH1_{G33A}$, $JFH1_{WT}$ and $JFH1_{GND}$. As shown in Fig. 3.25B, $JFH1_{G33A}$ secreted a similar number of RNA containing particles as $JFH1_{WT}$. To test the sedimentation equilibrium of these particles, sucrose gradient ultracentrifugation analysis was performed. The $JFH1_{G33A}$ RNA containing particles displayed a similar sedimentation pattern to $JFH1_{WT}$ with the peak RNA quantities residing within fractions 6-8 (Fig. 3.25C and D). The low level infectivity detected for $JFH1_{G33A}$ was found in the lighter density fractions (fractions 3-6), suggesting the $JFH1_{G33A}$ infectious particles are of a similar buoyant density to $JFH1_{WT}$. As expected, the serial passaging $JFH1_{G33A}$-transfected cells resulted in a progressive increase in extracellular viral titers (Fig. 3.26A) and further passaging experiments performed on this mutant confirmed that this behaviour was reproducible (Fig. 3.26B). Sequence analysis of the $JFH1_{G33A}$ core protein from passage 6 virus (Fig. 3.26C) revealed the presence of second-site core mutations. Importantly, no core mutations were detected in the genome of the passage 6 $JFH1_{WT}$ virus. Overall, a total of 4 different second-site mutations in core were identified, all of which were located in very close proximity to the original engineered substitution and coincided with the increase in infectious virus (Fig. 3.26D). Interestingly, these same four mutations were documented previously from $JFH1_{G33A}$ passaging experiments (Dalrymple, 2007).

To determine if these additional core mutations were responsible for the enhanced infectivity of $JFH1_{G33A}$ seen during passaging, these second-site changes were engineered individually into the original $JFH1_{G33A}$ genome by site-directed mutagenesis as described in section 2.2.3.9. Unlike $JFH1_{G33A}$, these double core mutants displayed comparable cell-free infectivity's to $JFH1_{WT}$ (Fig. 3.27A), indicating these second core mutations are compensatory mutations. No changes were observed in the intracellular RNA replication levels for $JFH1_{G33A}$ or the double mutants (Fig. 3.27B), implying that the G33A mutation only negates infectious virus assembly. Next, the replication kinetics of each double mutant was examined following infection. Virus obtained 72 h post-electroporation was used to inoculate naïve cells at an m.o.i. of 0.1 and 0.01 $TCID_{50}$ per cell. The levels of infectious progeny virus release and intracellular viral RNA replication were then measured at 24, 48 and 72 h after infection. Surprisingly, apart from $JFH1_{G33A/L37S}$ the remaining double core mutants displayed lower replication levels than $JFH1_{WT}$. The greatest reduction was observed for $JFH1_{G33A/V34A}$, which had the lowest infectivity and intracellular RNA replication values at each time-point for each m.o.i. (Figs. 3.28A-D).

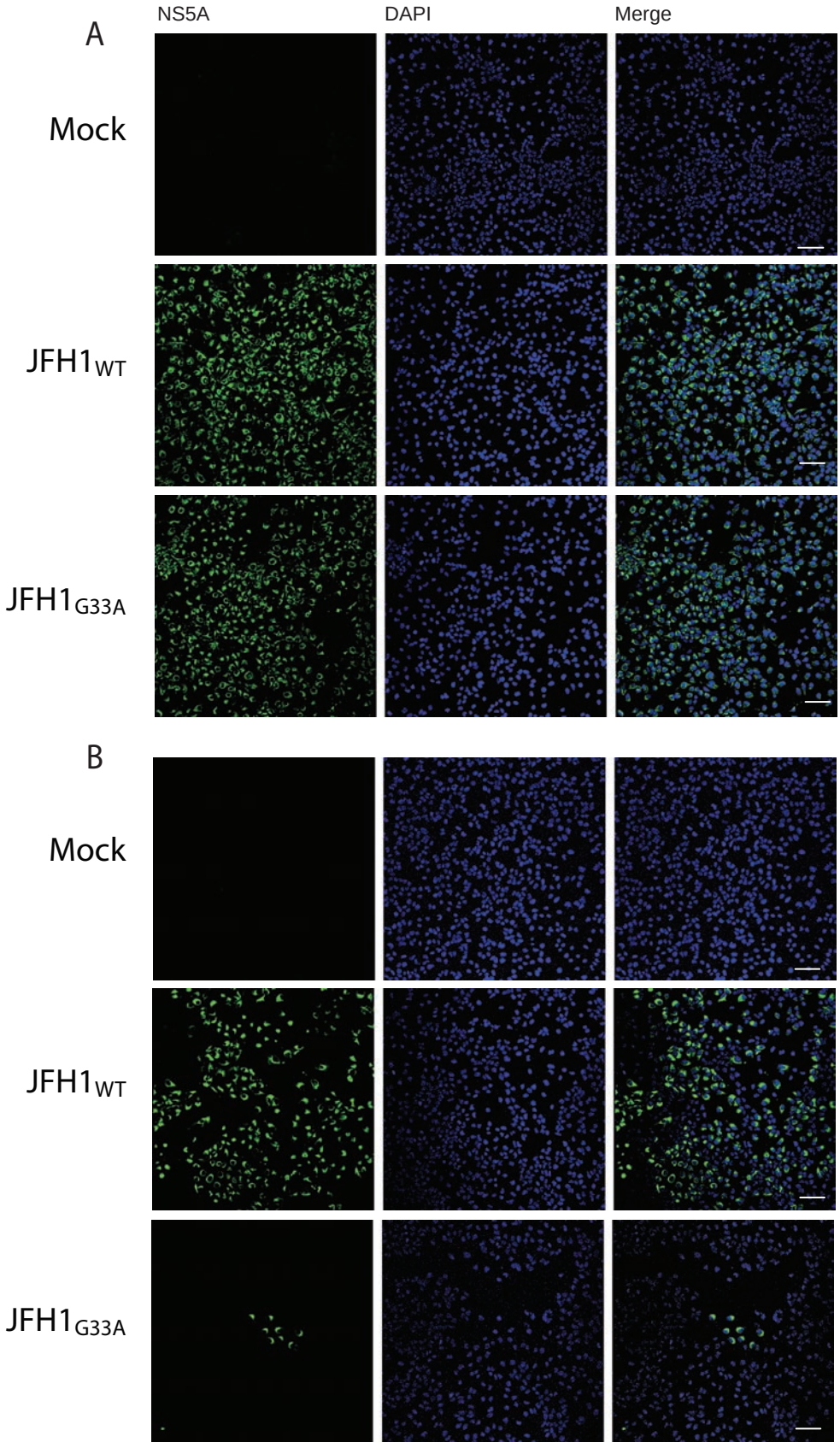

Figure 3.24. NS5A expression from JFH1$_{G33A}$-electroporated and -infected cells.

(A) Huh-7 cells were electroporated with 10 µg of JFH1$_{WT}$ and JFH1$_{G33A}$ viral RNA. At 72 h post-incubation, the cells were fixed and probed with the anti-NS5A mAb 9E10. (B) Naïve Huh-7 cells were inoculated with the culture medium obtained at 72 h post-electroporation with JFH1$_{WT}$ and JFH1$_{G33A}$. At 48 h post-incubation, the cells were fixed and probed with the anti-NS5A mAb 9E10. Scale bar, 100 µm.

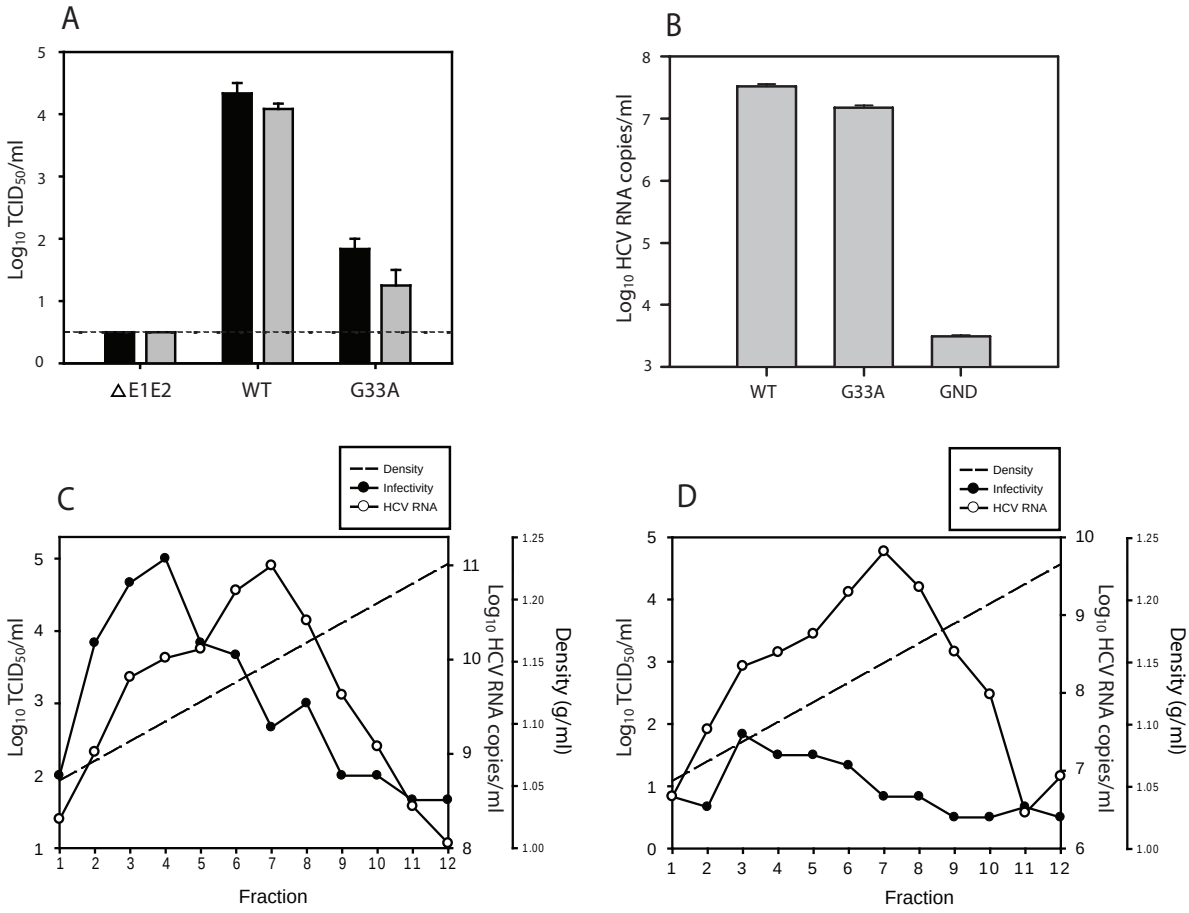

Figure 3.25. Requirement of JFH1$_{G33A}$ for virus release.

(A) Huh-7 cells were electroporated with the genomes specified and 48 h later the cell-released (black bars) and cell-associated (grey bars) infectivity were determined by $TCID_{50}$ assay. Mean values and standard errors of from two independent experiments are shown. Dotted line indicates assay sensitivity. (B) Genomic RNA levels purified by sedimentation of culture supernatants through a sucrose cushion were measured by RT-qPCR at 120 h post-electroporation. Error bars indicate variability of the assay. (C and D) Culture medium from Huh-7 cells electroporated with (C) JFH1$_{WT}$ and (D) JFH1$_{G33A}$ were purified through a sucrose cushion. The pelleted virus then underwent 20-60 % sucrose gradient ultracentrifugation. The infectivity and genomic RNA levels of gradient fractions were determined by $TCID_{50}$ assay and RT-qPCR, respectively.

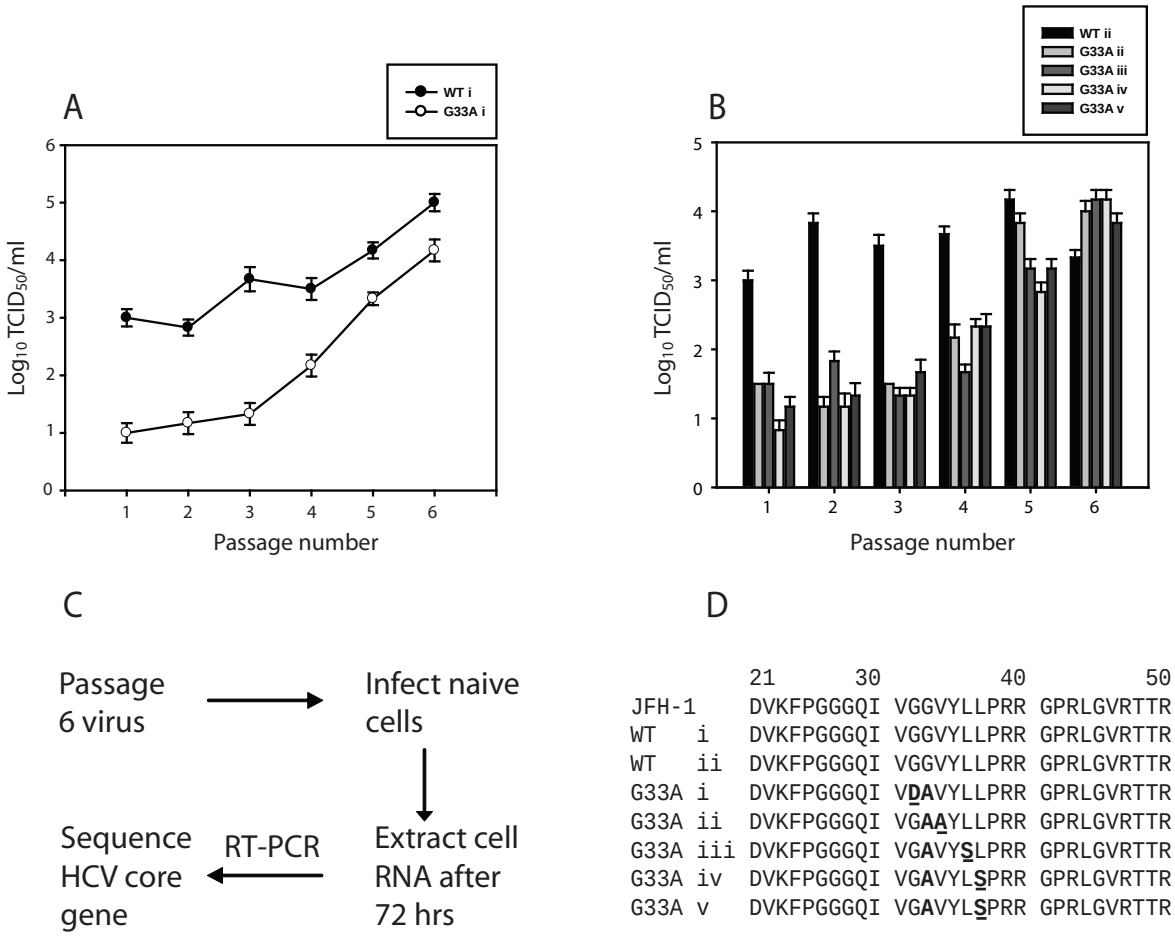

Figure 3.26. Reversion properties of JFH1$_{G33A}$.

(A) Cells electroporated with JFH1$_{G33A}$ or JFH1$_{WT}$ genomes were passaged 6 times. At each passage the infectivity of the cell culture supernatant was determined by TCID$_{50}$ assay. Error bars demonstrate variability of the TCID$_{50}$ assay. (B) Repeat passaging experiments on JFH1$_{G33A}$-electroporated cells. (C) Methodology for sequencing the core gene from passage 6 virus. (D) Mutations identified in the JFH1$_{G33A}$ core protein sequence from each passaging experiment with the engineered G33A mutation shown in bold and the second-site mutation underlined in bold. Roman numerals represent different passaging experiments.

Given that these second-site mutations are located within or close to the DDX3 binding region of core, the level of core-DDX3 association was measured. First, colocalisation studies were done by staining cells for core and DDX3 at 72 h post-electroporation. As shown in the representative images in Fig. 3.29, varying levels of core-DDX3 colocalisation were observed for each mutant. Core-DDX3 colocalisation was diminished by $JFH1_{G33A/V34A}$, whereas $JFH1_{G33A/L37S}$ emulated the complete colocalisation observed for $JFH1_{WT}$. Mixed populations of cells were found for $JFH1_{G32D/G33A}$ and $JFH1_{G33A/L36S}$ with colocalisation being observed in 35 and 21 % of cells counted, respectively (Fig. 3.29.). To determine the level of core-DDX3 interaction in cells replicating these double mutants, the co-IP assay described in section 3.1.3 was implemented. However, prior to this, the reactivity of these mutated core proteins to mAb C7-50 was analysed by immunoblotting. Cell lysates obtained from Huh-7 cells electroporated with each viral RNA were immunoblotted using mAb C7-50 in combination with the anti-NS5A mAb 9E10. These mAbs are suitable to use in combination as they were known not to cross react with other proteins (Appendix 2). The presence of NS5A but barely detectable levels of core protein from the double mutant lysates indicated none of these mutated core proteins bound C7-50 (Fig. 3.30A). Next, these lysates were immunoblotted using pAb R308 and biotinylated pAb BR526. As shown in Fig. 3.30B, R308 detected similar levels of core protein in each lysate confirming that the double mutations did not affect core stability. BR526 detected the core expressed by all mutants except $JFH1_{G33A/L37S}$, indicating that these two mutations reduce the antibody binding affinity. Although, R308 recognised each mutant core protein, it was not suitable for immunoblotting of precipitated lysates due to the potential cross reactivity caused by the R648 rabbit IgGs. This problem was not applicable to BR526 as it was biotin labelled and thus requires a stretavidin-HRP conjugate. Unfortunately, due to the reduced affinity of BR526 to $JFH1_{G33A/L37S}$ this mutant had to be excluded from the co-IP assay. As shown in Fig. 3.30C, $JFH1_{G32D/G33A}$ and $JFH1_{G33A/L36S}$ core protein was co-immunoprecipitated in much lower amounts than the WT protein. However, the $JFH1_{G33A/V34A}$ core was not co-immunoprecipitated at all, indicating the interaction was abrogated. It should be noted that BR526 had a poor affinity for core mutants $JFH1_{I30A}$ and $JFH1_{G33A}$ (Appendix 3) that were also shown not to be recognised by C7-50 (Fig. 3.9A) and therefore could not be used in the co-IP assay with this antibody. Next, the stability of these double mutations during persistent infection was measured. Virus from each double mutant was used to infect naïve Huh-7 cells alongside $JFH1_{WT}$ at an equally low m.o.i. At the time of subconfluency, these cells were split 1:10 for a total of 5 passages. At passage 5 the cell medium was assayed for infectious virus, the

cells were tested for core-DDX3 colocalisation, and the core gene from intracellular viral RNA was sequenced. As summarised in Fig. 3.30D, each mutant had similar levels of virus release to the $JFH1_{WT}$ indicating that they can persistently infect cells during serial passages. Moreover, each mutation appears stable as no changes to the core gene sequence or core-DDX3 colocalisation was observed in passage 5 cells.

3.2.4. $JFH1_{F24A}$ and $JFH1_{G33A/V34A}$ have Reduced Virus Spread

The results from sections 3.2.2 and 3.2.3 indicate that core mutations F24A and G33A/V34A both impede JFH1 viral spread. To better understand the nature of these abnormalities, further experiments were performed on these mutants. IF analysis at 72 h post-infection showed that the foci produced by both $JFH1_{G33A/V34A}$ and $JFH1_{F24A}$ had fewer infected cells per focus compared to $JFH1_{WT}$ (Fig. 3.31A and B). In addition, the individual NS5A-positive cells within each focus were generally less bright for each core mutant (Fig. 3.31A). These observations further support the notion that these core mutants are less efficient at spreading in cell culture. Given that both viruses replicate efficiently following electroporation of the viral RNA into cells, the defect likely acts at an early stage during infection, possibly before the release of the infectious genome into the cytoplasm. Given that the viral envelope glycoproteins are unaltered this defect is unlikely to occur during virus binding and entry. However, to experimentally exclude the possibility of an entry problem, the ability of $JFH1_{G33A/V34A}$ and $JFH1_{F24A}$ to bind and infect cells during a standard infection was measured. In this experiment, the internalised and cell-surface attached viruses were distinguished by their sensitivity to trypsin digestion. Cells were infected with virus according to protocols I or II (Fig. 3.31C). Following virus attachment (1 h at 4 ^{o}C) or standard infection, cells were either washed in cold medium or treated with trypsin for 30 min at 4 ^{o}C. The latter treatment degrades the cell-bound virus but not the internalised particle, which is able to proceed with subsequent stages of entry and replication. After appropriate treatment, cells were cultivated for 48 h following which infectivity was determined (Fig. 3.31D). After 3 h at 37 ^{o}C, ~ 80 % of the cell-associated WT and core mutant viruses were resistant to trypsin digestion and therefore represent the fraction of internalized viruses. In contrast, after 1 h at 4 ^{o}C, more than 95 % of the WT and core mutant viruses were inactivated by trypsin proteolysis, indicating that this treatment is efficient at degrading the vast majority of cell-bound virus (Fig. 3.31D). Therefore, during the 3 h time frame the degree of internalization is similar for all viruses,

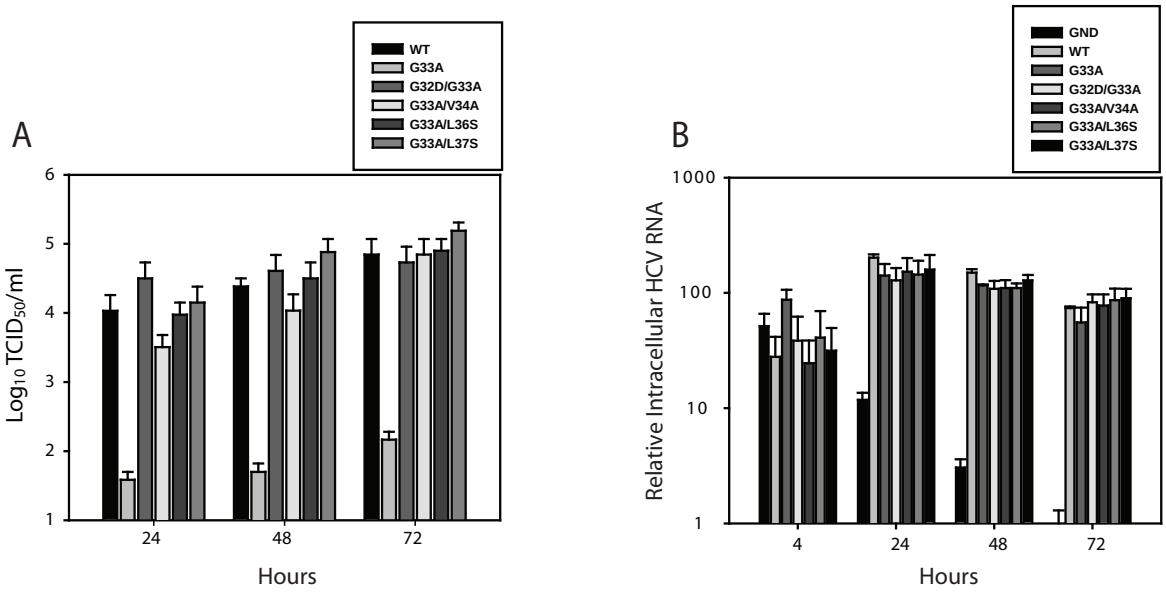

Figure 3.27. Second-site mutations compensate JFH1$_{G33A}$ virus assembly.

(A) Infectious virus production and (B) intracellular HCV RNA replication at 24, 48 and 72 h post-electroporation into Huh-7 cells of JFH1$_{G33A}$ RNA with and without the second-site mutations, as determined by $TCID_{50}$ and RT-qPCR, respectively. The relative RNA levels were normalised to the GND value at 72 h. Means and error ranges from two independent experiments are given.

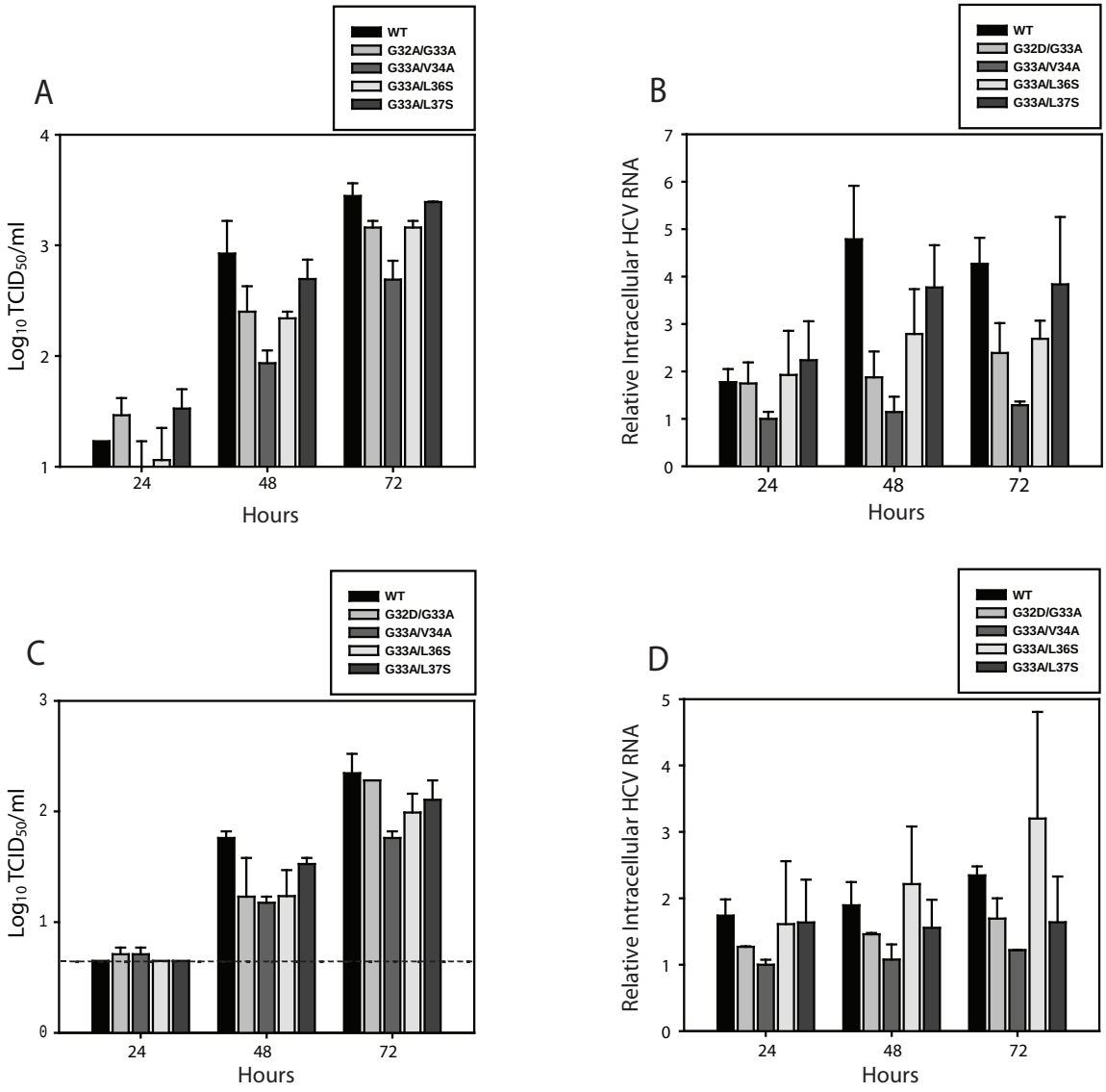

Figure 3.28. Infection kinetics of double core mutant viruses.

Naïve Huh-7 cells were infected with $JFH1_{WT}$ or mutant viruses at an m.o.i. of 0.1 (A and B) and 0.01 (C and D) as indicated. At 24, 48, or 72 h post-infection, the released virus yield (A and C) and the intracellular HCV RNA levels (B and D) were determined by $TCID_{50}$ and RT-qPCR, respectively. The relative RNA levels were normalised to $JFH1_{G33A/V34A}$ at 24 h. Means and error ranges from two independent experiments are given. Dotted line indicates cut-off of the $TCID_{50}$ assay.

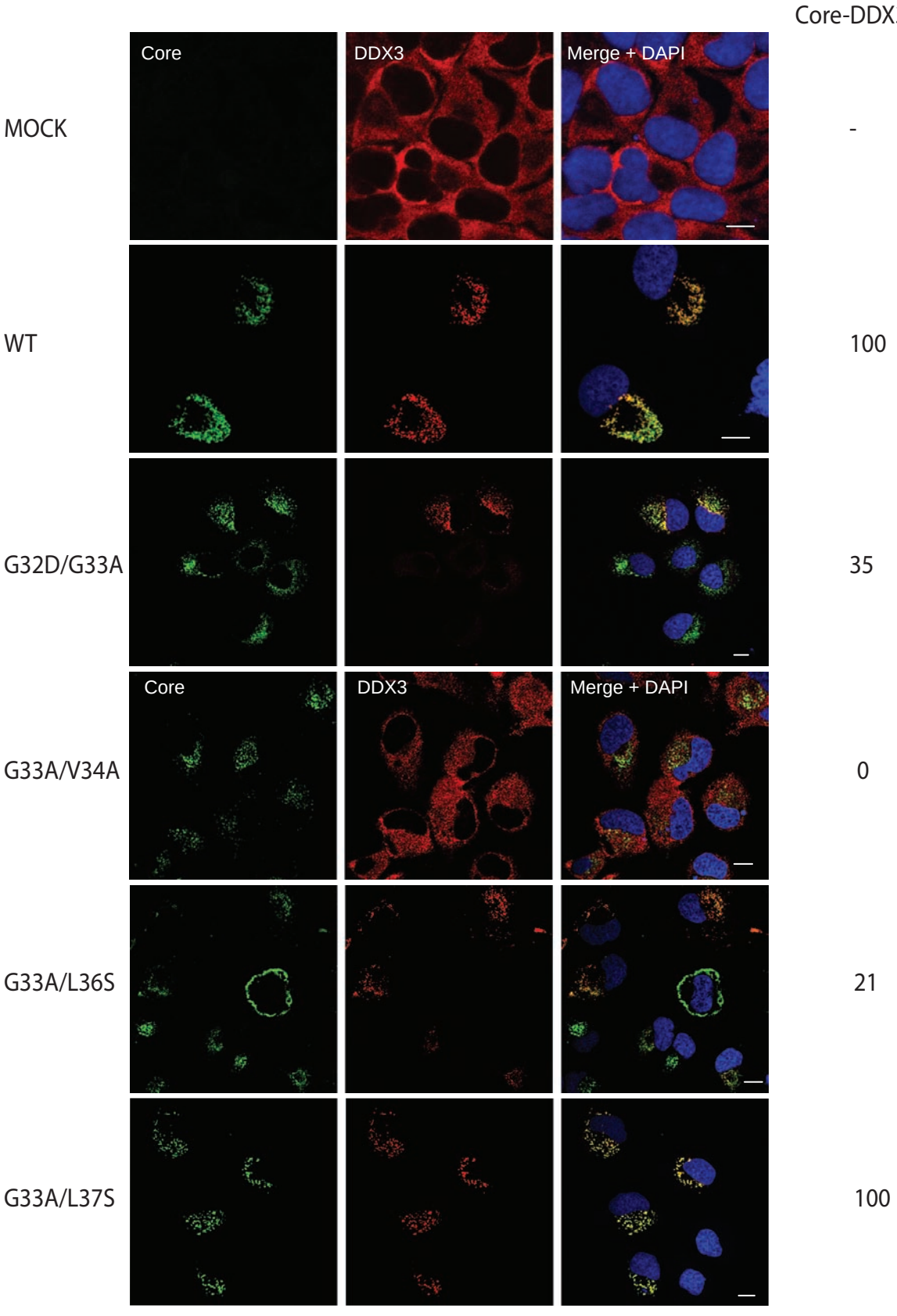

Figure 3.29. The localisation of DDX3 in cells replicating the double core mutants.

Huh-7 cells were electroporated with the indicated viral RNAs were fixed at 72 h post-incubation and analysed by confocal microscopy for the intracellular distribution of core and DDX3 using antibodies R308 and AO196, respectively. The percentage of cells (n=200) displaying core-DDX3 colocalisation is stated next to each image. Scale bar, 10 μm.

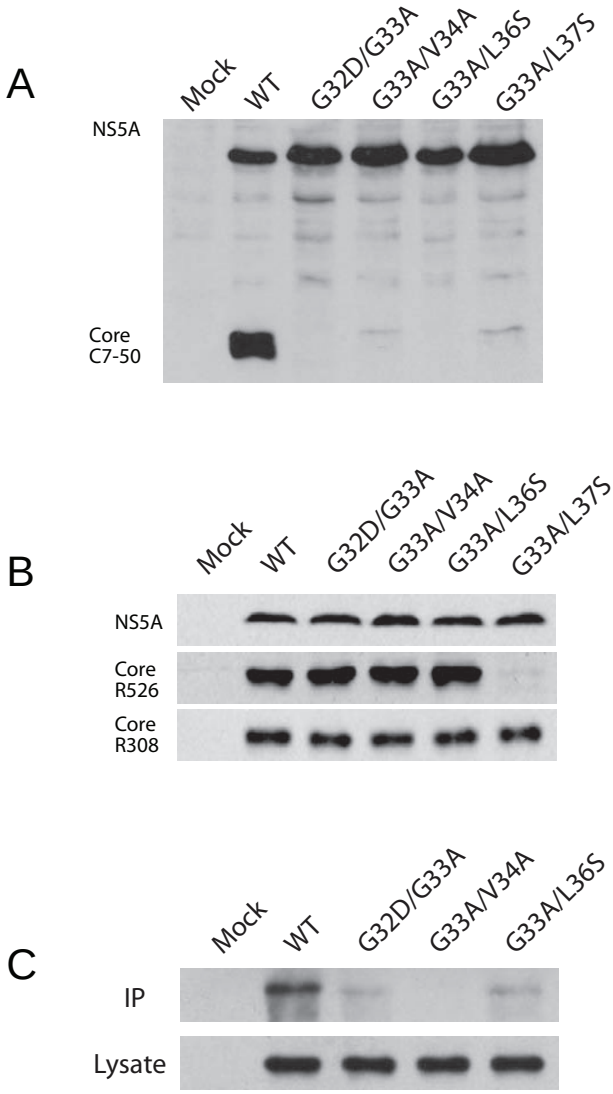

D

Virus	WT	G32D/G33A	G33A/V34A	G33A/L36S	G33A/L37S
$log_{10}TCID_{50}$/ml	4.58	4.58	4.5	4.42	4.58
% Core-DDX3	100	46	0	15	100
Core Sequence	No change	No change	No change	No change	No change

Figure 3.30. Analysis of JFH1 core double mutant viruses.

(A and B) Huh-7 cells electroporated with viral RNAs as shown were subjected to immunoblotting at 72 h post-incubation using anti-NS5A mAb 9E10, anti-core antibodies mAb C7-50, biotinylated pAb BR526 and pAb R308. (C) Analysis of the interaction of DDX3 with core mutants. Huh-7 cells were electroporated with the indicated viral RNAs and HCV core co-immunoprecipitated at 72 h post-incubation using R648 followed by immunoblotting with BR526. (D) Persistent infection of Huh-7 cells with the JFH1 core mutant viruses. Cells were infected at an m.o.i. of 0.005 and passaged 1:10 at the time of subconfluency for 5 passages. At passage 5 the infectivity of the culture medium was assayed by $TCID_{50}$ assay, the percentage of cells (n=200) displaying core-DDX3 colocalisation was determined by IF and the viral core gene was sequenced from total cell RNA following RT-PCR.

indicating that the delayed spread of $JFH1_{V34A}$ and $JFH1_{F24A}$ is not attributed to virus binding and entry into the host cell.

3.2.5. Discussion

The results in section 3.1.6 confirmed that the core-DDX3 interaction was not required for virus replication as the viral fitness of the $JFH1_{Y35A}$ mutant that failed to bind DDX3 was unaltered. Nevertheless, there were other mutant viruses characterised in this section that were clearly attenuated. One of these was $JFH1_{G33A}$, which was defective in the assembly of infectious virus particles but not intracellular viral RNA replication as observed by the presence of NS5A. Further characterisation of this mutant was not performed in this section due to the inability of $JFH1_{G33A}$ to bind to core mAb C7-50, which prevented its DDX3 binding properties from being ascertained. However, $JFH1_{G33A}$ was chosen for further analysis in order to gain better insight into the reasons for its deficiency in infectious virus release. The results showed that $JFH1_{G33A}$ has no effect on intracellular viral RNA replication or the secretion of non-infectious particles. Its major defect is a large reduction in infectious virion assembly, which strikingly can be rescued by closely positioned compensatory mutations within core. Unfortunately, the underlying reason for the intriguing phenotype of $JFH1_{G33A}$ can only be speculated upon at this time. There are many potential explanations giving the broad functional properties that this region of core has been assigned. Currently, these include RNA binding, homo-oligomerisation, and the interaction with numerous cellular factors. This domain also harbours the residues required for generation of the F protein (Section 1.11.4) and the nucleotides that comprise the two highly conserved stem-loop structures SL47 and SL87 (Section 1.11.5). Alterations to the F protein sequence are likely to be irrelevant as two independent studies found that the F protein was dispensable for HCV replication *in vitro* and *in vivo* (McMullan *et al.*, 2007; Vassilaki *et al.*, 2008). To date, only one study has performed a comprehensive aa mutagenesis on core protein to determine its effects on HCVcc replication (Murray *et al.*, 2007). However, this study avoided mutagenesis within the first 57 residues of domain I to avoid complications caused by the presence of SL47 and SL87, which are known to influence viral RNA replication (McMullan *et al.*, 2007; Vassilaki *et al.*, 2008). Indeed, the G33 codon is located within a base pairing region of SL87. To determine if the nucleotide change that created the G33A mutation caused any structural re-arrangements of SL47 and SL87, the sequence was entered into the mfold web server for nucleic acid folding and hybridization prediction (Zuker, 2003). As shown in Fig. 3.32A, this change created no

structural alterations to either stem-loop. This is supported by the proficiency of the $JFH1_{G33A}$ genome in RNA replication. Therefore, the defect in infectious particle assembly is more likely caused by alterations to the protein structure. Although, the BLOSUM62 mutation matrix (Fig. 3.17) indicate glycine can tolerate substitutions with other small residues such as alanine (log-odds score = 0), the unique structure of glycine can mean that even neutral mutations can be forbidden in certain contexts. Glycine is the simplest aa due to its side chain containing only a single hydrogen (Fig. 3.19), as apposed to a carbon as is the case for all other aas. For this reason, glycine has more conformational flexibility allowing it to reside in regions of protein structures that are forbidden to all other aas, such as tight turns (Betts & Russell, 2003). Thus, in the case of a highly conserved glycine, such as G33 even neutral alanine substitutions can have a major impact. In addition, the NMR structure of WT core residues 2-45 (unpublished data, Protein Data bank I.D. 1CWX, http://hepatitis.ibcp.fr) has identified a helix-loop-helix motif between residues 17-37 (Dr Francois Penin, personnal communication). Interestingly, G33A and the four compensatory mutations all reside within the proposed helix 2 (Fig. 3.33). It is plausible that this helix is crucial for the infectious particle assembly process and the properties of glycine at position 33 are required for its integrity. It is important to note that other than V34A, which is considered a neutral change, the remaining compensatory mutations are disfavoured substitutions with log-odds scores of -1 for G32D and -2 for both L36S and L37S (Fig. 3.17). It is interesting to speculate that such drastic reversion mutations may be necessary to repair the structural damage caused by G33A. It is intriguing that despite the reversion mutations having similar effects on infectious virus production following electroporation, the particles produced have dissimilar infection kinetics. This is exemplified by the $JFH1_{G33A/V34A}$ virus that displayed the lowest levels of virus release and intracellular HCV RNA levels following infection. Strikingly, the nucleotide changes that created the G33A/V34A substitutions are predicted to alter the complete stem-loop structure of SL87. In contrast, no alterations in SL47 or SL87 are predicted to arise by the nucleotide changes corresponding to the remaining double mutants (Fig. 3.33C). Therefore, these results suggest the structural integrity of SL87 is required for the efficient spread of JFH1 virus in cell culture.

A marked reduction in infection kinetics was also observed for $JFH1_{F24A}$ during its initial characterisation (Section 3.1.6). To further investigate the impact of residue F24 in virus proliferation, aa substitutions to leucine, isoleucine, valine and tyrosine were engineered at this position. The virus replication levels of these four mutants was then characterised alongside the original F24A mutant virus. Despite some modulation in viral titers at 24 and

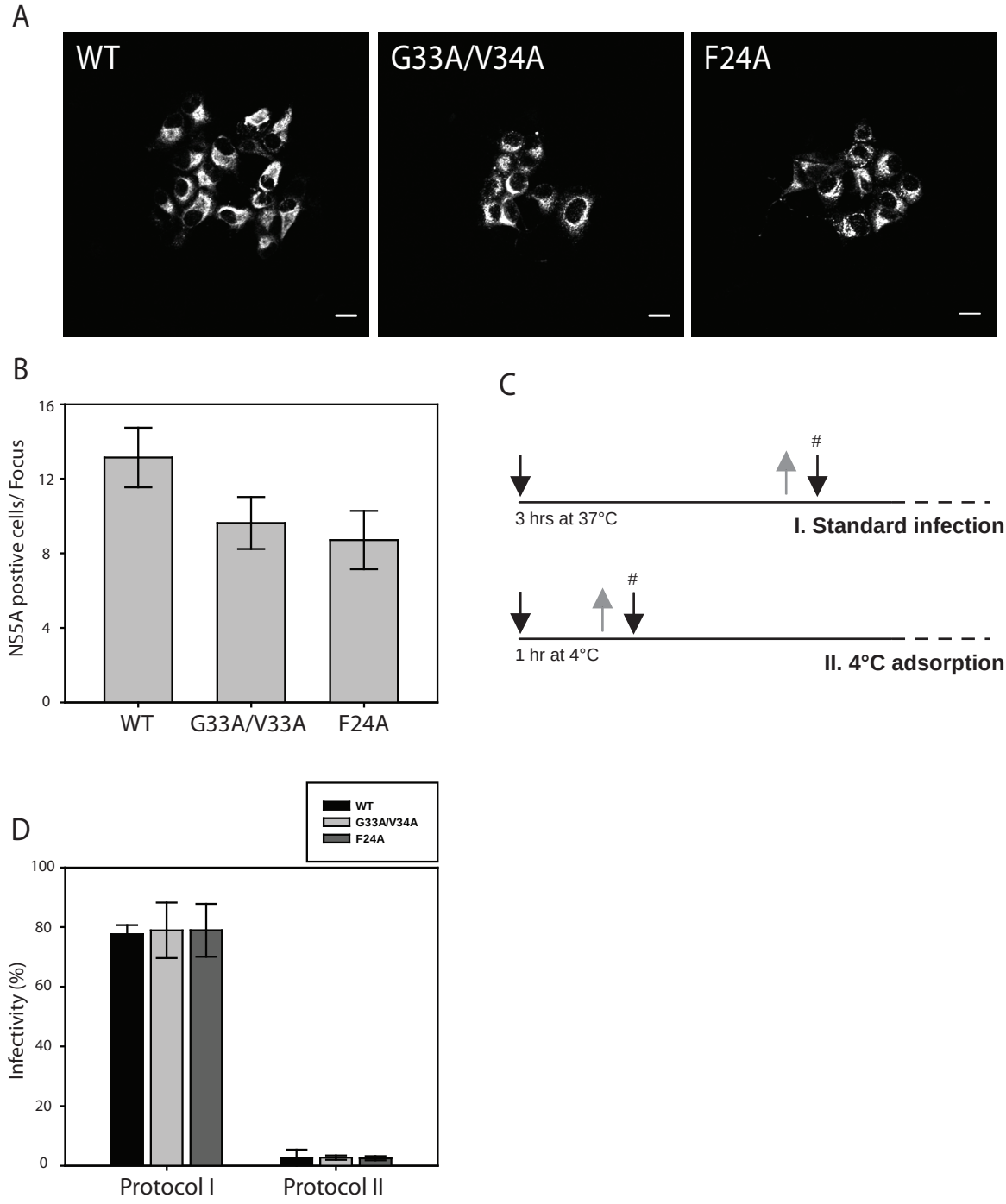

Figure 3.31. JFH1$_{G33A/V34A}$ and JFH1$_{F24A}$ have reduced virus spread.

(A) Huh-7 cells were infected with the indicated virus. At 72 h post-infection cells were fixed, probed with the anti-NS5A mAb 9E10 and analyzed by confocal microscopy. The laser intensity was kept constant for each image. Scale bar, 20 μm. (B) The average number of NS5A-positive cells from 24 individual foci was determined. Means and error ranges of three independent infections are shown. (C) Protocols used in the binding and internalization assay. Protocol I corresponds to a standard infection where the virus added to the cells was incubated for 3 h at 37 ^{o}C after which the cells are washed and treated before being incubated further in fresh medium for 48 h. Protocol II involves a cell binding step for 1 h at 4 ^{o}C, which allows synchronization of virus attachment to cells but not virus entry. Black arrows indicate virus inoculations. Grey arrows represent virus removal and the cells being washed and treated with trypsin (test cells) or medium (control cells) for 30 min at 4 ^{o}C. #, addition of fresh medium to control cells or resuspension of test cells in fresh medium. (D) The percentage infectivity values for each mutant and JFH1$_{WT}$ obtained from protocols I and II with trypsin treatment normalised to those obtained with the control treatment. Means and error ranges from two independent experiments are shown.

48 h post-electroporation, all mutants achieved titers comparable to that of $JFH1_{WT}$ at the 72 h time-point. However, the infection experiments revealed that the replication levels of the $JFH1_{F24A}$ virus was consistently lower than the other mutants over a 72 h period. The phenotype of $JFH1_{F24A}$ was very similar to that of $JFH1_{G33A/V34A}$ where virus particles are efficiently assembled but are defective in spreading following infection. Indeed, further characterisation of both these mutants found that they each share a defect that acts at an early stage post-infection, following virus binding and internalisation. Importantly, the F24 codon is situated in the upper stem of SL47. Given the predicted alterations to SL87 caused by the G33A/V34A changes (Fig. 3.32C), it was important to test what effects the nucleotide substitutions that created each F24 mutation had on SL47. Mfold analysis indicated that all but one of the phenylalanine mutations ($JFH1_{F24L}$) could potentially rearrange the structure of SL47 (Fig. 3.32B). Interestingly, $JFH1_{F24L}$ was the most closely matched to $JFH1_{WT}$ with respect to RNA replication and virus release levels post-electroporation and post-infection. Mfold analysis indicated that $JFH1_{F24I}$, $JFH1_{F24V}$, and $JFH1_{F24Y}$ likely cause minor changes that affect the number of nucleotides occupying the two loops of SL47, whereas $JFH1_{F24A}$ could re-order the entire structure, separating SL47 into two smaller stem-loops. Thus, the similar anomalies in viral spread from both $JFH1_{G33A/V34A}$ and $JFH1_{F24A}$ suggest both SL47 and SL87 function in viral infection.

From the evidence presented in section 3.2, it seems more likely that the F24 mutations, particulary F24A, effect virus infectivity by acting on the underlying RNA sequence as opposed to the protein. However, the properties of the aa substitutions introduced at this position can explain somewhat the effects observed on core-DDX3 binding. Substitutions with the smaller aliphatic residues L, I, and V reduced the core-DDX3 interaction to similar levels as the alanine change. These effects, together with the improved interaction generated by the favourable F24Y change, suggests an aromatic side chain at this position is crucial for maintaining a stable contact between the two proteins.

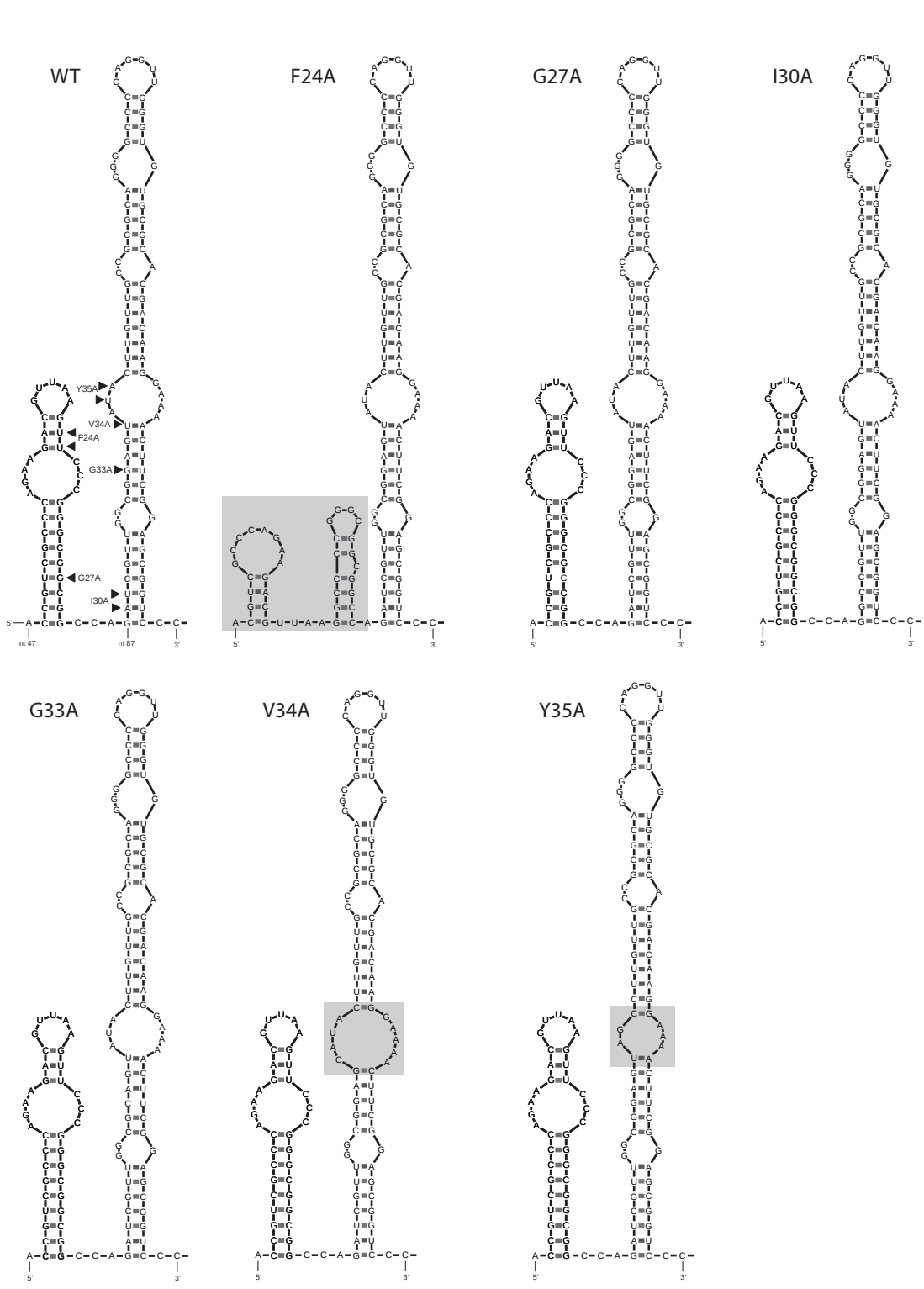

Figure 3.32. Effect of core mutations on the predicted structures of stem loops SL47 and SL87.

The sequences incorporating SL47 and SL87 (nucleotides 388-507 with respect to the 5' end of the JFH1 genome) with the indicated nucleotide substitutions that create the core mutants described in section (A) 3.1.6, (B) 3.2.2, (C) 3.2.3 were entered into the mfold web server for nucleic acid folding and hybridization prediction. The nucleotides substituted to create each mutant are marked with black arrows in the WT structure. Shaded boxes represent regions in the stem-loops altered by nucleotide substitution.

B

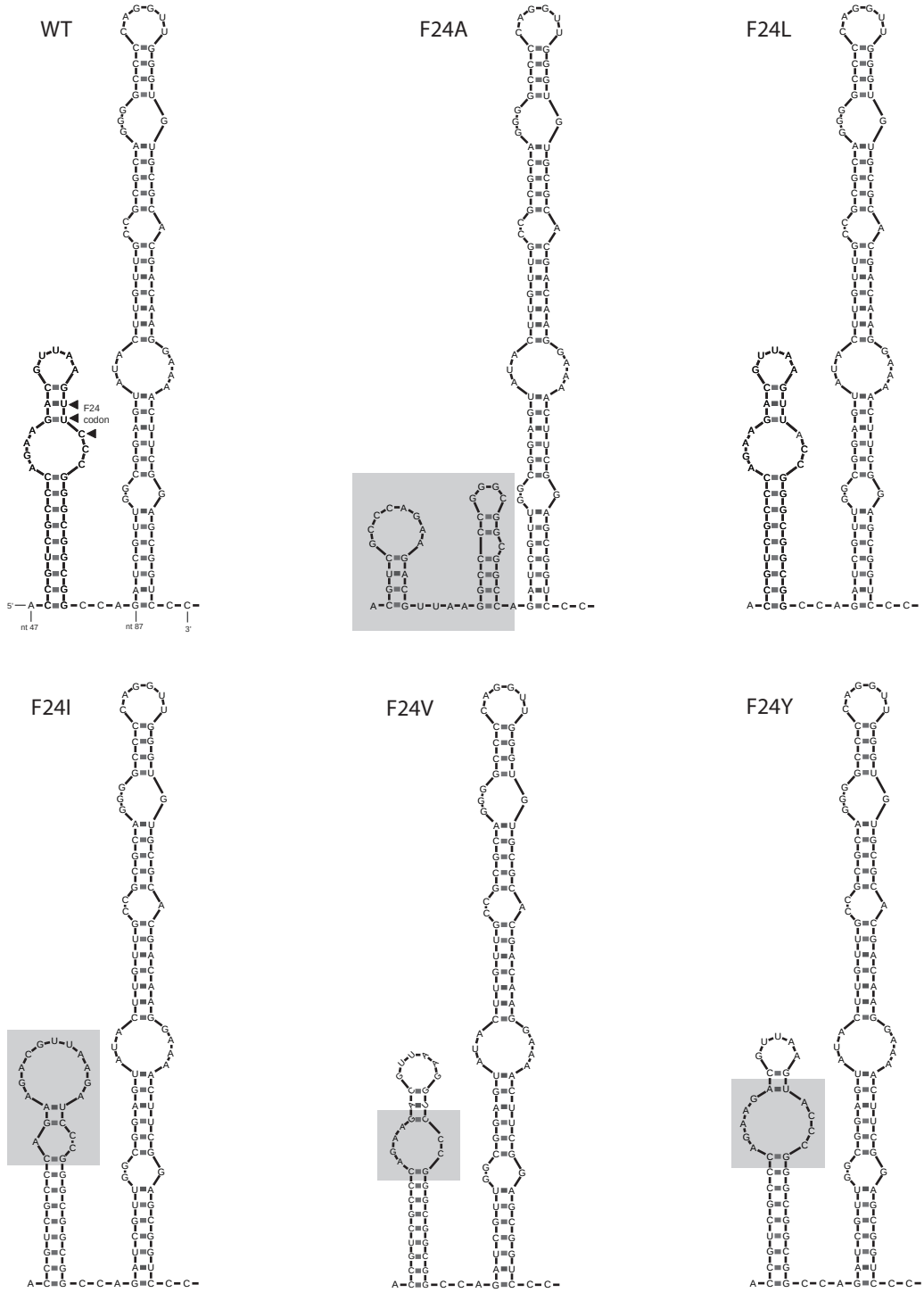

C

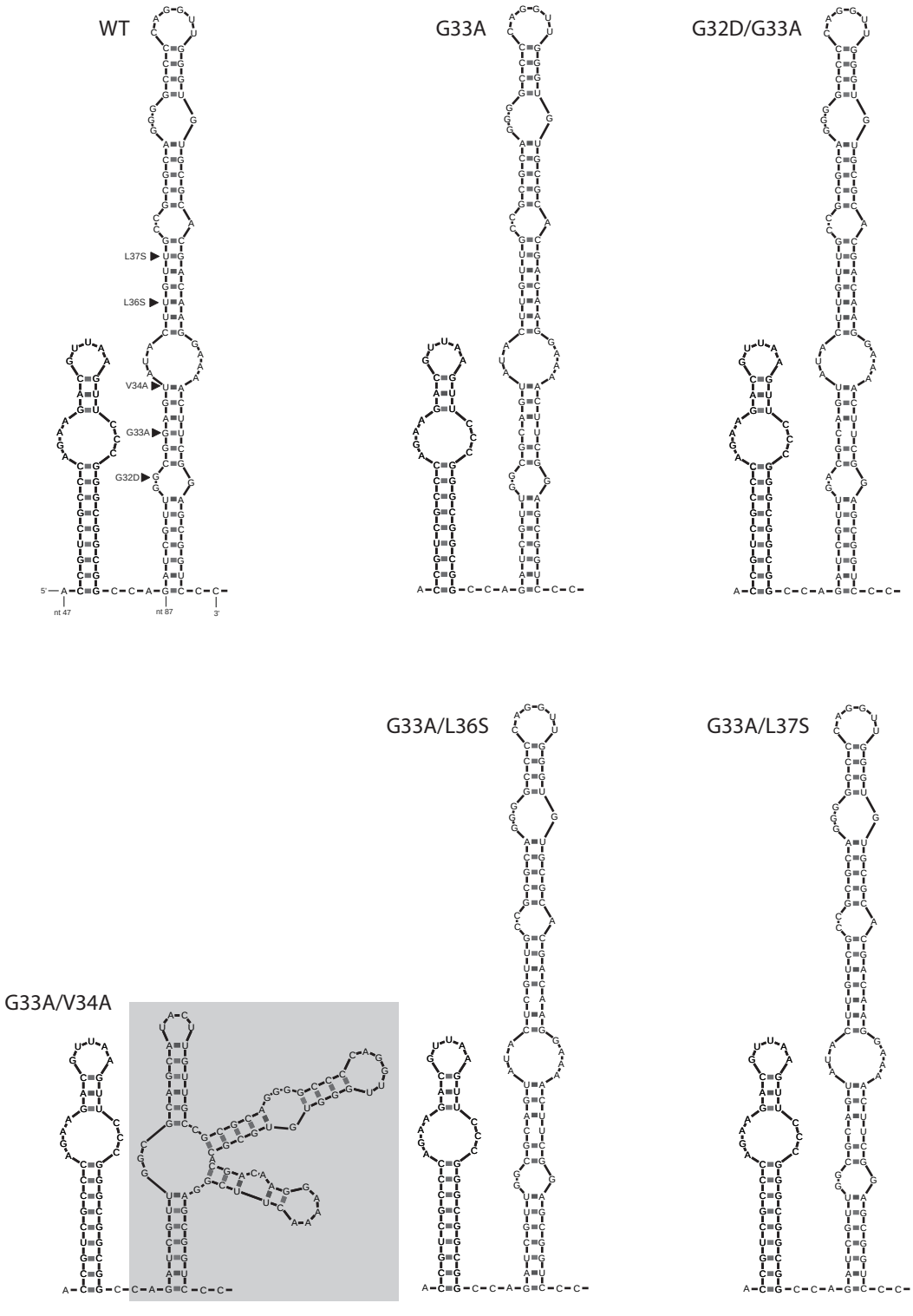
WT
L37S
L36S
V34A
G33A
G32D
5'
nt 47
nt 87
3'
G33A
G32D/G33A
G33A/L36S
G33A/L37S
G33A/V34A

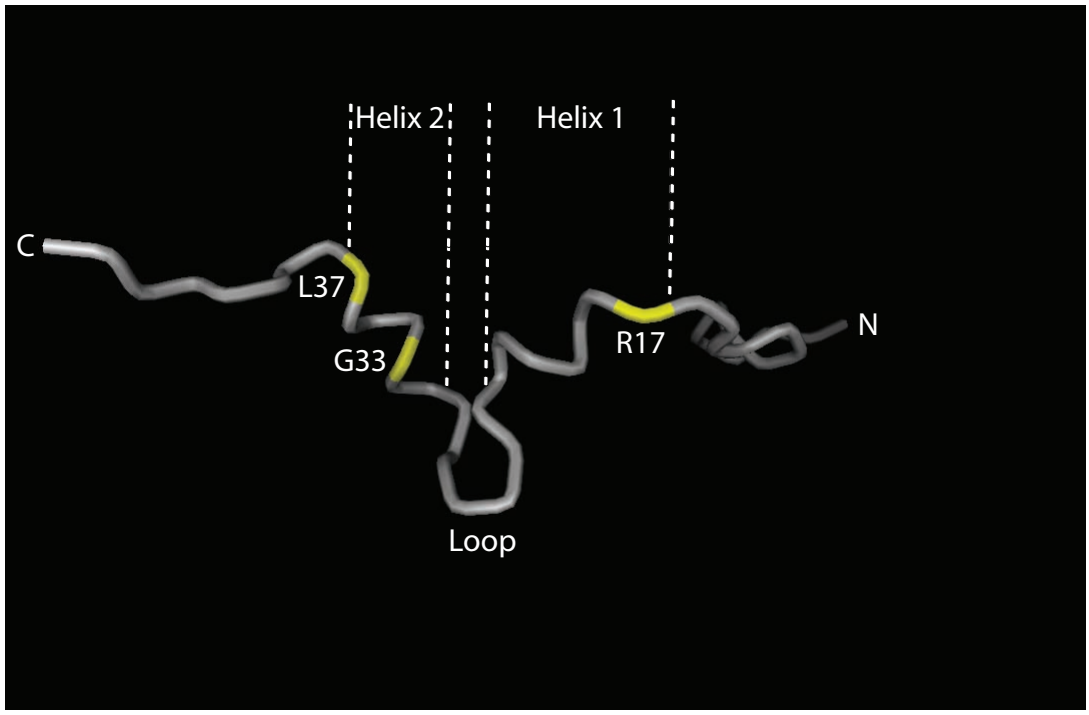

Figure 3.33. NMR model of core residues 2-45 proposed by Ladaviere *et al*. (Protein Data Bank I.D. 1CWX).

For simplicity, the protein backbone (grey tube) is shown without atoms. Residues of interest are marked on the protein backbone in yellow. The helix-loop-helix motif present between residues R17 and L37 is indicated as well as the location of G33A within helix 2. The peptide N- and C-termini are indicated.

4 Conclusions

4.1. Summary

A number of revelations have emerged from this study regarding the role of DDX3 and its interaction with HCV core protein in virus morphogenesis. In addition, a novel function for domain I of core in virus assembly and spread was uncovered. The findings in this study are recapitulated below, followed by a discussion section exploring some possible theories relating to the major findings of this work.

1. Core protein can be specifically co-immunoprecipitated from JFH1-electroporated cell lysates using an anti-DDX3 antibody, confirming this interaction occurs during authentic viral replication.

2. The redistribution of DDX3 within cells replicating JFH1 was purely dependent on the stable expression of core protein.

3. Mutations in JFH1 core that disrupted core-DDX3 colocalisation did not alter the core-LD association.

4. Co-IP assay identified a previously generated JFH1 core alanine mutant ($JFH1_{Y35A}$) that thwarted the core-DDX3 interaction.

5. Detailed characterisation studies found that the replication kinetics of $JFH1_{Y35A}$ resembled $JFH1_{WT}$.

6. DDX3 knockdown from Huh-7 cells severely impaired the replication of $JFH1_{WT}$ and $JFH1_{Y35A}$ following infection.

7. Viral protein expression levels were unchanged when DDX3 was silenced in cells replicating $JFH1_{\Delta E1E2(WT)}$ and $JFH1_{\Delta E1E2(Y35A)}$.

8. DDX3, like core, co-sedimented with the $JFH1_{WT}$ extracellular virus particles but was less prevalent on $JFH1_{Y35A}$ particles.

9. Core mutation G33A impaired the assembly of infectious virus particles but caused no alteration to intracellular RNA synthesis or the secretion of non-infectious RNA containing particles.

10. Four separate compensatory mutations in core altered the assembly phenotype of $JFH1_{G33A}$ to emulate that of $JFH1_{WT}$. These assembly competent double core mutants had diverse phenotypes in terms of their infection kinetics and capacity to bind DDX3.

11. Mutagenesis of the phenylalanine residue at position 24 in core protein revealed that this aa is an important determinant for DDX3 binding. Certain mutations at this position also had negative affects on viral spread.

12. Mutants $JFH1_{G33A/V34A}$ and $JFH1_{F24A}$ significantly reduced viral spread, which was likely caused by the respective nucleotide substitutions altering the confirmation of RNA stem loops SL87 and SL47, respectively.

4.2. The Core-DDX3 Interaction and HCV Replication

The HCV core-DDX3 interaction was first shown in cells transiently transfected with constructs expressing the genotype 1a core, but in the absence of virus replication and fully productive infection (Mamiya & Worman, 1999; Owsianka & Patel, 1999; You *et al.*, 1999). The HCVcc system made it possible here to analyse the effects of this interaction on the full viral life cycle. Given the importance of DDX3 in the life cycle of several viruses including HCV, it was surprising to find no alterations to HCVcc proliferation when the interaction was disrupted. Although, the replication data from $JFH1_{Y35A}$ appear conclusive, there are several counter arguments that must be considered when interpreting these results. One possibility that cannot be discounted is the lack of DDX3 interaction with core could be supplanted by recruiting another cellular factor(s) by HCV. In line with this, another DEAD-box protein, DDX1 is present on LDs alongside DDX3 in core expressing Hep39 cells (Sato *et al.*, 2006). It is interesting to note that DDX1, like DDX3, has been implicated in the nuclear export of HIV-1 RNA, where the two proteins indeed may conceivably act in concert with each other in carrying out this function (Fang *et al.*, 2004; Yedavalli *et al.*, 2004). Furthermore, DDX5 has also been reported to interact with core and NS5B (Goh *et al.*, 2004; Kang *et al.*, 2005). Such related cellular proteins may be

functionally interchangeable with DDX3 during virus replication. Another major complicating factor in interpreting these results is the unique features of the HCVcc system. Given the peculiarities in the HCV strain and cell line used it is questionable whether HCVcc truly represents HCV replication *in vivo*. The permissive nature of Huh-7 cells may be related to the marked differences in the host environment relative to other liver cell lines and primary human hepatocytes that are naturally infected by HCV. In the context of this study, several reports have described increased expression levels of DDX3 in tumour cell lines and thus it is conceivable that Huh-7 hepatoma cells have an excess of DDX3 compared to normal hepatocytes. Therefore, if HCV sequesters DDX3 to concentrate this protein at the virus assembly and replication sites, it is possible the high expression levels of DDX3 in Huh-7 cells make the core-DDX3 interaction obsolete. Also, the JFH1 strain is atypical among all HCV isolates, because it is the only isolate that replicates without requiring replication-enhancing mutations. JFH1 may contain genetic alterations that provide advantages for viral replication but at the same time make functions exerted by the core-DDX3 interaction dispensable.

4.3. Requirement of DDX3 for HCV Replication

It is intriguing that DDX3 is essential for HCV replication, yet this effect appears to be independent of its interaction with core. This effect is not caused by cell death as reports described previously and this study found no changes to cell viability following DDX3 silencing, at least up to 96 h (Ariumi *et al.*, 2007; Randall *et al.*, 2007). Another explanation is that knockdown of DDX3 has an indirect role on HCV replication. Despite the exact function(s) of DDX3 being unknown, the large number of cellular processes that it has been implicated in suggests that the protein is a very important component of the cell. Thus, downregulating its functions may affect an alternate pathway utilised by HCV during replication, subsequently causing these negative effects on virus replication. The exact mechanism by which HCV uses this host factor is unclear, however the work from this study indicates that the effects are more relevant in the virus infection setting rather than during viral RNA synthesis. However, there are important differences between the data in this study and those of Ariumi *et al*. (2007) that need to be discussed. Ariumi *et al*. (2007) found a 50 % decrease in the RNA levels of the JFH1 SGR following DDX3 knockdown, although this decrease in replication was not confirmed by protein expression or colony forming units. Similarly, a 45 % drop in HCV RNA levels was observed in the

present study for $JFH1_{\Delta E1E2(WT)}$ in DDX3 knockdown cells. However, unlike the reduction in HCV RNA, the core protein expression levels were unaltered in the knockdown cells. This suggests that the viral genome translation is not altered by DDX3 silencing but either less RNA is being synthesised or more RNA is being subjected to degradation. The RT-qPCR probe used in this study is designed to quantify the total positive-strand HCV RNA within cells and therefore cannot decipher what proportion of molecules are functioning within viral replication complexes. Indeed, studies have shown that positive-, negative- and double-stranded HCV RNA molecules are dispersed throughout the cytoplasm of infected cells and are not solely confined to the viral replication compartments (Miyanari *et al.*, 2007; Targett-Adams *et al.*, 2008a). Thus, it is possible that DDX3 binds to rogue RNA molecules and delays their degradation. Indeed, DDX3 has been shown to interact with 3' UTR of the HCV genome (Harris *et al.*, 2006). However, the results with $JFH1_{\Delta E1E2(Y35A)}$ contradict this theory as both the HCV RNA and core protein levels were unchanged in the knockdown cells replicating these genomes. While this result implicates the involvement of the core-DDX3 interaction in this event, it doesn't explain the HCV RNA reductions obtained with the SGR that does not possess core (Ariumi *et al.*, 2007). Clearly, further knockdown studies are required to resolve these discrepancies. In contrast, to the differences observed with $JFH1_{\Delta E1E2(WT)}$ and $JFH1_{\Delta E1E2(Y35A)}$, infection of DDX3 knockdown cells with the $JFH1_{WT}$ and $JFH1_{Y35A}$ infectious virus gave identical results for intracellular HCV RNA levels, virus release and protein expression. This implies that the mechanism inhibiting infection is the same for both viruses. Clearly, the results with the full-length JFH1 virus and the $JFH1_{\Delta E1E2}$ genomes suggest that DDX3 functions at an early event in the virus lifecycle prior to the release of the genome into the cytoplasm. However, Ariumi *et al*. (2007) also showed DDX3 knockdown in cells harbouring a full-length genotype 1b replicon severely inhibited RNA replication (>90 %) and colony formation after cell selection. This result opposes the theory of DDX3 knockdown only affecting HCV in the infection setting. However, this effect could well be genotype-dependent as Ariumi *et al*. (2007) found that their genotype 1b core protein had a greatly increased binding capacity to DDX3 compared to JFH1 core, which was barely detectable in their co-IP assay. Thus, it is possible that the core-DDX3 interaction has an important function in the productive RNA replication of this particular genotype.

4.4. Is DDX3 a Component of the Virion?

The co-sedimentation of DDX3 with $JFH1_{WT}$ extracellular core was an intriguing finding. However, this result doesn't necessarily prove that DDX3 is a component of the virus particle. The first critique of this finding is the detection of core protein only within the lower density fractions corresponding to the peak HCV RNA content. To strengthen the possibility of DDX3 being present on HCV it must be shown to co-sediment with the core and envelope proteins of infectious virions. It is widely reported that the RNA containing particles sediment differently to the infectious virions and are present in greater numbers (Chang *et al.*, 2007; Gastaminza *et al.*, 2006; Grove *et al.*, 2008; Lindenbach *et al.*, 2005). As with the results in this study, these particles have been shown to co-sediment with core protein (Gastaminza *et al.*, 2006). It is possible that DDX3 may only be present on these denser particles and not on the infectious virion. Indeed, it has been reported that DDX3 is a host component of HCMV non-infectious dense bodies but not of the infectious viral progeny (Varnum *et al.*, 2004). Dense bodies constitute the majority of a virion preparation obtained from HCMV-infected fibroblasts, but as for the HCV RNA containing particles, their significance during infection is unknown. DDX3 was also recently shown to be encapsidated into HBV particles, although the exact mechanism and physiological relevance behind these findings remain to be determined (Wang *et al.*, 2009).

Another logical explanation for the co-sedimentation of DDX3 with core is the contamination of the virus preparation with cell debris. Ideally, the purity of the fractions should be assessed by EM following negative staining to check for no obvious contamination by cellular debris (Shaw *et al.*, 2008). Also, to determine whether the cellular proteins are really an integral part of the virion or perhaps derived from a microvesicle or exosome that co-purified with the virus, an Optiprep gradient should be used. Unlike sucrose, Optiprep medium maintains iso-osmotic conditions at high densities and is therefore particularly good at separating membranous organelles such as enveloped viruses and microvesicles (Shaw *et al.*, 2008). This would be a crucial assay to show whether DDX3 is really co-purifying with virus particles or just cellular organelles with similar densities. Another possibility is the adherence of DDX3 to the virion exterior due to contaminating levels of the protein in the virion preparation. This theory is plausible given the large amount of cell death and debris generated by the electroporation procedure. Unfortunately, the above possibilities could not be investigated in the present study due to

time constraints. However, the gradient results on the $JFH1_{Y35A}$ virus particles provide a strong argument against the above criticisms. The reduced core: DDX3 protein ratio observed by immunoblotting from fractions 6 and 7 imply the cells replicating this mutant secrete less DDX3 into the culture medium. Also, the leftward shift observed in the infectious and RNA particle buoyant density of $JFH1_{Y35A}$ could be due to a decrease in the DDX3 content of the particle. These two points allude to the possibility of DDX3 being a component of both types of particles through its intracellular interaction with core protein. However, further research is needed to ascertain whether or not these two events are coincidental.

Knowledge of the protein composition of infectious viral particles is an important prerequisite for functional studies, as it focuses the analysis on specific proteins and their roles during assembly and/or infection. Enveloped viruses have considerable potential to incorporate both viral and host proteins into their membrane(s) as well as inside the envelope, and these can be present at low levels, making their detection difficult. Mass spectrometry (MS) approaches have been invaluable in the identification of the viral and cellular protein content of many different viruses. Examples of well characterised envelope viruses and the number of host proteins associated to these are listed in Table 5.

Table 5. Numbers of host proteins found on enveloped viruses by MS

Virus	Number of host proteins	Reference
HIV-1	253	Chertova *et al*. (2006)
Influenza	36	Shaw *et al*. (2008)
HSV-1	49	Loret *et al*. (2008)
HCMV	71	Varnum *et al*. (2004)
EBV	6	Johannsen *et al*. (2004)
KSHV	21	Zhu *et al*. (2005)
Vaccinia virus	23	Chung *et al*. (2006)

Some cellular proteins may be specifically recruited and packaged into the virion, presumably via an interaction with either a viral protein or the viral genome. There is a high probability that such proteins are actively involved in the virus life cycle, either at late stages during virus assembly and egress from the producer cell or at early stages of entry into the new target cell. It seems unlikely that all of the 253 cellular proteins identified in HIV-1 virions (Table 5) are of functional significance, and some may be packaged accidentally due to their abundance and cellular localization (Chertova *et al.*, 2006).

Detailed functional studies will be needed to determine which of the packaged cellular proteins actually contribute to HIV-1 infection. Perhaps one of the best characterised host proteins found on HIV-1 virions is cyclophilin A (CypA). This host protein is incorporated onto the virion through its association with virus capsid. Most importantly, it is the only incorporated cellular protein shown to be critical for viral infectivity. Its exact role in infectivity is debateable, with some authors arguing for a role in early events of the replication cycle, such as uncoating, and others for a role in late events, such as maturation (Scarlata & Carter, 2003). From the MS studies it has become apparent that there is some overlap in the nature of the host proteins incorporated into the different enveloped viruses. For example, actin is present in all the enveloped virions listed in Table 5 and all but EBV incorporate annexin A2 and CypA. The heat shock proteins HSC70 and HSC90 are also common host proteins with the former being present in all the virions from Table 5, except Influenza. It remains to be determined whether these cellular proteins play a conserved functional role in these virions or are simply passenger proteins that are accidentally packed due to their location. Importantly, a recent mass spectrometric analysis performed on purified J6/JFH1 virions identified the presence of HSC70. It was demonstrated that HCV particles from cell culture and patient sera could be immunogold labelled with an anti-HSC70 primary antibody. Also, HCVcc infection could be efficiently inhibited by anti-HSC70 antibodies implying that the virion requires this component for an early step in infection. However, RNAi studies also found HSC70 was important for infectious particle secretion. Although the mechanism by which HSC70 is incorporated into the particle was not demonstrated it was speculated to occur through the binding to an HSC70 substrate-binding domain present on E2 (Parent *et al.*, 2009). While this study was able to show potential functions of HSC70 on the virion, the present study was unable to show any possible function for DDX3 that would explains its presence on the virus. Nevertheless, the results provide a strong basis for future research into this subject.

4.5. The Core-DDX3 Interaction and HCV-Associated Pathogenesis

With the data from this study indicating that the core-DDX3 interaction does not function in virus replication, the possibility of this interaction being pathogenesis related must be explored. Indeed, core protein has been widely implicated in modulating cellular functions, mainly due to its interaction with numerous host factors (Table 4). In particular, one could

anticipate an involvement of the core-DDX3 interaction in apoptosis and immune evasion given the recent evidence stating a role for DDX3 in each of these processes. As described in section 1.11.6, both pro- and anti-apoptotic effects of core protein have been described with the conflicting nature of these reports likely caused by the different core expression systems and cell lines used. It is widely reported in the literature that Huh-7 cells and derived subclones undergo considerable apoptotis during HCVcc infection (Deng *et al.*, 2008; Lan *et al.*, 2008; Mateu *et al.*, 2008; Sekine-Osajima *et al.*, 2008). These effects could be inflicted directly or indirectly by the virus through a number of mechanisms given that virtually all HCV proteins have been shown to modulate the cell death process (Fischer *et al.*, 2007). However, the core-DDX3 interaction could potentially contribute to such effects as both proteins have links to apoptosis. As DDX3 is a component of an anti-apoptotic death receptor complex (Sun *et al.*, 2008), its sequestration by core may release this inhibitory cap to allow for stronger apoptotic signalling upon death receptor stimulation initiated by the viral infection. Indeed, several viruses are known to induce apoptosis actively at later stages of infection, including HIV-1, human adenovirus, influenza and parvoviruses. This process may represent a mechanism by which the virus can disseminate progeny to neighbouring cells while also evading induction of host inflammatory and immune responses (Teodoro & Branton, 1997). Thus, HCV core may have been adapted to antagonize apoptosis before an antiviral defence is instituted by the host cell. Indeed, DDX3 has been shown to positively regulate IFN-induction through its interaction with kinases IKK-ε (Schroder *et al.*, 2008), TBK1 (Soulat *et al.*, 2008) and IPS-1 (Oshiumi *et al*., 2010). Moreover, Schroder *et al*. (2008) found that a direct interaction between the vaccinia virus K7 protein and DDX3 could inhibit IFN-induction. Core protein may also be employing a similar strategy as K7 to limit the quantity of DDX3 available in the cell to perform this innate immune function during virus infection. Thus, it is possible that the core-DDX3 interaction modulates both cellular processes, establishing a complex interplay between these two events during infection to function as an early evasion strategy from the host defence. However, if this theory is true then one would expect $JFH1_{Y35A}$ to be attenuated in virus replication as it is unable to counteract the cell defences via this particular mechanism. It is possible that Huh-7 cells lack efficient innate immune defences making the replication characteristics of $JFH1_{WT}$ and $JFH1_{Y35A}$ indistinguishable from one another. This would partly explain why Huh-7 cells are the only cell line capable of supporting high levels of HCV RNA replication. It is also important to note that the studies reporting the roles of DDX3 in apoptosis and innate immunity were conducted in cell lines other than Huh-7 cells. The possible contributions of this interaction to clinical manifestations of viral disease cannot be discounted. Indeed, differential

regulation of DDX3 has been reported in a number of tumours, including HCC (Botlagunta *et al*., 2008; Chang *et al*., 2006; Chao *et al*., 2006; Huang *et al*., 2004), suggesting it may be involved in HCV-associated pathogenesis. Although, no differences in DDX3 expression levels were observed between HCVcc-infected cultured cells and uninfected cells, its relevance *in vivo* from a long-term disease perspective warrants further investigation.

4.6. The Importance of Core Residue Glycine 33

Of all the core mutants characterised in this project, $JFH1_{G33A}$ has by far the most compelling phenotype. Despite being unable to decipher its level of interaction with DDX3, the findings with the other mutants convincingly exclude changes to the core-DDX3 interaction as an explanation for the $JFH1_{G33A}$ phenotype. This mutation is located within a highly conserved and multifunctional region of core protein and its coding gene and thus, a number of explanations could be proposed as to why this change significantly reduces infectious virus release. These are:

1. Disrupting a core-cellular protein interaction that is important for virus assembly. As shown in Table 4, domain I of core protein interacts with a number of cellular proteins with binding sites that include residue G33.

2. The inability of the mutant core to bind HCV RNA and thereby disallowing its proper encapsidation into infectious particles. The RNA binding region of core has been broadly mapped to residues 1-75 (Santolini *et al.*, 1994).

3. Impaired nucleocapsid assembly. Core multimerisation requires domain I, which may be compromised by G33A preventing the formation of the nucleocapsid during virion assembly.

4. Dissociation between core and NS5A. A recent study found an interaction between core and NS5A that was required for infectious particle production (Masaki *et al.*, 2008). This study mapped the interacting residues to domain III of NS5A, although the binding region in core was not identified. G33A may disjoin this interaction, which would explain the loss in infectivity.

Whatever the explanation for this defect, the G33A mutation is not completely lethal as the virus can generate reversion mutations in core to restore virion assembly. Since the development of HCVcc, there have been several reports of compensatory mutations that rescue the phenotype of assembly defective mutants and chimeric viruses (Gottwein *et al.*, 2009; Murray *et al.*, 2007; Phan *et al.*, 2009; Yi *et al.*, 2007). This is likely caused by the high error-rate of nucleotide substitutions by the NS5B polymerase during viral genome synthesis allowing the selection of reversion variants. It would be interesting to characterise the phenotypes of the second core mutations in the absence of the G33A change. However, the V34A mutation was initially identified as an important residue for the core-DDX3 interaction and was tentatively characterised in section 3.1.6. From these data this mutant appeared to be competent for virus RNA replication and infectious particle release. Despite restoring infectious virus assembly, the second-site core mutations caused differential expansion kinetics to the virus at early time-points post-infection. This was most indicative for $JFH1_{G33A/V34A}$ virus particles, which displayed the lowest level of virus spread. A likely explanation for these findings is the V34A mutation being selected by $JFH1_{G33A}$ to restore the core protein conformation required for infectious virus assembly but as a negative consequence the nucleotide change alters an RNA structure important in viral spread. The gross alterations to SL87 appear to be caused by the combined nucleotide substitutions of G33A and V34A, as very little effect to this stem loop is observed by each individual mutation (Fig. 3.32A). $JFH1_{G33A/V34A}$ was still capable of persistently infecting cells in culture over serial passages without further changes to the core sequence. Thus, the defect of $JFH1_{G33A/V34A}$ may be short-lived and only apparent at early time-points post-infection. Each double mutant also displayed lower levels of core-DDX3 interaction, supporting the notion that these second mutations do not fully reinstate the WT protein structure. The ability of this mutant virus to select compensatory mutations that are deleterious to DDX3 binding further highlights the core-DDX3 interaction playing no role in virus replication.

4.7. The Importance of Core Residue Phenylalanine 24

The phenylanine residue at position 24 was further investigated due to its profound effect on the productive infection of JFH1. This phenotype was confirmed by the more detailed characterisation of this mutant alongside $JFH1_{F24L}$, $JFH1_{F24I}$, $JFH1_{F24V}$ and $JFH1_{F24Y}$, where $JFH1_{F24A}$ displayed the greatest decrease in infection kinetics. The phenotype of $JFH1_{F24A}$ was remarkably similar to that of $JFH1_{G33A/V34A}$ in that infectious virus particles

could be generated efficiently from electroporated cells but these were relatively inefficient at expanding in culture following infection. As with $JFH1_{G33A/V34A,}$ these effects did not compromise the ability of the virus to persist during long-term culture. It is intriguing to speculate that the similar defects in viral spread for $JFH1_{G33A/V34A}$ and $JFH1_{F24A}$ are caused by rearrangements to the functional RNA elements in which their codons are positioned. Indeed, the RNA folding predictions show that of all the mutants generated in this study, only $JFH1_{F24A}$ and $JFH1_{G33A/V34A}$ caused major alterations to SL47 and SL87, respectively (Fig. 3.32A-C). It is possible that the integrity of SL47 and SL87 may be necessary for efficient virus infection. Our results pinpoint the defect of both mutants to an early stage following virus entry and before the release of the infectious genome into the cell cytoplasm. One could speculate that these RNA secondary structures play a role in the translocation of the genome from the internalized, disassembling nucleocapsid to the translation initiation sites of the cell. The importance of SL47 and SL87 in HCVcc propagation has been analysed in a previous study by introducing silent mutations predicted to disrupt these stem-loops into the infectious genome (Vassilaki *et al.*, 2008). However, the effects of these stem-loop disruptions on virus spread were not tested. Instead, this study monitored virus release and RNA replication following electroporation of JFH1 RNA into Huh-7.5 cells, where they found delayed kinetics in both processes. These defects were found to be caused by reduced translation levels of the viral genome at early time-points (Vassilaki *et al.*, 2008). Mutant $JFH1_{G27A}$ was the only mutant characterised in the present study that possessed delayed replication kinetics post-electroporation (Fig. 3.10). However, mfold analysis found the nucleotide substitutions that created the G27A did not change the conformation of SL47 (Fig. 3.32A), suggesting that the phenotype may be more relevant at the protein level. It is interesting that these delayed replication kinetics were not observed in either $JFH1_{G33A/V34A}$ or $JFH1_{F24A}$ following electroporation given how disruptive these mutations were to the structures of their respective stem loop. Nevertheless, these data provide important insights into a potentially novel function of these RNA structures in virus infection. Additionally, at the protein level these aa substitutions have provided further insights into the importance of this residue in the binding of core to DDX3. The differential binding of each phenylalanine mutant to DDX3 along with their replication properties again strengthen the previous findings that this interaction is not required for HCVcc replication. $JFH1_{F24Y}$ was an especially important finding as it demonstrates that this interaction can be increased without affecting viral proliferation.

4.8. Finishing Statement

The aim of this project was to resolve the role of the core-DDX3 interaction in HCV replication. After characterising a panel of core mutant viruses, a lack of correlation between the level of core-DDX3 binding and virus replication was found to exist, strongly suggesting this virus-host interaction is dispensable for HCV propagation in cell culture. As well as fulfilling the major aim of this project, preliminary results were obtained regarding the importance of DDX3 in an early infection stage as well as its potential incorporation into the virus particle. Together, the above results suggest this multifunctional cellular protein may have several roles in the HCV lifecycle. Furthermore, two core mutants ($JFH1_{G33A}$ and $JFH1_{F24A}$) were selected for further characterisation given their unique properties that appeared to be unrelated to the core-DDX3 interaction. Predictive structural modelling provided useful insights into the alterations caused by these mutations at the RNA level, which may be related to the peculiar phenotypes of these mutant viruses in cell culture. Undoubtedly, the data and reagents generated in this project will be of great utility for future studies investigating both the functions(s) of DDX3 in the HCV lifecycle and the importance of core domain I for virus assembly and spread.

Appendices

Appendix 1: Primers used for core mutagenesis and sequencing

Primer Name	Sequence (5'-3')	Function
JFH1 NegRT	TTGCGAGTGCCCCGGGA	Used to reverse transcribe negative-strand HCV JFH1 core sequence
NA7	CAC TCC GCC ATG AAT CAC TC	Used to sequence 5' UTR and core gene
NA11	GTCTCGTAGACCGTGC	Used to amplify and sequence core gene
NA12	GCCAGTGGAGCGCCGATCTTT G	Used to sequence core gene
NA13	CAAAGATCGGCGCTCCACTGG C	Used to sequence core gene
NA14	GTATTCTTCACCTGGGCAGC	Used to amplify and sequence core gene
NA15	CCTGTTGTCCTGCATCACCG	Used to sequence E1 gene
NA18	CGTGCAACAGCGCCTCCAAC	Used to sequence E1 gene
NA72	CGGCCAGATCGTTGACGCAGT ATACTTGTTGC	Forward primer for site-directed mutagenesis of G32D in G33A JFH1 plasmid
NA73	GCAACAAGTATACTGCGTCAA CGATCTGGCCG	Reverse primer for site-directed mutagenesis of G32D in G33A JFH1 plasmid
NA74	CGTTGGCGCAGCATACTTGTT GCCGC	Forward primer for site-directed mutagenesis of V34 A in G33A JFH1 plasmid
NA75	GCGGCAACAAGTATGCTGCGC CAACG	Reverse primer for site-directed mutagenesis of V34 A in G33A JFH1 plasmid
NA76	GTTGGCGCAGTATACTCGTTG CCGCGCAGG	Forward primer for site-directed mutagenesis of L36S in G33A JFH1 plasmid
NA77	CCTGCGCGGCAACGAGTATAC TGCGCCAAC	Reverse primer for site-directed mutagenesis of L36S in G33A JFH1 plasmid
NA78	GTTGGCGCAGTATACTTGTCG CCGCGCAGG	Forward primer for site-directed mutagenesis of L37S in G33A JFH1 plasmid
NA 79	CCTGCGCGGCGACAAGTATAC TGCGCCAAC	Reverse primer for site-directed mutagenesis of L37S in G33A JFH1 plasmid
NA82	CCAGAAGACGTTAAGTACCCG GGCGGCGGCCAG	Forward primer for site-directed mutagenesis of F24Y in pJFH1
NA83	CTGGCCGCCGCCCGGGTACTT AACGTCTTCTGG	Reverse primer for site-directed mutagenesis of F24Y in pJFH1
NA84	CCAGAAGACGTTAAGTTACCG	Forward primer for site-directed

	GGCGGCGGCCAG	mutagenesis of F24L in pJFH1
NA85	CTGGCCGCCGCCCGGTAACTT AACGTCTTCTGG	Reverse primer for site-directed mutagenesis of F24L in pJFH1
NA86	CCAGAAGACGTTAAGATCCCG GGCGGCGGCCAG	Forward primer for site-directed mutagenesis of F24I in pJFH1
NA87	CTGGCCGCCGCCCGGGATCTT AACGTCTTCTGG	Reverse primer for site-directed mutagenesis of F24I in pJFH1
NA88	CCAGAAGACGTTAAGGTCCCG GGCGGCGGCCAG	Forward primer for site-directed mutagenesis of F24V in pJFH1
NA89	CTGGCCGCCGCCCGGGACCTT AACGTCTTCTGG	Reverse primer for site-directed mutagenesis of F24V in pJFH1
RA16	TCTGCGGAACCGGTGAGTAC	Used to amplify HCV JFH1 5'NCR
RA17	GCACTCGCAAGCGCCCTATC	Used to amplify HCV JFH1 5'NCR

Appendix 2: Binding of mAbs to JFH1-electroporated Huh-7 cell lysates when used alone or in combination with other mAbs

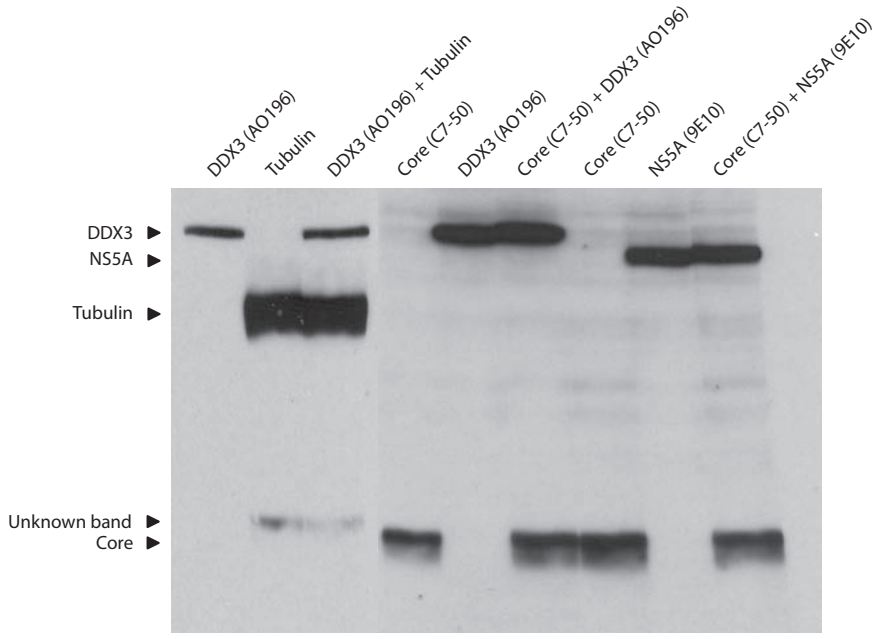

Appendix 3: Binding of core antibodies to $JFH1_{I30A}$, $JFH1_{G33A}$-electroporated Huh-7 cell lysates

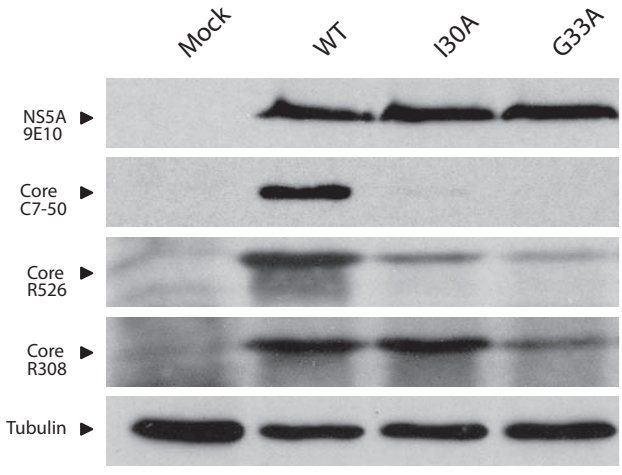

References

Acton, S., Rigotti, A., Landschulz, K. T., Xu, S., Hobbs, H. H. & Krieger, M. (1996). Identification of scavenger receptor SR-BI as a high density lipoprotein receptor. *Science* **271**, 518-520.

Acton, S. L., Scherer, P. E., Lodish, H. F. & Krieger, M. (1994). Expression cloning of SR-BI, a CD36-related class B scavenger receptor. *J Biol Chem* **269**, 21003-21009.

Agnello, V., Abel, G., Elfahal, M., Knight, G. B. & Zhang, Q. X. (1999). Hepatitis C virus and other flaviviridae viruses enter cells via low density lipoprotein receptor. *Proc Natl Acad Sci U S A* **96**, 12766-12771.

Ago, H., Adachi, T., Yoshida, A., Yamamoto, M., Habuka, N., Yatsunami, K. & Miyano, M. (1999). Crystal structure of the RNA-dependent RNA polymerase of hepatitis C virus. *Structure* **7**, 1417-1426.

Ait-Goughoulte, M., Banerjee, A., Meyer, K., Mazumdar, B., Saito, K., Ray, R. B. & Ray, R. (2009). Hepatitis C virus core protein interacts with fibrinogen-beta and attenuates cytokine stimulated acute-phase response. *Hepatology* **51**, 1505-1513.

Ait-Goughoulte, M., Hourioux, C., Patient, R., Trassard, S., Brand, D. & Roingeard, P. (2006). Core protein cleavage by signal peptide peptidase is required for hepatitis C virus-like particle assembly. *J Gen Virol* **87**, 855-860.

Ali, N. & Siddiqui, A. (1995). Interaction of polypyrimidine tract-binding protein with the 5' noncoding region of the hepatitis C virus RNA genome and its functional requirement in internal initiation of translation. *J Virol* **69**, 6367-6375.

Ali, N. & Siddiqui, A. (1997). The La antigen binds 5' noncoding region of the hepatitis C virus RNA in the context of the initiator AUG codon and stimulates internal ribosome entry site-mediated translation. *Proc Natl Acad Sci U S A* **94**, 2249-2254.

Alisi, A., Giambartolomei, S., Cupelli, F., Merlo, P., Fontemaggi, G., Spaziani, A. & Balsano, C. (2003). Physical and functional interaction between HCV core protein and the different p73 isoforms. *Oncogene* **22**, 2573-2580.

Alter, H. J., Purcell, R. H., Holland, P. V. & Popper, H. (1978). Transmissible agent in non-A, non-B hepatitis. *Lancet* **1**, 459-463.

Alter, H. J. & Seeff, L. B. (2000). Recovery, persistence, and sequelae in hepatitis C virus infection: a perspective on long-term outcome. *Semin Liver Dis* **20**, 17-35.

Alter, M. J. (2007). Epidemiology of hepatitis C virus infection. *World J Gastroenterol* **13**, 2436-2441.

Alter, M. J., Kruszon-Moran, D., Nainan, O. V., McQuillan, G. M., Gao, F., Moyer, L. A., Kaslow, R. A. & Margolis, H. S. (1999). The prevalence of hepatitis C virus infection in the United States, 1988 through 1994. *N Engl J Med* **341**, 556-562.

Andre, P., Komurian-Pradel, F., Deforges, S., Perret, M., Berland, J. L., Sodoyer, M., Pol, S., Brechot, C., Paranhos-Baccala, G. & Lotteau, V. (2002). Characterization of low- and very-low-density hepatitis C virus RNA-containing particles. *J Virol* **76**, 6919-6928.

Angus, A. G., Dalrymple, D., Boulant, S., McGivern, D. R., Clayton, R. F., Scott, M. J., Adair, R., Graham, S., Owsianka, A. M., Targett-Adams, P., Li, K., Wakita, T., McLauchlan, J., Lemon, S. M. & Patel, A. H. (2010). Requirement of cellular DDX3 for hepatitis C virus replication is unrelated to its interaction with the viral core protein. *J Gen Virol* **91**, 122-132.

Aoki, H., Hayashi, J., Moriyama, M., Arakawa, Y. & Hino, O. (2000). Hepatitis C virus core protein interacts with 14-3-3 protein and activates the kinase Raf-1. *J Virol* **74**, 1736-1741.

Aoyagi, K., Ohue, C., Iida, K., Kimura, T., Tanaka, E., Kiyosawa, K. & Yagi, S. (1999). Development of a simple and highly sensitive enzyme immunoassay for hepatitis C virus core antigen. *J Clin Microbiol* **37**, 1802-1808.

Appel, N., Pietschmann, T. & Bartenschlager, R. (2005). Mutational analysis of hepatitis C virus nonstructural protein 5A: potential role of differential phosphorylation in RNA replication and identification of a genetically flexible domain. *J Virol* **79**, 3187-3194.

Appel, N., Zayas, M., Miller, S., Krijnse-Locker, J., Schaller, T., Friebe, P., Kallis, S., Engel, U. & Bartenschlager, R. (2008). Essential role of domain III of nonstructural protein 5A for hepatitis C virus infectious particle assembly. *PLoS Pathog* **4**, e1000035.

Ariumi, Y., Kuroki, M., Abe, K., Dansako, H., Ikeda, M., Wakita, T. & Kato, N. (2007). DDX3 DEAD-box RNA helicase is required for hepatitis C virus RNA replication. *J Virol* **81**, 13922-13926.

Bain, C., Parroche, P., Lavergne, J. P., Duverger, B., Vieux, C., Dubois, V., Komurian-Pradel, F., Trepo, C., Gebuhrer, L., Paranhos-Baccala, G., Penin, F. & Inchauspe, G. (2004). Memory T-cell-mediated immune responses specific to an alternative core protein in hepatitis C virus infection. *J Virol* **78**, 10460-10469.

Bamber, M., Murray, A. K., Weller, I. V., Morelli, A., Scheuer, P. J., Thomas, H. C. & Sherlock, S. (1981). Clinical and histological features of a group of patients with sporadic non-A, non-B hepatitis. *J Clin Pathol* **34**, 1175-1180.

Barba, G., Harper, F., Harada, T., Kohara, M., Goulinet, S., Matsuura, Y., Eder, G., Schaff, Z., Chapman, M. J., Miyamura, T. & Brechot, C. (1997). Hepatitis C virus core protein shows a cytoplasmic localization and associates to cellular lipid storage droplets. *Proc Natl Acad Sci U S A* **94**, 1200-1205.

Baril, M. & Brakier-Gingras, L. (2005). Translation of the F protein of hepatitis C virus is initiated at a non-AUG codon in a +1 reading frame relative to the polyprotein. *Nucleic Acids Res* **33**, 1474-1486.

Bartenschlager, R., Ahlborn-Laake, L., Mous, J. & Jacobsen, H. (1993). Nonstructural protein 3 of the hepatitis C virus encodes a serine-type proteinase required for cleavage at the NS3/4 and NS4/5 junctions. *J Virol* **67**, 3835-3844.

Bartenschlager, R., Ahlborn-Laake, L., Mous, J. & Jacobsen, H. (1994). Kinetic and structural analyses of hepatitis C virus polyprotein processing. *J Virol* **68**, 5045-5055.

Bartenschlager, R., Frese, M. & Pietschmann, T. (2004). Novel insights into hepatitis C virus replication and persistence. *Adv Virus Res* **63**, 71-180.

Bartenschlager, R. & Sparacio, S. (2007). Hepatitis C virus molecular clones and their replication capacity in vivo and in cell culture. *Virus Res* **127**, 195-207.

Barth, H., Schafer, C., Adah, M. I., Zhang, F., Linhardt, R. J., Toyoda, H., Kinoshita-Toyoda, A., Toida, T., Van Kuppevelt, T. H., Depla, E., Von Weizsacker, F., Blum, H. E. & Baumert, T. F. (2003). Cellular binding of hepatitis C virus envelope glycoprotein E2 requires cell surface heparan sulfate. *J Biol Chem* **278**, 41003-41012.

Bartosch, B., Dubuisson, J. & Cosset, F. L. (2003a). Infectious hepatitis C virus pseudo-particles containing functional E1-E2 envelope protein complexes. *J Exp Med* **197**, 633-642.

Bartosch, B., Vitelli, A., Granier, C., Goujon, C., Dubuisson, J., Pascale, S., Scarselli, E., Cortese, R., Nicosia, A. & Cosset, F. L. (2003b). Cell entry of hepatitis C virus requires a set of co-receptors that include the CD81 tetraspanin and the SR-B1 scavenger receptor. *J Biol Chem* **278**, 41624-41630.

Battegay, M., Fikes, J., Di Bisceglie, A. M., Wentworth, P. A., Sette, A., Celis, E., Ching, W. M., Grakoui, A., Rice, C. M., Kurokohchi, K. & et al. (1995). Patients with chronic hepatitis C have circulating cytotoxic T cells which recognize

hepatitis C virus-encoded peptides binding to HLA-A2.1 molecules. *J Virol* **69**, 2462-2470.

Beck, J. & Nassal, M. (2007). Hepatitis B virus replication. *World J Gastroenterol* **13**, 48-64.

Behrens, S. E., Tomei, L. & De Francesco, R. (1996). Identification and properties of the RNA-dependent RNA polymerase of hepatitis C virus. *Embo J* **15**, 12-22.

Bellentani, S. & Tiribelli, C. (2001). The spectrum of liver disease in the general population: lesson from the Dionysos study. *J Hepatol* **35**, 531-537.

Benali-Furet, N. L., Chami, M., Houel, L., De Giorgi, F., Vernejoul, F., Lagorce, D., Buscail, L., Bartenschlager, R., Ichas, F., Rizzuto, R. & Paterlini-Brechot, P. (2005). Hepatitis C virus core triggers apoptosis in liver cells by inducing ER stress and ER calcium depletion. *Oncogene* **24**, 4921-4933.

Benedicto, I., Molina-Jimenez, F., Bartosch, B., Cosset, F. L., Lavillette, D., Prieto, J., Moreno-Otero, R., Valenzuela-Fernandez, A., Aldabe, R., Lopez-Cabrera, M. & Majano, P. L. (2009). The tight junction-associated protein occludin is required for a postbinding step in hepatitis C virus entry and infection. *J Virol* **83**, 8012-8020.

Benhamou, Y., Bochet, M., Di Martino, V., Charlotte, F., Azria, F., Coutellier, A., Vidaud, M., Bricaire, F., Opolon, P., Katlama, C. & Poynard, T. (1999). Liver fibrosis progression in human immunodeficiency virus and hepatitis C virus coinfected patients. The Multivirc Group. *Hepatology* **30**, 1054-1058.

Beran, R. K., Lindenbach, B. D. & Pyle, A. M. (2009). The NS4A protein of hepatitis C virus promotes RNA-coupled ATP hydrolysis by the NS3 helicase. *J Virol* **83**, 3268-3275.

Berenguer, M., Ferrell, L., Watson, J., Prieto, M., Kim, M., Rayon, M., Cordoba, J., Herola, A., Ascher, N., Mir, J., Berenguer, J. & Wright, T. L. (2000). HCV-related fibrosis progression following liver transplantation: increase in recent years. *J Hepatol* **32**, 673-684.

Betts, M. J. Russell, R, B. (2003). Amino Acid properties and consequences of substitutions. In Bioinformatics for Geneticists, Barnes & Gray, Wiley.

Bhattacherjee, V., Prescott, L. E., Pike, I., Rodgers, B., Bell, H., El-Zayadi, A. R., Kew, M. C., Conradie, J., Lin, C. K., Marsden, H. & et al. (1995). Use of NS-4 peptides to identify type-specific antibody to hepatitis C virus genotypes 1, 2, 3, 4, 5 and 6. *J Gen Virol* **76**, 1737-1748.

Binder, M., Quinkert, D., Bochkarova, O., Klein, R., Kezmic, N., Bartenschlager, R. & Lohmann, V. (2007). Identification of determinants involved in initiation of hepatitis C virus RNA synthesis by using intergenotypic replicase chimeras. *J Virol* **81**, 5270-5283.

Bissig, K. D., Le, T. T., Woods, N. B. & Verma, I. M. (2007). Repopulation of adult and neonatal mice with human hepatocytes: a chimeric animal model. *Proc Natl Acad Sci U S A* **104**, 20507-20511.

Bissig, K. D., Wieland, S. F., Tran, P., Isogawa, M., Le, T. T., Chisari, F. V. & Verma, I. M (2010). Human liver chimeric mice provide a model for hepatitis B and C virus infection and treatment. *J Clin Invest* **120**, 924-30.

Biswal, B. K., Cherney, M. M., Wang, M., Chan, L., Yannopoulos, C. G., Bilimoria, D., Nicolas, O., Bedard, J. & James, M. N. (2005). Crystal structures of the RNA-dependent RNA polymerase genotype 2a of hepatitis C virus reveal two conformations and suggest mechanisms of inhibition by non-nucleoside inhibitors. *J Biol Chem* **280**, 18202-18210.

Bjoro, K., Froland, S. S., Yun, Z., Samdal, H. H. & Haaland, T. (1994). Hepatitis C infection in patients with primary hypogammaglobulinemia after treatment with contaminated immune globulin. *N Engl J Med* **331**, 1607-1611.

Bjoro, K., Skaug, K., Haaland, T. & Froland, S. S. (1999). Long-term outcome of chronic hepatitis C virus infection in primary hypogammaglobulinaemia. *QJM* **92**, 433-441.

Blanchard, E., Belouzard, S., Goueslain, L., Wakita, T., Dubuisson, J., Wychowski, C. & Rouille, Y. (2006). Hepatitis C virus entry depends on clathrin-mediated endocytosis. *J Virol* **80**, 6964-6972.

Blasiole, D. A., Davis, R. A. & Attie, A. D. (2007). The physiological and molecular regulation of lipoprotein assembly and secretion. *Mol Biosyst* **3**, 608-619.

Blight, K. J., Kolykhalov, A. A. & Rice, C. M. (2000). Efficient initiation of HCV RNA replication in cell culture. *Science* **290**, 1972-1974.

Blight, K. J., McKeating, J. A., Marcotrigiano, J. & Rice, C. M. (2003). Efficient replication of hepatitis C virus genotype 1a RNAs in cell culture. *J Virol* **77**, 3181-3190.

Blight, K. J., McKeating, J. A. & Rice, C. M. (2002). Highly permissive cell lines for subgenomic and genomic hepatitis C virus RNA replication. *J Virol* **76**, 13001-13014.

Blight, K. J. & Rice, C. M. (1997). Secondary structure determination of the conserved 98-base sequence at the 3' terminus of hepatitis C virus genome RNA. *J Virol* **71**, 7345-7352.

Bode, J. G., Ludwig, S., Ehrhardt, C., Albrecht, U., Erhardt, A., Schaper, F., Heinrich, P. C. & Haussinger, D. (2003). IFN-alpha antagonistic activity of HCV core protein involves induction of suppressor of cytokine signaling-3. *Faseb J* **17**, 488-490.

Booth, J. C., Kumar, U., Webster, D., Monjardino, J. & Thomas, H. C. (1998). Comparison of the rate of sequence variation in the hypervariable region of E2/NS1 region of hepatitis C virus in normal and hypogammaglobulinemic patients. *Hepatology* **27**, 223-227.

Botarelli, P., Brunetto, M. R., Minutello, M. A., Calvo, P., Unutmaz, D., Weiner, A. J., Choo, Q. L., Shuster, J. R., Kuo, G., Bonino, F. & et al. (1993). T-lymphocyte response to hepatitis C virus in different clinical courses of infection. *Gastroenterology* **104**, 580-587.

Botlagunta, M., Vesuna, F., Mironchik, Y., Raman, A., Lisok, A., Winnard, P., Jr., Mukadam, S., Van Diest, P., Chen, J. H., Farabaugh, P., Patel, A. H. & Raman, V. (2008). Oncogenic role of DDX3 in breast cancer biogenesis. *Oncogene* **27**, 3912-3922.

Boulant, S., Becchi, M., Penin, F. & Lavergne, J. P. (2003). Unusual multiple recoding events leading to alternative forms of hepatitis C virus core protein from genotype 1b. *J Biol Chem* **278**, 45785-45792.

Boulant, S., Douglas, M. W., Moody, L., Budkowska, A., Targett-Adams, P. & McLauchlan, J. (2008). Hepatitis C virus core protein induces lipid droplet redistribution in a microtubule- and dynein-dependent manner. *Traffic* **9**, 1268-1282.

Boulant, S., Targett-Adams, P. & McLauchlan, J. (2007). Disrupting the association of hepatitis C virus core protein with lipid droplets correlates with a loss in production of infectious virus. *J Gen Virol* **88**, 2204-2213.

Boulant, S., Vanbelle, C., Ebel, C., Penin, F. & Lavergne, J. P. (2005). Hepatitis C virus core protein is a dimeric alpha-helical protein exhibiting membrane protein features. *J Virol* **79**, 11353-11365.

Bradley, D., McCaustland, K., Krawczynski, K., Spelbring, J., Humphrey, C. & Cook, E. H. (1991). Hepatitis C virus: buoyant density of the factor VIII-derived isolate in sucrose. *J Med Virol* **34**, 206-208.

Bradrick, S. S., Walters, R. W. & Gromeier, M. (2006). The hepatitis C virus 3'-untranslated region or a poly(A) tract promote efficient translation subsequent to the initiation phase. *Nucleic Acids Res* **34**, 1293-1303.

Brass, V., Bieck, E., Montserret, R., Wolk, B., Hellings, J. A., Blum, H. E., Penin, F. & Moradpour, D. (2002). An amino-terminal amphipathic alpha-helix mediates membrane association of the hepatitis C virus nonstructural protein 5A. *J Biol Chem* **277**, 8130-8139.

Bressanelli, S., Tomei, L., Roussel, A., Incitti, I., Vitale, R. L., Mathieu, M., De Francesco, R. & Rey, F. A. (1999). Crystal structure of the RNA-dependent RNA polymerase of hepatitis C virus. *Proc Natl Acad Sci U S A* **96**, 13034-13039.

Brillanti, S., Foli, M., Gaiani, S., Masci, C., Miglioli, M. & Barbara, L. (1993). Persistent hepatitis C viraemia without liver disease. *Lancet* **341**, 464-465.

Bukh, J., Purcell, R. H. & Miller, R. H. (1992). Sequence analysis of the 5' noncoding region of hepatitis C virus. *Proc Natl Acad Sci U S A* **89**, 4942-4946.

Bukh, J., Purcell, R. H. & Miller, R. H. (1994). Sequence analysis of the core gene of 14 hepatitis C virus genotypes. *Proc Natl Acad Sci U S A* **91**, 8239-8243.

Burlone, M. E. & Budkowska, A. (2009). Hepatitis C virus cell entry: role of lipoproteins and cellular receptors. *J Gen Virol* **90**, 1055-1070.

Carrere-Kremer, S., Montpellier-Pala, C., Cocquerel, L., Wychowski, C., Penin, F. & Dubuisson, J. (2002). Subcellular localization and topology of the p7 polypeptide of hepatitis C virus. *J Virol* **76**, 3720-3730.

Caruthers, J. M., Johnson, E. R. & McKay, D. B. (2000). Crystal structure of yeast initiation factor 4A, a DEAD-box RNA helicase. *Proc Natl Acad Sci U S A* **97**, 13080-13085.

Caruthers, J. M. & McKay, D. B. (2002). Helicase structure and mechanism. *Curr Opin Struct Biol* **12**, 123-133.

Castera, L., Chouteau, P., Hezode, C., Zafrani, E. S., Dhumeaux, D. & Pawlotsky, J. M. (2005). Hepatitis C virus-induced hepatocellular steatosis. *Am J Gastroenterol* **100**, 711-715.

Catanese, M. T., Ansuini, H., Graziani, R., Huby, T., Moreau, M., Ball, J. K., Paonessa, G., Rice, C. M., Cortese, R., Vitelli, A. & Nicosia, A. (2010). Role of scavenger receptor class B type I in hepatitis C virus entry: kinetics and molecular determinants. *J Virol* **84**, 34-43.

Catanese, M. T., Graziani, R., von Hahn, T., Moreau, M., Huby, T., Paonessa, G., Santini, C., Luzzago, A., Rice, C. M., Cortese, R., Vitelli, A. & Nicosia, A. (2007). High-avidity monoclonal antibodies against the human scavenger class B type I receptor efficiently block hepatitis C virus infection in the presence of high-density lipoprotein. *J Virol* **81**, 8063-8071.

Chang, J., Yang, S. H., Cho, Y. G., Hwang, S. B., Hahn, Y. S. & Sung, Y. C. (1998). Hepatitis C virus core from two different genotypes has an oncogenic potential but is not sufficient for transforming primary rat embryo fibroblasts in cooperation with the H-ras oncogene. *J Virol* **72**, 3060-3065.

Chang, K. M., Rehermann, B., McHutchison, J. G., Pasquinelli, C., Southwood, S., Sette, A. & Chisari, F. V. (1997). Immunological significance of cytotoxic T lymphocyte epitope variants in patients chronically infected by the hepatitis C virus. *J Clin Invest* **100**, 2376-2385.

Chang, K. M., Thimme, R., Melpolder, J. J., Oldach, D., Pemberton, J., Moorhead-Loudis, J., McHutchison, J. G., Alter, H. J. & Chisari, F. V. (2001). Differential CD4(+) and CD8(+) T-cell responsiveness in hepatitis C virus infection. *Hepatology* **33**, 267-276.

Chang, K. S., Jiang, J., Cai, Z. & Luo, G. (2007). Human apolipoprotein e is required for infectivity and production of hepatitis C virus in cell culture. *J Virol* **81**, 13783-13793.

Chang, P. C., Chi, C. W., Chau, G. Y., Li, F. Y., Tsai, Y. H., Wu, J. C. & Wu Lee, Y. H. (2006). DDX3, a DEAD box RNA helicase, is deregulated in hepatitis virus-associated hepatocellular carcinoma and is involved in cell growth control. *Oncogene* **25**, 1991-2003.

Chao, C. H., Chen, C. M., Cheng, P. L., Shih, J. W., Tsou, A. P. & Lee, Y. H. (2006). DDX3, a DEAD box RNA helicase with tumor growth-suppressive property and transcriptional regulation activity of the p21waf1/cip1 promoter, is a candidate tumor suppressor. *Cancer Res* **66**, 6579-6588.

Chen, C. M., You, L. R., Hwang, L. H. & Lee, Y. H. (1997). Direct interaction of hepatitis C virus core protein with the cellular lymphotoxin-beta receptor modulates the signal pathway of the lymphotoxin-beta receptor. *J Virol* **71**, 9417-9426.

Chen, S. Y., Kao, C. F., Chen, C. M., Shih, C. M., Hsu, M. J., Chao, C. H., Wang, S. H., You, L. R. & Lee, Y. H. (2003). Mechanisms for inhibition of hepatitis B virus gene expression and replication by hepatitis C virus core protein. *J Biol Chem* **278**, 591-607.

Chertova, E., Chertov, O., Coren, L. V., Roser, J. D., Trubey, C. M., Bess, J. W., Jr., Sowder, R. C., 2nd, Barsov, E., Hood, B. L., Fisher, R. J., Nagashima, K., Conrads, T. P., Veenstra, T. D., Lifson, J. D. & Ott, D. E. (2006). Proteomic and biochemical analysis of purified human immunodeficiency virus type 1 produced from infected monocyte-derived macrophages. *J Virol* **80**, 9039-9052.

Choo, Q. L., Kuo, G., Ralston, R., Weiner, A., Chien, D., Van Nest, G., Han, J., Berger, K., Thudium, K., Kuo, C. & et al. (1994). Vaccination of chimpanzees against infection by the hepatitis C virus. *Proc Natl Acad Sci U S A* **91**, 1294-1298.

Choo, Q. L., Kuo, G., Weiner, A. J., Overby, L. R., Bradley, D. W. & Houghton, M. (1989). Isolation of a cDNA clone derived from a blood-borne non-A, non-B viral hepatitis genome. *Science* **244**, 359-362.

Choo, Q. L., Richman, K. H., Han, J. H., Berger, K., Lee, C., Dong, C., Gallegos, C., Coit, D., Medina-Selby, R., Barr, P. J. & et al. (1991). Genetic organization and diversity of the hepatitis C virus. *Proc Natl Acad Sci U S A* **88**, 2451-2455.

Choo, S. H., So, H. S., Cho, J. M. & Ryu, W. S. (1995). Association of hepatitis C virus particles with immunoglobulin: a mechanism for persistent infection. *J Gen Virol* **76**, 2337-2341.

Christie, J. M., Healey, C. J., Watson, J., Wong, V. S., Duddridge, M., Snowden, N., Rosenberg, W. M., Fleming, K. A., Chapel, H. & Chapman, R. W. (1997). Clinical outcome of hypogammaglobulinaemic patients following outbreak of acute hepatitis C: 2 year follow up. *Clin Exp Immunol* **110**, 4-8.

Chuang, R. Y., Weaver, P. L., Liu, Z. & Chang, T. H. (1997). Requirement of the DEAD-Box protein ded1p for messenger RNA translation. *Science* **275**, 1468-1471.

Chung, C. S., Chen, C. H., Ho, M. Y., Huang, C. Y., Liao, C. L. & Chang, W. (2006). Vaccinia virus proteome: identification of proteins in vaccinia virus intracellular mature virion particles. *J Virol* **80**, 2127-2140.

Clarke, B. (1997). Molecular virology of hepatitis C virus. *J Gen Virol* **78**, 2397-2410.

Clayton, R. F., Owsianka, A., Aitken, J., Graham, S., Bhella, D. & Patel, A. H. (2002). Analysis of antigenicity and topology of E2 glycoprotein present on recombinant hepatitis C virus-like particles. *J Virol* **76**, 7672-7682.

Cocquerel, L., Kuo, C. C., Dubuisson, J. & Levy, S. (2003). CD81-dependent binding of hepatitis C virus E1E2 heterodimers. *J Virol* **77**, 10677-10683.

Cordin, O., Banroques, J., Tanner, N. K. & Linder, P. (2006). The DEAD-box protein family of RNA helicases. *Gene* **367**, 17-37.

Cordin, O., Tanner, N. K., Doere, M., Linder, P. & Banroques, J. (2004). The newly discovered Q motif of DEAD-box RNA helicases regulates RNA-binding and helicase activity. *Embo J* **23**, 2478-2487.

Cormier, E. G., Durso, R. J., Tsamis, F., Boussemart, L., Manix, C., Olson, W. C., Gardner, J. P. & Dragic, T. (2004a). L-SIGN (CD209L) and DC-SIGN (CD209) mediate transinfection of liver cells by hepatitis C virus. *Proc Natl Acad Sci U S A* **101**, 14067-14072.

Cormier, E. G., Tsamis, F., Kajumo, F., Durso, R. J., Gardner, J. P. & Dragic, T. (2004b). CD81 is an entry coreceptor for hepatitis C virus. *Proc Natl Acad Sci U S A* **101**, 7270-7274.

de Lucas, S., Bartolome, J. & Carreno, V. (2005). Hepatitis C virus core protein down-regulates transcription of interferon-induced antiviral genes. *J Infect Dis* **191**, 93-99.

Dalrymple, D. (2007). Identification of hepatitis C Virus Core Protein Residues Critical for the Interaction with the Cellular DEAD-box Helicase DDX3 and their Functional Relevance. In *MRC Virology Unit* University of Glasgow, Glasgow.

Deckert, J., Hartmuth, K., Boehringer, D., Behzadnia, N., Will, C. L., Kastner, B., Stark, H., Urlaub, H. & Luhrmann, R. (2006). Protein composition and electron microscopy structure of affinity-purified human spliceosomal B complexes isolated under physiological conditions. *Mol Cell Biol* **26**, 5528-5543.

Deleersnyder, V., Pillez, A., Wychowski, C., Blight, K., Xu, J., Hahn, Y. S., Rice, C. M. & Dubuisson, J. (1997). Formation of native hepatitis C virus glycoprotein complexes. *J Virol* **71**, 697-704.

Deng, L., Adachi, T., Kitayama, K., Bungyoku, Y., Kitazawa, S., Ishido, S., Shoji, I. & Hotta, H. (2008). Hepatitis C virus infection induces apoptosis through a Bax-triggered, mitochondrion-mediated, caspase 3-dependent pathway. *J Virol* **82**, 10375-10385.

Di Bisceglie, A. M., Goodman, Z. D., Ishak, K. G., Hoofnagle, J. H., Melpolder, J. J. & Alter, H. J. (1991). Long-term clinical and histopathological follow-up of chronic posttransfusion hepatitis. *Hepatology* **14**, 969-974.

Di Martino, V., Rufat, P., Boyer, N., Renard, P., Degos, F., Martinot-Peignoux, M., Matheron, S., Le Moing, V., Vachon, F., Degott, C., Valla, D. & Marcellin, P. (2001). The influence of human immunodeficiency virus coinfection on chronic hepatitis C in injection drug users: a long-term retrospective cohort study. *Hepatology* **34**, 1193-1199.

Diaz, O., Delers, F., Maynard, M., Demignot, S., Zoulim, F., Chambaz, J., Trepo, C., Lotteau, V. & Andre, P. (2006). Preferential association of Hepatitis C virus with apolipoprotein B48-containing lipoproteins. *J Gen Virol* **87**, 2983-2991.

Dienes, H. P., Popper, H., Arnold, W. & Lobeck, H. (1982). Histologic observations in human hepatitis non-A, non-B. *Hepatology* **2**, 562-571.

Diepolder, H. M., Hoffmann, R. M., Gerlach, J. T., Zachoval, R., Jung, M. C. & Pape, G. R. (1998). Immunopathogenesis of HCV infection. *Curr Stud Hematol Blood Transfus* **62**, 135-151.

Diepolder, H. M., Zachoval, R., Hoffmann, R. M., Wierenga, E. A., Santantonio, T., Jung, M. C., Eichenlaub, D. & Pape, G. R. (1995). Possible mechanism involving T-lymphocyte response to non-structural protein 3 in viral clearance in acute hepatitis C virus infection. *Lancet* **346**, 1006-1007.

Domitrovich, A. M., Diebel, K. W., Ali, N., Sarker, S. & Siddiqui, A. (2005). Role of La autoantigen and polypyrimidine tract-binding protein in HCV replication. *Virology* **335**, 72-86.

Doughty, A. L., Spencer, J. D., Cossart, Y. E. & McCaughan, G. W. (1998). Cholestatic hepatitis after liver transplantation is associated with persistently high serum hepatitis C virus RNA levels. *Liver Transpl Surg* **4**, 15-21.

Drummer, H. E., Maerz, A. & Poumbourios, P. (2003). Cell surface expression of functional hepatitis C virus E1 and E2 glycoproteins. *FEBS lett* **546**, 385-390.

Dubuisson, J., Hsu, H. H., Cheung, R. C., Greenberg, H. B., Russell, D. G. & Rice, C. M. (1994). Formation and intracellular localization of hepatitis C virus envelope glycoprotein complexes expressed by recombinant vaccinia and Sindbis viruses. *J Virol* **68**, 6147-6160.

Egger, D., Wolk, B., Gosert, R., Bianchi, L., Blum, H. E., Moradpour, D. & Bienz, K. (2002). Expression of hepatitis C virus proteins induces distinct membrane alterations including a candidate viral replication complex. *J Virol* **76**, 5974-5984.

Einav, S. & Koziel, M. J. (2002). Immunopathogenesis of hepatitis C virus in the immunosuppressed host. *Transpl Infect Dis* **4**, 85-92.

El-Hage, N. & Luo, G. (2003). Replication of hepatitis C virus RNA occurs in a membrane-bound replication complex containing nonstructural viral proteins and RNA. *J Gen Virol* **84**, 2761-2769.

Elazar, M., Cheong, K. H., Liu, P., Greenberg, H. B., Rice, C. M. & Glenn, J. S. (2003). Amphipathic helix-dependent localization of NS5A mediates hepatitis C virus RNA replication. *J Virol* **77**, 6055-6061.

Elazar, M., Liu, P., Rice, C. M. & Glenn, J. S. (2004). An N-terminal amphipathic helix in hepatitis C virus (HCV) NS4B mediates membrane association, correct localization of replication complex proteins, and HCV RNA replication. *J Virol* **78**, 11393-11400.

Elmore, S. (2007). Apoptosis: a review of programmed cell death. *Toxicol Pathol* **35**, 495-516.

Evans, M. J., von Hahn, T., Tscherne, D. M., Syder, A. J., Panis, M., Wolk, B., Hatziioannou, T., McKeating, J. A., Bieniasz, P. D. & Rice, C. M. (2007). Claudin-1 is a hepatitis C virus co-receptor required for a late step in entry. *Nature* **446**, 801-805.

Failla, C., Tomei, L. & De Francesco, R. (1994). Both NS3 and NS4A are required for proteolytic processing of hepatitis C virus nonstructural proteins. *J Virol* **68**, 3753-3760.

Fang, J., Kubota, S., Yang, B., Zhou, N., Zhang, H., Godbout, R. & Pomerantz, R. J. (2004). A DEAD box protein facilitates HIV-1 replication as a cellular co-factor of Rev. *Virology* **330**, 471-480.

Farci, P., Alter, H. J., Shimoda, A., Govindarajan, S., Cheung, L. C., Melpolder, J. C., Sacher, R. A., Shih, J. W. & Purcell, R. H. (1996a). Hepatitis C virus-associated fulminant hepatic failure. *N Engl J Med* **335**, 631-634.

Farci, P., Alter, H. J., Wong, D., Miller, R. H., Shih, J. W., Jett, B. & Purcell, R. H. (1991). A long-term study of hepatitis C virus replication in non-A, non-B hepatitis. *N Engl J Med* **325**, 98-104.

Farci, P., Shimoda, A., Wong, D., Cabezon, T., De Gioannis, D., Strazzera, A., Shimizu, Y., Shapiro, M., Alter, H. J. & Purcell, R. H. (1996b). Prevention of hepatitis C virus infection in chimpanzees by hyperimmune serum against the hypervariable region 1 of the envelope 2 protein. *Proc Natl Acad Sci U S A* **93**, 15394-15399.

Feinstone, S. M., Kapikian, A. Z., Purcell, R. H., Alter, H. J. & Holland, P. V. (1975). Transfusion-associated hepatitis not due to viral hepatitis type A or B. *N Engl J Med* **292**, 767-770.

Feinstone, S. M., Mihalik, K. B., Kamimura, T., Alter, H. J., London, W. T. & Purcell, R. H. (1983). Inactivation of hepatitis B virus and non-A, non-B hepatitis by chloroform. *Infect Immun* **41**, 816-821.

Feray, C., Caccamo, L., Alexander, G. J., Ducot, B., Gugenheim, J., Casanovas, T., Loinaz, C., Gigou, M., Burra, P., Barkholt, L., Esteban, R., Bizollon, T., Lerut, J., Minello-Franza, A., Bernard, P. H., Nachbaur, K., Botta-Fridlund, D., Bismuth, H., Schalm, S. W. & Samuel, D. (1999). European collaborative study on factors influencing outcome after liver transplantation for hepatitis C. European Concerted Action on Viral Hepatitis (EUROHEP) Group. *Gastroenterology* **117**, 619-625.

Fischer, R., Baumert, T. & Blum, H. E. (2007). Hepatitis C virus infection and apoptosis. *World J Gastroenterol* **13**, 4865-4872.

Flajolet, M., Rotondo, G., Daviet, L., Bergametti, F., Inchauspe, G., Tiollais, P., Transy, C. & Legrain, P. (2000). A genomic approach of the hepatitis C virus generates a protein interaction map. *Gene* **242**, 369-379.

Forns, X., Thimme, R., Govindarajan, S., Emerson, S. U., Purcell, R. H., Chisari, F. V. & Bukh, J. (2000). Hepatitis C virus lacking the hypervariable region 1 of the second envelope protein is infectious and causes acute resolving or persistent infection in chimpanzees. *Proc Natl Acad Sci U S A* **97**, 13318-13323.

Foy, E., Li, K., Wang, C., Sumpter, R., Jr., Ikeda, M., Lemon, S. M. & Gale, M., Jr. (2003). Regulation of interferon regulatory factor-3 by the hepatitis C virus serine protease. *Science* **300**, 1145-1148.

Franca, R., Belfiore, A., Spadari, S. & Maga, G. (2007). Human DEAD-box ATPase DDX3 shows a relaxed nucleoside substrate specificity. *Proteins* **67**, 1128-1137.

Frank, C., Mohamed, M. K., Strickland, G. T., Lavanchy, D., Arthur, R. R., Magder, L. S., El Khoby, T., Abdel-Wahab, Y., Aly Ohn, E. S., Anwar, W. & Sallam, I. (2000). The role of parenteral antischistosomal therapy in the spread of hepatitis C virus in Egypt. *Lancet* **355**, 887-891.

Frasca, L., Del Porto, P., Tuosto, L., Marinari, B., Scotta, C., Carbonari, M., Nicosia, A. & Piccolella, E. (1999). Hypervariable region 1 variants act as TCR antagonists for hepatitis C virus-specific CD4+ T cells. *J Immunol* **163**, 650-658.

Frick, D. N., Rypma, R. S., Lam, A. M. & Gu, B. (2004). The nonstructural protein 3 protease/helicase requires an intact protease domain to unwind duplex RNA efficiently. *J Biol Chem* **279**, 1269-1280.

Friebe, P. & Bartenschlager, R. (2002). Genetic analysis of sequences in the 3' nontranslated region of hepatitis C virus that are important for RNA replication. *J Virol* **76**, 5326-5338.

Friebe, P., Lohmann, V., Krieger, N. & Bartenschlager, R. (2001). Sequences in the 5' nontranslated region of hepatitis C virus required for RNA replication. *J Virol* **75**, 12047-12057.

Fried, M. W., Shiffman, M. L., Reddy, K. R., Smith, C., Marinos, G., Goncales, F. L., Jr., Haussinger, D., Diago, M., Carosi, G., Dhumeaux, D., Craxi, A., Lin, A., Hoffman, J. & Yu, J. (2002). Peginterferon alfa-2a plus ribavirin for chronic hepatitis C virus infection. *N Engl J Med* **347**, 975-982.

Fukushi, S., Okada, M., Kageyama, T., Hoshino, F. B., Nagai, K. & Katayama, K. (2001). Interaction of poly(rC)-binding protein 2 with the 5'-terminal stem loop of the hepatitis C-virus genome. *Virus Res* **73**, 67-79.

Furuse, M., Hirase, T., Itoh, M., Nagafuchi, A., Yonemura, S., Tsukita, S. & Tsukita, S. (1993). Occludin: a novel integral membrane protein localizing at tight junctions. *J Cell Biol* **123**, 1777-1788.

Gale, M., Jr., Blakely, C. M., Kwieciszewski, B., Tan, S. L., Dossett, M., Tang, N. M., Korth, M. J., Polyak, S. J., Gretch, D. R. & Katze, M. G. (1998). Control of PKR protein kinase by hepatitis C virus nonstructural 5A protein: molecular mechanisms of kinase regulation. *Mol Cell Biol* **18**, 5208-5218.

Gale, M., Jr. & Foy, E. M. (2005). Evasion of intracellular host defence by hepatitis C virus. *Nature* **436**, 939-945.

Gane, E. J., Portmann, B. C., Naoumov, N. V., Smith, H. M., Underhill, J. A., Donaldson, P. T., Maertens, G. & Williams, R. (1996). Long-term outcome of hepatitis C infection after liver transplantation. *N Engl J Med* **334**, 815-820.

Gastaminza, P., Cheng, G., Wieland, S., Zhong, J., Liao, W. & Chisari, F. V. (2008). Cellular determinants of hepatitis C virus assembly, maturation, degradation, and secretion. *J Virol* **82**, 2120-2129.

Gastaminza, P., Kapadia, S. B. & Chisari, F. V. (2006). Differential biophysical properties of infectious intracellular and secreted hepatitis C virus particles. *J Virol* **80**, 11074-11081.

Gee, S. L. & Conboy, J. G. (1994). Mouse erythroid cells express multiple putative RNA helicase genes exhibiting high sequence conservation from yeast to mammals. *Gene* **140**, 171-177.

Germi, R., Crance, J. M., Garin, D., Guimet, J., Lortat-Jacob, H., Ruigrok, R. W., Zarski, J. P. & Drouet, E. (2002). Cellular glycosaminoglycans and low density lipoprotein receptor are involved in hepatitis C virus adsorption. *J Med Virol* **68**, 206-215.

Ghebrehiwet, B., Lim, B. L., Kumar, R., Feng, X. & Peerschke, E. I. (2001). gC1q-R/p33, a member of a new class of multifunctional and multicompartmental cellular proteins, is involved in inflammation and infection. *Immunol Rev* **180**, 65-77.

Goffard, A., Callens, N., Bartosch, B., Wychowski, C., Cosset, F. L., Montpellier, C. & Dubuisson, J. (2005). Role of N-linked glycans in the functions of hepatitis C virus envelope glycoproteins. *J Virol* **79**, 8400-8409.

Goh, P. Y., Tan, Y. J., Lim, S. P., Lim, S. G., Tan, Y. H. & Hong, W. J. (2001). The hepatitis C virus core protein interacts with NS5A and activates its caspase-mediated proteolytic cleavage. *Virology* **290**, 224-236.

Goh, P. Y., Tan, Y. J., Lim, S. P., Tan, Y. H., Lim, S. G., Fuller-Pace, F. & Hong, W. (2004). Cellular RNA helicase p68 relocalization and interaction with the hepatitis C virus (HCV) NS5B protein and the potential role of p68 in HCV RNA replication. *J Virol* **78**, 5288-5298.

Gosert, R., Egger, D., Lohmann, V., Bartenschlager, R., Blum, H. E., Bienz, K. & Moradpour, D. (2003). Identification of the hepatitis C virus RNA replication complex in Huh-7 cells harboring subgenomic replicons. *J Virol* **77**, 5487-5492.

Gotto, J. & Dusheiko, G. M. (2004). Hepatitis C and treatment with pegylated interferon and ribavirin. *Int J Biochem Cell Biol* **36**, 1874-1877.

Gottwein, J. M., Scheel, T. K., Jensen, T. B., Lademann, J. B., Prentoe, J. C., Knudsen, M. L., Hoegh, A. M. & Bukh, J. (2009). Development and characterization of hepatitis C virus genotype 1-7 cell culture systems: role of CD81 and scavenger receptor class B type I and effect of antiviral drugs. *Hepatology* **49**, 364-377.

Goueslain, L., Alsaleh, K., Horellou, P., Roingeard, P., Descamps, V., Duverlie, G., Ciczora, Y., Wychowski, C., Dubuisson, J. & Rouille, Y. (2010). Identification of Gbf1 as a Cellular Factor Required for Hepatitis C Virus RNA Replication. *J Virol* **84**, 773-87.

Grakoui, A., Hanson, H. L. & Rice, C. M. (2001). Bad time for Bonzo? Experimental models of hepatitis C virus infection, replication, and pathogenesis. *Hepatology* **33**, 489-495.

Grakoui, A., McCourt, D. W., Wychowski, C., Feinstone, S. M. & Rice, C. M. (1993a). Characterization of the hepatitis C virus-encoded serine proteinase: determination of proteinase-dependent polyprotein cleavage sites. *J Virol* **67**, 2832-2843.

Grakoui, A., McCourt, D. W., Wychowski, C., Feinstone, S. M. & Rice, C. M. (1993b). A second hepatitis C virus-encoded proteinase. *Proc Natl Acad Sci U S A* **90**, 10583-10587.

Gretton, S. N., Taylor, A. I. & McLauchlan, J. (2005). Mobility of the hepatitis C virus NS4B protein on the endoplasmic reticulum membrane and membrane-associated foci. *J Gen Virol* **86**, 1415-1421.

Griffin, S., Clarke, D., McCormick, C., Rowlands, D. & Harris, M. (2005). Signal peptide cleavage and internal targeting signals direct the hepatitis C virus p7 protein to distinct intracellular membranes. *J Virol* **79**, 15525-15536.

Griffin, S., StGelais, C., Owsianka, A. M., Patel, A. H., Rowlands, D. & Harris, M. (2008). Genotype-dependent sensitivity of hepatitis C virus to inhibitors of the p7 ion channel. *Hepatology* **48**, 1779-1790.

Griffin, S. D., Beales, L. P., Clarke, D. S., Worsfold, O., Evans, S. D., Jaeger, J., Harris, M. P. & Rowlands, D. J. (2003). The p7 protein of hepatitis C virus forms

an ion channel that is blocked by the antiviral drug, Amantadine. *FEBS lett* **535**, 34-38.

Grove, J., Huby, T., Stamataki, Z., Vanwolleghem, T., Meuleman, P., Farquhar, M., Schwarz, A., Moreau, M., Owen, J. S., Leroux-Roels, G., Balfe, P. & McKeating, J. A. (2007). Scavenger receptor BI and BII expression levels modulate hepatitis C virus infectivity. *J Virol* **81**, 3162-3169.

Grove, J., Nielsen, S., Zhong, J., Bassendine, M. F., Drummer, H. E., Balfe, P. & McKeating, J. A. (2008). Identification of a residue in hepatitis C virus E2 glycoprotein that determines scavenger receptor BI and CD81 receptor dependency and sensitivity to neutralizing antibodies. *J Virol* **82**, 12020-12029.

Gruner, N. H., Gerlach, T. J., Jung, M. C., Diepolder, H. M., Schirren, C. A., Schraut, W. W., Hoffmann, R., Zachoval, R., Santantonio, T., Cucchiarini, M., Cerny, A. & Pape, G. R. (2000). Association of hepatitis C virus-specific CD8+ T cells with viral clearance in acute hepatitis C. *J Infect Dis* **181**, 1528-1536.

Gururajan, R., Perry-O'Keefe, H., Melton, D. A. & Weeks, D. L. (1991). The Xenopus localized messenger RNA An3 may encode an ATP-dependent RNA helicase. *Nature* **349**, 717-719.

Haber, M. M., West, A. B., Haber, A. D. & Reuben, A. (1995). Relationship of aminotransferases to liver histological status in chronic hepatitis C. *Am J Gastroenterol* **90**, 1250-1257.

Hahm, B., Kim, Y. K., Kim, J. H., Kim, T. Y. & Jang, S. K. (1998). Heterogeneous nuclear ribonucleoprotein L interacts with the 3' border of the internal ribosomal entry site of hepatitis C virus. *J Virol* **72**, 8782-8788.

Hanoulle, X., Verdegem, D., Badillo, A., Wieruszeski, J. M., Penin, F. & Lippens, G. (2009). Domain 3 of non-structural protein 5A from hepatitis C virus is natively unfolded. *Biochem Biophys Res Commun* **381**, 634-638.

Haqshenas, G., Mackenzie, J. M., Dong, X. & Gowans, E. J. (2007). Hepatitis C virus p7 protein is localized in the endoplasmic reticulum when it is encoded by a replication-competent genome. *J Gen Virol* **88**, 134-142.

Harris, D., Zhang, Z., Chaubey, B. & Pandey, V. N. (2006). Identification of cellular factors associated with the 3'-nontranslated region of the hepatitis C virus genome. *Mol Cell Proteomics* **5**, 1006-1018.

Harris, H. J., Farquhar, M. J., Mee, C. J., Davis, C., Reynolds, G. M., Jennings, A., Hu, K., Yuan, F., Deng, H., Hubscher, S. G., Han, J. H., Balfe, P. & McKeating, J. A. (2008). CD81 and claudin 1 coreceptor association: role in hepatitis C virus entry. *J Virol* **82**, 5007-5020.

He, L. F., Alling, D., Popkin, T., Shapiro, M., Alter, H. J. & Purcell, R. H. (1987). Determining the size of non-A, non-B hepatitis virus by filtration. *J Infect Dis* **156**, 636-640.

Heckel, J. L., Sandgren, E. P., Degen, J. L., Palmiter, R. D. & Brinster, R. L. (1990). Neonatal bleeding in transgenic mice expressing urokinase-type plasminogen activator. *Cell* **62**, 447-456.

Helle, F., Goffard, A., Morel, V., Duverlie, G., McKeating, J., Keck, Z. Y., Foung, S., Penin, F., Dubuisson, J. & Voisset, C. (2007). The neutralizing activity of anti-hepatitis C virus antibodies is modulated by specific glycans on the E2 envelope protein. *J Virol* **81**, 8101-8111.

Henikoff, S. & Henikoff, J. G. (1992). Amino acid substitution matrices from protein blocks. *Proc Natl Acad Sci U S A* **89**, 10915-10919.

Henke, J. I., Goergen, D., Zheng, J., Song, Y., Schuttler, C. G., Fehr, C., Junemann, C. & Niepmann, M. (2008). microRNA-122 stimulates translation of hepatitis C virus RNA. *Embo J* **27**, 3300-3310.

Hezode, C., Roudot-Thoraval, F., Zafrani, E. S., Dhumeaux, D. & Pawlotsky, J. M. (2004). Different mechanisms of steatosis in hepatitis C virus genotypes 1 and 3 infections. *J Viral Hepat* **11**, 455-458.

Hijikata, M., Mizushima, H., Akagi, T., Mori, S., Kakiuchi, N., Kato, N., Tanaka, T., Kimura, K. & Shimotohno, K. (1993a). Two distinct proteinase activities required for the processing of a putative nonstructural precursor protein of hepatitis C virus. *J Virol* **67**, 4665-4675.

Hijikata, M., Shimizu, Y. K., Kato, H., Iwamoto, A., Shih, J. W., Alter, H. J., Purcell, R. H. & Yoshikura, H. (1993b). Equilibrium centrifugation studies of hepatitis C virus: evidence for circulating immune complexes. *J Virol* **67**, 1953-1958.

Hoffmann, R. M., Diepolder, H. M., Zachoval, R., Zwiebel, F. M., Jung, M. C., Scholz, S., Nitschko, H., Riethmuller, G. & Pape, G. R. (1995). Mapping of immunodominant CD4+ T lymphocyte epitopes of hepatitis C virus antigens and their relevance during the course of chronic infection. *Hepatology* **21**, 632-638.

Honda, M., Brown, E. A. & Lemon, S. M. (1996a). Stability of a stem-loop involving the initiator AUG controls the efficiency of internal initiation of translation on hepatitis C virus RNA. *RNA* **2**, 955-968.

Honda, M., Ping, L. H., Rijnbrand, R. C., Amphlett, E., Clarke, B., Rowlands, D. & Lemon, S. M. (1996b). Structural requirements for initiation of translation by internal ribosome entry within genome-length hepatitis C virus RNA. *Virology* **222**, 31-42.

Honda, M., Rijnbrand, R., Abell, G., Kim, D. & Lemon, S. M. (1999). Natural variation in translational activities of the 5' nontranslated RNAs of hepatitis C virus genotypes 1a and 1b: evidence for a long-range RNA-RNA interaction outside of the internal ribosomal entry site. *J Virol* **73**, 4941-4951.

Hoofnagle, J. H. (1997). Hepatitis C: the clinical spectrum of disease. *Hepatology* **26**, 15S-20S.

Hope, R. G. & McLauchlan, J. (2000). Sequence motifs required for lipid droplet association and protein stability are unique to the hepatitis C virus core protein. *J Gen Virol* **81**, 1913-1925.

Hope, R. G., Murphy, D. J. & McLauchlan, J. (2002). The domains required to direct core proteins of hepatitis C virus and GB virus-B to lipid droplets share common features with plant oleosin proteins. *J Biol Chem* **277**, 4261-4270.

Horner, S. M. & Gale, M., Jr. (2009). Intracellular innate immune cascades and interferon defenses that control hepatitis C virus. *J Interferon Cytokine Res* **29**, 489-498.

Hsieh, T. Y., Matsumoto, M., Chou, H. C., Schneider, R., Hwang, S. B., Lee, A. S. & Lai, M. M. (1998). Hepatitis C virus core protein interacts with heterogeneous nuclear ribonucleoprotein K. *J Biol Chem* **273**, 17651-17659.

Hsu, M., Zhang, J., Flint, M., Logvinoff, C., Cheng-Mayer, C., Rice, C. M. & McKeating, J. A. (2003). Hepatitis C virus glycoproteins mediate pH-dependent cell entry of pseudotyped retroviral particles. *Proc Natl Acad Sci U S A* **100**, 7271-7276.

Huang, H., Sun, F., Owen, D. M., Li, W., Chen, Y., Gale, M., Jr. & Ye, J. (2007a). Hepatitis C virus production by human hepatocytes dependent on assembly and secretion of very low-density lipoproteins. *Proc Natl Acad Sci U S A* **104**, 5848-5853.

Huang, J. S., Chao, C. C., Su, T. L., Yeh, S. H., Chen, D. S., Chen, C. T., Chen, P. J. & Jou, Y. S. (2004). Diverse cellular transformation capability of overexpressed genes in human hepatocellular carcinoma. *Biochem Biophys Res Commun* **315**, 950-958.

Huang, L., Hwang, J., Sharma, S. D., Hargittai, M. R., Chen, Y., Arnold, J. J., Raney, K. D. & Cameron, C. E. (2005). Hepatitis C virus nonstructural protein 5A (NS5A) is an RNA-binding protein. *J Biol Chem* **280**, 36417-36428.

Huang, Y., Staschke, K., De Francesco, R. & Tan, S. L. (2007b). Phosphorylation of hepatitis C virus NS5A nonstructural protein: a new paradigm for phosphorylation-dependent viral RNA replication? *Virology* **364**, 1-9.

Hughes, M., Griffin, S. & Harris, M. (2009). Domain III of NS5A contributes to both RNA replication and assembly of hepatitis C virus particles. *J Gen Virol* **90**, 1329-1334.

Hugle, T., Fehrmann, F., Bieck, E., Kohara, M., Krausslich, H. G., Rice, C. M., Blum, H. E. & Moradpour, D. (2001). The hepatitis C virus nonstructural protein 4B is an integral endoplasmic reticulum membrane protein. *Virology* **284**, 70-81.

Hussy, P., Langen, H., Mous, J. & Jacobsen, H. (1996). Hepatitis C virus core protein: carboxy-terminal boundaries of two processed species suggest cleavage by a signal peptide peptidase. *Virology* **224**, 93-104.

Igney, F. H. & Krammer, P. H. (2002). Death and anti-death: tumour resistance to apoptosis. *Nat Rev Cancer* **2**, 277-288.

Ikeda, M., Yi, M., Li, K. & Lemon, S. M. (2002). Selectable subgenomic and genome-length dicistronic RNAs derived from an infectious molecular clone of the HCV-N strain of hepatitis C virus replicate efficiently in cultured Huh7 cells. *J Virol* **76**, 2997-3006.

Isherwood, B. J. & Patel, A. H. (2005). Analysis of the processing and transmembrane topology of the E2p7 protein of hepatitis C virus. *J Gen Virol* **86**, 667-676.

Ishii, K., Rosa, D., Watanabe, Y., Katayama, T., Harada, H., Wyatt, C., Kiyosawa, K., Aizaki, H., Matsuura, Y., Houghton, M., Abrignani, S. & Miyamura, T. (1998). High titers of antibodies inhibiting the binding of envelope to human cells correlate with natural resolution of chronic hepatitis C. *Hepatology* **28**, 1117-1120.

Ito, T., Tahara, S. M. & Lai, M. M. (1998). The 3'-untranslated region of hepatitis C virus RNA enhances translation from an internal ribosomal entry site. *J Virol* **72**, 8789-8796.

Ivashkina, N., Wolk, B., Lohmann, V., Bartenschlager, R., Blum, H. E., Penin, F. & Moradpour, D. (2002). The hepatitis C virus RNA-dependent RNA polymerase membrane insertion sequence is a transmembrane segment. *J Virol* **76**, 13088-13093.

Jamieson, D. J. & Beggs, J. D. (1991). A suppressor of yeast spp81/ded1 mutations encodes a very similar putative ATP-dependent RNA helicase. *Mol Microbiol* **5**, 805-812.

Jeang, K. T. & Yedavalli, V. (2006). Role of RNA helicases in HIV-1 replication. *Nucleic Acids Res* **34**, 4198-4205.

Jin, D. Y., Wang, H. L., Zhou, Y., Chun, A. C., Kibler, K. V., Hou, Y. D., Kung, H. & Jeang, K. T. (2000). Hepatitis C virus core protein-induced loss of LZIP function correlates with cellular transformation. *Embo J* **19**, 729-740.

Jirasko, V., Montserret, R., Appel, N., Janvier, A., Eustachi, L., Brohm, C., Steinmann, E., Pietschmann, T., Penin, F. & Bartenschlager, R. (2008). Structural and functional characterization of nonstructural protein 2 for its role in hepatitis C virus assembly. *J Biol Chem* **283**, 28546-28562.

Johannsen, E., Luftig, M., Chase, M. R., Weicksel, S., Cahir-McFarland, E., Illanes, D., Sarracino, D. & Kieff, E. (2004). Proteins of purified Epstein-Barr virus. *Proc Natl Acad Sci U S A* **101**, 16286-16291.

Jones, C. T., Murray, C. L., Eastman, D. K., Tassello, J. & Rice, C. M. (2007). Hepatitis C virus p7 and NS2 proteins are essential for production of infectious virus. *J Virol* **81**, 8374-8383.

Jones, D. M., Patel, A. H., Targett-Adams, P. & McLauchlan, J. (2009). The hepatitis C virus NS4B protein can trans-complement viral RNA replication and modulates production of infectious virus. *J Virol* **83**, 2163-2177.

Jopling, C. L., Schutz, S. & Sarnow, P. (2008). Position-dependent function for a tandem microRNA miR-122-binding site located in the hepatitis C virus RNA genome. *Cell Host Microbe* **4**, 77-85.

Jopling, C. L., Yi, M., Lancaster, A. M., Lemon, S. M. & Sarnow, P. (2005). Modulation of hepatitis C virus RNA abundance by a liver-specific MicroRNA. *Science* **309**, 1577-1581.

Kaito, M., Watanabe, S., Tsukiyama-Kohara, K., Yamaguchi, K., Kobayashi, Y., Konishi, M., Yokoi, M., Ishida, S., Suzuki, S. & Kohara, M. (1994). Hepatitis C virus particle detected by immunoelectron microscopic study. *J Gen Virol* **75**, 1755-1760.

Kanai, Y., Dohmae, N. & Hirokawa, N. (2004). Kinesin transports RNA: isolation and characterization of an RNA-transporting granule. *Neuron* **43**, 513-525.

Kaneko, T., Moriyama, T., Udaka, K., Hiroishi, K., Kita, H., Okamoto, H., Yagita, H., Okumura, K. & Imawari, M. (1997). Impaired induction of cytotoxic T lymphocytes by antagonism of a weak agonist borne by a variant hepatitis C virus epitope. *Euro J Immunol* **27**, 1782-1787.

Kang, S. M., Shin, M. J., Kim, J. H. & Oh, J. W. (2005). Proteomic profiling of cellular proteins interacting with the hepatitis C virus core protein. *Proteomics* **5**, 2227-2237.

Kapadia, S. B., Barth, H., Baumert, T., McKeating, J. A. & Chisari, F. V. (2007). Initiation of hepatitis C virus infection is dependent on cholesterol and cooperativity between CD81 and scavenger receptor B type I. *J Virol* **81**, 374-383.

Kapadia, S. B. & Chisari, F. V. (2005). Hepatitis C virus RNA replication is regulated by host geranylgeranylation and fatty acids. *Proc Natl Acad Sci U S A* **102**, 2561-2566.

Kashiwakuma, T., Hasegawa, A., Kajita, T., Takata, A., Mori, H., Ohta, Y., Tanaka, E., Kiyosawa, K., Tanaka, T., Tanaka, S., Hattori, N. & Kohara, M. (1996). Detection of hepatitis C virus specific core protein in serum of patients by a sensitive fluorescence enzyme immunoassay (FEIA). *J Immunol Methods* **190**, 79-89.

Kato, N., Ootsuyama, Y., Ohkoshi, S., Nakazawa, T., Sekiya, H., Hijikata, M. & Shimotohno, K. (1992a). Characterization of hypervariable regions in the putative envelope protein of hepatitis C virus. *Biochem Biophys Res Commun* **189**, 119-127.

Kato, N., Ootsuyama, Y., Tanaka, T., Nakagawa, M., Nakazawa, T., Muraiso, K., Ohkoshi, S., Hijikata, M. & Shimotohno, K. (1992b). Marked sequence diversity in the putative envelope proteins of hepatitis C viruses. *Virus Res* **22**, 107-123.

Kato, N., Sekiya, H., Ootsuyama, Y., Nakazawa, T., Hijikata, M., Ohkoshi, S. & Shimotohno, K. (1993). Humoral immune response to hypervariable region 1 of the putative envelope glycoprotein (gp70) of hepatitis C virus. *J Virol* **67**, 3923-3930.

Kato, T., Date, T., Miyamoto, M., Furusaka, A., Tokushige, K., Mizokami, M. & Wakita, T. (2003). Efficient replication of the genotype 2a hepatitis C virus subgenomic replicon. *Gastroenterology* **125**, 1808-1817.

Katoh, M., Tateno, C., Yoshizato, K. & Yokoi, T. (2008). Chimeric mice with humanized liver. *Toxicology* **246**, 9-17.

Kaul, A., Woerz, I., Meuleman, P., Leroux-Roels, G. & Bartenschlager, R. (2007). Cell culture adaptation of hepatitis C virus and in vivo viability of an adapted variant. *J Virol* **81**, 13168-13179.

Kawamura, T., Furusaka, A., Koziel, M. J., Chung, R. T., Wang, T. C., Schmidt, E. V. & Liang, T. J. (1997). Transgenic expression of hepatitis C virus structural proteins in the mouse. *Hepatology* **25**, 1014-1021.

Kenny-Walsh, E. (1999). Clinical outcomes after hepatitis C infection from contaminated anti-D immune globulin. Irish Hepatology Research Group. *N Engl J Med* **340**, 1228-1233.

Kiiver, K., Merits, A., Ustav, M. & Zusinaite, E. (2006). Complex formation between hepatitis C virus NS2 and NS3 proteins. *Virus Res* **117**, 264-272.

Kim, D. W., Gwack, Y., Han, J. H. & Choe, J. (1995). C-terminal domain of the hepatitis C virus NS3 protein contains an RNA helicase activity. *Biochem Biophys Res Commun* **215**, 160-166.

Kim, J. L., Morgenstern, K. A., Griffith, J. P., Dwyer, M. D., Thomson, J. A., Murcko, M. A., Lin, C. & Caron, P. R. (1998). Hepatitis C virus NS3 RNA helicase domain with a bound oligonucleotide: the crystal structure provides insights into the mode of unwinding. *Structure* **6**, 89-100.

Kim, M., Ha, Y. & Park, H. J. (2006). Structural requirements for assembly and homotypic interactions of the hepatitis C virus core protein. *Virus Res* **122**, 137-143.

Kim, Y. K., Kim, C. S., Lee, S. H. & Jang, S. K. (2002). Domains I and II in the 5' nontranslated region of the HCV genome are required for RNA replication. *Biochem Biophys Res Commun* **290**, 105-112.

Kim, Y. S., Lee, S. G., Park, S. H. & Song, K. (2001). Gene structure of the human DDX3 and chromosome mapping of its related sequences. *Mol Cells* **12**, 209-214.

Kittlesen, D. J., Chianese-Bullock, K. A., Yao, Z. Q., Braciale, T. J. & Hahn, Y. S. (2000). Interaction between complement receptor gC1qR and hepatitis C virus core protein inhibits T-lymphocyte proliferation. *J Clin Invest* **106**, 1239-1249.

Klein, K. C., Polyak, S. J. & Lingappa, J. R. (2004). Unique features of hepatitis C virus capsid formation revealed by de novo cell-free assembly. *J Virol* **78**, 9257-9269.

Ko, L. J. & Prives, C. (1996). p53: puzzle and paradigm. *Genes Dev* **10**, 1054-1072.

Kolykhalov, A. A., Agapov, E. V., Blight, K. J., Mihalik, K., Feinstone, S. M. & Rice, C. M. (1997). Transmission of hepatitis C by intrahepatic inoculation with transcribed RNA. *Science* **277**, 570-574.

Kolykhalov, A. A., Feinstone, S. M. & Rice, C. M. (1996). Identification of a highly conserved sequence element at the 3' terminus of hepatitis C virus genome RNA. *J Virol* **70**, 3363-3371.

Koutsoudakis, G., Kaul, A., Steinmann, E., Kallis, S., Lohmann, V., Pietschmann, T. & Bartenschlager, R. (2006). Characterization of the early steps of hepatitis C virus infection by using luciferase reporter viruses. *J Virol* **80**, 5308-5320.

Koziel, M. J., Dudley, D., Afdhal, N., Choo, Q. L., Houghton, M., Ralston, R. & Walker, B. D. (1993). Hepatitis C virus (HCV)-specific cytotoxic T lymphocytes recognize epitopes in the core and envelope proteins of HCV. *J Virol* **67**, 7522-7532.

Koziel, M. J., Dudley, D., Afdhal, N., Grakoui, A., Rice, C. M., Choo, Q. L., Houghton, M. & Walker, B. D. (1995). HLA class I-restricted cytotoxic T lymphocytes specific for hepatitis C virus. Identification of multiple epitopes and characterization of patterns of cytokine release. *J Clin Invest* **96**, 2311-2321.

Kremsdorf, D. & Brezillon, N. (2007). New animal models for hepatitis C viral infection and pathogenesis studies. *World J Gastroenterol* **13**, 2427-2435.

Krieger, N., Lohmann, V. & Bartenschlager, R. (2001). Enhancement of hepatitis C virus RNA replication by cell culture-adaptive mutations. *J Virol* **75**, 4614-4624.

Krieger, S. E., Zeisel, M. B., Davis, C., Thumann, C., Harris, H. J., Schnober, E. K., Mee, C., Soulier, E., Royer, C., Lambotin, M., Grunert, F., Dao Thi, V. L., Dreux, M., Cosset, F. L., McKeating, J. A., Schuster, C. & Baumert, T. F. (2009). Inhibition of hepatitis C virus infection by anti-claudin-1 antibodies is mediated by neutralization of E2-CD81-Claudin-1 associations. *Hepatology* **51**, 1144-57.

Lahn, B. T. & Page, D. C. (1997). Functional coherence of the human Y chromosome. *Science* **278**, 675-680.

Lai, M. C., Lee, Y. H. & Tarn, W. Y. (2008). The DEAD-box RNA helicase DDX3 associates with export messenger ribonucleoproteins as well as tip-associated protein and participates in translational control. *Mol Biol Cell* **19**, 3847-3858.

Lan, L., Gorke, S., Rau, S. J., Zeisel, M. B., Hildt, E., Himmelsbach, K., Carvajal-Yepes, M., Huber, R., Wakita, T., Schmitt-Graeff, A., Royer, C., Blum, H. E., Fischer, R. & Baumert, T. F. (2008). Hepatitis C virus infection sensitizes human hepatocytes to TRAIL-induced apoptosis in a caspase 9-dependent manner. *J Immunol* **181**, 4926-4935.

Landmann, L. & Marbet, P. (2004). Colocalisation yields superior results after image restoration. *Micro Res Tech* **64**, 103-112.

Large, M. K., Kittlesen, D. J. & Hahn, Y. S. (1999). Suppression of host immune response by the core protein of hepatitis C virus: possible implications for hepatitis C virus persistence. *J Immunol* **162**, 931-938.

Lauer, G. M., Ouchi, K., Chung, R. T., Nguyen, T. N., Day, C. L., Purkis, D. R., Reiser, M., Kim, A. Y., Lucas, M., Klenerman, P. & Walker, B. D. (2002). Comprehensive analysis of CD8(+)-T-cell responses against hepatitis C virus reveals multiple unpredicted specificities. *J Virol* **76**, 6104-6113.

Lavanchy, D. (1999). Hepatitis C: public health strategies. *J Hepatol* **31 Suppl 1**, 146-151.

Lavie, M., Goffard, A. & Dubuisson, J. (2007). Assembly of a functional HCV glycoprotein heterodimer. *Curr Issues Mol Biol* **9**, 71-86.

Lavillette, D., Morice, Y., Germanidis, G., Donot, P., Soulier, A., Pagkalos, E., Sakellariou, G., Intrator, L., Bartosch, B., Pawlotsky, J. M. & Cosset, F. L. (2005). Human serum facilitates hepatitis C virus infection, and neutralizing responses inversely correlate with viral replication kinetics at the acute phase of hepatitis C virus infection. *J Virol* **79**, 6023-6034.

Law, M., Maruyama, T., Lewis, J., Giang, E., Tarr, A. W., Stamataki, Z., Gastaminza, P., Chisari, F. V., Jones, I. M., Fox, R. I., Ball, J. K., McKeating, J. A., Kneteman, N. M. & Burton, D. R. (2008). Broadly neutralizing antibodies protect against hepatitis C virus quasispecies challenge. *Nat Med* **14**, 25-27.

Lechner, F., Wong, D. K., Dunbar, P. R., Chapman, R., Chung, R. T., Dohrenwend, P., Robbins, G., Phillips, R., Klenerman, P. & Walker, B. D. (2000). Analysis of successful immune responses in persons infected with hepatitis C virus. *J Exp Med* **191**, 1499-1512.

Lee, C. S., Dias, A. P., Jedrychowski, M., Patel, A. H., Hsu, J. L. & Reed, R. (2008). Human DDX3 functions in translation and interacts with the translation initiation factor eIF3. *Nucleic Acids Res* **36**, 4708-4718.

Lefkowitch, J. H., Schiff, E. R., Davis, G. L., Perrillo, R. P., Lindsay, K., Bodenheimer, H. C., Jr., Balart, L. A., Ortego, T. J., Payne, J., Dienstag, J. L. & et al. (1993). Pathological diagnosis of chronic hepatitis C: a multicenter comparative study with chronic hepatitis B. The Hepatitis Interventional Therapy Group. *Gastroenterology* **104**, 595-603.

Lemon, S. M., Lerat, H., Weinman, S. A. & Honda, M. (2000). A transgenic mouse model of steatosis and hepatocellular carcinoma associated with chronic hepatitis C virus infection in humans. *Trans Am Clin Climatol Assoc* **111**, 146-156; discussion 156-147.

Lerat, H., Honda, M., Beard, M. R., Loesch, K., Sun, J., Yang, Y., Okuda, M., Gosert, R., Xiao, S. Y., Weinman, S. A. & Lemon, S. M. (2002). Steatosis and liver cancer in transgenic mice expressing the structural and nonstructural proteins of hepatitis C virus. *Gastroenterology* **122**, 352-365.

Lerat, H., Kammoun, H. L., Hainault, I., Merour, E., Higgs, M. R., Callens, C., Lemon, S. M., Foufelle, F. & Pawlotsky, J. M. (2009). Hepatitis C virus (HCV) proteins induce lipogenesis and defective triglyceride secretion in transgenic mice. *J Biol Chem* **284**, 33455-74.

Lerat, H., Rumin, S., Habersetzer, F., Berby, F., Trabaud, M. A., Trepo, C. & Inchauspe, G. (1998). In vivo tropism of hepatitis C virus genomic sequences in

hematopoietic cells: influence of viral load, viral genotype, and cell phenotype. *Blood* **91**, 3841-3849.

Leroy, P., Alzari, P., Sassoon, D., Wolgemuth, D. & Fellous, M. (1989). The protein encoded by a murine male germ cell-specific transcript is a putative ATP-dependent RNA helicase. *Cell* **57**, 549-559.

Lesburg, C. A., Cable, M. B., Ferrari, E., Hong, Z., Mannarino, A. F. & Weber, P. C. (1999). Crystal structure of the RNA-dependent RNA polymerase from hepatitis C virus reveals a fully encircled active site. *Nat Struct Biol* **6**, 937-943.

Levy, S., Todd, S. C. & Maecker, H. T. (1998). CD81 (TAPA-1): a molecule involved in signal transduction and cell adhesion in the immune system. *Ann Rev Immunol* **16**, 89-109.

Li, X. D., Sun, L., Seth, R. B., Pineda, G. & Chen, Z. J. (2005). Hepatitis C virus protease NS3/4A cleaves mitochondrial antiviral signaling protein off the mitochondria to evade innate immunity. *Proc Natl Acad Sci U S A* **102**, 17717-17722.

Liang, Y., Kang, C. B. & Yoon, H. S. (2006). Molecular and structural characterization of the domain 2 of hepatitis C virus non-structural protein 5A. *Mol Cells* **22**, 13-20.

Lin, C., Kwong, A. D. & Perni, R. B. (2006a). Discovery and development of VX-950, a novel, covalent, and reversible inhibitor of hepatitis C virus NS3.4A serine protease. *Infec Disord Drug Targets* **6**, 3-16.

Lin, C., Lindenbach, B. D., Pragai, B. M., McCourt, D. W. & Rice, C. M. (1994a). Processing in the hepatitis C virus E2-NS2 region: identification of p7 and two distinct E2-specific products with different C termini. *J Virol* **68**, 5063-5073.

Lin, C., Pragai, B. M., Grakoui, A., Xu, J. & Rice, C. M. (1994b). Hepatitis C virus NS3 serine proteinase: trans-cleavage requirements and processing kinetics. *J Virol* **68**, 8147-8157.

Lin, K., Perni, R. B., Kwong, A. D. & Lin, C. (2006b). VX-950, a novel hepatitis C virus (HCV) NS3-4A protease inhibitor, exhibits potent antiviral activities in HCv replicon cells. *Antimicrob Agents Chemother* **50**, 1813-1822.

Lin, W., Kim, S. S., Yeung, E., Kamegaya, Y., Blackard, J. T., Kim, K. A., Holtzman, M. J. & Chung, R. T. (2006c). Hepatitis C virus core protein blocks interferon signaling by interaction with the STAT1 SH2 domain. *J Virol* **80**, 9226-9235.

Lindenbach, B. D., Evans, M. J., Syder, A. J., Wolk, B., Tellinghuisen, T. L., Liu, C. C., Maruyama, T., Hynes, R. O., Burton, D. R., McKeating, J. A. & Rice, C. M. (2005). Complete replication of hepatitis C virus in cell culture. *Science* **309**, 623-626.

Lindenbach, B. D., Meuleman, P., Ploss, A., Vanwolleghem, T., Syder, A. J., McKeating, J. A., Lanford, R. E., Feinstone, S. M., Major, M. E., Leroux-Roels, G. & Rice, C. M. (2006). Cell culture-grown hepatitis C virus is infectious in vivo and can be recultured in vitro. *Proc Natl Acad Sci U S A* **103**, 3805-3809.

Lindenbach, B. D., Pragai, B. M., Montserret, R., Beran, R. K., Pyle, A. M., Penin, F. & Rice, C. M. (2007). The C terminus of hepatitis C virus NS4A encodes an electrostatic switch that regulates NS5A hyperphosphorylation and viral replication. *J Virol* **81**, 8905-8918.

Linder, P., Lasko, P. F., Ashburner, M., Leroy, P., Nielsen, P. J., Nishi, K., Schnier, J. & Slonimski, P. P. (1989). Birth of the D-E-A-D box. *Nature* **337**, 121-122.

Lindstrom, H., Lundin, M., Haggstrom, S. & Persson, M. A. (2006). Mutations of the Hepatitis C virus protein NS4B on either side of the ER membrane affect the efficiency of subgenomic replicons. *Virus Res* **121**, 169-178.

Linnen, J., Wages, J., Jr., Zhang-Keck, Z. Y., Fry, K. E., Krawczynski, K. Z., Alter, H., Koonin, E., Gallagher, M., Alter, M., Hadziyannis, S., Karayiannis, P., Fung, K., Nakatsuji, Y., Shih, J. W., Young, L., Piatak, M., Jr., Hoover, C., Fernandez, J., Chen, S., Zou, J. C., Morris, T., Hyams, K. C., Ismay, S., Lifson, J. D., Hess, G., Foung, S. K., Thomas, H., Bradley, D., Margolis, H. &

Kim, J. P. (1996). Molecular cloning and disease association of hepatitis G virus: a transfusion-transmissible agent. *Science* **271**, 505-508.

Liu, Q., Tackney, C., Bhat, R. A., Prince, A. M. & Zhang, P. (1997). Regulated processing of hepatitis C virus core protein is linked to subcellular localization. *J Virol* **71**, 657-662.

Liu, S., Yang, W., Shen, L., Turner, J. R., Coyne, C. B. & Wang, T. (2009). Tight junction proteins claudin-1 and occludin control hepatitis C virus entry and are downregulated during infection to prevent superinfection. *J Virol* **83**, 2011-2014.

Lo, S. Y., Masiarz, F., Hwang, S. B., Lai, M. M. & Ou, J. H. (1995). Differential subcellular localization of hepatitis C virus core gene products. *Virology* **213**, 455-461.

Lo, S. Y., Selby, M. J. & Ou, J. H. (1996). Interaction between hepatitis C virus core protein and E1 envelope protein. *J Virol* **70**, 5177-5182.

Logvinoff, C., Major, M. E., Oldach, D., Heyward, S., Talal, A., Balfe, P., Feinstone, S. M., Alter, H., Rice, C. M. & McKeating, J. A. (2004). Neutralizing antibody response during acute and chronic hepatitis C virus infection. *Proc Natl Acad Sci U S A* **101**, 10149-10154.

Lohmann, V., Hoffmann, S., Herian, U., Penin, F. & Bartenschlager, R. (2003). Viral and cellular determinants of hepatitis C virus RNA replication in cell culture. *J Virol* **77**, 3007-3019.

Lohmann, V., Korner, F., Dobierzewska, A. & Bartenschlager, R. (2001). Mutations in hepatitis C virus RNAs conferring cell culture adaptation. *J Virol* **75**, 1437-1449.

Lohmann, V., Korner, F., Herian, U. & Bartenschlager, R. (1997). Biochemical properties of hepatitis C virus NS5B RNA-dependent RNA polymerase and identification of amino acid sequence motifs essential for enzymatic activity. *J Virol* **71**, 8416-8428.

Lohmann, V., Korner, F., Koch, J., Herian, U., Theilmann, L. & Bartenschlager, R. (1999). Replication of subgenomic hepatitis C virus RNAs in a hepatoma cell line. *Science* **285**, 110-113.

Loo, Y. M., Owen, D. M., Li, K., Erickson, A. K., Johnson, C. L., Fish, P. M., Carney, D. S., Wang, T., Ishida, H., Yoneyama, M., Fujita, T., Saito, T., Lee, W. M., Hagedorn, C. H., Lau, D. T., Weinman, S. A., Lemon, S. M. & Gale, M., Jr. (2006). Viral and therapeutic control of IFN-beta promoter stimulator 1 during hepatitis C virus infection. *Proc Natl Acad Sci U S A* **103**, 6001-6006.

Lorenz, I. C., Marcotrigiano, J., Dentzer, T. G. & Rice, C. M. (2006). Structure of the catalytic domain of the hepatitis C virus NS2-3 protease. *Nature* **442**, 831-835.

Loret, S., Guay, G. & Lippe, R. (2008). Comprehensive characterization of extracellular herpes simplex virus type 1 virions. *J Virol* **82**, 8605-8618.

Lozach, P. Y., Amara, A., Bartosch, B., Virelizier, J. L., Arenzana-Seisdedos, F., Cosset, F. L. & Altmeyer, R. (2004). C-type lectins L-SIGN and DC-SIGN capture and transmit infectious hepatitis C virus pseudotype particles. *J Biol Chem* **279**, 32035-32045.

Lozach, P. Y., Lortat-Jacob, H., de Lacroix de Lavalette, A., Staropoli, I., Foung, S., Amara, A., Houles, C., Fieschi, F., Schwartz, O., Virelizier, J. L., Arenzana-Seisdedos, F. & Altmeyer, R. (2003). DC-SIGN and L-SIGN are high affinity binding receptors for hepatitis C virus glycoprotein E2. *J Biol Chem* **278**, 20358-20366.

Lu, W., Lo, S. Y., Chen, M., Wu, K., Fung, Y. K. & Ou, J. H. (1999). Activation of p53 tumor suppressor by hepatitis C virus core protein. *Virology* **264**, 134-141.

Luik, P., Chew, C., Aittoniemi, J., Chang, J., Wentworth, P., Jr., Dwek, R. A., Biggin, P. C., Venien-Bryan, C. & Zitzmann, N. (2009). The 3-dimensional structure of a hepatitis C virus p7 ion channel by electron microscopy. *Proc Natl Acad Sci U S A* **106**, 12712-12716.

Lundin, M., Monne, M., Widell, A., Von Heijne, G. & Persson, M. A. (2003). Topology of the membrane-associated hepatitis C virus protein NS4B. *J Virol* **77**, 5428-5438.

Luo, G., Hamatake, R. K., Mathis, D. M., Racela, J., Rigat, K. L., Lemm, J. & Colonno, R. J. (2000). De novo initiation of RNA synthesis by the RNA-dependent RNA polymerase (NS5B) of hepatitis C virus. *J Virol* **74**, 851-863.

Ma, Y., Yates, J., Liang, Y., Lemon, S. M. & Yi, M. (2008). NS3 helicase domains involved in infectious intracellular hepatitis C virus particle assembly. *J Virol* **82**, 7624-7639.

Macdonald, A., Crowder, K., Street, A., McCormick, C., Saksela, K. & Harris, M. (2003). The hepatitis C virus non-structural NS5A protein inhibits activating protein-1 function by perturbing ras-ERK pathway signaling. *J Biol Chem* **278**, 17775-17784.

Maillard, P., Huby, T., Andreo, U., Moreau, M., Chapman, J. & Budkowska, A. (2006). The interaction of natural hepatitis C virus with human scavenger receptor SR-BI/Cla1 is mediated by ApoB-containing lipoproteins. *Faseb J* **20**, 735-737.

Mamiya, N. & Worman, H. J. (1999). Hepatitis C virus core protein binds to a DEAD box RNA helicase. *J Biol Chem* **274**, 15751-15756.

Martinez-Sierra, C., Arizcorreta, A., Diaz, F., Roldan, R., Martin-Herrera, L., Perez-Guzman, E. & Giron-Gonzalez, J. A. (2003). Progression of chronic hepatitis C to liver fibrosis and cirrhosis in patients coinfected with hepatitis C virus and human immunodeficiency virus. *Clin Infect Dis* **36**, 491-498.

Marusawa, H., Hijikata, M., Chiba, T. & Shimotohno, K. (1999). Hepatitis C virus core protein inhibits Fas- and tumor necrosis factor alpha-mediated apoptosis via NF-kappaB activation. *J Virol* **73**, 4713-4720.

Masaki, T., Suzuki, R., Murakami, K., Aizaki, H., Ishii, K., Murayama, A., Date, T., Matsuura, Y., Miyamura, T., Wakita, T. & Suzuki, T. (2008). Interaction of hepatitis C virus nonstructural protein 5A with core protein is critical for the production of infectious virus particles. *J Virol* **82**, 7964-7976.

Mateu, G., Donis, R. O., Wakita, T., Bukh, J. & Grakoui, A. (2008). Intragenotypic JFH1 based recombinant hepatitis C virus produces high levels of infectious particles but causes increased cell death. *Virology* **376**, 397-407.

Matsuda, J., Suzuki, M., Nozaki, C., Shinya, N., Tashiro, K., Mizuno, K., Uchinuno, Y. & Yamamura, K. (1998). Transgenic mouse expressing a full-length hepatitis C virus cDNA. *Jpn J Cancer Res* **89**, 150-158.

Matsumoto, M., Hsieh, T. Y., Zhu, N., VanArsdale, T., Hwang, S. B., Jeng, K. S., Gorbalenya, A. E., Lo, S. Y., Ou, J. H., Ware, C. F. & Lai, M. M. (1997). Hepatitis C virus core protein interacts with the cytoplasmic tail of lymphotoxin-beta receptor. *J Virol* **71**, 1301-1309.

Matsumoto, M., Hwang, S. B., Jeng, K. S., Zhu, N. & Lai, M. M. (1996). Homotypic interaction and multimerization of hepatitis C virus core protein. *Virology* **218**, 43-51.

McCaughan, G. W., McGuinness, P. H., Bishop, G. A., Painter, D. M., Lien, A. S., Tulloch, R., Wylie, B. R. & Archer, G. T. (1992). Clinical assessment and incidence of hepatitis C RNA in 50 consecutive RIBA-positive volunteer blood donors. *The Med J Aust* **157**, 231-233.

McGuinness, P. H., Bishop, G. A., Painter, D. M., Chan, R. & McCaughan, G. W. (1996). Intrahepatic hepatitis C RNA levels do not correlate with degree of liver injury in patients with chronic hepatitis C. *Hepatology* **23**, 676-687.

McLauchlan, J. (2009). Lipid droplets and hepatitis C virus infection. *Biochim Biophys Acta* **1791**, 552-559.

McLauchlan, J., Lemberg, M. K., Hope, G. & Martoglio, B. (2002). Intramembrane proteolysis promotes trafficking of hepatitis C virus core protein to lipid droplets. *Embo J* **21**, 3980-3988.

McMullan, L. K., Grakoui, A., Evans, M. J., Mihalik, K., Puig, M., Branch, A. D., Feinstone, S. M. & Rice, C. M. (2007). Evidence for a functional RNA element in the hepatitis C virus core gene. *Proc Natl Acad Sci U S A* **104**, 2879-2884.

Meertens, L., Bertaux, C., Cukierman, L., Cormier, E., Lavillette, D., Cosset, F. L. & Dragic, T. (2008). The tight junction proteins claudin-1, -6, and -9 are entry cofactors for hepatitis C virus. *J Virol* **82**, 3555-3560.

Meertens, L., Bertaux, C. & Dragic, T. (2006). Hepatitis C virus entry requires a critical postinternalization step and delivery to early endosomes via clathrin-coated vesicles. *J Virol* **80**, 11571-11578.

Melen, K., Fagerlund, R., Nyqvist, M., Keskinen, P. & Julkunen, I. (2004). Expression of hepatitis C virus core protein inhibits interferon-induced nuclear import of STATs. *J Med Virol* **73**, 536-547.

Mercer, D. F., Schiller, D. E., Elliott, J. F., Douglas, D. N., Hao, C., Rinfret, A., Addison, W. R., Fischer, K. P., Churchill, T. A., Lakey, J. R., Tyrrell, D. L. & Kneteman, N. M. (2001). Hepatitis C virus replication in mice with chimeric human livers. *Nat Med* **7**, 927-933.

Merz, C., Urlaub, H., Will, C. L. & Luhrmann, R. (2007). Protein composition of human mRNPs spliced in vitro and differential requirements for mRNP protein recruitment. *RNA* **13**, 116-128.

Meuleman, P., Hesselgesser, J., Paulson, M., Vanwolleghem, T., Desombere, I., Reiser, H. & Leroux-Roels, G. (2008). Anti-CD81 antibodies can prevent a hepatitis C virus infection in vivo. *Hepatology* **48**, 1761-1768.

Meuleman, P. & Leroux-Roels, G. (2008). The human liver-uPA-SCID mouse: a model for the evaluation of antiviral compounds against HBV and HCV. *Antiviral Res* **80**, 231-238.

Meunier, J. C., Engle, R. E., Faulk, K., Zhao, M., Bartosch, B., Alter, H., Emerson, S. U., Cosset, F. L., Purcell, R. H. & Bukh, J. (2005). Evidence for cross-genotype neutralization of hepatitis C virus pseudo-particles and enhancement of infectivity by apolipoprotein C1. *Proc Natl Acad Sci U S A* **102**, 4560-4565.

Meylan, E., Curran, J., Hofmann, K., Moradpour, D., Binder, M., Bartenschlager, R. & Tschopp, J. (2005). Cardif is an adaptor protein in the RIG-I antiviral pathway and is targeted by hepatitis C virus. *Nature* **437**, 1167-1172.

Michalak, J. P., Wychowski, C., Choukhi, A., Meunier, J. C., Ung, S., Rice, C. M. & Dubuisson, J. (1997). Characterization of truncated forms of hepatitis C virus glycoproteins. *J Gen Virol* **78**, 2299-2306.

Mink, M. A., Benichou, S., Madaule, P., Tiollais, P., Prince, A. M. & Inchauspe, G. (1994). Characterization and mapping of a B-cell immunogenic domain in hepatitis C virus E2 glycoprotein using a yeast peptide library. *Virology* **200**, 246-255.

Missale, G., Bertoni, R., Lamonaca, V., Valli, A., Massari, M., Mori, C., Rumi, M. G., Houghton, M., Fiaccadori, F. & Ferrari, C. (1996). Different clinical behaviors of acute hepatitis C virus infection are associated with different vigor of the anti-viral cell-mediated immune response. *J Clin Invest* **98**, 706-714.

Miyamoto, H., Okamoto, H., Sato, K., Tanaka, T. & Mishiro, S. (1992). Extraordinarily low density of hepatitis C virus estimated by sucrose density gradient centrifugation and the polymerase chain reaction. *J Gen Virol* **73**, 715-718.

Miyamura, T. & Matsuura, Y. (1993). Structural proteins of hepatitis C virus. *Trends Microbiol* **1**, 229-231.

Miyanari, Y., Atsuzawa, K., Usuda, N., Watashi, K., Hishiki, T., Zayas, M., Bartenschlager, R., Wakita, T., Hijikata, M. & Shimotohno, K. (2007). The lipid droplet is an important organelle for hepatitis C virus production. *Nat Cell Biol* **9**, 1089-1097.

Mohd-Ismail, N. K., Deng, L., Sukumaran, S. K., Yu, V. C., Hotta, H. & Tan, Y. J. (2009). The hepatitis C virus core protein contains a BH3 domain that regulates apoptosis through specific interaction with human Mcl-1. *J Virol* **83**, 9993-10006.

Mohsen, A. H., Easterbrook, P. J., Taylor, C., Portmann, B., Kulasegaram, R., Murad, S., Wiselka, M. & Norris, S. (2003). Impact of human immunodeficiency virus (HIV) infection on the progression of liver fibrosis in hepatitis C virus infected patients. *Gut* **52**, 1035-1040.

Molina, S., Castet, V., Fournier-Wirth, C., Pichard-Garcia, L., Avner, R., Harats, D., Roitelman, J., Barbaras, R., Graber, P., Ghersa, P., Smolarsky, M., Funaro, A., Malavasi, F., Larrey, D., Coste, J., Fabre, J. M., Sa-Cunha, A. & Maurel, P. (2007). The low-density lipoprotein receptor plays a role in the infection of primary human hepatocytes by hepatitis C virus. *J Hepatol* **46**, 411-419.

Mondelli, M. U., Cerino, A., Boender, P., Oudshoorn, P., Middeldorp, J., Fipaldini, C., La Monica, N. & Habets, W. (1994). Significance of the immune response to a major, conformational B-cell epitope on the hepatitis C virus NS3 region defined by a human monoclonal antibody. *J Virol* **68**, 4829-4836.

Moradpour, D., Brass, V., Bieck, E., Friebe, P., Gosert, R., Blum, H. E., Bartenschlager, R., Penin, F. & Lohmann, V. (2004). Membrane association of the RNA-dependent RNA polymerase is essential for hepatitis C virus RNA replication. *J Virol* **78**, 13278-13284.

Moradpour, D., Englert, C., Wakita, T. & Wands, J. R. (1996). Characterization of cell lines allowing tightly regulated expression of hepatitis C virus core protein. *Virology* **222**, 51-63.

Moriishi, K., Okabayashi, T., Nakai, K., Moriya, K., Koike, K., Murata, S., Chiba, T., Tanaka, K., Suzuki, R., Suzuki, T., Miyamura, T. & Matsuura, Y. (2003). Proteasome activator PA28gamma-dependent nuclear retention and degradation of hepatitis C virus core protein. *J Virol* **77**, 10237-10249.

Moriya, K., Todoroki, T., Tsutsumi, T., Fujie, H., Shintani, Y., Miyoshi, H., Ishibashi, K., Takayama, T., Makuuchi, M., Watanabe, K., Miyamura, T., Kimura, S. & Koike, K. (2001). Increase in the concentration of carbon 18 monounsaturated fatty acids in the liver with hepatitis C: analysis in transgenic mice and humans. *Biochem Biophys Res Commun* **281**, 1207-1212.

Moriya, K., Yotsuyanagi, H., Shintani, Y., Fujie, H., Ishibashi, K., Matsuura, Y., Miyamura, T. & Koike, K. (1997). Hepatitis C virus core protein induces hepatic steatosis in transgenic mice. *J Gen Virol* **78**, 1527-1531.

Mottola, G., Cardinali, G., Ceccacci, A., Trozzi, C., Bartholomew, L., Torrisi, M. R., Pedrazzini, E., Bonatti, S. & Migliaccio, G. (2002). Hepatitis C virus nonstructural proteins are localized in a modified endoplasmic reticulum of cells expressing viral subgenomic replicons. *Virology* **293**, 31-43.

Murray, C. L., Jones, C. T., Tassello, J. & Rice, C. M. (2007). Alanine scanning of the hepatitis C virus core protein reveals numerous residues essential for production of infectious virus. *J Virol* **81**, 10220-10231.

Nahmias, Y., Goldwasser, J., Casali, M., van Poll, D., Wakita, T., Chung, R. T. & Yarmush, M. L. (2008). Apolipoprotein B-dependent hepatitis C virus secretion is inhibited by the grapefruit flavonoid naringenin. *Hepatology* **47**, 1437-1445.

Nasoff, M. S., Zebedee, S. L., Inchauspe, G. & Prince, A. M. (1991). Identification of an immunodominant epitope within the capsid protein of hepatitis C virus. *Proc Natl Acad Sci U S A* **88**, 5462-5466.

Negro, F., Pacchioni, D., Shimizu, Y., Miller, R. H., Bussolati, G., Purcell, R. H. & Bonino, F. (1992). Detection of intrahepatic replication of hepatitis C virus RNA by in situ hybridization and comparison with histopathology. *Proc Natl Acad Sci U S A* **89**, 2247-2251.

Nelson, D. R., Marousis, C. G., Davis, G. L., Rice, C. M., Wong, J., Houghton, M. & Lau, J. Y. (1997). The role of hepatitis C virus-specific cytotoxic T lymphocytes in chronic hepatitis C. *J Immunol* **158**, 1473-1481.

Neumann-Haefelin, C., Blum, H. E., Chisari, F. V. & Thimme, R. (2005). T cell response in hepatitis C virus infection. *J Clin Virol* **32**, 75-85.

Neumann, A. U., Lam, N. P., Dahari, H., Gretch, D. R., Wiley, T. E., Layden, T. J. & Perelson, A. S. (1998). Hepatitis C viral dynamics in vivo and the antiviral efficacy of interferon-alpha therapy. *Science* **282**, 103-107.

Nielsen, S. U., Bassendine, M. F., Burt, A. D., Bevitt, D. J. & Toms, G. L. (2004). Characterization of the genome and structural proteins of hepatitis C virus resolved from infected human liver. *J Gen Virol* **85**, 1497-1507.

Nielsen, S. U., Bassendine, M. F., Burt, A. D., Martin, C., Pumeechockchai, W. & Toms, G. L. (2006). Association between hepatitis C virus and very-low-density lipoprotein (VLDL)/LDL analyzed in iodixanol density gradients. *J Virol* **80**, 2418-2428.

NIH Consensus. (2002). National Institutes of Health Consensus Development Conference Statement: Management of hepatitis C 2002 (June 10-12, 2002). *Gastroenterology* **123**, 2082-2099.

Nolandt, O., Kern, V., Muller, H., Pfaff, E., Theilmann, L., Welker, R. & Krausslich, H. G. (1997). Analysis of hepatitis C virus core protein interaction domains. *J Gen Virol* **78**, 1331-1340.

Novak, J. E. & Kirkegaard, K. (1994). Coupling between genome translation and replication in an RNA virus. *Genes Dev* **8**, 1726-1737.

Ogino, T., Fukuda, H., Imajoh-Ohmi, S., Kohara, M. & Nomoto, A. (2004). Membrane binding properties and terminal residues of the mature hepatitis C virus capsid protein in insect cells. *J Virol* **78**, 11766-11777.

Oh, J. W., Ito, T. & Lai, M. M. (1999). A recombinant hepatitis C virus RNA-dependent RNA polymerase capable of copying the full-length viral RNA. *J Virol* **73**, 7694-7702.

Oka, K., Nagano-Fujii, M., Yoshida, I., Hidajat, R., Deng, L., Akutsu, M. & Hotta, H. (2003). Hepatitis C virus core protein selectively inhibits synthesis and accumulation of p21/Waf1 and certain nuclear proteins. *Microbiol Immunol* **47**, 429-438.

Okamoto, K., Mori, Y., Komoda, Y., Okamoto, T., Okochi, M., Takeda, M., Suzuki, T., Moriishi, K. & Matsuura, Y. (2008). Intramembrane processing by signal peptide peptidase regulates the membrane localization of hepatitis C virus core protein and viral propagation. *J Virol* **82**, 8349-8361.

Onji, M., Kikuchi, T., Kumon, I., Masumoto, T., Nadano, S., Kajino, K., Horiike, N. & Ohta, Y. (1992). Intrahepatic lymphocyte subpopulations and HLA class I antigen expression by hepatocytes in chronic hepatitis C. *Hepato-gastroenterology* **39**, 340-343.

Op De Beeck, A., Cocquerel, L. & Dubuisson, J. (2001). Biogenesis of hepatitis C virus envelope glycoproteins. *J Gen Virol* **82**, 2589-2595.

Op De Beeck, A., Voisset, C., Bartosch, B., Ciczora, Y., Cocquerel, L., Keck, Z., Foung, S., Cosset, F. L. & Dubuisson, J. (2004). Characterization of functional hepatitis C virus envelope glycoproteins. *J Virol* **78**, 2994-3002.

Oshiumi, H., Sakai, K., Matsumoto, M. & Seya, T. (2010). DEAD/H BOX 3 (DDX3) helicase binds the RIG-I adaptor IPS-1 to up-regulate IFN-beta inducing potential. *Euro J Immunol* **40**, 940-8.

Owsianka, A., Clayton, R. F., Loomis-Price, L. D., McKeating, J. A. & Patel, A. H. (2001). Functional analysis of hepatitis C virus E2 glycoproteins and virus-like particles reveals structural dissimilarities between different forms of E2. *J Gen Virol* **82**, 1877-1883.

Owsianka, A., Tarr, A. W., Juttla, V. S., Lavillette, D., Bartosch, B., Cosset, F. L., Ball, J. K. & Patel, A. H. (2005). Monoclonal antibody AP33 defines a broadly neutralizing epitope on the hepatitis C virus E2 envelope glycoprotein. *J Virol* **79**, 11095-11104.

Owsianka, A. M. & Patel, A. H. (1999). Hepatitis C virus core protein interacts with a human DEAD box protein DDX3. *Virology* **257**, 330-340.

Pallaoro, M., Lahm, A., Biasiol, G., Brunetti, M., Nardella, C., Orsatti, L., Bonelli, F., Orru, S., Narjes, F. & Steinkuhler, C. (2001). Characterization of the hepatitis C virus NS2/3 processing reaction by using a purified precursor protein. *J Virol* **75**, 9939-9946.

Pang, P. S., Jankowsky, E., Planet, P. J. & Pyle, A. M. (2002). The hepatitis C viral NS3 protein is a processive DNA helicase with cofactor enhanced RNA unwinding. *Embo J* **21**, 1168-1176.

Parent, R., Qu, X., Petit, M. A. & Beretta, L. (2009). The heat shock cognate protein 70 is associated with hepatitis C virus particles and modulates virus infectivity. *Hepatology* **49**, 1798-1809.

Park, S. H., Lee, S. G., Kim, Y. & Song, K. (1998). Assignment of a human putative RNA helicase gene, DDX3, to human X chromosome bands p11.3-->p11.23. *Cytogenet Cell Genet* **81**, 178-179.

Pasquinelli, C., Shoenberger, J. M., Chung, J., Chang, K. M., Guidotti, L. G., Selby, M., Berger, K., Lesniewski, R., Houghton, M. & Chisari, F. V. (1997). Hepatitis C virus core and E2 protein expression in transgenic mice. *Hepatology* **25**, 719-727.

Pause, A., Methot, N. & Sonenberg, N. (1993). The HRIGRXXR region of the DEAD box RNA helicase eukaryotic translation initiation factor 4A is required for RNA binding and ATP hydrolysis. *Mol Cell Biol* **13**, 6789-6798.

Pause, A. & Sonenberg, N. (1992). Mutational analysis of a DEAD box RNA helicase: the mammalian translation initiation factor eIF-4A. *Embo J* **11**, 2643-2654.

Pavio, N. & Lai, M. M. (2003). The hepatitis C virus persistence: how to evade the immune system? *J Biosci* **28**, 287-304.

Pavlovic, D., Neville, D. C., Argaud, O., Blumberg, B., Dwek, R. A., Fischer, W. B. & Zitzmann, N. (2003). The hepatitis C virus p7 protein forms an ion channel that is inhibited by long-alkyl-chain iminosugar derivatives. *Proc Natl Acad Sci U S A* **100**, 6104-6108.

Perlemuter, G., Sabile, A., Letteron, P., Vona, G., Topilco, A., Chretien, Y., Koike, K., Pessayre, D., Chapman, J., Barba, G. & Brechot, C. (2002). Hepatitis C virus core protein inhibits microsomal triglyceride transfer protein activity and very low density lipoprotein secretion: a model of viral-related steatosis. *Faseb J* **16**, 185-194.

Pestka, J. M., Zeisel, M. B., Blaser, E., Schurmann, P., Bartosch, B., Cosset, F. L., Patel, A. H., Meisel, H., Baumert, J., Viazov, S., Rispeter, K., Blum, H. E., Roggendorf, M. & Baumert, T. F. (2007). Rapid induction of virus-neutralizing antibodies and viral clearance in a single-source outbreak of hepatitis C. *Proc Natl Acad Sci U S A* **104**, 6025-6030.

Pestova, T. V., Shatsky, I. N., Fletcher, S. P., Jackson, R. J. & Hellen, C. U. (1998). A prokaryotic-like mode of cytoplasmic eukaryotic ribosome binding to the initiation codon during internal translation initiation of hepatitis C and classical swine fever virus RNAs. *Genes Dev* **12**, 67-83.

Pflugheber, J., Fredericksen, B., Sumpter, R., Jr., Wang, C., Ware, F., Sodora, D. L. & Gale, M., Jr. (2002). Regulation of PKR and IRF-1 during hepatitis C virus RNA replication. *Proc Natl Acad Sci U S A* **99**, 4650-4655.

Phan, T., Beran, R. K., Peters, C., Lorenz, I. C. & Lindenbach, B. D. (2009). Hepatitis C virus NS2 protein contributes to virus particle assembly via opposing epistatic interactions with the E1-E2 glycoprotein and NS3-NS4A enzyme complexes. *J Virol* **83**, 8379-8395.

Pietschmann, T., Kaul, A., Koutsoudakis, G., Shavinskaya, A., Kallis, S., Steinmann, E., Abid, K., Negro, F., Dreux, M., Cosset, F. L. & Bartenschlager, R. (2006). Construction and characterization of infectious intragenotypic and intergenotypic hepatitis C virus chimeras. *Proc Natl Acad Sci U S A* **103**, 7408-7413.

Pietschmann, T., Lohmann, V., Kaul, A., Krieger, N., Rinck, G., Rutter, G., Strand, D. & Bartenschlager, R. (2002). Persistent and transient replication of full-length hepatitis C virus genomes in cell culture. *J Virol* **76**, 4008-4021.

Pileri, P., Uematsu, Y., Campagnoli, S., Galli, G., Falugi, F., Petracca, R., Weiner, A. J., Houghton, M., Rosa, D., Grandi, G. & Abrignani, S. (1998). Binding of hepatitis C virus to CD81. *Science* **282**, 938-941.

Ploss, A., Evans, M. J., Gaysinskaya, V. A., Panis, M., You, H., de Jong, Y. P. & Rice, C. M. (2009). Human occludin is a hepatitis C virus entry factor required for infection of mouse cells. *Nature* **457**, 882-886.

Pockros, P., Nelson, D., Godofsky, E., Rodriguez-Torres, M., Everson, G. T., Fried, M. W., Ghalib, R., Harrison, S., Nyberg, L., Shiffman, M. L., Chan, A. & Hill, G. (2008). High relapse rate seen at week 72 for patients treated with R1626 combination therapy. *Hepatology* **48**, 1349-1350.

Poynard, T., Bedossa, P. & Opolon, P. (1997). Natural history of liver fibrosis progression in patients with chronic hepatitis C. The OBSVIRC, METAVIR, CLINIVIR, and DOSVIRC groups. *Lancet* **349**, 825-832.

Poynard, T., McHutchison, J., Manns, M., Trepo, C., Lindsay, K., Goodman, Z., Ling, M. H. & Albrecht, J. (2002). Impact of pegylated interferon alfa-2b and ribavirin on liver fibrosis in patients with chronic hepatitis C. *Gastroenterology* **122**, 1303-1313.

Prieto, M., Berenguer, M., Rayon, J. M., Cordoba, J., Arguello, L., Carrasco, D., Garcia-Herola, A., Olaso, V., De Juan, M., Gobernado, M., Mir, J. & Berenguer, J. (1999). High incidence of allograft cirrhosis in hepatitis C virus genotype 1b infection following transplantation: relationship with rejection episodes. *Hepatology* **29**, 250-256.

Prince, A. M., Brotman, B., Grady, G. F., Kuhns, W. J., Hazzi, C., Levine, R. W. & Millian, S. J. (1974). Long-incubation post-transfusion hepatitis without serological evidence of exposure to hepatitis-B virus. *Lancet* **2**, 241-246.

Quinkert, D., Bartenschlager, R. & Lohmann, V. (2005). Quantitative analysis of the hepatitis C virus replication complex. *J Virol* **79**, 13594-13605.

Racanelli, V., Sansonno, D., Piccoli, C., D'Amore, F. P., Tucci, F. A. & Dammacco, F. (2001). Molecular characterization of B cell clonal expansions in the liver of chronically hepatitis C virus-infected patients. *J Immunol* **167**, 21-29.

Ragni, M. V. & Belle, S. H. (2001). Impact of human immunodeficiency virus infection on progression to end-stage liver disease in individuals with hemophilia and hepatitis C virus infection. *J Infect Dis* **183**, 1112-1115.

Randall, G., Panis, M., Cooper, J. D., Tellinghuisen, T. L., Sukhodolets, K. E., Pfeffer, S., Landthaler, M., Landgraf, P., Kan, S., Lindenbach, B. D., Chien, M., Weir, D. B., Russo, J. J., Ju, J., Brownstein, M. J., Sheridan, R., Sander, C., Zavolan, M., Tuschl, T. & Rice, C. M. (2007). Cellular cofactors affecting hepatitis C virus infection and replication. *Proc Natl Acad Sci U S A* **104**, 12884-12889.

Ray, R. B., Lagging, L. M., Meyer, K. & Ray, R. (1996). Hepatitis C virus core protein cooperates with ras and transforms primary rat embryo fibroblasts to tumorigenic phenotype. *J Virol* **70**, 4438-4443.

Ray, R. B., Lagging, L. M., Meyer, K., Steele, R. & Ray, R. (1995). Transcriptional regulation of cellular and viral promoters by the hepatitis C virus core protein. *Virus Res* **37**, 209-220.

Ray, R. B., Meyer, K., Steele, R., Shrivastava, A., Aggarwal, B. B. & Ray, R. (1998a). Inhibition of tumor necrosis factor (TNF-alpha)-mediated apoptosis by hepatitis C virus core protein. *J Biol Chem* **273**, 2256-2259.

Ray, R. B., Steele, R., Meyer, K. & Ray, R. (1997). Transcriptional repression of p53 promoter by hepatitis C virus core protein. *J Biol Chem* **272**, 10983-10986.

Ray, R. B., Steele, R., Meyer, K. & Ray, R. (1998b). Hepatitis C virus core protein represses p21WAF1/Cip1/Sid1 promoter activity. *Gene* **208**, 331-336.

Ray, S. C., Wang, Y. M., Laeyendecker, O., Ticehurst, J. R., Villano, S. A. & Thomas, D. L. (1999). Acute hepatitis C virus structural gene sequences as predictors of persistent viremia: hypervariable region 1 as a decoy. *J Virol* **73**, 2938-2946.

Reed, K. E. & Rice, C. M. (2000). Overview of hepatitis C virus genome structure, polyprotein processing, and protein properties. *Curr Top Microbiol Immunol* **242**, 55-84.

Rehermann, B., Chang, K. M., McHutchinson, J., Kokka, R., Houghton, M., Rice, C. M. & Chisari, F. V. (1996). Differential cytotoxic T-lymphocyte responsiveness to the hepatitis B and C viruses in chronically infected patients. *J Virol* **70**, 7092-7102.

Reynolds, J. E., Kaminski, A., Carroll, A. R., Clarke, B. E., Rowlands, D. J. & Jackson, R. J. (1996). Internal initiation of translation of hepatitis C virus RNA: the ribosome entry site is at the authentic initiation codon. *RNA* **2**, 867-878.

Robertson, B., Myers, G., Howard, C., Brettin, T., Bukh, J., Gaschen, B., Gojobori, T., Maertens, G., Mizokami, M., Nainan, O., Netesov, S., Nishioka, K., Shin i, T., Simmonds, P., Smith, D., Stuyver, L. & Weiner, A. (1998). Classification, nomenclature, and database development for hepatitis C virus (HCV) and related viruses: proposals for standardization. International Committee on Virus Taxonomy. *Arch Virol* **143**, 2493-2503.

Rocak, S. & Linder, P. (2004). DEAD-box proteins: the driving forces behind RNA metabolism. *Nat Rev Mol Cell Biol* **5**, 232-241.

Roohvand, F., Maillard, P., Lavergne, J. P., Boulant, S., Walic, M., Andreo, U., Goueslain, L., Helle, F., Mallet, A., McLauchlan, J. & Budkowska, A. (2009). Initiation of hepatitis C virus infection requires the dynamic microtubule network: role of the viral nucleocapsid protein. *J Biol Chem* **284**, 13778-13791.

Rosenberg, P. M., Farrell, J. J., Abraczinskas, D. R., Graeme-Cook, F. M., Dienstag, J. L. & Chung, R. T. (2002). Rapidly progressive fibrosing cholestatic hepatitis--hepatitis C virus in HIV coinfection. *Am J Gastroenterol* **97**, 478-483.

Rosner, A. & Rinkevich, B. (2007). The DDX3 subfamily of the DEAD box helicases: divergent roles as unveiled by studying different organisms and in vitro assays. *Curr Med Chem* **14**, 2517-2525.

Rouille, Y., Helle, F., Delgrange, D., Roingeard, P., Voisset, C., Blanchard, E., Belouzard, S., McKeating, J., Patel, A. H., Maertens, G., Wakita, T., Wychowski, C. & Dubuisson, J. (2006). Subcellular localization of hepatitis C virus structural proteins in a cell culture system that efficiently replicates the virus. *J Virol* **80**, 2832-2841.

Ruggieri, A., Harada, T., Matsuura, Y. & Miyamura, T. (1997). Sensitization to Fas-mediated apoptosis by hepatitis C virus core protein. *Virology* **229**, 68-76.

Russell, R. S., Meunier, J. C., Takikawa, S., Faulk, K., Engle, R. E., Bukh, J., Purcell, R. H. & Emerson, S. U. (2008). Advantages of a single-cycle production assay to study cell culture-adaptive mutations of hepatitis C virus. *Proc Natl Acad Sci U S A* **105**, 4370-4375.

Sabile, A., Perlemuter, G., Bono, F., Kohara, K., Demaugre, F., Kohara, M., Matsuura, Y., Miyamura, T., Brechot, C. & Barba, G. (1999). Hepatitis C virus core protein binds to apolipoprotein AII and its secretion is modulated by fibrates. *Hepatology* **30**, 1064-1076.

Saito, K., Meyer, K., Warner, R., Basu, A., Ray, R. B. & Ray, R. (2006). Hepatitis C virus core protein inhibits tumor necrosis factor alpha-mediated apoptosis by a protective effect involving cellular FLICE inhibitory protein. *J Virol* **80**, 4372-4379.

Sakai, A., Claire, M. S., Faulk, K., Govindarajan, S., Emerson, S. U., Purcell, R. H. & Bukh, J. (2003). The p7 polypeptide of hepatitis C virus is critical for infectivity and contains functionally important genotype-specific sequences. *Proc Natl Acad Sci U S A* **100**, 11646-11651.

Sansonno, D. & Dammacco, F. (2005). Hepatitis C virus, cryoglobulinaemia, and vasculitis: immune complex relations. *Lancet Infec Dis* **5**, 227-236.

Santolini, E., Migliaccio, G. & La Monica, N. (1994). Biosynthesis and biochemical properties of the hepatitis C virus core protein. *J Virol* **68**, 3631-3641.

Santolini, E., Pacini, L., Fipaldini, C., Migliaccio, G. & Monica, N. (1995). The NS2 protein of hepatitis C virus is a transmembrane polypeptide. *J Virol* **69**, 7461-7471.

Sarobe, P., Lasarte, J. J., Casares, N., Lopez-Diaz de Cerio, A., Baixeras, E., Labarga, P., Garcia, N., Borras-Cuesta, F. & Prieto, J. (2002). Abnormal priming of CD4(+) T cells by dendritic cells expressing hepatitis C virus core and E1 proteins. *J Virol* **76**, 5062-5070.

Sato, S., Fukasawa, M., Yamakawa, Y., Natsume, T., Suzuki, T., Shoji, I., Aizaki, H., Miyamura, T. & Nishijima, M. (2006). Proteomic profiling of lipid droplet proteins in hepatoma cell lines expressing hepatitis C virus core protein. *J Biochem* **139**, 921-930.

Scaffidi, C., Fulda, S., Srinivasan, A., Friesen, C., Li, F., Tomaselli, K. J., Debatin, K. M., Krammer, P. H. & Peter, M. E. (1998). Two CD95 (APO-1/Fas) signaling pathways. *Embo J* **17**, 1675-1687.

Scarlata, S. & Carter, C. (2003). Role of HIV-1 Gag domains in viral assembly. *Biochim Biophys Acta* **1614**, 62-72.

Scarselli, E., Ansuini, H., Cerino, R., Roccasecca, R. M., Acali, S., Filocamo, G., Traboni, C., Nicosia, A., Cortese, R. & Vitelli, A. (2002). The human scavenger receptor class B type I is a novel candidate receptor for the hepatitis C virus. *Embo J* **21**, 5017-5025.

Scheuer, P. J., Ashrafzadeh, P., Sherlock, S., Brown, D. & Dusheiko, G. M. (1992). The pathology of hepatitis C. *Hepatology* **15**, 567-571.

Schluger, L. K., Sheiner, P. A., Thung, S. N., Lau, J. Y., Min, A., Wolf, D. C., Fiel, I., Zhang, D., Gerber, M. A., Miller, C. M. & Bodenheimer, H. C., Jr. (1996). Severe recurrent cholestatic hepatitis C following orthotopic liver transplantation. *Hepatology* **23**, 971-976.

Schroder, M., Baran, M. & Bowie, A. G. (2008). Viral targeting of DEAD box protein 3 reveals its role in TBK1/IKKepsilon-mediated IRF activation. *Embo J* **27**, 2147-2157.

Scott, M. J. (2002). Characterisation of a Human DEAD-box Protein DDX3 and its Interaction with Hepatitis C Virus Core Protein. In *MRC Virology Unit* University of Glasgow, Glasgow.

Seeff, L. B., Buskell-Bales, Z., Wright, E. C., Durako, S. J., Alter, H. J., Iber, F. L., Hollinger, F. B., Gitnick, G., Knodell, R. G., Perrillo, R. P. & et al. (1992). Long-term mortality after transfusion-associated non-A, non-B hepatitis. The National Heart, Lung, and Blood Institute Study Group. *N Engl J Med* **327**, 1906-1911.

Seeff, L. B., Hollinger, F. B., Alter, H. J., Wright, E. C., Cain, C. M., Buskell, Z. J., Ishak, K. G., Iber, F. L., Toro, D., Samanta, A., Koretz, R. L., Perrillo, R. P., Goodman, Z. D., Knodell, R. G., Gitnick, G., Morgan, T. R., Schiff, E. R., Lasky, S., Stevens, C., Vlahcevic, R. Z., Weinshel, E., Tanwandee, T., Lin, H. J. & Barbosa, L. (2001). Long-term mortality and morbidity of transfusion-associated non-A, non-B, and type C hepatitis: A National Heart, Lung, and Blood Institute collaborative study. *Hepatology* **33**, 455-463.

Sekine-Osajima, Y., Sakamoto, N., Mishima, K., Nakagawa, M., Itsui, Y., Tasaka, M., Nishimura-Sakurai, Y., Chen, C. H., Kanai, T., Tsuchiya, K., Wakita, T., Enomoto, N. & Watanabe, M. (2008). Development of plaque assays for hepatitis C virus-JFH1 strain and isolation of mutants with enhanced cytopathogenicity and replication capacity. *Virology* **371**, 71-85.

Selby, M. J., Glazer, E., Masiarz, F. & Houghton, M. (1994). Complex processing and protein:protein interactions in the E2:NS2 region of HCV. *Virology* **204**, 114-122.

Serebrov, V. & Pyle, A. M. (2004). Periodic cycles of RNA unwinding and pausing by hepatitis C virus NS3 helicase. *Nature* **430**, 476-480.
Sharara, A. I. (1997). Chronic hepatitis C. *South Med J* **90**, 872-877.
Shavinskaya, A., Boulant, S., Penin, F., McLauchlan, J. & Bartenschlager, R. (2007). The lipid droplet binding domain of hepatitis C virus core protein is a major determinant for efficient virus assembly. *J Biol Chem* **282**, 37158-37169.
Shaw, M. L., Stone, K. L., Colangelo, C. M., Gulcicek, E. E. & Palese, P. (2008). Cellular proteins in influenza virus particles. *PLoS Pathog* **4**, e1000085.
Shepard, C. W., Finelli, L. & Alter, M. J. (2005). Global epidemiology of hepatitis C virus infection. *Lancet infec Dis* **5**, 558-567.
Shi, S. T., Polyak, S. J., Tu, H., Taylor, D. R., Gretch, D. R. & Lai, M. M. (2002). Hepatitis C virus NS5A colocalizes with the core protein on lipid droplets and interacts with apolipoproteins. *Virology* **292**, 198-210.
Shih, C. M., Lo, S. J., Miyamura, T., Chen, S. Y. & Lee, Y. H. (1993). Suppression of hepatitis B virus expression and replication by hepatitis C virus core protein in HuH-7 cells. *J Virol* **67**, 5823-5832.
Shih, J. W., Tsai, T. Y., Chao, C. H. & Wu Lee, Y. H. (2008). Candidate tumor suppressor DDX3 RNA helicase specifically represses cap-dependent translation by acting as an eIF4E inhibitory protein. *Oncogene* **27**, 700-714.
Shimakami, T., Hijikata, M., Luo, H., Ma, Y. Y., Kaneko, S., Shimotohno, K. & Murakami, S. (2004). Effect of interaction between hepatitis C virus NS5A and NS5B on hepatitis C virus RNA replication with the hepatitis C virus replicon. *J Virol* **78**, 2738-2748.
Shin, K., Fogg, V. C. & Margolis, B. (2006). Tight junctions and cell polarity. *Ann Rev Cell Dev Biol* **22**, 207-235.
Simister, P., Schmitt, M., Geitmann, M., Wicht, O., Danielson, U. H., Klein, R., Bressanelli, S. & Lohmann, V. (2009). Structural and functional analysis of hepatitis C virus strain JFH1 polymerase. *J Virol* **83**, 11926-11939.
Simmonds, P. (2004). Genetic diversity and evolution of hepatitis C virus - 15 years on. *J Gen Virol* **85**, 3173-3188.
Smirnova, I. S., Aksenov, N. D., Kashuba, E. V., Payakurel, P., Grabovetsky, V. V., Zaberezhny, A. D., Vonsky, M. S., Buchinska, L., Biberfeld, P., Hinkula, J. & Isaguliants, M. G. (2006). Hepatitis C virus core protein transforms murine fibroblasts by promoting genomic instability. *Cell Oncol* **28**, 177-190.
Song, Y., Friebe, P., Tzima, E., Junemann, C., Bartenschlager, R. & Niepmann, M. (2006). The hepatitis C virus RNA 3'-untranslated region strongly enhances translation directed by the internal ribosome entry site. *J Virol* **80**, 11579-11588.
Soriano, V., Peters, M. G. & Zeuzem, S. (2009). New therapies for hepatitis C virus infection. *Clin Infect Dis* **48**, 313-320.
Soto, B., Sanchez-Quijano, A., Rodrigo, L., del Olmo, J. A., Garcia-Bengoechea, M., Hernandez-Quero, J., Rey, C., Abad, M. A., Rodriguez, M., Sales Gilabert, M., Gonzalez, F., Miron, P., Caruz, A., Relimpio, F., Torronteras, R., Leal, M. & Lissen, E. (1997). Human immunodeficiency virus infection modifies the natural history of chronic parenterally-acquired hepatitis C with an unusually rapid progression to cirrhosis. *J Hepatol* **26**, 1-5.
Soulat, D., Burckstummer, T., Westermayer, S., Goncalves, A., Bauch, A., Stefanovic, A., Hantschel, O., Bennett, K. L., Decker, T. & Superti-Furga, G. (2008). The DEAD-box helicase DDX3X is a critical component of the TANK-binding kinase 1-dependent innate immune response. *Embo J* **27**, 2135-2146.
Spangberg, K., Goobar-Larsson, L., Wahren-Herlenius, M. & Schwartz, S. (1999). The La protein from human liver cells interacts specifically with the U-rich region in the hepatitis C virus 3' untranslated region. *J Hum Virol* **2**, 296-307.
Steinmann, D., Barth, H., Gissler, B., Schurmann, P., Adah, M. I., Gerlach, J. T., Pape, G. R., Depla, E., Jacobs, D., Maertens, G., Patel, A. H., Inchauspe, G.,

Liang, T. J., Blum, H. E. & Baumert, T. F. (2004). Inhibition of hepatitis C virus-like particle binding to target cells by antiviral antibodies in acute and chronic hepatitis C. *J Virol* **78**, 9030-9040.

Steinmann, E., Penin, F., Kallis, S., Patel, A. H., Bartenschlager, R. & Pietschmann, T. (2007a). Hepatitis C virus p7 protein is crucial for assembly and release of infectious virions. *PLoS Pathog* **3**, e103.

Steinmann, E., Whitfield, T., Kallis, S., Dwek, R. A., Zitzmann, N., Pietschmann, T. & Bartenschlager, R. (2007b). Antiviral effects of amantadine and iminosugar derivatives against hepatitis C virus. *Hepatology* **46**, 330-338.

Stryer, L. (1988) Biochemistry 3rd Edition, Freeman & Company.

Su, A. I., Pezacki, J. P., Wodicka, L., Brideau, A. D., Supekova, L., Thimme, R., Wieland, S., Bukh, J., Purcell, R. H., Schultz, P. G. & Chisari, F. V. (2002). Genomic analysis of the host response to hepatitis C virus infection. *Proc Natl Acad Sci U S A* **99**, 15669-15674.

Sumpter, R., Jr., Loo, Y. M., Foy, E., Li, K., Yoneyama, M., Fujita, T., Lemon, S. M. & Gale, M., Jr. (2005). Regulating intracellular antiviral defense and permissiveness to hepatitis C virus RNA replication through a cellular RNA helicase, RIG-I. *J Virol* **79**, 2689-2699.

Sun, M., Song, L., Li, Y., Zhou, T. & Jope, R. S. (2008). Identification of an antiapoptotic protein complex at death receptors. *Cell Death Differ* **15**, 1887-1900.

Suzich, J. A., Tamura, J. K., Palmer-Hill, F., Warrener, P., Grakoui, A., Rice, C. M., Feinstone, S. M. & Collett, M. S. (1993). Hepatitis C virus NS3 protein polynucleotide-stimulated nucleoside triphosphatase and comparison with the related pestivirus and flavivirus enzymes. *J Virol* **67**, 6152-6158.

Suzuki, R., Matsuura, Y., Suzuki, T., Ando, A., Chiba, J., Harada, S., Saito, I. & Miyamura, T. (1995). Nuclear localization of the truncated hepatitis C virus core protein with its hydrophobic C terminus deleted. *J Gen Virol* **76**, 53-61.

Tabor, E., Gerety, R. J., Drucker, J. A., Seeff, L. B., Hoofnagle, J. H., Jackson, D. R., April, M., Barker, L. F. & Pineda-Tamondong, G. (1978). Transmission of non-A, non-B hepatitis from man to chimpanzee. *Lancet* **1**, 463-466.

Taguchi, T., Nagano-Fujii, M., Akutsu, M., Kadoya, H., Ohgimoto, S., Ishido, S. & Hotta, H. (2004). Hepatitis C virus NS5A protein interacts with 2',5'-oligoadenylate synthetase and inhibits antiviral activity of IFN in an IFN sensitivity-determining region-independent manner. *J Gen Virol* **85**, 959-969.

Tai, C. L., Chi, W. K., Chen, D. S. & Hwang, L. H. (1996). The helicase activity associated with hepatitis C virus nonstructural protein 3 (NS3). *J Virol* **70**, 8477-8484.

Takahashi, M., Yamada, G., Miyamoto, R., Doi, T., Endo, H. & Tsuji, T. (1993). Natural course of chronic hepatitis C. *Am J Gastroenterol* **88**, 240-243.

Takamizawa, A., Mori, C., Fuke, I., Manabe, S., Murakami, S., Fujita, J., Onishi, E., Andoh, T., Yoshida, I. & Okayama, H. (1991). Structure and organization of the hepatitis C virus genome isolated from human carriers. *J Virol* **65**, 1105-1113.

Takehara, T., Hayashi, N., Mita, E., Hagiwara, H., Ueda, K., Katayama, K., Kasahara, A., Fusamoto, H. & Kamada, T. (1992). Detection of the minus strand of hepatitis C virus RNA by reverse transcription and polymerase chain reaction: implications for hepatitis C virus replication in infected tissue. *Hepatology* **15**, 387-390.

Tanaka, T., Kato, N., Cho, M. J., Sugiyama, K. & Shimotohno, K. (1996). Structure of the 3' terminus of the hepatitis C virus genome. *J Virol* **70**, 3307-3312.

Tanaka, Y., Shimoike, T., Ishii, K., Suzuki, R., Suzuki, T., Ushijima, H., Matsuura, Y. & Miyamura, T. (2000). Selective binding of hepatitis C virus core protein to synthetic oligonucleotides corresponding to the 5' untranslated region of the viral genome. *Virology* **270**, 229-236.

Tanji, Y., Kaneko, T., Satoh, S. & Shimotohno, K. (1995). Phosphorylation of hepatitis C virus-encoded nonstructural protein NS5A. *J Virol* **69**, 3980-3986.

Tanner, N. K., Cordin, O., Banroques, J., Doere, M. & Linder, P. (2003). The Q motif: a newly identified motif in DEAD box helicases may regulate ATP binding and hydrolysis. *Mol cell* **11**, 127-138.

Targett-Adams, P., Boulant, S. & McLauchlan, J. (2008a). Visualization of double-stranded RNA in cells supporting hepatitis C virus RNA replication. *J Virol* **82**, 2182-2195.

Targett-Adams, P., Chambers, D., Gledhill, S., Hope, R. G., Coy, J. F., Girod, A. & McLauchlan, J. (2003). Live cell analysis and targeting of the lipid droplet-binding adipocyte differentiation-related protein. *J Biol Chem* **278**, 15998-16007.

Targett-Adams, P., Hope, G., Boulant, S. & McLauchlan, J. (2008b). Maturation of hepatitis C virus core protein by signal peptide peptidase is required for virus production. *J Biol Chem* **283**, 16850-16859.

Taylor, D. R., Shi, S. T., Romano, P. R., Barber, G. N. & Lai, M. M. (1999). Inhibition of the interferon-inducible protein kinase PKR by HCV E2 protein. *Science* **285**, 107-110.

Taylor, W. R. (1986). The classification of amino acid conservation. *J Theor Biol* **119**, 205-218.

Tellinghuisen, T. L., Evans, M. J., von Hahn, T., You, S. & Rice, C. M. (2007). Studying hepatitis C virus: making the best of a bad virus. *J Virol* **81**, 8853-8867.

Tellinghuisen, T. L., Foss, K. L. & Treadaway, J. (2008a). Regulation of hepatitis C virion production via phosphorylation of the NS5A protein. *PLoS Pathog* **4**, e1000032.

Tellinghuisen, T. L., Foss, K. L., Treadaway, J. C. & Rice, C. M. (2008b). Identification of residues required for RNA replication in domains II and III of the hepatitis C virus NS5A protein. *J Virol* **82**, 1073-1083.

Tellinghuisen, T. L., Marcotrigiano, J., Gorbalenya, A. E. & Rice, C. M. (2004). The NS5A protein of hepatitis C virus is a zinc metalloprotein. *J Biol Chem* **279**, 48576-48587.

Tellinghuisen, T. L., Marcotrigiano, J. & Rice, C. M. (2005). Structure of the zinc-binding domain of an essential component of the hepatitis C virus replicase. *Nature* **435**, 374-379.

Teodoro, J. G. & Branton, P. E. (1997). Regulation of apoptosis by viral gene products. *J Virol* **71**, 1739-1746.

Thimme, R., Oldach, D., Chang, K. M., Steiger, C., Ray, S. C. & Chisari, F. V. (2001). Determinants of viral clearance and persistence during acute hepatitis C virus infection. *J Exp Med* **194**, 1395-1406.

Thomas, D. L., Astemborski, J., Rai, R. M., Anania, F. A., Schaeffer, M., Galai, N., Nolt, K., Nelson, K. E., Strathdee, S. A., Johnson, L., Laeyendecker, O., Boitnott, J., Wilson, L. E. & Vlahov, D. (2000). The natural history of hepatitis C virus infection: host, viral, and environmental factors. *Jama* **284**, 450-456.

Thomson, B. J. (2009). Hepatitis C virus: the growing challenge. *Brit Med Bull* **89**, 153-167.

Thomssen, R., Bonk, S., Propfe, C., Heermann, K. H., Kochel, H. G. & Uy, A. (1992). Association of hepatitis C virus in human sera with beta-lipoprotein. *Med Microbiol Immunol* **181**, 293-300.

Thomssen, R., Bonk, S. & Thiele, A. (1993). Density heterogeneities of hepatitis C virus in human sera due to the binding of beta-lipoproteins and immunoglobulins. *Med Microbiol Immunol* **182**, 329-334.

Tomei, L., Failla, C., Santolini, E., De Francesco, R. & La Monica, N. (1993). NS3 is a serine protease required for processing of hepatitis C virus polyprotein. *J Virol* **67**, 4017-4026.

Toth, C. M., Pascual, M., Chung, R. T., Graeme-Cook, F., Dienstag, J. L., Bhan, A. K. & Cosimi, A. B. (1998). Hepatitis C virus-associated fibrosing cholestatic hepatitis after renal transplantation: response to interferon-alpha therapy. *Transplantation* **66**, 1254-1258.

Tsai, S. L., Chen, Y. M., Chen, M. H., Huang, C. Y., Sheen, I. S., Yeh, C. T., Huang, J. H., Kuo, G. C. & Liaw, Y. F. (1998). Hepatitis C virus variants circumventing cytotoxic T lymphocyte activity as a mechanism of chronicity. *Gastroenterology* **115**, 954-965.

Tsukiyama-Kohara, K., Iizuka, N., Kohara, M. & Nomoto, A. (1992). Internal ribosome entry site within hepatitis C virus RNA. *J Virol* **66**, 1476-1483.

Tuplin, A., Evans, D. J. & Simmonds, P. (2004). Detailed mapping of RNA secondary structures in core and NS5B-encoding region sequences of hepatitis C virus by RNase cleavage and novel bioinformatic prediction methods. *J Gen Virol* **85**, 3037-3047.

Urushihara, A., Sodeyama, T., Matsumoto, A. & Tanaka, E. (1994). Changes in antibody titers to hepatitis C virus following interferon therapy for chronic infection. *J Med Virol* **42**, 348-356.

Vanwolleghem, T., Bukh, J., Meuleman, P., Desombere, I., Meunier, J. C., Alter, H., Purcell, R. H. & Leroux-Roels, G. (2008). Polyclonal immunoglobulins from a chronic hepatitis C virus patient protect human liver-chimeric mice from infection with a homologous hepatitis C virus strain. *Hepatology* **47**, 1846-1855.

Vanwolleghem, T., Meuleman, P., Libbrecht, L., Roskams, T., De Vos, R. & Leroux-Roels, G. (2007). Ultra-rapid cardiotoxicity of the hepatitis C virus protease inhibitor BILN 2061 in the urokinase-type plasminogen activator mouse. *Gastroenterology* **133**, 1144-1155.

Vaquer, P., Canet, R., Llompart, A., Riera, J., Obrador, A. & Gaya, J. (1994). Histological evolution of chronic hepatitis C. Factors related to progression. *Liver* **14**, 265-269.

Varaklioti, A., Vassilaki, N., Georgopoulou, U. & Mavromara, P. (2002). Alternate translation occurs within the core coding region of the hepatitis C viral genome. *J Biol Chem* **277**, 17713-17721.

Varnum, S. M., Streblow, D. N., Monroe, M. E., Smith, P., Auberry, K. J., Pasa-Tolic, L., Wang, D., Camp, D. G., 2nd, Rodland, K., Wiley, S., Britt, W., Shenk, T., Smith, R. D. & Nelson, J. A. (2004). Identification of proteins in human cytomegalovirus (HCMV) particles: the HCMV proteome. *J Virol* **78**, 10960-10966.

Vassilaki, N., Friebe, P., Meuleman, P., Kallis, S., Kaul, A., Paranhos-Baccala, G., Leroux-Roels, G., Mavromara, P. & Bartenschlager, R. (2008). Role of the hepatitis C virus core+1 open reading frame and core cis-acting RNA elements in viral RNA translation and replication. *J Virol* **82**, 11503-11515.

Vassilaki, N. & Mavromara, P. (2003). Two alternative translation mechanisms are responsible for the expression of the HCV ARFP/F/core+1 coding open reading frame. *J Biol Chem* **278**, 40503-40513.

Villano, S. A., Vlahov, D., Nelson, K. E., Cohn, S. & Thomas, D. L. (1999). Persistence of viremia and the importance of long-term follow-up after acute hepatitis C infection. *Hepatology* **29**, 908-914.

Voisset, C., Callens, N., Blanchard, E., Op De Beeck, A., Dubuisson, J. & Vu-Dac, N. (2005). High density lipoproteins facilitate hepatitis C virus entry through the scavenger receptor class B type I. *J Biol Chem* **280**, 7793-7799.

von Hahn, T., Yoon, J. C., Alter, H., Rice, C. M., Rehermann, B., Balfe, P. & McKeating, J. A. (2007). Hepatitis C virus continuously escapes from neutralizing antibody and T-cell responses during chronic infection in vivo. *Gastroenterology* **132**, 667-678.

Wakita, T., Pietschmann, T., Kato, T., Date, T., Miyamoto, M., Zhao, Z., Murthy, K., Habermann, A., Krausslich, H. G., Mizokami, M., Bartenschlager, R. & Liang, T. J. (2005). Production of infectious hepatitis C virus in tissue culture from a cloned viral genome. *Nat Med* **11**, 791-796.

Walewski, J. L., Keller, T. R., Stump, D. D. & Branch, A. D. (2001). Evidence for a new hepatitis C virus antigen encoded in an overlapping reading frame. *RNA* **7**, 710-721.

Walker, J. E., Saraste, M., Runswick, M. J. & Gay, N. J. (1982). Distantly related sequences in the alpha- and beta-subunits of ATP synthase, myosin, kinases and other ATP-requiring enzymes and a common nucleotide binding fold. *Embo J* **1**, 945-951.

Wang, C., Sarnow, P. & Siddiqui, A. (1993). Translation of human hepatitis C virus RNA in cultured cells is mediated by an internal ribosome-binding mechanism. *J Virol* **67**, 3338-3344.

Wang, F., Yoshida, I., Takamatsu, M., Ishido, S., Fujita, T., Oka, K. & Hotta, H. (2000a). Complex formation between hepatitis C virus core protein and p21Waf1/Cip1/Sdi1. *Biochem Biophys Res Commun* **273**, 479-484.

Wang, H., Kim, S. & Ryu, W. S. (2009). DDX3 DEAD-Box RNA helicase inhibits hepatitis B virus reverse transcription by incorporation into nucleocapsids. *J Virol* **83**, 5815-5824.

Wang, W. K., Chen, M. Y., Chuang, C. Y., Jeang, K. T. & Huang, L. M. (2000b). Molecular biology of human immunodeficiency virus type 1. *J Microbiol Immunol Infect* **33**, 131-140.

Waris, G., Sarker, S. & Siddiqui, A. (2004). Two-step affinity purification of the hepatitis C virus ribonucleoprotein complex. *RNA* **10**, 321-329.

Watashi, K., Hijikata, M., Tagawa, A., Doi, T., Marusawa, H. & Shimotohno, K. (2003). Modulation of retinoid signaling by a cytoplasmic viral protein via sequestration of Sp110b, a potent transcriptional corepressor of retinoic acid receptor, from the nucleus. *Mol Cell Biol* **23**, 7498-7509.

Weiner, A., Erickson, A. L., Kansopon, J., Crawford, K., Muchmore, E., Hughes, A. L., Houghton, M. & Walker, C. M. (1995). Persistent hepatitis C virus infection in a chimpanzee is associated with emergence of a cytotoxic T lymphocyte escape variant. *Proc Natl Acad Sci U S A* **92**, 2755-2759.

Weiner, A. J., Brauer, M. J., Rosenblatt, J., Richman, K. H., Tung, J., Crawford, K., Bonino, F., Saracco, G., Choo, Q. L., Houghton, M. & et al. (1991). Variable and hypervariable domains are found in the regions of HCV corresponding to the flavivirus envelope and NS1 proteins and the pestivirus envelope glycoproteins. *Virology* **180**, 842-848.

Weiner, A. J., Geysen, H. M., Christopherson, C., Hall, J. E., Mason, T. J., Saracco, G., Bonino, F., Crawford, K., Marion, C. D., Crawford, K. A. & et al. (1992). Evidence for immune selection of hepatitis C virus (HCV) putative envelope glycoprotein variants: potential role in chronic HCV infections. *Proc Natl Acad Sci U S A* **89**, 3468-3472.

Wiese, M., Berr, F., Lafrenz, M., Porst, H. & Oesen, U. (2000). Low frequency of cirrhosis in a hepatitis C (genotype 1b) single-source outbreak in germany: a 20-year multicenter study. *Hepatology* **32**, 91-96.

Wolk, B., Sansonno, D., Krausslich, H. G., Dammacco, F., Rice, C. M., Blum, H. E. & Moradpour, D. (2000). Subcellular localization, stability, and trans-cleavage competence of the hepatitis C virus NS3-NS4A complex expressed in tetracycline-regulated cell lines. *J Virol* **74**, 2293-2304.

Wong, D. K., Dudley, D. D., Dohrenwend, P. B., Lauer, G. M., Chung, R. T., Thomas, D. L. & Walker, B. D. (2001). Detection of diverse hepatitis C virus (HCV)-specific cytotoxic T lymphocytes in peripheral blood of infected persons by screening for responses to all translated proteins of HCV. *J Virol* **75**, 1229-1235.

Wood, J., Frederickson, R. M., Fields, S. & Patel, A. H. (2001). Hepatitis C virus 3'X region interacts with human ribosomal proteins. *J Virol* **75**, 1348-1358.

Xu, Z., Choi, J., Yen, T. S., Lu, W., Strohecker, A., Govindarajan, S., Chien, D., Selby, M. J. & Ou, J. (2001). Synthesis of a novel hepatitis C virus protein by ribosomal frameshift. *Embo J* **20**, 3840-3848.

Yamaga, A. K. & Ou, J. H. (2002). Membrane topology of the hepatitis C virus NS2 protein. *J Biol Chem* **277**, 33228-33234.

Yanagi, M., Purcell, R. H., Emerson, S. U. & Bukh, J. (1997). Transcripts from a single full-length cDNA clone of hepatitis C virus are infectious when directly transfected into the liver of a chimpanzee. *Proc Natl Acad Sci U S A* **94**, 8738-8743.

Yanagi, M., St Claire, M., Emerson, S. U., Purcell, R. H. & Bukh, J. (1999). In vivo analysis of the 3' untranslated region of the hepatitis C virus after in vitro mutagenesis of an infectious cDNA clone. *Proc Natl Acad Sci U S A* **96**, 2291-2295.

Yao, N., Hesson, T., Cable, M., Hong, Z., Kwong, A. D., Le, H. V. & Weber, P. C. (1997). Structure of the hepatitis C virus RNA helicase domain. *Nat Struct Biol* **4**, 463-467.

Yao, Z. Q., Nguyen, D. T., Hiotellis, A. I. & Hahn, Y. S. (2001). Hepatitis C virus core protein inhibits human T lymphocyte responses by a complement-dependent regulatory pathway. *J Immunol* **167**, 5264-5272.

Yao, Z. Q., Praythер, D., Trabue, C., Dong, Z. P. & Moorman, J. (2008). Differential regulation of SOCS-1 signalling in B and T lymphocytes by hepatitis C virus core protein. *Immunology* **125**, 197-207.

Yasui, K., Wakita, T., Tsukiyama-Kohara, K., Funahashi, S. I., Ichikawa, M., Kajita, T., Moradpour, D., Wands, J. R. & Kohara, M. (1998). The native form and maturation process of hepatitis C virus core protein. *J Virol* **72**, 6048-6055.

Yedavalli, V. S., Neuveut, C., Chi, Y. H., Kleiman, L. & Jeang, K. T. (2004). Requirement of DDX3 DEAD box RNA helicase for HIV-1 Rev-RRE export function. *Cell* **119**, 381-392.

Yi, M. & Lemon, S. M. (2003). Structure-function analysis of the 3' stem-loop of hepatitis C virus genomic RNA and its role in viral RNA replication. *RNA* **9**, 331-345.

Yi, M., Ma, Y., Yates, J. & Lemon, S. M. (2007). Compensatory mutations in E1, p7, NS2, and NS3 enhance yields of cell culture-infectious intergenotypic chimeric hepatitis C virus. *J Virol* **81**, 629-638.

Yoshida, I., Oka, K., Hidajat, R., Nagano-Fujii, M., Ishido, S. & Hotta, H. (2001). Inhibition of p21/Waf1/Cip1/Sdi1 expression by hepatitis C virus core protein. *Microbiol Immunol* **45**, 689-697.

You, L. R., Chen, C. M., Yeh, T. S., Tsai, T. Y., Mai, R. T., Lin, C. H. & Lee, Y. H. (1999). Hepatitis C virus core protein interacts with cellular putative RNA helicase. *J Virol* **73**, 2841-2853.

Zarski, J. P., Bohn, B., Bastie, A., Pawlotsky, J. M., Baud, M., Bost-Bezeaux, F., Tran van Nhieu, J., Seigneurin, J. M., Buffet, C. & Dhumeaux, D. (1998). Characteristics of patients with dual infection by hepatitis B and C viruses. *J Hepatol* **28**, 27-33.

Zhang, J., Randall, G., Higginbottom, A., Monk, P., Rice, C. M. & McKeating, J. A. (2004). CD81 is required for hepatitis C virus glycoprotein-mediated viral infection. *J Virol* **78**, 1448-1455.

Zheng, A., Yuan, F., Li, Y., Zhu, F., Hou, P., Li, J., Song, X., Ding, M. & Deng, H. (2007). Claudin-6 and claudin-9 function as additional coreceptors for hepatitis C virus. *J Virol* **81**, 12465-12471.

Zhong, J., Gastaminza, P., Cheng, G., Kapadia, S., Kato, T., Burton, D. R., Wieland, S. F., Uprichard, S. L., Wakita, T. & Chisari, F. V. (2005). Robust hepatitis C virus infection in vitro. *Proc Natl Acad Sci U S A* **102**, 9294-9299.

Zhong, W., Uss, A. S., Ferrari, E., Lau, J. Y. & Hong, Z. (2000). De novo initiation of RNA synthesis by hepatitis C virus nonstructural protein 5B polymerase. *J Virol* **74**, 2017-2022.

Zhu, F. X., Chong, J. M., Wu, L. & Yuan, Y. (2005). Virion proteins of Kaposi's sarcoma-associated herpesvirus. *J Virol* **79**, 800-811.

Zhu, N., Khoshnan, A., Schneider, R., Matsumoto, M., Dennert, G., Ware, C. & Lai, M. M. (1998). Hepatitis C virus core protein binds to the cytoplasmic domain of tumor necrosis factor (TNF) receptor 1 and enhances TNF-induced apoptosis. *J Virol* **72**, 3691-3697.

Zhu, N., Ware, C. F. & Lai, M. M. (2001). Hepatitis C virus core protein enhances FADD-mediated apoptosis and suppresses TRADD signaling of tumor necrosis factor receptor. *Virology* **283**, 178-187.

Zuker, M. (2003). Mfold web server for nucleic acid folding and hybridization prediction. *Nucleic Acids Res* **31**, 3406-3415.